Emerging Frontiers in Science and Technology: Integrating Physics, Materials, and Energy Systems

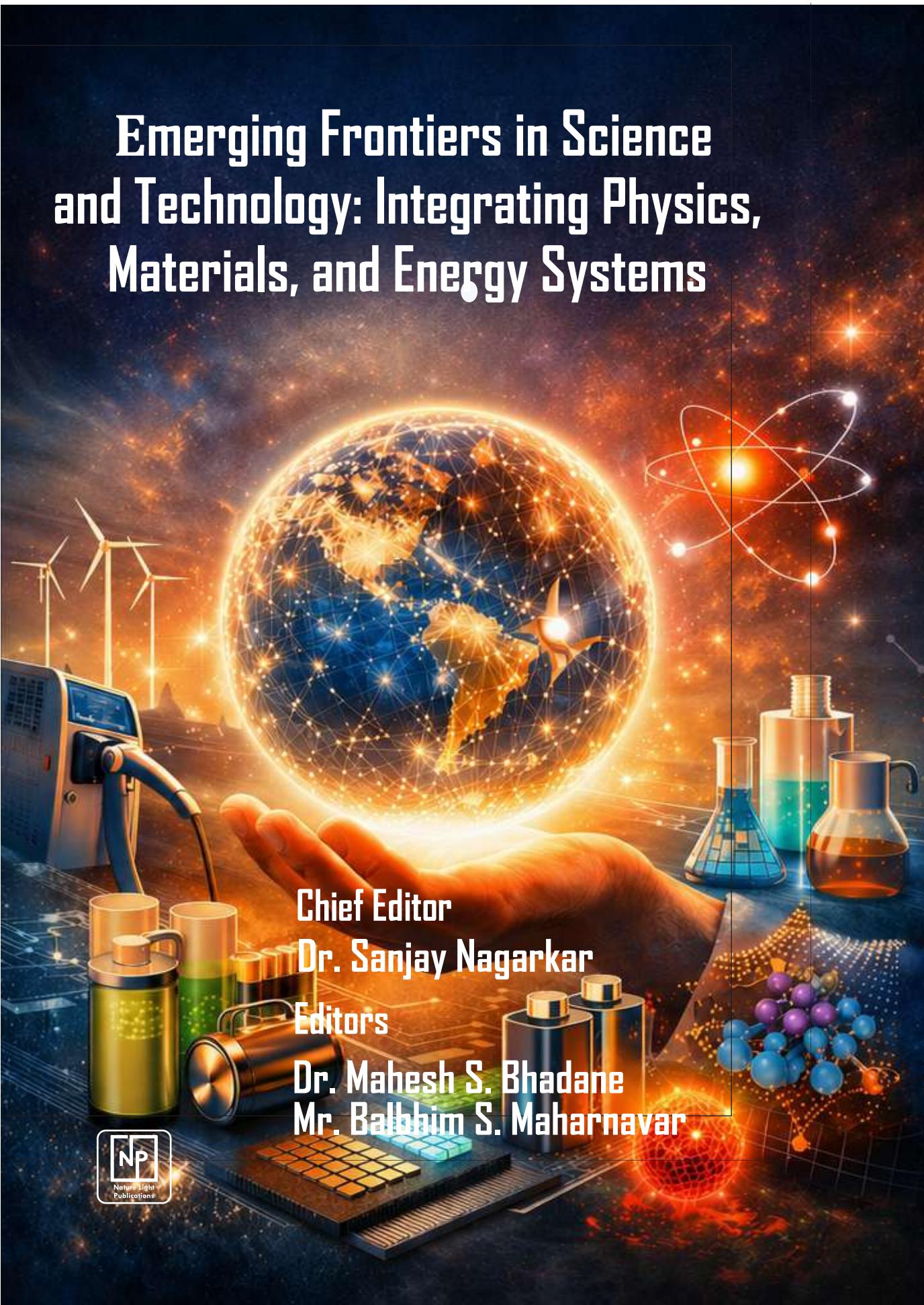

Chief Editor
Dr. Sanjay Nagarkar

Editors
Dr. Mahesh S. Bhadane
Mr. Balbhim S. Maharnavar

NP
Nature Light Publications

Emerging Frontiers in Science and Technology: Integrating Physics, Materials, and Energy Systems

Dr. Sanjay Nagarkar
Dr. Mahesh S. Bhadane
Mr. Balbhim S. Maharnavar

Nature Light Publications

Emerging Frontiers in Science and Technology: Integrating Physics, Materials, and Energy Systems

Chief Editor

Dr. Sanjay Nagarkar

Editors

Dr. Mahesh S. Bhadane

Mr. Balbhim S. Maharnavar

An International Edition

ISBN No.- 978-93-49938-40-3

Published & Printed By

Nature Light Publications

309 West 11, Manjari VSI Road, Manjari Bk.,
Haveli, Pune- 412 307.
Website: www.naturelightpublications.com
Email: naturelightpublications@gmail.com
Contact No: +91 9822489040 / 9922489040

Emerging Frontiers in Science and Technology: Integrating Physics, Materials, and Energy Systems

An Edited Book by

Department of Physics

Compiled as an outcome of

National Conference in 'Innovations in Science and Technology'

Organized by

Internal Quality Assurance Cell, along with Botany, Chemistry, Physics, Zoology, Geography, Mathematics and Computer Science departments of Dada Patil Mahavidyalaya, Karjat, Dist. Ahilyanagar

On 7th of March 2026

Nature Light Publications

Chief Editor

Sanjay Nagarkar

Professor & Principal
Rayat Shikshan Sanstha's,
Dada Patil Mahavidyalaya, Karjat 414402
Dist. Ahilyanagar, Maharashtra
India

Editors

Mahesh Bhadane
Assistant Professor &
Head, Physics

Balbhim Maharnavar
Assistant Professor
Physics

Co-Editors

Amol R. Pardeshi
Assistant Professor
Physics

Sahadev Kangude
Assistant Professor
Physics

Rutuja Malave
Assistant Professor
Physics

Sampada Karpe
Assistant Professor
Physics

Mangal Mhaske
Assistant Professor
Physics

Rani Gaikwad
Assistant Professor
Physics

Rayat Shikshan Sanstha's,
Dada Patil Mahavidyalaya, Karjat 414402
Dist. Ahilyanagar, Maharashtra
India

Preface

The contemporary era of scientific advancement is marked by unprecedented integration across disciplines, where physics, materials science, and energy systems converge to address some of the most pressing global challenges. Rapid developments in nanotechnology, semiconductor physics, advanced materials, and sustainable energy solutions have transformed the landscape of modern science and technology. The present edited volume, "Emerging Frontiers in Science and Technology: Integrating Physics, Materials, and Energy Systems," is a comprehensive compilation that reflects these dynamic and interdisciplinary advancements.

This volume brings together a rich collection of research contributions from scholars and scientists, covering both fundamental principles and cutting-edge innovations. The initial chapters focus on radiation physics and luminescence studies, including thermoluminescence, photoluminescence, and optically stimulated luminescence. These works highlight the importance of dosimetric materials in applications such as radiation measurement and medical therapies, including proton therapy.

A significant portion of this book is devoted to the study of advanced materials and nanotechnology. Contributions on rare earth–activated materials, polymer composites for radiation shielding, and crystal defect engineering provide insights into the design and development of functional materials. The exploration of quantum dots, carbon quantum dots, and nanostructured materials further emphasizes their critical role in sensing, photonics, and energy-related applications.

The volume also highlights innovations in semiconductor physics and optoelectronic materials, including studies on nonlinear optical materials, silicon nanowire heterostructures, and emerging semiconductor technologies. These advancements are essential for the development of next-generation electronic and photonic devices.

Another key theme of this book is the application of theoretical and computational approaches in modern science. Chapters on density functional theory, quantum tunneling, and galaxy rotation curves illustrate

how theoretical physics continues to expand our understanding of both microscopic and cosmic phenomena. Additionally, the integration of Artificial Intelligence in physics research represents a transformative trend, enabling accelerated materials discovery and enhanced data analysis.

Energy systems and sustainability form a central focus of this volume. A large number of contributions are dedicated to energy storage technologies, particularly supercapacitors, lithium-ion and sodium-ion batteries, and advanced electrode materials. Studies on layered double hydroxides, carbon-based nanostructures, and metal oxide nanocomposites demonstrate ongoing efforts to develop efficient and sustainable energy storage solutions.

Furthermore, the book explores renewable energy and environmental sustainability through topics such as solar energy materials, photocatalysts, hydrogen evolution reactions, and nanotechnology for environmental protection. These contributions underline the critical role of science and technology in achieving sustainable development goals.

The editors believe that this volume will serve as a valuable resource for researchers, students, and professionals in physics, materials science, and energy engineering. It not only presents recent trends and technological advancements but also encourages interdisciplinary collaboration and innovation.

We express our sincere gratitude to all contributors for their scholarly efforts and to the reviewers for their valuable insights. We also acknowledge the support of our institution and organizing committee in successfully bringing out this publication.

It is our hope that this book will inspire further research, foster innovation, and contribute to the advancement of sustainable and technologically advanced solutions for the future.

Mahesh Bhadane
Balbhim Maharnavar

Department of Physics
Rayat Shikshan Sanstha's,
Dada Patil Mahavidyalaya, Karjat
414402
Dist. Ahilyanagar, Maharashtra, India

Emerging Frontiers in Science and Technology: Integrating Physics, Materials, and Energy Systems

Table of Content

Effect of Different Radiation Sources on Glow Curve Properties of $CaSO_4$: Dy Thermoluminescent Phosphor

Mahesh S. Bhadane

Head, Department of Physics, Rayat Shikshan Sanstha's Dada Patil Mahavidyalaya Karjat, Dist-Ahilyanagar-414402

Email: mbhadane24@gmail.com

Article DOI Link: https://zenodo.org/uploads/19785530

DOI: 10.5281/zenodo.19785530

Abstract

Thermoluminescent phosphors are widely used in radiation dosimetry due to their high sensitivity and stability. Among them, $CaSO_4$ (Zeff. = 15.6) is one of the most effective materials for measuring ionizing radiation. This chapter discusses the effect of different radiation sources on the glow curve properties of $CaSO_4$: Dy thermoluminescent phosphor. Exposure to various radiations such as gamma rays, x-rays, electron, thermal neutron, and ion-beam leads to the formation of trapping centers that influence the intensity, peak position, and shape of the glow curve. These variations are important for understanding the trapping and recombination mechanisms within the phosphor material. The study of radiation-induced glow curve modifications provides valuable insight into the dosimetric performance and practical applications of $CaSO_4$: Dy in radiation monitoring and dosimetry.

Keywords: $CaSO_4$: Dy, Glow Curve, Thermoluminescence, Radiation, Dosimetry

Introduction

$CaSO_4$: Dy is one of the most sensitive thermoluminescent phosphors used in radiation dosimetry. When exposed to ionizing radiation, electrons and holes are trapped at defect sites within the crystal lattice. Upon heating, these trapped charge carriers are released and recombine at luminescent centers, producing light known as thermoluminescence [1]. The intensity of emitted light as a function of temperature is represented by a glow curve. The glow curve of $CaSO_4$ typically exhibits prominent peaks between 200–240 °C, which are associated with stable trapping centers responsible for dosimetric applications [2]. The position, intensity, and shape of these peaks depend on several factors such as radiation dose, type of radiation, heating rate, and material preparation methods. Changes in glow curve structure provide important information about trap depth, recombination probability, and kinetic parameters of the phosphor material [3].

Different radiation sources can influence the glow curve characteristics of $CaSO_4$ by creating varying densities of trapping centers. High-energy radiation such as gamma rays and electron beams generally produce deeper traps and higher TL intensity, while lower-energy radiation may lead to variations in peak structure and sensitivity [4]. Therefore, glow curve analysis plays a crucial role in evaluating the dosimetric performance and radiation response of $CaSO_4$: Dy phosphors.

Synthesis Routes

The synthesis of $CaSO_4$:Dy TL phosphor can be achieved through several preparation methods. Common synthesis routes are solid-state reaction [5], co-precipitation [6], sol–gel method [7], acid re-crystallization [8], and wet chemical techniques [9]. Among these, the co-precipitation method is widely used because it allows better control over dopant concentration and particle homogeneity. In a typical synthesis process, calcium and dysprosium precursors are mixed in aqueous solution, followed by precipitation using suitable reagents. The obtained precipitate is then filtered, dried, and annealed at elevated temperatures to achieve proper crystallization.

Discussion of Thermoluminescence Glow Curve of $CaSO_4$: Dy under Different Radiation Sources:

The glow curve profiles shown in Figures 1–4, further illustrate how the TL intensity and peak structure depend on radiation type, particle energy, and fluence. For example, the glow curves obtained under swift heavy ion irradiation show increasing intensity with increasing ion fluence, indicating a higher density of trapping centers. Similarly, neutron-irradiated samples display systematic changes in TL intensity with increasing neutron fluence. These observations confirm that radiation–matter interaction strongly influences defect formation and charge trapping processes in $CaSO_4$ phosphor. Therefore, understanding the effect of different radiation sources on TL glow curve behavior is essential for optimizing the dosimetric performance of this phosphor for radiation monitoring and detector applications.

The TL glow curve characteristics of $CaSO_4$ phosphor vary significantly depending on the type of radiation used for irradiation and the synthesis route employed. The data summarized in Table 1 show that multiple glow peaks appear in the temperature range of approximately 411–748 K when the material is exposed to different radiation sources such as γ-rays, swift heavy ions, ion beams, thermal neutrons, electrons, and X-rays. These peaks correspond to various trapping centers formed in the crystal lattice during irradiation. For γ-ray irradiation from ^{60}Co, four prominent glow peaks at 411, 498, 569, and 652 K are observed for samples prepared by the chemical co-precipitation method. The

presence of multiple peaks indicates the formation of several trapping levels with different activation energies. In contrast, irradiation with 100 MeV O^{7+} swift heavy ions produce glow peaks at 434, 554, and 646 K. The shift of peak positions to higher temperatures suggests the creation of deeper trapping centers due to the high electronic energy loss associated with swift heavy ions.Similarly, irradiation with a 75 MeV C^{6+} ion beam results in two major peaks at 439 and 483 K, indicating relatively fewer but stable trapping centers. Thermal neutron exposure using a ^{252}Cf source produces a dominant peak around 513 K for samples synthesized through the acid recrystallization method. Neutron interactions can generate defect centers through nuclear reactions, which modify the glow curve structure.Electron irradiation with 6 MeV energy produces multiple peaks at 437, 545, 638, and 748 K, suggesting complex trapping and recombination mechanisms. In the case of high-energy X-ray exposure (above 500 keV), two peaks at 463 and 503 K are observed, reflecting the formation of moderate depth traps.

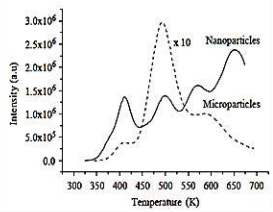

Fig. 1: TL Glow curves of $CaSO_4$:Dy micro and nano exposed to 10 Gy (reproduced with permission from ref. 10, copyright 2006, Elsevier)

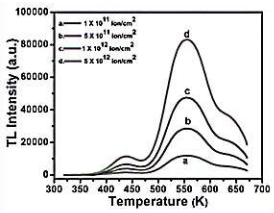

Fig.2: Glow curve of $CaSO_4$:Dy irradiated with 100 MeV O^{7+} SHI at different fluences.(reproduced with permission from ref. 11, copyright 2006, AIP)

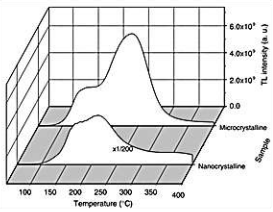

Fig. 3: Typical TL glow curves of $CaSO_4$:Dy nano- and microcrystalline samples exposed to 1 × 1011 ions cm^2 (reproduced with permission from ref. 12, copyright 2008, IOP)

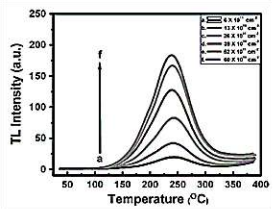

Fig. 4: Glow curve of $CaSO_4$:Dy microphosphor irradiated with thermal neutrons (reproduced with permission from ref. 12, copyright 2016, Elsevier)

Table 1: Comparative TL glow peak positions of $CaSO_4$: Dy for various irradiation sources.

Sr. No.	TL Glow Curve (°C)	Irradiated Source	Synthesis Route	Ref.
1.	411, 498, 569 and 652 K.	^{60}Co γ -Rays	chemical co-precipitation method	10
2.	434, 554, and 646 K	100 MeV O^{7+} SHI		11
3.	439 & 483 K	75 MeV C^{6+} ion beam		12
4.	513 K	^{252}Cf 4 Thermal Neutron	Acid re-crystallization	8
5.	437,545,638, and	6 MeV Energy	chemical co-	13

	748 K	Electron	precipitation	
6.	463 & 503K	500 keV X-Ray	-	14

Conclusion

The variation in the TL glow curve of Calcium Sulfate doped with Dysprosium ($CaSO_4$: Dy) under different radiation sources arises mainly from differences in energy deposition mechanisms and linear energy transfer (LET). Low-LET radiations such as X-rays, and gamma rays deposit energy sparsely within the lattice, producing relatively isolated electron and hole trapping centers. This generally results in well-defined dosimetric glow peaks with moderate trap populations. In contrast, high-LET radiations such as thermal neutrons (through nuclear reactions) and swift heavy ions create dense ionization tracks and complex defect clusters. These dense energy tracks increase defect population and may introduce deeper or additional trapping levels, which can modify the intensity and structure of the TL glow curve. Therefore, the observed variations in glow peak position and intensity reflect the nature of radiation–matter interaction and the resulting defect distribution within the $CaSO_4$: Dy crystal lattice, which is crucial for understanding its radiation response and dosimetric behavior.

References

1. S. W. S.McKeever, Thermoluminescence of Solids, Cambridge University Press, 1985.
2. C. Furetta, Handbook of Thermoluminescence, World Scientific Publishing, 2003.
3. Y. S. Horowitz, Thermoluminescence and Thermoluminescent Dosimetry, CRC Press, 1984.
4. L. Bøtter-Jensen et al., Opti. Stim. Lumin. Dos., Elsevier, 2003.
5. Resmi G. Nair et al., Ceramics International, 44, 3 (2018) 3492-3496.
6. R. Lakshmanan et al., Radiation Protection Dosimetry, 1321, (2008) 42–50.
7. Muhammad Ilham Bayquni et al., AIP Conf. Proc. 2967 (2024) 020006.
8. M. S. Bhadane et al., Journal of Luminescence, 170 (2016) 226-230.
9. Muhammad Ilham Bayqun, et.al, AIP Conf. Proc. 3065 (2024) 020037.
10. Numan Salah et al., Radiation Measurements 41 (2006) 40 – 47.
11. M. S. Bhadane et al., AIP Conference Proceedings 2115, 030143 (2019)
12. N. Salah, Journal of Physics D: Applied Physics 41 (2008) 155302(6pp)
13. N. T. Mandlink, Radiation Protection and Environment 34(3):p 185-189, Jul–Sep 2011.
14. A. Aypar, The International Journal of Applied Radiation and Isotopes, 29, 6, (1978) 369-372.

SHI Effects in Thermoluminescent Dosimetric Materials

Modhale Reshma B., Mahesh S. Bhadane

Department of Physics, Rayat Shikshan Sanstha's Dada Patil Mahavidyalaya Karjat, Dist-Ahilyanagar-414402

Email: modhalereshma9@gmail.com

Article DOI Link: https://zenodo.org/uploads/19785622

DOI: 10.5281/zenodo.19785622

Abstract

Swift heavy ions (SHIs) are highly energetic charged particles with energies typically exceeding 1 MeV/u that deposit extremely high energy densities in solid materials. When SHIs interact with thermoluminescent (TL) materials, they induce structural modifications, defect generation, and the formation of trapping centers that significantly influence the thermoluminescence behavior of dosimetric phosphors. The interaction of SHIs with matter mainly occurs through two energy loss mechanisms: electronic energy loss and nuclear energy loss. At high ion energies, electronic stopping dominates, producing intense ionization and excitation along the ion trajectory and leading to the formation of latent ion tracks and defect centers. These defects act as trapping and recombination sites responsible for TL emission during thermal stimulation. Investigating SHI-induced TL behavior is important for understanding radiation damage processes and developing dosimetric materials for high-energy particle environments such as accelerator facilities, nuclear reactors, and space missions. Various phosphors including borates, aluminates, silicates, and oxides have been explored to evaluate their TL response, trap characteristics, and radiation stability under SHI irradiation.

Keywords: SHI (Swift Heavy Ion), Thermoluminescence, Dosimeter, Phosphor, Radiation

Introduction

Thermoluminescence (TL) is a widely used phenomenon in radiation dosimetry where trapped charge carriers produced by ionizing radiation are released upon heating and recombine at luminescence centers, emitting light proportional to the absorbed radiation dose. TL materials are extensively used in medical radiation monitoring, environmental dosimetry, nuclear facilities, and space research [1]. Traditionally, TL phosphors have been studied under γ-rays, X-rays, and β-particles. However, the increasing use of particle accelerators and heavy ion

beams in research, medical therapy, and space science has necessitated the study of TL response under swift heavy ion (SHI) irradiation. Swift heavy ions possess very high kinetic energy and can deposit enormous energy densities along their paths in materials, creating unique radiation damage features known as ion tracks.

The energy deposition of SHIs produces localized excitation, ionization, and lattice disorder, leading to the formation of defect centers and trapping states. These defects significantly influence the TL glow curve shape, intensity, and trapping parameters. The study of TL properties under SHI irradiation provides valuable information about radiation damage mechanisms, defect dynamics, and the suitability of phosphors for high-energy particle dosimetry. Several inorganic phosphors including oxides, aluminates, borates, and silicates have been investigated for their TL response under SHI irradiation. These studies reveal that heavy ion irradiation can enhance or modify trap density, create new glow peaks, and influence luminescence efficiency depending on the material composition and irradiation conditions.

Ion Radiation Mechanism

When energetic ions pass through matter, they lose energy through interactions with electrons and atomic nuclei. The total stopping power is generally divided into two components:

$$\frac{dE}{dx} = \left(\frac{dE}{dx}\right)_e + \left(\frac{dE}{dx}\right)_n$$

Where,

$\left(\frac{dE}{dx}\right)_e$ = electronic energy loss and $\left(\frac{dE}{dx}\right)_n$ = nuclear energy loss

These processes determine the extent of structural damage and defect generation in the irradiated material [2].

- **Electronic Energy Loss**

Electronic energy loss occurs due to interactions between the incoming ion and the electrons of the target material. At the high energies typical of swift heavy ions (SHIs), electronic stopping dominates. The incident ion transfers energy to the electronic system through ionization, electronic excitation, and electron cascade processes [2]. The high energy deposition along the ion trajectory leads to the formation of latent tracks consisting of amorphous or highly defective regions within the crystal lattice. These tracks can extend several micrometres in length with nanometre-scale diameters. The resulting electronic excitations generate defect centers that act as trapping levels responsible for

thermoluminescence (TL) emission.

- **Nuclear Energy Loss**

Nuclear energy loss occurs through elastic collisions between the incoming ion and target nuclei and becomes significant at lower ion energies. These collisions cause atomic displacements, vacancy formation, interstitial defects, and lattice disorder. Although nuclear stopping is smaller than electronic stopping for SHIs, it still contributes to point defect formation and modifies recombination centers and trap distributions in TL phosphors.

Interaction Mechanism of Swift Heavy Ions with TL Materials

When a swift heavy ion penetrates a solid, it generates a cylindrical damage zone along its trajectory due to intense electronic excitation. The interaction mechanism can be explained through two widely accepted models:

- Thermal Spike Model: The thermal spike model suggests that the energy deposited by the ion rapidly heats the lattice within a small cylindrical region to extremely high temperatures for a very short time (~10^{-12} s). This transient heating causes: local melting, amorphization, defect formation.
- Coulomb Explosion Model: In the Coulomb explosion model, strong ionization leads to the removal of electrons from atoms along the ion track. The positively charged ions repel each other, causing lattice disruption and atomic displacement. Both models explain the formation of defect structures that significantly influence the TL properties of irradiated phosphors [2].

Table 1: TL Phosphors Studied Under Swift Heavy Ion Irradiation

No	TL Phosphor	Ion Beam Used	Key Observation	Ref. No.
1	$CaMoO_4$: Dy	Li^{3+}, C^{6+}, Ag^{7+}	TL intensity varies with ion species	3
2	$LiMgBO_3$: Dy	Ag^{9+}	Complex glow curve peaks observed	4
3	MgB_4O_7: Eu	Ag^{7+}, Ni^{7+}	Good linear TL response for SHI dosimetry	5
4	$CdSiO_3$: Ce	Si^{7+}	TL peaks influenced by ion fluence	6
5	Y_2O_3: Eu	Ni^{7+}, Ag^{9+}, Au^{8+}	Loss of crystallinity after irradiation	7
6	Al_2O_3	Au^{9+}	Broad TL glow peaks observed	8
7	$SrAl_2O_4$:Eu,Dy	Ag^{9+}	Increased trap density after SHI	9
8	$SrAl_2O_4$: Eu	120 MeV Ag^{9+}	Enhanced afterglow intensity	10

9	$CaSrAl_2Si_2O_8$: Eu	Fe, Si, C, N, Ne, & He	Future development of LLP	11
10	LiF:Mg,Ti & LiF:Mg,Cu,P	krypton and xenon	High-dose TL characteristics	12
11	$LiNaSO_4$: Eu	^7Li	Strong TL peaks	13
12	$CaSO_4$: Dy	O^{7+}	High sensitivity TL response	14
13	$SrSO_4$: Eu	SHI	Increased trapping centers	15
14	CaF_2: Yb	Ni^{7+}	Enhanced glow peak intensity	16

Discussion

Swift heavy ion irradiation produces significant modifications in TL phosphors due to the extremely high energy deposition along the ion track. Several important effects are commonly observed: defect formation, modification of TL glow curves, trap density enhancement, structural disorder, and strong dose and fluence dependence. The TL response of phosphors under SHI irradiation strongly depends on ion fluence. Typically, TL intensity increases with fluence up to a threshold, while beyond this level defect recombination, track overlapping, and partial lattice amorphization may reduce the TL output. In some materials, SHI irradiation can also create new trapping centers that appear as additional glow peaks in the TL glow curve, indicating changes in defect structure and recombination dynamics within the host lattice.

Future Scope

The study of swift heavy ion (SHI) effects in thermoluminescent dosimetric materials offers significant opportunities for advancing radiation detection technologies. Future research can focus on the development of novel TL phosphors with enhanced radiation hardness and higher sensitivity for high-energy ion environments. Investigations on nanostructured and composite phosphor materials may provide improved trap stability and luminescence efficiency under SHI irradiation. Advanced characterization techniques such as high-resolution microscopy and spectroscopic analysis can help understand ion track formation and defect evolution in greater detail. Additionally, integrating simulation tools such as SRIM and Monte Carlo modeling will enable better prediction of energy loss processes and defect generation mechanisms. Studies on the fluence dependence and long-term stability of TL signals are also important for reliable dosimetry applications. Furthermore, exploring SHI-induced modifications in different host lattices and dopant combinations may lead to the discovery of next-generation TL materials suitable for accelerator facilities, heavy ion therapy, and space radiation monitoring.

References

1. B. C. Bhatt, Radiation Protection and Environment 34(1) (2011)6-16.
2. Ragnar Hellborg, Harry J. Whitlow, and Yanwen Zhang, Ion Beams in Nanosci. and Techno., Springer Heidelberg Dordrecht London New York.
3. S. Dutta et. al., Journal of Luminescence 170 (2016) 42-49.
4. A.K. Bedyal et. al., Ceramics International 42 (2016) 18529-18535.
5. K. H. Gavhane et. al., Optical Materials 150 (2024) 115205.
6. C. Manjunatha et. al., Journal of Luminescence 134 (2013) 358-368.
7. S Som et. al., Luminescence. 2014 Aug;29(5):480-91.
8. K.R. Nagabhushana et al., Journal of Luminescence 131 (2011) 764-767.
9. A.K. Bedyal et. al., Radiation Physics and Chemistry 122(2016) 48-54.
10. Zhan, T et. al., RSC Advances, 2(1) (2012)328-332.
11. T. Z. Zhan et. al., AIP Advances 2 (2012) 032116.
12. W. Gieszczyk et al., Radiation Measurements 51–52(2013) 7-12.
13. Numan Salah et. al., Journal of Luminescence 121,2 (2006) 497-506.
14. Mahesh S. Bhadane et. al., AIP Conf. Proc. 2115(2019) 030143.
15. Tianzhuo Zhan et al., Meet. Abstr. MA2011-02 (2011) 2635.
16. C. Pandurangappa et al., NIMB, 269(2011) 185-188.

Role of Luminescence Dosimetry in Proton Therapy

[1]Kishor Gavhane, [2]Vipul S. Ghemud

[1]Department of Physics, Savitribai Phule Pune University, Pune 411007, India

[2]Department of Physics, BJS's Arts, Science & Commerce College, Pune 412207, India

Email: kishor.gavhane5@gmail.com

Article DOI Link: https://zenodo.org/uploads/19785741

DOI: 10.5281/zenodo.19785741

Abstract

Nowadays the proton ion therapy has recognized as one of the best progressive modalities in the field of radiation oncology, due to delivering the superior and accurate dose conformity as compare to the conventional photon-based radiotherapy. The main advantage of the proton therapy consists of, deposition of accurate and precise dose deposition within the Bragg peak region. LiF based thermoluminescent materials, Al2O3:C based optically stimulated luminescence, Ag doped glasses act as radio-photoluminescent materials offers versatile solutions for proton therapy. In luminescence dosimetry, specially Thermoluminescence Dosimeters (TLD's) and Optically Stimulated Luminescence Dosimeters (OSLD's) are plays vital role in the proton therapy for the accurate dosimetric verifications such as dose gradients and sensitivity to range uncertainties. This chapter includes the main interactions of proton ions with the luminescent phosphor materials, directing on the Linear Energy Transform (LET) dependent responses variations and improvement tactics. In addition to that, developments in phosphors and LET dependent materials which are highlighting how revolutions in material science improve the usefulness of luminescence dosimetry in current proton therapy.

Keywords: Thermoluminescence, optically stimulated luminescence, Dosimetry, Proton Therapy.

Introduction

In the field of radiation oncology proton beam therapy signifies an important development. In which, major practices with high-energy protons to deliver extremely conformal radiation doses to cancer tumours. The exceptional physical properties of protons contain Braggs peak, permit them to deposit the most of their beam energy accurately at particular part and depth inside the body. Therefore, clinicians allow to deliver high energy of radiation doses to tumours

and reduced to exposed nearby healthy tissues. Thus, treating the critical organs in the human body where long-term side effects must be carefully managed. TL and OSL both the techniques mostly based on the luminescent materials that stores energy when exposed to radiation and later release it as light or photons after stimulation. The properties of dosimeters such as tissue-equivalent features, small physical size, low thermal fading, and high sensitivity make them perfect for in- phantom measurements

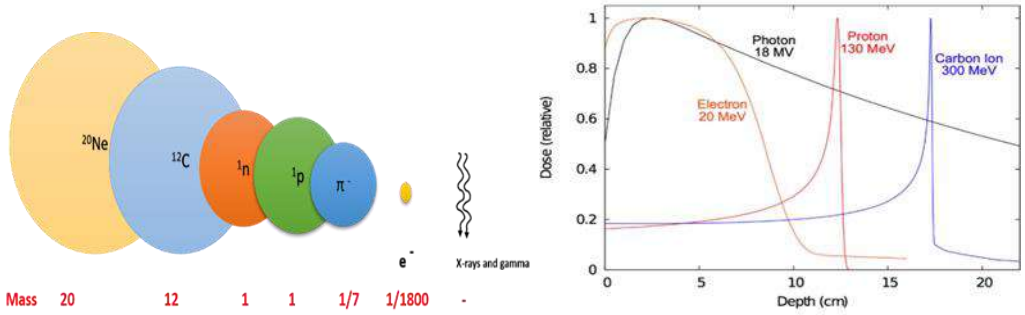

Figure 1: Comparison of various clinical radiation beams with (a) their mass of ions and (b) dose distributions as a function of depth in water [1]

Proton Beam Characteristics and Dosimetric Challenges

In proton therapy, due to its exceptional depth-dose distribution properties dominated by the Bragg peak, where maximum of the energy of proton beams exactly deposited around the end of its range as shown in fig 1. In addition to that, the mass of the proton ion is much larger as compare to photon and electron. Due to the unique physical characteristics of proton ion beams, mainly the Bragg peak phenomenon, maximum energy is deposited within the tumour volume although minimizing radiation exposure to nearby healthy tissues throughout cancer treatment. In treatment of tumour having finite thickness several energies are jointly form a Spread-Out Bragg Peak (SOBP) for uniform target coverage. The resultant sharp distal dose fall-off allows extraordinary sparing of organs-at-risk. Though, Linear Energy Transfer (LET) variation rises expressively close to SOBP edge, varying relative biological effectiveness (RBE) and possibly causing unpredicted normal tissue toxicity. The detectors such as ionization chambers and diodes, face challenges in averaging volume and LET dependence requiring progressive improvement approaches for precise proton dosimetry [2].

Fundamentals of TL and OSL Dosimetry

The interaction of ionizing radiations with phosphor materials, form an electron-hole pairs which are trapped in the defects. The detects are formed known as luminescent centres or the trapping centres which are plays very crucial role in storing the dose in the phosphor material. The subsequent readout process

contains the stimulation in form of thermal and optical energy in TL and OSL respectively. Some of the common phosphor materials such as LiF:Mg,Ti [3], LiF: Mg,Cu,P, [4]and oxide based Al2O3:C [5] materials are used in personal and medical dosimetric applications due to its high sensitivity, low tissue equivalent number, low fading and decent dynamic ranges [6].

Role of TL and OSL in Proton Therapy Applications

In proton therapy, TL and OSL techniques are showing their main importance due to their adaptability in complex dose distributions, and exceptional dosimetric properties. Thus, at the time of beam commissioning, TL and OSL dosimeters playing role verification of depth-dose curves, Bragg peaks and SOBP. In addition to that, compact size of the dosimeters at several depths in the phantoms to improve the accuracy and precision in the treatment planning. In patient-specific quality assurance (QA), these passive dosimeters are playing important role to measure point verification water phantoms. Also, in pencil beam scanning (PBS) systems TL and OSL dosimeters can evaluate exact locating accuracy and collective dose distribution after placed in arrays or fixed in thin films. We can also place these dosimeters on the body of patients to monitor actual dose distributions which comes under part of in vivo dosimetry. Therefore, TL and OSL dosimeters used in proton therapy for their instant readout ability and reusability, determining steep dose gradients close to distal edge of the proton beam where accurate dosimetric authentication is critical [6–8].

LET Dependence and Quenching Effects

In the TLD's and OSLD's, the response of dosimeters is reliant on the LET of the incident radiations, and in case of charged particles the phenomenon shows high complexity mailnly in space dosimetry and particle therapy. At the end of the energy range, LET in the charged particles boosted dramatically and producing an appearances Bragg peak. Therefore, in the particle tracks sharp growth in the ionization density observed and this might be happened due to quenching effects. Due to improvement in quenching luminescent phosphor materials lose its efficiency per unit absorbed dose. Hence, LET based calibrations and correction factors are very important for consistent dosimetric quantification [9].

Current Limitations and Future Developments

When we think about the proton therapy, there are certain restriction in case of TL and OSL dosimetry. Fading in the material and saturation observe at high doses can disturb the measurement accurateness, which required accurate calibration work. In addition to that, batch variability in detector sensitivity also required separate calibration for specific work. The expansion of LET-independent or LET compensated phosphors is consequently a critical research

priority. Thus, the computational based tactics and the artificial intelligence models might be offer to resolve the difficulties in the relating luminescent response with LET spectra and beam parameters, refining real-time dosimetric accuracy [10].

Conclusion

Thermoluminescent (TL) and optically stimulated luminescent (OSL) dosimeters function as balancing radiation detectors in proton therapy due to their high detection sensitivity and satisfactory spatial resolution. They are extensively functional in beam commissioning, repetitive quality assurance, and in vivo dose assessment. However, variations in detector response under high linear energy transfer (LET) conditions demand LET-specific calibration and correction, particularly near the distal edge of the Bragg peak. Continuing improvement in phosphor synthesis, response modelling, and data-driven improvement systems is probable to expand dosimetric accuracy. The combination of advanced materials with smart analytical methods places luminescence dosimetry as a capable technique for next-generation precision proton therapy.

References

1. A. Kaiser, J.G. Eley, et al., Journal of Visualized Experiments, (2019).
2. Muñoz, I. D. et al. Physics in medicine and biology, 69 (2024) 135004.
3. Y.S. Horowitz, S. Mahajna, Radiation Protection Dosimetry, 3 (1999) 169–194.
4. N. Salah, P.D. Sahare, A.A. Rupasov, Journal of Luminescence, 124 (2007) 357–364.
5. M.S. Akselrod, et al., Radiation Protection Dosimetry, 32 (1990) 15-20.
6. S. McKeever, E. G. Yukihara, Fundamentals and Applications, John Wiley & Sons, (2011).
7. W.L. Mclaughlin, M.F. Desrosiers, Radiation Physics and Chemistry (1995), 46 1163–1174.
8. K.C. Jones, C.M. Seghal, S. Avery, Physics in Medicine & Biology, 61 (2016) 2213–2242.
9. L. V. Spencer, F.H. Attix, A Theory of Cavity Ionization, Radiation Research, 3 (1955) 239.
10. F. H. Attix, Introduction to radiological physics and radiation dosimetry, WILEY WSH, (2008).

Thermoluminescence Dosimetry: Fundamentals and Emerging Research Areas for Beginners

[1]M. A. Padvi, [2]Mahesh S. Bhadane

[1]Department of Physics, S.S.G.M Science, Gautam Arts and Sanjivani Commerce College, Kopargaon, Ahilyanagar-423601.

[2]Department of Physics, Rayat Shikshan Sanstha's Dada Patil Mahavidyalaya Karjat, Dist-Ahilyanagar-414402

Email: mbhadane24@gmail.com

Article DOI Link: https://zenodo.org/uploads/19785841

DOI: 10.5281/zenodo.19785841

Abstract

Thermoluminescence dosimetry (TLD) measures ionizing radiation using materials that store energy in traps and emit light upon heating. This chapter outlines fundamental principles, energy band theory, glow curve analysis, material synthesis, optimization parameters, and characterization techniques. It also discusses irradiation sources, material requirements, applications, limitations, and emerging research trends, providing a systematic foundation for students to conduct experimental research in TL materials.

Introduction

Thermoluminescence dosimetry (TLD) is a well-established technique used for measuring ionizing radiation by utilizing the thermoluminescent properties of certain crystalline materials. When a thermoluminescent material is exposed to ionizing radiation, a fraction of the absorbed energy becomes stored in the form of trapped charge carriers within the crystal lattice defects. Upon heating, these trapped electrons and holes recombine and release the stored energy in the form of visible or ultraviolet light, known as thermoluminescence (TL) [1,2]. Thermoluminescent dosimeters are widely used in medical radiation monitoring, environmental radiation assessment, nuclear industry, space research, and radiation processing facilities. Materials such as LiF, $CaSO_4$: Dy, CaF2: Dy, Al_2O_3:C, and MgB_4O_7 have been extensively studied as TLD phosphors due to their high sensitivity and reproducibility. For undergraduate and postgraduate students in physics and materials science, the study of TL provides an excellent opportunity to understand radiation–matter interaction, defect behaviour, luminescence mechanisms, and solid-state materials characterization. A systematic understanding of these aspects allows students to design and perform

experimental projects related to TL materials [2,3].

Fundamental Concepts of TL [4]

Before beginning experimental work, students must understand the basic physics behind TL. TL can be understood in two simple stages:

Stage 1: Energy Storage Mechanism (Fig. 1 a–c)

As shown in Fig. 1 (a), before irradiation, electrons remain in the valence band of the phosphor material. Due to defects or doping, some intermediate energy levels (traps) are formed between the valence band and conduction band. When ionizing radiation interacts with the material (Fig. 1 (b)), electrons are excited from the valence band to the conduction band. After irradiation (Fig. 1. (c)), some electrons become trapped in these metastable states, storing the absorbed radiation energy.

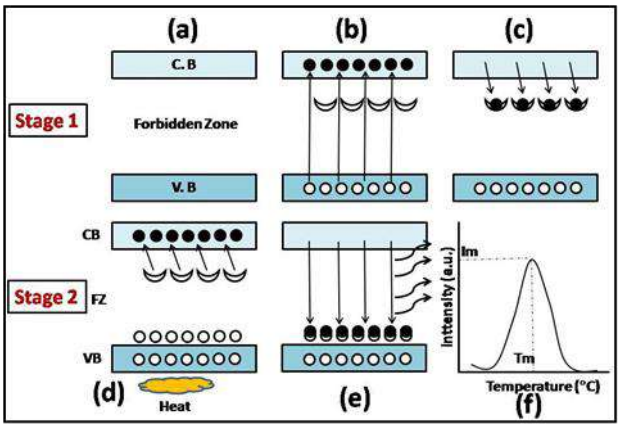

Fig. 1: Image shows energy storage process (a), (b), and (c) and energy release process (d) and (e). 'f' shows typical TL glow peak.[4]

Stage 2: Energy Release (Fig. 1 d–f)

When the material is heated (Fig. 1 (d)), trapped electrons gain thermal energy and move to the conduction band. These electrons then recombine with holes at luminescence centers (Fig. 1 (e)), releasing energy as light. The emitted light intensity, measured as a function of temperature, produces a typical TL glow curve (Fig. 1 (f)).

1. TL Glow Curve

A glow curve is a plot of emitted light intensity versus temperature. Each peak in the glow curve corresponds to a specific trap depth and activation energy. By analyzing glow curves, researchers can determine important parameters such as: Trap depth (E), Frequency factor (s), Order of kinetics, and Stability of trapping centers. The TL response is measured using a TL reader. During measurement, the sample is heated at a constant heating rate, typically between 1–10 °C/s. Methods such as peak shape, initial rise, and curve fitting deconvolution are

commonly used for trap parameter calculations. These parameters determine the suitability of a material for dosimetric applications.

2. Requirements of an Ideal Thermoluminescent Dosimetric Material

The TL phosphor and the chosen glow peak should meet the following criteria: [5,6]

a) The TL material should ideally exhibit a single, well-defined glow peak.
b) It must possess high TL sensitivity.
c) The emission spectrum should lie in the visible region (i.e. 400–500 nm.).
d) Thermal fading should be minimal.
e) The glow peak maximum should preferably occur around 200 °C.
f) The selected dosimetric glow peak should not show thermal quenching.
g) It should be tissue-equivalent.
h) Cost-effective, easy to synthesize, and require a simple annealing procedure.
i) A linear relationship between absorbed dose and emitted light intensity should be maintained over a broad dose range.
j) The material should be insensitive to ambient light exposure.

3. Experimental Methodology for TL Material Preparation

Students interested in developing new TL phosphors must follow systematic experimental protocols.

- **Selection of Host Material**

The host lattice plays a critical role in determining luminescence properties. Common host materials include oxides, sulfates, borates, and aluminates. The host should have good thermal stability and ability to accommodate dopant ions.

- **Choice of Dopant/Impurity**

Rare-earth ions such as Dy^{3+}, Eu^{3+}, Tb^{3+}, or Ce^{3+} or others are often used as activators because they introduce luminescent centers and modify trapping structures.

- **Doping Concentration Optimization**

Dopant concentration significantly affects TL intensity. Therefore, different molar concentrations (for example 0.1–5 mol%) should be systematically prepared and evaluated to determine the optimum concentration.

- **Synthesis Techniques**

Several synthesis techniques are commonly used in TL phosphor preparation. The most popular orders are the Chemical Co-Precipitation method, Solid State diffusion method, Combustion method, Hydrothermal method, and Sol-gel also use sometime.

4. Optimization Parameters in TL Materials

After synthesis, key parameters such as dopant concentration, calcination temperature, and temperature–time conditions must be optimized to achieve maximum TL performance. TL intensity increases up to an optimum dopant level (beyond which concentration quenching occurs), while proper control of calcination and sintering conditions governs crystallinity, defect formation, and luminescent efficiency.

5. Characterization of Prepared Materials

After synthesis, systematic characterization is essential to confirm successful material preparation. Structural characterization using XRD confirms the phase purity and crystal structure of the synthesized material, while SEM and EDS provide information about morphology, particle size, and elemental composition including dopant presence. Photoluminescence (PL) spectroscopy identifies luminescent centers and emission transitions, ensuring the material possesses the desired structural and optical properties.

6. Irradiation Sources Used in TL Studies

Thermoluminescent materials are exposed to different radiation sources to study their dosimetric response. Common irradiation sources include: Gamma radiation (Co-60, Cs-137), Beta radiation (Sr-90), X-rays, Heavy ions, Neutron, and electron radiation. Generally, Gamma irradiation using Co-60 sources is most commonly used in laboratory studies due to its stable and well-defined radiation output.

Importance and Applications of Thermoluminescence Dosimetry

Thermoluminescence dosimetry plays a critical role in radiation monitoring and safety.

Major applications include:

a) *Personal radiation monitoring for workers in nuclear facilities and hospitals.*
b) *Medical radiation therapy dosimetry for accurate dose measurement in cancer treatment.*
c) *Environmental radiation monitoring to assess natural background radiation.*
d) *Archaeological dating through thermoluminescence dating techniques.*
e) *Space radiation studies for monitoring cosmic radiation exposure.*
f) *Due to its high sensitivity and reliability, TLD remains one of the most widely used passive radiation dosimetry techniques.*

Limitations of Thermoluminescence Dosimetry

Despite its advantages, TL dosimetry also has some limitations.

a) *Signal fading over time*
b) *Destructive readout (information is lost after heating)*

c) Complex glow curve structures in some materials
d) Dependence on heating rate and readout conditions

These limitations motivate ongoing research to develop new materials with improved stability and sensitivity.

Emerging Research Areas in Thermoluminescence

Recent advances in thermoluminescence research aim at developing high-performance TL phosphors and exploring novel material systems. Emerging areas include nanostructured materials, rare-earth doped oxides, heavy-ion induced defect studies, computational modeling of trapping centers, and highly sensitive environmental dosimeters. These developments focus on enhancing trapping efficiency and overall sensitivity for modern radiation monitoring applications.

Conclusion

Thermoluminescence dosimetry is an interdisciplinary field combining solid-state physics, materials science, and radiation physics. For undergraduate and postgraduate students, understanding the fundamental concepts of TL, synthesis methods, material characterization, and glow curve analysis provides a strong foundation for experimental research. A systematic approach involving material synthesis, optimization of dopant concentration, structural characterization, irradiation studies, and glow curve analysis enables students to design meaningful research projects in this field. With growing applications in radiation safety, medical physics, and space science, thermoluminescence continues to remain an important and evolving area of scientific research.

References

1. R. Chen, S. W. S. McKeever, Theory of Thermoluminescence and Related Phenomena. World Scientific, 1997.
2. S. W. S.McKeever, Thermoluminescence of Solids, Cambridge University Press, 1985.
3. Y. S. Horowitz, Thermoluminescence and Thermoluminescent Dosimetry. CRC Press, 1984.
4. M. S. Bhadane, Development of Sulphate, Fluoride and Oxide-based, Nanophosphor for Gamma, Electron and Ion Dosimetry for Personal and Medical Applications, PhD. Thesis, Savitribai Phule Pune University, Pune, India (2018).
5. A. J. J. Bos, High Sensitivity Thermoluminescent Dosimetry. Nuclear Instruments and Methods in Physics Research Section B, 184(2001) 3-28.
6. Dr. Munish Kumar, Principles of Thermoluminescence Dosimetry; https://share.google/gADfKYb3urXECyxqg.

Photoluminescence and Thermoluminescence: Fundamental Principles and Applications

[1,2] Sandhya B. Deshmukh, [1]Kishor H. Gavhane

[1]Microtron Accelerator Laboratory, Department of Physics, Savitribai Phule Pune University, Pune, 411007, India

[2]Department of Physics, Rayat Shikshan Sanstha's Dada Patil Mahavidyalaya, Karjat, Dist-Ahilyanagar, 414402, India

Email: sandhyadeshmukh0479@gmail.com

Article DOI Link: https://zenodo.org/uploads/19786854

DOI: 10.5281/zenodo.19786854

Abstract

Photoluminescence (PL) and thermoluminescence (TL) are broadly employed techniques for investigating the optical behaviour and radiation response of phosphor materials. PL arises when light is emitted following optical excitation, providing insights into structural features, defect levels, and energy transfer processes. TL, in contrast, is a radiation-induced phenomenon in which trapped charge carriers are released during controlled heating, producing light emission. This property makes TL particularly valuable in radiation dosimetry and dose measurement. This chapter presents an overview of the fundamental principles, physical mechanisms, and applications of PL and TL. The complementary relationship between PL and TL techniques is highlighted, demonstrating how they jointly advance the understanding of luminescent materials.

Keywords: Photoluminescence, Thermoluminescence, Dosimetry.

Introduction

Luminescence refers to the emission of light arising from electronic transitions, distinct from thermal sources such as incandescence. Photoluminescence (PL) occurs when materials absorb photons typically in the ultraviolet or blue region stimulating electrons from the valence band to the conduction band. These excited electrons subsequently relax radiatively, producing visible light. Thermoluminescence (TL), by contrast, involves the storage of energy from prior exposure to ionizing radiation (e.g., gamma rays or X-rays) in defect-related traps. Upon controlled heating, the trapped charges are released, recombine, and emit light. Both PL and TL processes are significantly influenced by dopants, which enhance their efficiency and sensitivity. For example, Ce^{3+} ions improve

PL emission efficiency, while Dy^{3+} ions increase TL sensitivity. These luminescence mechanisms underpin the development of advanced phosphor materials for diverse applications, including solid-state lighting (such as white LEDs), display technologies (OLEDs), optical sensors, and radiation dosimeters. Beyond their technological utility, PL and TL provide valuable insights into band structures, impurity states, defect distributions, and radiation dose measurements, making them indispensable tools in both fundamental research and applied sciences [1–8].

Photoluminescence

- **Fundamental Principles**

PL occurs when a material absorbs electromagnetic radiation, typically ultraviolet or visible light, exciting electrons from the valence band or defect levels to upper energy states in the conduction band or localized traps. Subsequent excitation, electrons undergo rapid thermalization through phonon emission, losing excess energy before radiative recombination produces lower-energy photons.

This process reveals band gap energies, impurity states, and lattice disorders in semiconductors, phosphors, and nanomaterials. Key materials include direct bandgap semiconductors (GaN, GaAs, CdSe quantum dots), phosphors (YAG: Ce^{3+}, ZnS:Cu), and organic dyes, all of which exhibit strong PL due to efficient electron–hole recombination.

The released photon energy is usually red-shifted comparative to the absorbed light due to the Stokes shift ($\Delta E \approx 0.1–0.5$ eV), arising from lattice relaxation and electron–phonon coupling. Larger shifts often indicate stronger structural disorder or defect involvement.

- **Jablonski Diagram**

The Jablonski diagram illustrates the excitation and relaxation pathways of electrons in molecular and organic systems as shown in fig 1. Molecules occupy the ground state (S_0), singlet excited states (S_1, S_2, S_3), and the triplet state (T_1), each with vibrational sublevels.

When absorbed photon energy exceeds the (highest occupied molecular orbital) HOMO–LUMO (lowest unoccupied molecular orbital) gap, electrons are promoted to higher singlet states or vibronic levels of S_1. These states relax rapidly: higher singlets (S_2, S_3) undergo internal conversion (IC) to S_1, while vibronic relaxation within S_1 occurs in picoseconds. From S_1, intersystem crossing (ISC) can generate triplet states (T_1). Radiative transitions occur when electrons return from S_1 or T_1 to S_0. Spin-allowed transitions ($S_1 \rightarrow S_0$) occur within nanoseconds, while spin-forbidden transitions ($T_1 \rightarrow S_0$) are slower, ranging from microseconds to milliseconds. Typically, the emission spectrum resembles a mirror image of the absorption spectrum [9-12].

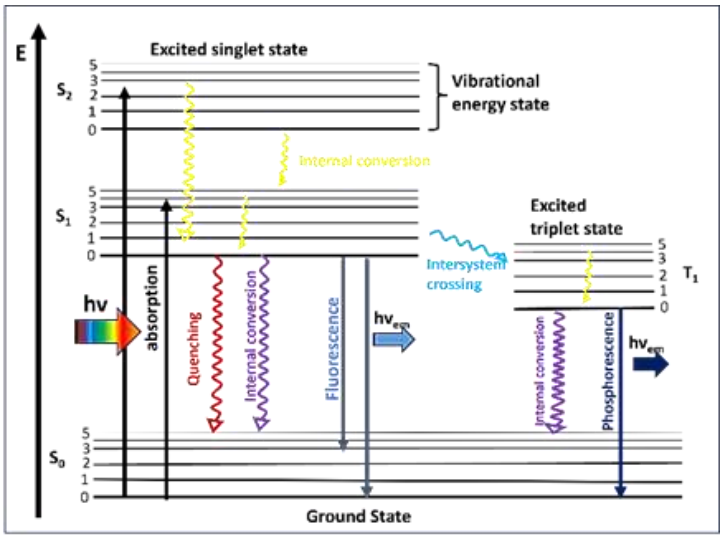

Fig. 1. *Jablonski diagram*

Applications

PL spectroscopy is widely applied across multiple fields:

- **Optoelectronics:** YAG: Ce^{3+} phosphors in white LEDs convert blue light into yellow, producing bright light with high color quality.
- **Displays:** Quantum dots such as CdSe generate sharp, tunable colors between 450–650 nm.
- **Sensors:** Ruthenium complexes detect oxygen, fluorescein measures pH, and pyrene derivatives aid in explosive detection.
- **Materials Science:** PL probes defects in semiconductors like GaN and assesses SiC crystal quality.
- **Biomedicine:** Quantum dots serve as biomarkers for imaging within living systems.

A major advantage of PL spectroscopy is its non-destructive nature and high sensitivity to trace impurities, making it essential for LED and phosphor research [13-17].

Thermoluminescence Mechanism:

Thermoluminescence (TL) is a widely used technique for measuring ionizing radiation. TL occurs when materials exposed to radiation store energy in the form of trapped electrons. Upon heating, these trapped electrons are released, recombine, and emit light [18]. The released intensity is proportionate to the absorbed radiation dose as shown in fig 2.

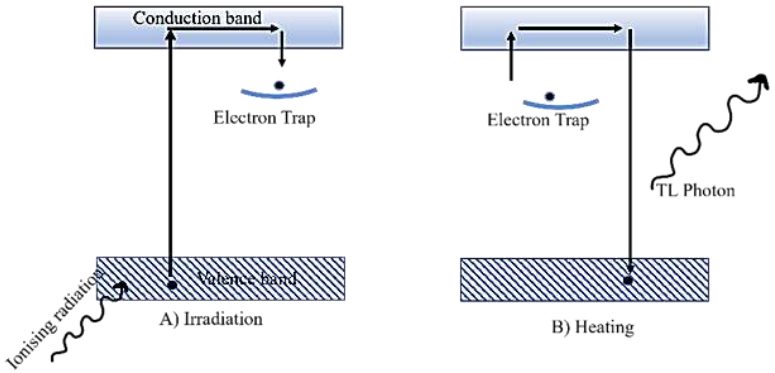

Fig. 2. A simplified energy level diagram to illustrate thermoluminescence process

Applications in Dosimetry

Thermoluminescence (TL) is extensively used in radiation dosimetry since of its versatility and reliability. It plays a main role in personal monitoring, serving track radiation exposure for workers in medical, nuclear, and industrial environments. In radiation protection, TL confirms compliance with safety standards by determining accumulated doses. It is also useful in environmental monitoring, where it detects radiation levels in soil, water, and air [19]. In the medical field, TL supports dosimetry for patients, confirming precise dose delivery throughout diagnostic imaging and radiotherapy [20].

Differences Between PL and TL

Table 1. Table of the difference between Photoluminescence and Thermoluminescence

Aspect	Photoluminescence	Thermoluminescence
Excitation	Optical photons	Ionizing radiation
Emission Trigger	Instant relaxation	Thermal ejection from traps
Timescale	ns-μs (FL), ms (PH)	s-min (25-400°C)
Key Output	Spectra, lifetimes	Glow curves, dose-response
Probes	Real-time defects/bandgaps	Cumulative dose, trap depths
Reversibility	Fully reversible	Fades unless re-irradiated
Dosimetry Mode	RL/OSL (real-time/optical)	TL (retrospective/thermal)

Applications of PL and TL

Table 2. Table of the Applications of Photoluminescence and Thermoluminescence

Technique	Key Applications	Dosimetry Examples
PL/OSL	LEDs, displays, sensors	Real-time RL (YAP:Ce), OSL badges (Al_2O_3:C, 1 μGy–10 Gy)
TL	Dosimetry	TLD-100 (LiF:Mg,Ti, personnel), quartz dating (>10^5 yr)

Upcoming Challenges in PL and TL Dosimetry

Despite their widespread use, PL and TL methods face notable challenges:

- **PL:** Thermal quenching above 100 °C reduces emission intensity, while efficiency droop at high currents limits device performance. The absence of stable narrow-band emitters restricts spectral precision.
- **TL:** Signal fading (5–20% per year), supralinearity at doses above 1 Gy, and instability under humidity compromise accuracy and reliability.

To address these issues, researchers are exploring tissue-equivalent hybrid materials and advanced multi-peak deconvolution methods. However, standardization of OSL and TL for extreme environments such as space remains incomplete. Promising solutions include perovskite materials and co-dopant strategies, which aim to improve stability, reduce quenching, and enhance spectral control [2,3,9].

References

1. Zurich Instruments, Photoluminescence Applications, Zurich Instruments Application Note, 2019.
2. U.S. NRC, Thermoluminescent Dosimeters Guide, U.S. Nuclear Regulatory Commission Technical Report, 2011.
3. H. A. Hoppe et al., Chemistry of Materials, 26 (2014) 3570-3578.
4. WikiDiff Contributors, Photoluminescence vs Thermoluminescence, WikiDiff Comparative Analysis, 2023.
5. Landauer Inc., "Thermoluminescent Dosimeters: Principles and Applications", Radiation Protection Dosimetry, 2024.
6. Intematix Corporation, SSL Phosphors: Materials for Solid State Lighting, Phosphor Technology Report, 2023.
7. J. Grimm et al., Journal of Vacuum Science & Technology A, 38 (2020) 063207.
8. Encyclopaedia Britannica Editors, Phosphor Chemistry and Luminescent Materials, Encyclopaedia Britannica, 2022.
9. Atkins, P., & de Paula, J. (2014). Atkins' Physical Chemistry (10th ed.). Oxford University Press.
10. Engel, T., & Reid, P. (2019). Physical Chemistry (4th ed.). Pearson.
11. Chemistry Libre Texts. (n.d.). Jablonski Diagram. Retrieved March 4, 2026, from https://chem.libretexts.org
12. Wikipedia contributors. Jablonski diagram. In Wikipedia. Retrieved March 4, 2026, from https://en.wikipedia.org/wiki/Jablonski_diagram
13. Blasse, G., & Grabmaier, B. C. (1994). Luminescent Materials. Springer.
14. Lakowicz, J. R. Principles of Fluorescence Spectroscopy (3rd ed.), (2006). Springer.
15. Chen, O., et al. Nature Materials, 12(5) (2013) 445–451.

16. Reshchikov, M. A., & Morkoç, H. Journal of Applied Physics, 97(6), (2005), 061301.
17. Medintz, I. L., et al."Quantum dot bioconjugates for imaging, labelling and sensing." Nature Materials, 4(6), (2005), 435–446.
18. M. Kumar, PRINCIPLES OF THERMOLUMINESCENCE DOSIMETRY, n.d.
19. McKeever, S. W. S., & Moscovitch, M. Thermoluminescence dosimetry materials: properties and uses. In Comprehensive Nuclear Materials (pp. 301-319), (2011).
20. Deme, S., Gal, J., & Schieber, C. Thermoluminescence dosimetry in medical physics. Journal of Radioanalytical and Nuclear Chemistry, 281(1), (2009). 175-178.

Crystal Defects and Their Influence on Thermoluminescent Properties

Ajay Dilip Vartha

Assistant Professor, Department of Physics, Loknete Ramsheth Thakur Arts, Science and Commerce College, Mokhada

Email: ajayvartha123@gmail.com

Article DOI Link: https://zenodo.org/uploads/19786935

DOI: 10.5281/zenodo.19786935

Abstract

Thermoluminescence (TL) is a defect-mediated luminescence phenomenon widely used in radiation dosimetry and solid-state research. In crystalline materials, intrinsic and extrinsic defects introduce localized energy levels within the forbidden band gap, forming trapping and recombination centers. Upon irradiation, electrons and holes are generated and subsequently captured at these defect sites. During controlled heating, trapped charge carriers are thermally released and recombine at luminescent centers, emitting light. The distribution, concentration, and depth of traps govern the structure of the TL glow curve, including peak position, intensity, and kinetic behavior. These defect characteristics directly determine key dosimetric properties such as sensitivity, linearity, stability, and fading. Controlled doping and defect engineering enable optimization of trap parameters to achieve reliable and reproducible dose measurements. Thus, understanding the relationship between crystal defects and thermoluminescent processes is essential for the development of efficient and stable TL materials for radiation detection applications.

Introduction

A crystal structure refers to the periodic arrangement of atoms, ions, or molecules in a solid material, forming a three-dimensional ordered pattern that extends throughout the crystal lattice [1]. The smallest repeating unit in a crystal is called the unit cell, and repetition of this unit cell generates the entire crystal structure [1,2]. The crystal structure can be described as a combination of a lattice and a basis, where the lattice represents a periodic array of points in space and the basis represents the group of atoms associated with each lattice point [1]. Crystalline solids are classified into seven crystal systems based on lattice parameters and angles, including cubic, tetragonal, orthorhombic, monoclinic, triclinic, hexagonal, and rhombohedral systems [2]. Crystal structure strongly influences

material properties such as density, electrical conductivity, mechanical strength, and optical behaviour [1]. Imperfections within the crystal lattice create localized energy levels inside the forbidden band gap that can trap charge carriers and influence luminescence processes [3,6]. Thermoluminescence is a luminescence phenomenon observed in insulating or semiconducting materials when they emit light upon heating after prior exposure to ionizing radiation [4]. This mechanism makes thermoluminescent materials useful for radiation dosimetry, archaeological dating, and environmental radiation monitoring [5,9].

Crystal Defects

Crystal defects are irregularities or imperfections in the periodic arrangement of atoms within a crystal lattice [1]. In real crystals, perfect ordering is rarely achieved because thermal fluctuations, impurity incorporation, and growth conditions introduce structural imperfections [2]. Defects can be classified into intrinsic defects, which occur naturally in the crystal lattice, and extrinsic defects, which are introduced through impurity doping [3]. Common point defects include vacancies, interstitial atoms, and substitutional impurities [1]. In ionic crystals, two important defect types are observed: Schottky defects, consisting of paired cation–anion vacancies, and Frenkel defects, where an ion moves from its lattice position to an interstitial site [2].

- **Formation of Defects**

Crystal defects can be generated through several mechanisms. Thermal excitation causes atoms to leave lattice sites and create vacancies [2]. Impurity doping during material synthesis introduces substitutional or interstitial defect centers that influence luminescent behaviour [3,6]. Ionizing radiation can displace atoms from lattice sites producing vacancy–interstitial pairs known as Frenkel pairs [4]. Crystal growth conditions such as rapid cooling or mechanical stress may also introduce defects into the crystal lattice [2]. Thermodynamically, the formation of defects lowers the Gibbs free energy of the crystal at finite temperature, making defect formation energetically favorable [2].

Effect of Defects on Thermoluminescence

Thermoluminescence is fundamentally controlled by defects because these defects create localized energy levels within the forbidden band gap that act as trapping and recombination centers [3,4].

When a TL material is exposed to ionizing radiation, electrons are excited from the valence band to the conduction band while holes remain in the valence band [4]. Some of these charge carriers become trapped at defect levels rather than recombining immediately [3]. During heating, trapped electrons gain sufficient thermal energy to escape from traps and return to the conduction band. These electrons migrate through the lattice and recombine with holes at luminescent

centers, releasing energy in the form of photons [4]. The resulting light emission forms the characteristic thermoluminescence glow curve [5].The theoretical description of thermoluminescence was first proposed through the Randall–Wilkins model of electron trapping and release [7], and later refined through detailed kinetic models describing glow curve behaviour [8].

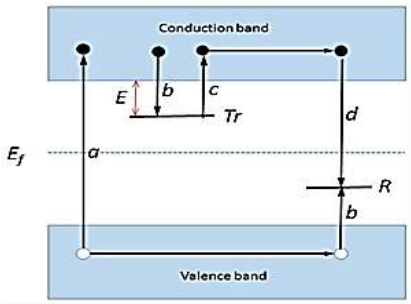

Figure 1. Energy band diagram illustrating trapping and recombination centers in thermoluminescent materials.

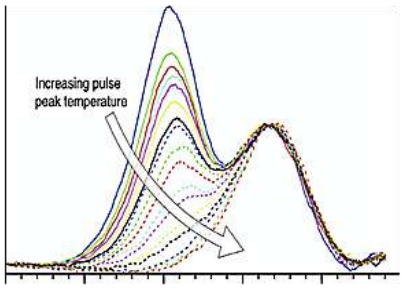

Figure 2. Typical thermoluminescence glow curve showing intensity as a function of temperature.

Trap Centers

Trap centers are defect-related energy levels within the forbidden band gap that capture and store radiation-induced charge carriers [3].The stability of trapped electrons depends on the trap depth (E), which represents the activation energy required for thermal release of trapped charge carriers [5].Shallow traps release carriers at lower temperatures, whereas deeper traps release carriers at higher temperatures and therefore contribute to more stable TL signals [5].The number and distribution of trap centers influence the intensity and temperature position of glow peaks observed in thermoluminescent materials [3,8].

Recombination Centers

Recombination centers are defect sites where electrons recombine with holes and produce light emission during thermoluminescence [3]. These centers are often associated with impurity ions or activator ions intentionally introduced into the host lattice to enhance luminescent efficiency [6]. Radiative recombination at these centers produces photons whose wavelength depends on the energy difference between excited and ground states of the luminescent center [6].

Glow Curve Structure

The thermoluminescence glow curve represents the variation of emitted light intensity as a function of temperature during controlled heating [4]. Each peak in the glow curve corresponds to a specific trap level in the band gap [5]. The temperature position of the glow peak depends mainly on trap depth and heating rate, while the shape of the peak depends on the kinetic order of the

recombination process [5,8]. Glow curve analysis methods are commonly used to determine kinetic parameters such as activation energy and frequency factor [5].

Dosimetric Properties

Thermoluminescent materials are widely used for radiation dose measurement due to their stable trapping and luminescence characteristics [4]. Important dosimetric parameters include dose-response linearity, sensitivity, fading behaviour, reproducibility, and energy dependence [4,9]. A linear dose–response relationship allows accurate determination of absorbed radiation dose [4]. Sensitivity depends on trap density and luminescence efficiency, while fading occurs due to gradual thermal release of trapped carriers at room temperature [5]. Advances in thermoluminescent dosimetry have improved the sensitivity and reliability of TL detectors used in radiation protection and medical physics [10].

Table 1. Examples of Thermoluminescent Materials Used in Radiation Dosimetry

TL Material	Activator	Application
LiF:Mg,Ti	Mg, Ti	Personal radiation dosimetry
$CaSO_4$: Dy	Dy	Environmental radiation monitoring
Al_2O_3:C	Carbon	High sensitivity TL dosimeters
CaF_2: Mn	Mn	Radiation detection

Conclusion

Thermoluminescence is fundamentally governed by crystal defects that introduce trapping and recombination centers within the band gap of a material [3]. Trap centers store radiation-induced charge carriers, while recombination centers facilitate light emission during heating [4]. The distribution and depth of traps determine the structure of the TL glow curve and influence key dosimetric properties such as sensitivity, linearity, and fading [5]. Controlled doping and defect engineering therefore play an important role in improving the performance of thermoluminescent materials used for radiation dosimetry [3,6,10].

References

1. C. Kittel, Introduction to Solid State Physics, 8th ed., Wiley, New York, 2004.
2. N. W. Ashcroft and N. D. Mermin, Solid State Physics, Holt, Rinehart and Winston, New York, 1976.
3. R. Chen and S. W. S. McKeever, Theory of Thermoluminescence and Related Phenomena, World Scientific, Singapore, 1997. DOI: https://doi.org/10.1142/3524
4. S. W. S. McKeever, Thermoluminescence of Solids, Cambridge University Press, Cambridge, 1985. DOI: https://doi.org/10.1017/CBO9780511564994
5. M. J. Aitken, Thermoluminescence Dating, Academic Press, London, 1985.

DOI: https://doi.org/10.1016/C2013-0-05954-2
6. G. Blasse and B. C. Grabmaier, Luminescence of Solids, Springer, Berlin, 1994. DOI: https://doi.org/10.1007/978-3-642-79017-1
7. J. T. Randall and M. H. F. Wilkins, "Phosphorescence and electron traps," Proceedings of the Royal Society A, 1945. DOI: https://doi.org/10.1098/rspa.1945.0024
8. A. J. J. Bos, "Theory of thermoluminescence," Radiation Measurements, 41, 2006. DOI: https://doi.org/10.1016/j.radmeas.2006.04.001
9. B. C. Bhatt, "Thermoluminescence dosimetry overview," Radiation Protection and Environment, 2011. DOI: https://doi.org/10.4103/0972-0464.85366
10. A. J. J. Bos, "High sensitivity thermoluminescence dosimetry," Nuclear Instruments and Methods in Physics Research B, 2001. DOI: https://doi.org/10.1016/S0168-583X(01)00717-6

Optically Stimulated Luminescence in Radiation Dosimetry: A Short Review

Sanika R. Ghadage, Mahesh S. Bhadane

Department of Physics, Rayat Shikshan Sanstha's Dada Patil Mahavidyalaya Karjat, Dist-Ahilyanagar-414402

Email: sanikaghadage3@gmail.com

Article DOI Link: https://zenodo.org/uploads/19787023

DOI: 10.5281/zenodo.19787023

Abstract

Optically Stimulated Luminescence (OSL) is a powerful technique for measuring ionizing radiation using luminescent materials. This chapter briefly reviews the working principle, commonly used phosphors such as Carbon-doped Aluminum Oxide, synthesis methods, and major applications in radiation dosimetry. The discussion highlights the importance of OSL materials for reliable radiation monitoring and safety.

Keywords: Al_2O_3:C, OSL, Radiation Dosimetry Phosphors, Luminescent Trap Centers, Defect Engineering in Oxides, Energy Storage Phosphor Materials

Introduction

Radiation dosimetry plays an important role in medical diagnostics, radiotherapy, nuclear industries, environmental monitoring, and space research. Accurate measurement of radiation exposure is essential for ensuring the safety of workers, patients, and the environment. Among various dosimetric techniques, Optically Stimulated Luminescence (OSL) has emerged as a reliable and highly sensitive method for radiation measurement.

OSL is a luminescence phenomenon in which a material emits light when it is exposed to optical stimulation after previously absorbing energy from ionizing radiation. The emitted light intensity is proportional to the absorbed radiation dose, which allows the determination of radiation exposure. OSL dosimeters offer several advantages such as high sensitivity, reusability, wide dose range, and the possibility of repeated readouts without destroying the stored signal [1].

In recent decades, OSL has gained considerable attention in fields such as personnel dosimetry, retrospective dosimetry, environmental monitoring, and geological dating. Materials like aluminium oxide (Al_2O_3:C) and beryllium oxide (BeO) have become widely used OSL phosphors due to their excellent luminescence characteristics and stability [2]. This chapter provides a concise

overview of the principles, materials, instrumentation, advantages, and applications of OSL in radiation dosimetry.

Basic Principle of OSL

The OSL phenomenon is based on the interaction between ionizing radiation and crystalline materials containing defects or impurities. These defects act as trapping centers for charge carriers. When ionizing radiation interacts with a luminescent material, electrons in the valence band gain energy and move to the conduction band. Some of these electrons become trapped in metastable energy levels within the band gap of the material. At the same time, holes may be trapped in other defect sites. These trapped charge carriers represent stored radiation energy in the material (Fig.1, Left side).

During optical stimulation, usually with visible or infrared light, the trapped electrons gain sufficient energy to escape from the traps and return to the conduction band. These electrons then recombine with holes at luminescence centers. This recombination process results in the emission of light photons (Fig.1, Right side). The intensity of this emitted light is proportional to the number of trapped electrons and therefore related to the absorbed radiation dose [3].

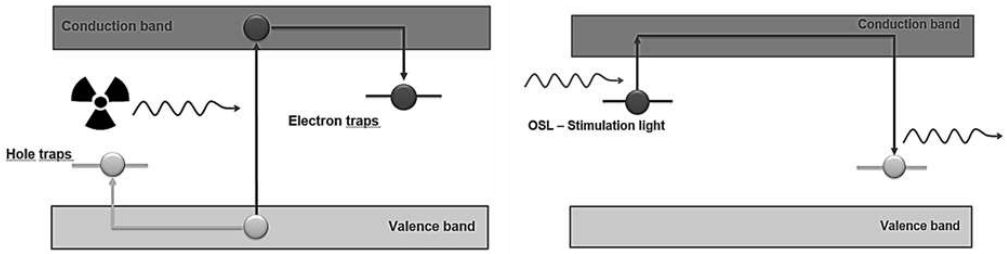

Fig. 1: Schematic diagram of the OSL mechanism.

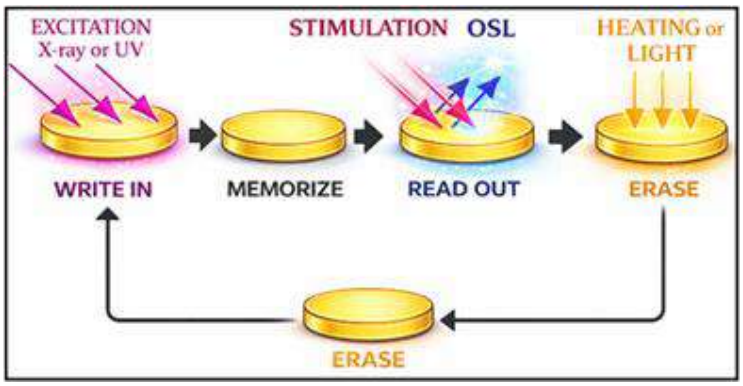

Fig. 2: Schematic representation of the OSL process showing the stages of energy storage and release.

As shown in Fig. 2, the diagram shows the working cycle of an OSL material. First, the material is exposed to X-ray or UV radiation, which excites electrons

and stores energy in the material (Write-in). The trapped charges remain stored in defect levels (Memorize). When the material is stimulated by light, the trapped electrons are released and emit luminescence, which is measured as the OSL signal (Read-out). Finally, heating or strong light removes the remaining trapped charges and resets the material so it can be used again (Erase).

The general process of OSL can be summarized in three steps:

- **Radiation Exposure:** Creation of electron–hole pairs and trapping of charges.
- **Energy Storage:** Electrons remain trapped in metastable states for long periods.
- **Optical Stimulation:** Light stimulation releases electrons, producing luminescence.

The emitted light is detected using sensitive photodetectors such as photomultiplier tubes (PMTs) or photodiodes.

Materials Used in OSL Dosimetry

The performance of an OSL dosimeter strongly depends on the properties of the phosphor material. An ideal OSL material should have high sensitivity, stable trapping centers, minimal fading, and good reproducibility. Several inorganic phosphors have been investigated for OSL applications. Among them, Al_2O_3:C (carbon-doped aluminum oxide) is the most widely used material due to its high sensitivity and excellent signal stability. Another promising material is beryllium oxide (BeO), which offers tissue-equivalent properties and good radiation response [4].

Some other materials such as LiF, $CaSO_4$, and $SrAl_2O_4$ have also been studied for OSL applications. Each material shows different luminescence efficiency, trapping structure, and response to radiation. These materials differ in their trap structures and luminescence efficiency, which directly influence their dosimetric performance [5,6].

Synthesis Methods for OSL Materials:

Several synthesis techniques are used to prepare high-quality OSL phosphors such as Carbon-doped Aluminum Oxide (Al_2O_3:C).

- **Sol–Gel Method:** Metal alkoxides or nitrates are dissolved in alcohol or water to form a homogeneous solution. A chelating agent (citric acid/ethylene glycol) is added to form a gel. Carbon sources like glucose or graphite are introduced for doping. The gel is dried and calcined at 800–1200 °C to obtain crystalline OSL phosphor. This method offers good compositional control and uniform dopant distribution.
- **Solid-State Reaction:** High-purity Al_2O_3 powder is mixed with a carbon

source and pressed into pellets. The mixture is sintered at high temperatures (1200–1600 °C) in a reducing atmosphere. It is a simple and widely used method for bulk phosphor production.

- **Combustion Method:** Metal nitrates and fuels (urea/glycine) are heated to trigger a self-sustained combustion reaction, producing fine phosphor powders rapidly with high surface area.

Advantages of OSL Dosimetry

Optically stimulated luminescence dosimetry offers several advantages compared with other radiation measurement techniques such as thermoluminescence dosimetry (TLD).

One of the most significant advantages is non-destructive readout. Unlike thermoluminescence, OSL signals can be read multiple times without completely erasing the stored information. This allows repeated measurements and improved accuracy. Another advantage is high sensitivity, which enables detection of very low radiation doses. OSL dosimeters also show a wide dynamic dose range, making them suitable for both low-dose and high-dose measurements. OSL systems are also relatively simple and fast, allowing rapid dose evaluation. Additionally, many OSL materials show good signal stability and low fading, which ensures reliable long-term measurements [7]. Because of these benefits, OSL has become an important technique in modern radiation monitoring systems.

Applications of OSL in Radiation Dosimetry

OSL technology has found widespread applications in several fields where accurate radiation monitoring is essential.

- **Personnel Dosimetry:** OSL dosimeters are widely used to monitor radiation exposure of workers in nuclear power plants, hospitals, and research laboratories. Commercial OSL badges based on Al_2O_3:C are commonly used for personal radiation monitoring.
- **Medical Dosimetry:** In radiotherapy and diagnostic radiology, accurate dose measurement is crucial for patient safety. OSL detectors are used for verifying radiation doses delivered during medical procedures.
- **Environmental Radiation Monitoring:** OSL detectors can measure background radiation levels in the environment. They are used around nuclear facilities and in environmental protection studies.
- **Retrospective Dosimetry:** OSL techniques can estimate past radiation exposure by analyzing materials such as building materials, ceramics, or electronic components.

- **Geological and Archaeological Dating:** Beyond radiation protection, OSL is also used for dating sediments and archaeological artifacts by determining the time elapsed since their last exposure to sunlight [8].

Future Perspectives

Research in OSL dosimetry continues to focus on the development of new phosphor materials with improved sensitivity, stability, and tissue equivalence. Nanostructured materials and rare-earth doped phosphors are being explored to enhance luminescence efficiency. Advances in instrumentation and signal processing are also improving measurement accuracy and reducing detection limits. Portable and automated OSL systems are being developed for field applications.

Another emerging area is the integration of OSL detectors in space missions and high-energy radiation environments, where precise radiation monitoring is essential for astronaut safety and spacecraft electronics [9].

Conclusion

OSL has become an important technique for radiation dosimetry due to its high sensitivity, reliability, and flexibility. The principle of OSL is based on the storage of radiation-induced energy in trapping centers and its release in the form of light when stimulated by optical sources. Various materials such as Al_2O_3:C, BeO, and LiF have been successfully used for OSL dosimetry applications. Modern OSL systems provide accurate and repeatable radiation measurements in medical, environmental, and industrial fields. Continuous research on new luminescent materials and improved instrumentation is expected to further enhance the performance and applications of OSL technology in the future.

References

1. McKeever, S. W. S., 2001, Nuclear Instruments and Methods in Physics Research B, 184, 29–54.
2. Akselrod, M. S., 2011, Radiation Protection Dosimetry, 144, 218–226.
3. Yukihara, E. G., McKeever, S. W. S., 2011, Wiley, 1, 1–362.
4. Sommer, M., Henniger, J., 2008, Radiation Measurements, 43, 353–356.
5. Hidehito Nanto and Go Okada 2023 Jpn. J. Appl. Phys. 62 010505
6. Botter-Jensen, L., McKeever, S. W. S., Wintle, A. G., 2003, Elsevier, 1, 1–355.
7. Akselrod, M. S., Kortov, V. S., Kravetsky, D. J., Gotlib, V. I., 1990, Radiation Protection Dosimetry, 33, 119–122.
8. Wintle, A. G., 2008, Boreas, 37, 471–482.
9. Yukihara, E. G., McKeever, S. W. S., 2014, Radiation Measurements, 71, 1–8.

Recent Development in Photoluminescent Phosphor Materials

Pardeshi Neha R., Kangude Sahadev H.

Department of Physics Rayat Shikshan Sanstha's Dada Patil Mahavidyalaya Karjat, Dist- Ahilyanagar-414402

Email: npardeshi273@gmail.com

Article DOI Link: https://zenodo.org/uploads/19787132

DOI: 10.5281/zenodo.19787132

Abstract

Phosphor materials have gained considerable interest due to their capability to efficiently transform absorbed energy into visible light. Over the years, research in this field has evolved from conventional rare-earth-doped phosphors to advanced materials such as sulfides, nitrides, fluorides, quantum dots, metal–organic frameworks, and carbon-based nanomaterials. These modern systems offer improved emission tunability, enhanced thermal and chemical stability, and broader application potential. The performance of a phosphor strongly depends on its composition, crystal structure, synthesis method, and energy-transfer processes. Because of these characteristics, photoluminescent phosphors play an important role in white light-emitting diodes, display devices, bioimaging, optical sensing, and anti-counterfeiting technologies. This chapter reviews recent advances in phosphor materials, covering their classification, mechanisms, applications, and future trends, with emphasis on efficient, sustainable, rare-earth-free systems.

Keywords: Photoluminescent phosphors; rare-earth ions; white LEDs; quantum dots; luminescent materials.

Introduction

Photoluminescent phosphors are luminescent solid materials that absorb incident radiation and subsequently emit visible light at longer wavelengths through radiative relaxation processes such as fluorescence or phosphorescence. Owing to their high emission efficiency and, in some cases, persistent afterglow properties, these materials are widely used in applications including light-emitting diode (LED) lighting, display technologies, bioimaging, safety signage, and anti-counterfeiting systems [1]. In phosphor materials, the host lattice forms a stable crystalline framework, while a small number of activator ions embedded within it serve as centers for light emission. Activator ions, such as rare-earth or transition metal ions like Eu^{2+} and Mn^{2+}, create discrete energy levels that allow absorbed

energy to be released as visible light efficiently [2]. The emission colour, intensity, and thermal stability of phosphors are strongly influenced by the nature of the activator ion and the local crystal field environment provided by the host lattice.

Recent advances in photoluminescent phosphor materials are largely driven by the demand for higher luminous efficiency, improved colour quality, and better thermal stability in solid-state lighting technologies. Rare-earth-activated phosphate phosphors have attracted considerable attention due to their excellent chemical stability and tunable luminescence properties. Current research focuses on optimizing energy-transfer mechanisms, modifying host crystal structures, and precisely controlling dopant composition and concentration [3]. These approaches significantly enhance emission intensity, improve colour rendering performance, and allow precise tuning of the emission spectrum, which is essential for the development of high-performance phosphor-converted white LEDs used in indoor and outdoor illumination, automotive lighting, horticulture systems, and biomedical applications [4].

Despite these advancements, phosphor performance often decreases at elevated operating temperatures due to thermal quenching, which reduces luminescence efficiency. Therefore, the development of thermally stable phosphor materials remains a major challenge and an important direction for future research [5].

Mechanism of Photoluminescence

Photoluminescent phosphors consist of a crystalline host lattice doped with small amounts of activator ions such as Eu^{2+} or Ce^{3+} that act as luminescent centers. When the material absorbs ultraviolet or visible radiation, electrons in the activator ions are excited to higher energy levels. As these electrons return to lower energy states, the absorbed energy is released in the form of photons, producing visible luminescence. The emission wavelength and intensity depend on the type of activator ion and the crystal field environment provided by the host lattice [6].

Rare-Earth-Doped Phosphor Materials

Rare-earth ions play an important role in the development of phosphor materials because they provide sharp and efficient emission bands. Europium, cerium, terbium, dysprosium, praseodymium, and gadolinium are among the most widely used activators. The luminescent properties of these ions strongly depend on the host lattice structure, synthesis method, and the surrounding crystal field environment [7].

Table 1: Examples of rare-earth-doped phosphor materials and their properties [Ref. 7-10]

Phosphor element	Synthesis method	Excitation nm	Emission nm	Color	Application
$CagMg_3Al_2Si_7O_{28}$; Eu^{2+}	Solid state	420	535	Green	WLEDs
$MgAl_2O_4$:Eu^{2+}	Solid State	394	615	Red	LED & energy storage
$GdMo_3Og$; Eu^{3+}	Solid state	280	395/645	Red/Blue	Solid State lightining
Gd^{3+} LZB glass	Melt quenching	265	311	Blue	Phototherapy lamps & UV-LED
$NaYF_4$:Gd^{3+}	Co-precipitation	27	311	Blue	Phototherapeutic lamp
KSrPO4:Dy3	Solid state	351/388	570	Green Yellow	Hight Powered LED
$GdSr_2(MoO_4)_{4:}2xSm^{3+}$	Sol-gel	405	-	Blue green	Indoor illumination/WELDs
YAG: Ce^{3+}	Low temperature co sintering	350	450	Red	High-Power WLEDs

Classification of Photoluminescent Phosphors

Photoluminescent phosphors can be classified based on their chemical composition and crystal structure. Oxide phosphors offer high chemical stability and are widely used in LEDs and display devices. Nitride phosphors provide excellent thermal stability and strong red emission, while fluoride phosphors exhibit low phonon energy and high luminescence efficiency. Sulfide phosphors produce intense emission but are less chemically stable. Emerging materials, including quantum dots, nanophosphors, metal–organic framework-based, and carbon-based phosphors, offer tunable emission and multifunctional applications, expanding the potential for modern lighting and sensing technologies [11]

Phosphor Converted White Light Emitting Diodes

Phosphor-converted white LEDs (pc-WLEDs) are widely used in modern lighting due to their high energy efficiency, long lifetime, and environmentally friendly operation. White light is typically produced either by combining a near-ultraviolet LED with red, green, and blue phosphors or by using a blue LED with a yellow-emitting phosphor. Key performance parameters include luminous efficacy, color rendering index (CRI), and correlated color temperature (CCT), which determine the quality and appearance of the emitted light. Pc-WLEDs are essential for applications in indoor and outdoor illumination, automotive lighting, and horticultural systems [12].

Challenges and Future Trends

Although photoluminescent phosphors have advanced greatly, several challenges remain. Thermal quenching at high operating temperatures can reduce emission efficiency. In addition, the cost and limited availability of rare-earth elements motivate the development of alternative activators and host materials. Future research is expected to focus on rare-earth-free phosphors, nanostructured materials, quantum dots, multifunctional phosphors, and sustainable synthesis routes

Conclusion

Photoluminescent phosphor materials represent a dynamic area of research spanning chemistry, and engineering, enabling advancement in lighting and display technologies. Innovation have progressed from early fluorescent lamps to highly engineered materials synthesized through precise solution-based methods, improving efficiency and performance. Current research emphasizes sustainability, cost-effectiveness, and reducing dependence on critical raw materials while enhancing luminous efficiency. Continued atomic-level control of light-emitting processes is expected to drive brighter, more energy-efficient, and environmentally friendly application

References

1. Hoppe, H. A. (2009). Angewandte Chemie International Edition, 48(20), 3572–3582.
2. Flomo, M. K., & Omoniyi, A. O. (2025). Next Nanotechnology, 8, 100234.
3. Qiao, J., Zhao, J., Liu, Q., & Xia, Z. (2019). Journal of Rare Earths.
4. Wan, Y., Liu, D., Yang, W., et al. (2025). J. Mater. Chem. C, 13, 16–30.
5. Huang, L., Chen, X., Wang, Q., et al. (2024). Journal of Luminescence, 278, 121500.
6. Wei, X., Yang, J., Hu, L., Cao, Y., Lai, J., Cao, F., Gu, J., & Cao, X. (2021). Journal of Materials Chemistry C.
7. Zhang, C., Li, H., Wang, Y., et al. (2023). Journal of Materials Science: Materials in Electronics, 34, 11245–11263.
8. Yadav, S., Kumar, D., Yadav, R. S., & Singh, A. K. (2022). SSRN Electronic Journal.
9. Tao, P., Liu, S.-J., & Wong, W.-Y. (2020). Advanced Optical Materials, 8, 2000985.
10. Zhang, C., & Lin, J. (2012). Chemical Society Reviews, 41(24), 7938–7961.
11. Ye, S., Xiao, F., Pan, Y. X., Ma, Y. Y., & Zhang, Q. Y. (2010). Materials Science and Engineering R, 71(1), 1–34.
12. Lin, Y.-C., Karlsson, M., & Bettinelli, M. (2016). Topics in Current Chemistry, 374, 21.

Advances in Polymer Composites for Radiation Shielding: A Comprehensive Overview

Prashant G. Ghule, Dinesh Kute

Applied Sciences & Humanities, Pimpri Chinchwad College of Engineering, Pune, Maharashtra, India

Email: prashantghule2808@gmail.com

Article DOI Link: https://zenodo.org/uploads/19787324

DOI: 10.5281/zenodo.19787324

Abstract

Polymer composites are revolutionizing radiation shielding by overcoming the limitations of lead and concrete. This work reviews recent advances, including lightweight polymer matrices with high-atomic-number fillers: bismuth, tungsten, and boron, which provide effective attenuation while reducing weight, toxicity, and rigidity. It covers radiation interaction mechanisms, polymer selection, environmentally friendly fillers, and challenges such as filler dispersion, mechanical trade-offs, and durability. Solutions like nanocomposites, multifunctional and multifilter materials, and 3D printing are discussed. Practical uses include medical physics, aerospace, nuclear decommissioning, and the nuclear industry. Overall, polymer composites are innovative technologies that improve radiation safety by addressing traditional material shortcomings.

Introduction

The discovery of ionizing radiation transformed fields like medicine, industry, and energy, but it also raised the crucial issue of protection. Exposure to X-rays, gamma rays, and neutrons can lead to genetic mutations and tissue damage [1]. The ALARA principle focuses on time, distance, and, especially, shielding, with shielding being the most practical safety measure [2].

For a century, lead has been the main shielding material because of its high atomic number (Z=82) and density (11.3 g/cm3), which offer effective photon attenuation. Nevertheless, lead-based shields pose a paradox: they protect from radiation but also introduce new risks. Lead aprons weighing 5-7 kg can cause musculoskeletal injuries in medical staff [3]. Additionally, lead is biologically toxic and environmentally persistent, and it has a weak absorption region between 40-88 keV. This chapter discusses how polymer-based composites overcome these challenges by merging lightweight, easy-to-process polymers with high-Z fillers to develop safer, more efficient shielding materials.

Fundamentals of Radiation Interaction

Understanding how radiation interacts with matter is crucial for designing effective shielding materials. Gamma-rays interact with matter mainly through three mechanisms. The photoelectric effect dominates at lower energies (10-300 keV), with probability proportional to Z4/E3, making high-Z materials particularly effective at these energies. Compton scattering is the primary mechanism at intermediate energies (300 keV to several MeV), with likelihood scaling linearly with Z. For energies above 1.02 MeV, pair production occurs, with probability scaling with Z2 [4].

Neutrons interact with nuclei via elastic and inelastic scattering, losing energy efficiently when colliding with nuclei of similar mass, such as hydrogen-rich materials [5]. They can also be absorbed through nuclear reactions. The effectiveness of shielding is measured using the linear attenuation coefficient (μ), the half-value layer (HVL), which is the thickness that reduces radiation intensity by 50%, and the mass attenuation coefficient (μ/ρ), which accounts for density [6].

The Polymer Matrix: Foundation of Flexible Shielding

The polymer matrix offers mechanical strength, flexibility, and ease of processing while dispersing functional fillers. The ideal matrices demonstrate durability, thermal stability, radiation resistance, and good compatibility with fillers [7].

Thermoplastics like high-density polyethylene (HDPE), polypropylene, and PVC are easy to process because they melt. HDPE is especially valued for neutron shielding owing to its high hydrogen content. Thermosets such as epoxy and polyurethane show superior mechanical properties but cannot be reshaped after curing, making them suitable for structural applications. Elastomers such as silicone rubber enable flexible shielding garments when comfort and mobility are essential [8].

Lead-Free Functional Fillers

Extensive research has examined alternative high-Z elements that balance effective radiation attenuation with biological safety. The development of composite materials relies heavily on uniform filler dispersion, since nanoparticles tend to agglomerate; surface functionalization with coupling agents enhances compatibility with hydrophobic polymers [9].

Bismuth (Bi, Z=83) stands out as the most promising substitute for lead. Its atomic number and density (9.8 g/cm3) are comparable to lead, and bismuth compounds are stable and notably non-toxic. Bismuth oxide (Bi2O3)/LDPE composites achieve about 80% attenuation of 47.9 keV X-rays with only 15% filler loading. At 40-50% loading, they provide lead-like attenuation while

maintaining flexibility [10].

Tungsten (W, Z=74) has the highest density among practical shielding elements at 19.3 g/cm3. Tungsten-polymer composites provide excellent attenuation at higher energies. Its high atomic density allows small tungsten volumes to achieve attenuation comparable to larger, less dense fillers, preserving polymer's mechanical properties.

Certain rare-earth elements, such as gadolinium (Gd, Z=64), exhibit unique shielding properties in which K-edges enhance absorption. Gadolinium also has the highest thermal neutron capture cross-section among elements.

For neutron shielding, boron carbide (B4C) and boron nitride dispersed in polyethylene are at the forefront. They combine hydrogen-rich moderation with effective neutron capture. The 10B isotope captures neutrons via the 10B(n,α)7Li reaction, producing no secondary gamma radiation, which is a considerable advantage over gadolinium compounds that emit gamma rays during capture, and lithium compounds that require higher loadings [11].

Engineering Applications in Radiation Safety

- **Medical Physics**

Medical devices require advanced shielding solutions. Traditional lead aprons cause back pain, shoulder strain, and fatigue, creating occupational hazards. Lead-free polymer composites address these issues [3]. Flexible aprons with bismuth or tungsten fillers deliver comparable attenuation with much less weight. Patient safety also improves with flexible, conformable shields worn directly on patients, which protect radiosensitive organs without the discomfort associated with rigid lead sheets [12].

- **Aerospace**

Space radiation involves galactic cosmic rays, solar particles, and secondary neutrons. NASA develops multifunctional composites that balance load-bearing and radiation shielding. High-hydrogen bismaleimide resins with boron carbide protect against radiation while maintaining strength. Polyethylene composites with boron or tungsten also provide effective shielding against galactic rays and solar protons. [13].

- **Nuclear Industry**

Nuclear facilities require shielding for operations, waste handling, and decommissioning. Polymer composites are ideal for temporary shielding and complex shapes. Spray-on boron coatings contain contamination by providing containment and shielding during decommissioning. Flexible polymer sheets wrap irregular parts, reducing disassembly and worker exposure. For spent fuel

transport, durable polymer composite liners enhance shielding by offering neutron moderation without added lead weight [14].

Emerging Trends in Shielding Materials

Nanocomposites represent a major advancement. Nanoparticles offer a higher surface area-to-volume ratio, allowing for more uniform dispersion. Graphene and carbon nanotubes are widely used as co-fillers, improving mechanical properties and enhancing thermal and electrical conductivity for secondary design needs [15].

Multifunctional materials can simultaneously block radiation, conduct heat, and ensure structural stability. Composites with boron nitride or aluminium nitride dissipate heat and shield against neutrons, preventing hot spots in waste storage [16].

Additive manufacturing allows customization of shields for specific needs. Fused deposition modelling with filled polymer filaments produces complex shapes that are unachievable with traditional methods. Patient-specific shields can be 3D printed from CT data for a perfect fit. Lattice structures reduce weight while maintaining effectiveness through scattering. [17].

Multi-filler Systems that combine multiple fillers, such as bismuth for gamma-ray shielding, boron for neutrons, and gadolinium to fill spectral gaps, offer broader protection than single fillers. Machine learning accelerates the discovery of optimal combinations by predicting performance from existing data.

Challenges and Future Pathways

Despite some progress, challenges persist. Effective filler dispersion is vital, as agglomeration can create weak points. Nanoparticles improve dispersion but pose handling difficulties. Balancing filler content and polymer properties requires optimization. Higher loadings enhance shielding but also make composites more brittle. Long-term durability under continuous radiation remains incompletely understood, with polymers potentially undergoing chain scission or crosslinking. Scaling up from lab to commercial production demands cost-efficient processing.

The future pathways are promising. Advances in computational methods accelerate materials discovery, additive manufacturing offers design flexibility, and environmental concerns drive the phase-out of lead. Together, these factors position polymer composites as the preferred materials for radiation protection.

Conclusion

Polymer-based composites are increasingly important for radiation shielding because they can replace toxic lead with safer alternatives such as bismuth oxide and tungsten oxide, while still offering effective protection. These composites are lightweight, flexible, and easier to manufacture than traditional shielding materials. Currently, research is shifting from replacing lead to creating advanced

multifunctional materials that combine mixed radiation shielding along with strong mechanical and thermal properties.

References

1. Reisz et al., Antioxidants & Redox Signaling, Mary Ann Liebert, 2014
2. Hendee et al., Seminars in Nuclear Medicine, Elsevier, 1986
3. Cheon et al., Korean Journal of Pain, Korean Pain Society, 2018
4. Ghule et al., Radiation Physics and Chemistry, Elsevier, 2024
5. Knoll et al., Radiation Detection and Measurement, John Wiley & Sons, 2010
6. El-Khatib et al., Materials (Basel), MDPI, 2022
7. Nambiar et al., ACS Applied Materials & Interfaces, American Chemical Society, 2012
8. Kameesy et al., International Journal of Advanced Research, IJAR, 2015
9. Toyen et al., Iranian Polymer Journal, Springer, 2018
10. Alshahri et al., Polymers (Basel), MDPI, 2021
11. Huo et al., Nuclear Materials and Energy, Elsevier, 2021
12. Wu et al., Applied Radiation and Isotopes, Elsevier, 2023
13. Venkatakrishnan et al., Journal of Applied Mechanical Engineering, OMICS Publishing, 2017
14. Akman et al., Radiation Physics and Chemistry, Elsevier, 2024
15. Mittal et al., In-Situ Synthesis of Polymer Nanocomposites, Wiley-VCH, 2011
16. Kiani et al., Scientific Reports, Nature Publishing Group, 2025
17. Knott et al., Composites Science and Technology, Elsevier, 2023

Basic Mathematics, Interpretation and Applications of Photoluminescence

[1]Nilesh Nana Mharsale, [2]Archana Satish Shirsat

[1]Dept. of Physics, M.V.P Samaj's Arts, Commerce and science College, Trymbakeshwar, Dist Nashik, Maharashtra, India-422212

[2]Dept. of Mathematics, Institute of engineering, Bhujbal Knowledge City, Adgaon Nashik, Maharashtra, India-422003

Email: nileshmharsale@gmail.com

Article DOI Link: https://zenodo.org/uploads/19787471

DOI: 10.5281/zenodo.19787471

Abstract

This chapter presents the principles, mathematical basis, and applications of photoluminescence, including excitation–emission processes, radiative recombination, quantum efficiency, energy–wavelength relations, and Gaussian analysis for band gap and defect studies. It also emphasizes the importance of PL in semiconductor characterization, photocatalysis, and optoelectronic devices.

Keywords: Photoluminescence, Energy Band Theory, Radiative Recombination, Quantum Efficiency, Gaussian Fitting, Carrier Lifetime, Defect States

Introduction

Luminescence is the emission of light after external energy absorption through electronic transitions. The theoretical foundation of thermoluminescence (TL) was established by McKeever [1], describing radiation-induced trapping of charge carriers in band-gap defects and their thermally stimulated release, producing glow curves governed by kinetic equations [1]. Early studies clarified defect-mediated recombination mechanisms [2, 3], enabling trap parameter evaluation and dosimetry [4, 5]. Comprehensive descriptions of luminescent materials were provided by Kitai [6, 7] and Blasse and Grabmaier [8], relating emission to transitions between discrete energy levels influenced by lattice symmetry and defects. Photoluminescence (PL) involves photon-induced recombination, while TL involves thermally stimulated emission after irradiation [1], [5], both modeled using transition probability and first- and general-order kinetics [1], [6]. Classical and modern studies confirmed the role of electronic transitions and defect states [9-11], with glow curve analysis explaining trap-controlled recombination [12,13]. Thus, TL and PL are complementary

techniques for investigating electronic transitions and defects in solids [1-3], [7-13].

Energy Band Theory of Solids

When atoms form a crystalline solid, their discrete energy levels split into continuous energy bands due to interatomic interactions, as described by band theory [14], which explains electrical, optical, and luminescent properties. Electrons occupy the valence band (VB) and conduction band (CB), separated by a forbidden energy gap (Eg) [14]; the VB contains strongly bound electrons requiring excitation [14], [16], while the CB contains free carriers responsible for conduction [14], [17]. The band gap, defined as $E_g = E_{CB} - E_{VB}$, determines electrical and photoluminescent behavior [14], [15], and materials are classified as conductors ($E_g \approx 0$), semiconductors (0.1–3 eV), and insulators ($E_g > 3$ eV) [14], [16].

Definition: Photoluminescence is a radiative recombination process used to study semiconductor optical and electronic properties. In materials such as ZnO, PL originates from band-to-band and defect-related transitions, providing information on band structure and defect states [18]. It is also sensitive to carrier lifetime and recombination dynamics due to its dependence on excess carrier density and non-radiative pathways [19].PL involves excitation, relaxation, and emission: photons with $h\nu_{exc} \geq E_g$ promote electrons to the conduction band, followed by non-radiative relaxation [20], and radiative recombination emitting photons with $h\nu < h\nu_{exc}$, producing a Stokes shift. Emission efficiency and quantum yield are key parameters for luminescent material evaluation [21].

Mathematical Interpretation of PL

- **Energy–Wavelength Relationship**

The energy–wavelength relationship is given by $E = h\nu = hc/\lambda$ where (h) is Planck's constant, ν is the frequency of light, c is the speed of light, and λ is the wavelength. From the photoluminescence (PL) spectrum, the band gap energy in electron volts can be calculated using the relation $E_g(eV) = 1240/(\lambda(nm))$

- **Radiative Recombination Rate**

PL results from radiative recombination of photo-generated electrons and holes in semiconductors, governing emission intensity and carrier dynamics [22]. The radiative recombination rate is given by $R = Bnp$, where n and p are electron and hole concentrations and B is the temperature- and band-structure-dependent coefficient [22]. TRPL analyzes carrier lifetime and decay behavior, revealing radiative and non-radiative mechanisms in advanced semiconductors such as halide perovskites [23]. Hence, $R = Bnp$ is the fundamental relation describing radiative PL processes [22], [23].

- **PL Intensity**

PL intensity is governed by radiative recombination of charge carriers in semiconductors. For band-to-band transitions, the radiative recombination rate is R = Bnp, where n and p are electron and hole concentrations, and B is the radiative recombination coefficient dependent on material properties and temperature [24]. Hence, IPL∝R=Bnp.

In real materials, radiative and non-radiative recombination occur simultaneously. Defects and impurities introduce non-radiative pathways that reduce emission efficiency. The quantum efficiency is defined as-

$$\eta = \frac{Rrad}{R_{rad} + R_{non-rod}}$$

where,

R_{rad} and $R_{non\text{-}rad}$ are radiative and non-radiative recombination rates, respectively [24].

Gaussian Fitting of PL Peaks

The Gaussian function is expressed as:

$$I(\lambda) = I0 \exp\left[-\frac{(\lambda - \lambda 0)^2}{2\sigma^2}\right]$$

where λ_0 is the peak wavelength, σ represents the standard deviation related to spectral width (FWHM), and I_0 is the maximum intensity. The parameter σ indicates peak broadening caused by structural disorder, electron–phonon interaction, or defects. Gaussian deconvolution is especially useful for resolving overlapping emission bands and analyzing changes induced by irradiation or chemical modification, making it an essential tool in PL spectral interpretation and semiconductor characterization [25].

Applications

PL is used to estimate the band gap of semiconductors like $BiFeO_3$, ZnO, and TiO_2 from emission spectra. It detects defect states and evaluates charge separation efficiency, where lower PL intensity indicates reduced recombination and improved photocatalytic activity. PL also aids in selecting materials for LEDs and laser diodes by analyzing emission characteristics.

Conclusion

Photoluminescence is an essential optical technique based on energy band theory and radiative recombination (R = Bnp). Its mathematical analysis enables precise evaluation of band gap, defects, and carrier dynamics, making it valuable for semiconductor, photocatalytic, and optoelectronic applications.

References

1. S. W. S. McKeever, Thermoluminescence of Solids. Cambridge, U.K.:

Cambridge University Press, 1985.
2. J. T. Randall and M. H. F. Wilkins, Proc. R. Soc. Lond. A, vol. 184, no. 999, pp. 365–389, 1945.
3. G. F. J. Garlick and A. F. Gibson, Proc. Phys. Soc., vol. 60, no. 6, pp. 574–590, 1948.
4. S. W. S. McKeever and R. H. Bube, Thermoluminescence of Solids. 1987, pp. 80–81.
5. Y. S. Horowitz, Ed., Thermoluminescence and Thermoluminescent Dosimetry. Boca Raton, FL, USA: CRC Press, 1984.
6. G. Kitis, J. M. Gomez-Ros, and J. W. N. Tuyn, "Thermoluminescence glow-curve analysis and kinetic models," 1998.
7. A. Kitai, Ed., Luminescent Materials and Applications. Hoboken, NJ, USA: John Wiley & Sons, 2008.
8. G. Blasse and B. C. Grabmaier, Berlin, Germany: Springer, 1994, pp. 1–9.
9. K. V. R. Murthy and H. S. Virk, vol. 347. Trans Tech Publications Ltd, 2014.
10. C. R. Ronda, Ed., Hoboken, NJ, USA: John Wiley & Sons, 2007.
11. F. E. Williams, J. Opt. Soc. Am., vol. 39, no. 8, pp. 648–654, 1949.
12. A. Y. Madkhli et al., Appl. Radiat. Isot., vol. 208, p. 111301, 2024.
13. J. Lumin., 2024.
14. S. H. Simon, The Oxford Solid State Basics. Oxford, U.K.: Oxford University Press, 2013.
15. Raman, Toatemperatuurse Fotoluminestsentsi ja Spektroskoopia Abil,
16. U. Shukla and S. Bari, J. Pure Appl. Ind. Phys., vol. 8, no. 5, pp. 25–31, 2018.
17. A. Buzzell and A. Mendizabal, Diss. Worcester Polytechnic Institute, 1919.
18. W. Shan et al., Appl. Phys. Lett., vol. 86, no. 19, 2005.
19. T. Trupke and R. A. Bardos, in Conf. Rec. 31st IEEE Photovoltaic Specialists Conf., 2005.
20. T. Aoki, 2019, pp. 157–202.
21. C. Würth et al., Anal. Bioanal. Chem., vol. 407, no. 1, pp. 59–78, 2015.
22. T. H. Gfroerer, Encyclopedia of Analytical Chemistry, vol. 67, p. 3810, 2000.
23. J. Chen et al., Phys. Chem. Chem. Phys., vol. 25, no. 11, pp. 7574–7588, 2023.
24. D. K. Schroder, 3rd ed. Hoboken, NJ, USA: John Wiley & Sons, 2015.
25. N. K. Fernando et al., J. Phys. Chem. A, vol. 125, no. 34, pp. 7473–7488, 2021.
26. N. K. Fernando et al., J. Phys. Chem. A, vol. 125, no. 34, pp. 7473–7488, 2021.

Growth, Theoretical, and Nonlinear Optical Studies of Glycine Glycinium Chloride: A Potential Semiorganic Nonlinear Optical Material

B. Uma

Assistant Professor, Department of Physics, Ethiraj College for Women, Chennai – 600 008, India

Email: uma2612@gmail.com

Article DOI Link: https://zenodo.org/uploads/19787557

DOI: 10.5281/zenodo.19787557

Abstract

Single crystals of Glycine Glycinium chloride (GGC) ($C_2H_6NO2^+$ $C_2H_5NO_2$. C^{l-}) with dimensions up to 15x4x1.5mm^3 have been grown successfully from aqueous solution at room temperature by slow solvent evaporation. The crystal belongs to orthorhombic structure with the space group P212121 and lattice parameters a= 5.3105 Å, b = 8.0983 Å, c = 18.0020 Å. Theoretical calculations of polarizability, useful for device fabrication, are performed using the Clausius-Mossotti equation and the Penn analysis, and the results are compared. The second-harmonic signal in the GGC crystal is confirmed by green emission using the Kurtz powder technique, and the SHG efficiency is 5.6 times that of KDP.

Keywords: Physics research, Energy materials.

Introduction

Over the past few years, research on nonlinear optical materials has received considerable attention due to their widespread use in the fabrication of electro-optic and integrated optical devices. The second-order nonlinear optical (SONLO) properties of molecular crystals have been deeply investigated for their potential applications in newly emerging areas such as optoelectronics, optical modulation, and optical signal processing. Optical non-linearity of the crystals with O-H bond has been extensively studied, as the donor-acceptor system enhances the optical activity to the desired level [1]. Though it is very difficult to grow large, optical-quality crystals of organic materials for device applications, amino acid family crystals can be obtained easily due to their high coordination during crystallization. Glycine is one of the simplest of all amino acids, whose complexes with mineral acids have high physical properties like ferroelastic, ferroelectric, or anti-ferroelectric behaviour [2].

Semiorganic materials have the potential to combine the high optical nonlinearity and chemical flexibility of organic materials with the thermal stability and mechanical robustness of inorganic materials [3]. Amino acids are interesting materials for NLO applications, as they contain a proton-donating carboxylic acid (-COO) group and a proton-accepting amino (NH2) group [4]. There are two forms of glycine: glycinium ions and zwitterions. Such a configuration of glycine ions interconnected by short O-H-O hydrogen bonds is regarded as particularly important for the ferroelectric behaviour of the crystal [5,8].

In the present investigation, single crystals of Glycine Glycinium Chloride (GGC) with dimensions up to 15x4x1.5 mm^3 have been grown by the slow evaporation technique and characterized by single-crystal XRD. Theoretical calculations of polarizability, useful for device fabrication, are performed using the Clausius-Mossotti equation and the Penn analysis, and their results are compared. The NLO activity of the crystal is also examined by the Kurtz powder test.

Experimental

- **Synthesis**

The salt of Glycine Glycinium Chloride (GGC) is synthesized by dissolving analar-grade glycine and concentrated hydrochloric acid in the stoichiometric ratio 2:1 in double-distilled water. The fine powder of GGC salt is obtained by constant slow evaporation at room temperature. The synthesized salt is further purified by repeated recrystallization. The reaction of synthesis is adhered to by the equation,

$$2(C_2H_5NO_2) + HCl \rightarrow C_2H_6NO_2 + C_2H_5NO_2.\ Cl^-$$

- **Crystal Growth**

The saturated solution of the crystal is obtained by dissolving the recrystallized or synthesized salt in double-distilled water under constant stirring. The homogenous solution obtained after thorough mixing is allowed to evaporate to form the seed crystal. A good quality seed crystal is selected and immersed in the supersaturated mother solution. Continuous, slow solvent evaporation at room temperature led to seed growth, and crystals up to 15x4x1.5 mm^3 were obtained over three months. The grown crystal exhibits a platelet structure with good optical transparency. A photograph of a grown crystal is shown in Fig. 1.

- **Characterization Studies**

Single-crystal X-ray diffraction analysis is performed on the crystal using an Enraf–Nonius CAD diffractometer with MoKα radiation (wavelength 0.71073Å) to determine the cell parameters. Relative second-harmonic generation was performed using the Kurtz powder technique to confirm the crystal's nonlinearity.

Results and Discussions

1. X-ray Crystallographic studies

- **Single-crystal X-ray diffraction studies**

Single-crystal X-ray diffraction studies of GGC single crystals were carried out using an Enraf–Nonius CAD diffractometer with MoKα radiation of wavelength 0.71073Å. A carefully cut crystal of dimensions 0.30 x 0.20 x 0.20 mm^3 is used for the analysis [9]. The crystallographic data obtained from single-crystal X-ray data of the GGC crystal are presented in Table 1. From the single-crystal X-ray diffraction analysis, it was observed that the crystal belongs to the orthorhombic system with the lattice parameters a = 5.3105Å, b = 8.0983Å, c = 18.0020Å, and space group P212121.

- **Theoretical measurements**

The valence electron plasma energy ħωp is given by

$$\hbar\omega_p = 28.8 \left(\frac{Z\rho}{M}\right)^{\frac{1}{2}} \text{----------[1]}$$

Where Z= ((4xZC) + (11xZH) + (2xZN) + (4xZO) + (1xZCl)) = 79 is the total number of valence electrons, ρ is the density and M is the molecular weight of the crystal. The Penn gap and the Fermi energy are explicitly dependent on the ħωp [10] which are given by

$$E_p = \frac{\hbar\omega_p}{(\varepsilon_\infty - 1)^{\frac{1}{2}}} \text{----------[2]}$$

$$E_F = 0.2948\ (\hbar\omega_p)^{\frac{4}{3}} \text{----------[3]}$$

The molecular polarizability 'α', is obtained by using the relation [11],

$$\alpha = \left[\frac{(\hbar\omega_p)^2 S_0}{(\hbar\omega_p)^2 S_0 + 3E_P^2}\right] \times \frac{M}{\rho} \times 0.396 \times 10^{-24} \text{----------[4]}$$

Where SO is a constant for the material, which is given by

$$S_O = 1 - \left[\frac{E_P}{4E_f}\right] + \frac{1}{3}\left[\frac{E_P}{4E_F}\right]^2 \text{----------[5]}$$

The value of α obtained agrees well with that of the Clausius – Mossotti equation, which is given by the relation,

$$\alpha = \frac{3M}{4\pi N_a \rho}\left(\frac{\varepsilon_\infty - 1}{\varepsilon_\infty + 2}\right) \text{----------[6]}$$

All these calculated theoretical data for the grown crystal are presented in Table

2.

2. Second Harmonic Generation (SHG)Property Studies

Kurtz [12] powder SHG test is performed to find the NLO property of the GGC crystal. The microcrystalline powdered sample packed in a capillary tube of diameter 0.154mm is illuminated using Spectra Physics Quanta Ray DHS2. Nd-YAG laser using the first harmonics output of 1064nm with the pulse width of 8ns and repetition rate 10Hz. The input laser energy incident on the powdered sample is 8.8mJ/pulse. The SHG signal at 532nm is detected at various points on the sample in transmission using a photomultiplier tube (PMT) and box averager. The SHG in the crystal is confirmed by the emission of green light. The microcrystalline KDP powder is used as the reference material. It is found that the frequency doubling efficiency of the GGC crystal is 5.6 times that of KDP. The high NLO efficiency demonstrates GGC's suitability for device fabrication in photonics and nonlinear optics, surpassing that of other semiorganic materials.

Conclusions

Optically transparent Glycine Glycinium Chloride crystals are successfully grown by the slow evaporation method from aqueous solution. The crystallinity of the grown crystal is confirmed by single-crystal XRD analysis. The polarizability calculated by the Penn analysis is verified using the Clausius-Mossotti equation, and the results indicate that the values agree well. Other important parameters, such as plasma energy and Fermi energy, are also calculated from single-crystal X-ray analysis. The SHG studies confirm the NLO property of the grown crystal, and the SHG efficiency of the GGC crystal is found to be 5.6 times higher than that of KDP. The NLO properties indicate that GGC crystals can be used effectively for photonics and opto-electronic device fabrication.

References

1. G. Anandhababu, P. Ramasamy, J. Crys. Growth, 310 (2008) 3561.
2. R. Sankar, C.M. Ragahavan, R. Mohan Kumar, R. Jayavel, J. Crys. Growth, 309(2007) 30
3. P.V. Dhanraj, N.P. Rajesh, Phys B, 405(2010) 4105
4. B.Narayana Moolya, S.M. Darmaprakash, J. Crys. Growth, 293 (2006) 86-92.
5. K. Ambujam, K. Rajarajan, S. Selvakumar, I. Vetha Potheher, Ginson P. Joseph, P. Sagayaraj, J. Crys. Growth, 286 (2006) 440-444.
6. T. Hahn, Z. Kristallogr. 113 (1960) 403.
7. S. Natarajan, C. Muthukrishnan, S. A. Bahadur, R. K. Rajaram, S.S. Rajan, Z. Kristallogr. 198(1992) 265.
8. K. Ambujam, K. Rajarajan, S. Selvakumar, J. Madhavan, Gulam Mohamed, P. Sagayaraj, J. Crys. Growth, 29 (2007) 657-662.

9. Oxford Diffraction (2010). CrysAlis PRO. Oxford Diffraction Ltd, Yarnton,Oxfordshire, England.
10. N.M. Ravindra, R. P. Bharadwaj, K. Sunil Kumar, V. K. Srivastava, Infra Phys. 21(1981)369.
11. N.M. Ravindra, V. K. Srivastava, Infrared Phys. 67 (1980) 20.
12. S.K. Kurtz, T.T.Perry, J.Appl. Phys. 39 (1968) 3798.

List of Figures

1. As grown single crystal of GGC crystal.

List of Tables

- Crystal data and structure refinement for GGC crystals
- Theoretical data of GGC crystal.

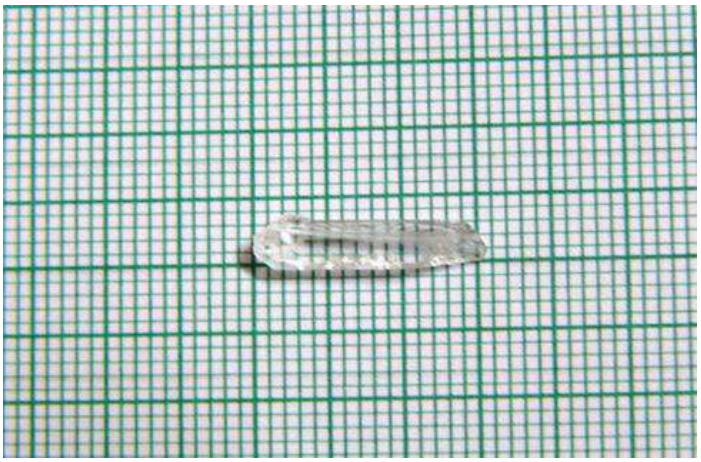

Fig.1. As-grown single crystal of GGC

Table 1. Crystal data and structure refinement for GGC crystals

Crystal size	0.30 x 0.20 x 0.20 mm^3
Empirical formula	$C_2 H_6 NO2^+$, $C_2 H_5 NO_2$, C^{l-}
Formula weight	186.60
Unit cell dimensions	a = 5.31050Å
b = 8.0983Å	
c = 18.0020Å	
Crystal system	Orthorhombic
Space group	P212121
Unit cell volume	774.19$Å^3$
No. of molecules per unit cell, Z	4
Temperature	293 K

Table 2. Theoretical data of GGC crystal.

Parameters	Values
Plasma energy (eV)	23.71
Penn gap energy (eV)	10.11
Fermi energy (eV)	20.08
Polarizability (cm^3)	
Penn analysis	2.848×10^{-23}
Clausius-Mossotti equation	2.990×10^{-23}

Rare Earth–Activated Materials in Photonics, Energy, and Biomedical Applications

[1]Preeti Padhye Kulkarni, [2]Kishor H. Gavhane

[1]School of Engineering, Ajeenkya D Y Patil University, Charholi Budruk, Pune, Maharashtra 412105, India

[2]Microtron Accelerator Laboratory, Department of Physics, S. P. Pune University, Pune 411007, India

Email: preetipadhye01@gmail.com

Article DOI Link: https://zenodo.org/uploads/19787656

DOI: 10.5281/zenodo.19787656

Abstract

Rare earth ions exhibit unique luminescent properties arising from intra-4f or 4f–5d transitions. Over the past decade, rare-earth-doped materials have appeared as a progressive group of luminescent optical markers, signifying significant potential as replacements for conventional organic fluorophores and semiconductor quantum dots. Due to their greater photostability, narrow emission bands, and extended luminescence lifetimes, these materials remain gradually employed across varied fields, with optoelectronic devices, energy conversion, bioassays, biomedical imaging, and materials research. Additionally, rare-earth-activated hybrid phosphors are key to developing multifunctional materials with tunable optical and magnetic properties. They enable nanostructured platforms that integrate multiple functionalities within a single system. By combining complementary components, these hybrids improve performance, reliability, scalability, and cost-effectiveness for advanced applications. Furthermore, extending their capabilities to radiation sensing, rare-earth-activated materials are widely explored in thermoluminescence (TL) applications. TL dosimeters based on such materials are extensively used in personnel and environmental monitoring, medical and clinical radiation therapy, in vivo dosimetry, nuclear medicine, etc. This chapter comprehensively discusses rare-earth-activated materials, highlighting their fundamental properties and diverse applications in photonics, energy conversion, and biomedical technologies.

Keywords: Rare-earth activated materials, luminescent properties, optoelectronics, energy harvesting, bioimaging, dosimetry

Introduction

Luminescent nanomaterials have gained significant attention for applications in displays, optoelectronics, bio-labelling, and solar cells. They are broadly classified into four types: A). semiconductor quantum and carbon dots, B). metal nanoclusters, C). metal-doped nanomaterials, and D). organic–inorganic hybrids. The luminescence of Q- dots, C- dots, and metal nanoclusters arises from quantum confinement effects, where precise control of particle size and surface passivation is essential for achieving efficient and color-tunable emission. In contrast, metal-doped nanomaterials and organic–inorganic hybrids exhibit luminescence from discrete emissive centers such as ions, complex ions, or molecules [1]. Here, we focus on trivalent rare-earth ion (RE) doped luminescent materials.

Rare-Earth-Activated Luminescent Materials

Rare-earth-activated luminescent phosphor materials have attracted significant attention due to their efficient down-conversion (DC) and up-conversion (UC) emissions, making them valuable complements to conventional semiconductors and dyes.

Selection of Suitable Host and Dopant Materials

An inorganic phosphor comprises a stable host lattice doped with optically active rare-earth ions as luminescent centers. Its emission efficiency depends on the proper selection of host structure, dopant type, and concentration.

Choice of Host Lattice

For efficient rare-earth (lanthanide; Ln) luminescence, the host lattice must have low phonon energy to minimize nonradiative losses and high chemical and thermal stability to ensure efficient emission.

Dopant Systems

- **Activators**

Luminescence is reached by doping minor amounts of trivalent lanthanide ions (Ln^{3+}) into a host lattice. These activators introduce discrete 4f energy levels that absorb excitation energy and produce characteristic emission.

Sensitizers

A sensitizer is a dopant ion that efficiently absorbs excitation energy and transfers it to a nearby activator. This mechanism enhances emission intensity, particularly when the activator exhibits weak absorption at the excitation wavelength.

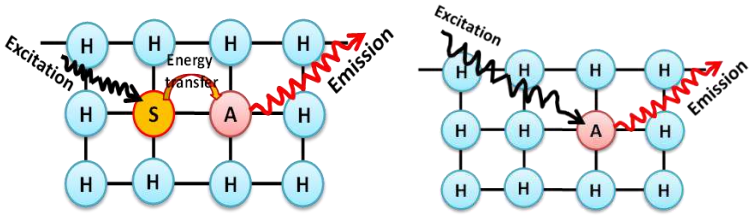

Fig. 1: (i) Activator (A) doped into host (H) lattice, (ii) Schematic of energy allocation after sensitizer (S) to activator (A) within the host lattice (H).

Unique Optical Properties

Optically active trivalent lanthanide (Ln^{3+})-doped materials are widely studied for their ladder-like discrete energy levels, which enable unique optical behavior. Their ability to produce multicolor emission under single-wavelength excitation makes them valuable for applications in displays, optical communication, bioimaging, diagnostics, lasers, solar cells, LEDs, and biomolecular sensing [2-3]. The exclusive photophysical behavior of rare-earth ions exhibits via 4f–4f and 4f–5d transitions. Shielding of 4f electrons by outer orbitals results in sharp emission bands with minimal environmental influence. Due to Laporte-forbidden 4f–4f transitions, lanthanides exhibit long excited-state lifetimes, enabling reduced cell background fluorescence. Rare-earth-doped nanoparticles also show negligible blinking because of the large number of emitters per particle. Thus, owing to their exceptional optical properties-high photostability, negligible blinking, sharp emission bands, large Stokes/anti-Stokes shifts, minimal autofluorescence interference, long excited-state lifetimes, and low cytotoxicity, rare-earth based materials are outstanding candidates for bioimaging and advanced biomedical applications [4], often outperforming conventional organic dyes and quantum dots. Furthermore, their high color purity and spectral stability also make them highly efficient for optoelectronic applications.

The emission efficiency of lanthanide ions is strongly governed by the host lattice, which facilitates efficient energy absorption and transfer. Various inorganic hosts such as oxides, sulphates, fluorides, vanadate's, phosphates, and orthoborates have been explored. Down conversion rare earth phosphors convert high-energy photons into lower-energy emission, whereas upconversion produces higher-energy emission from low-energy excitation via sequential energy transfer.

Solar energy conversion is constrained by the limited spectral absorption of conventional photoactive materials, which largely miss the NIR region. While dyes and quantum dots extend absorption into the visible range, stability issues limit their efficiency. Ln^{3+}-doped upconverting phosphor–semiconductor hybrids address this challenge by converting NIR photons into UV–visible light through anti-Stokes emission, thereby enhancing solar spectrum utilization and improving

photocatalytic and solar cell performance.

Beyond their tunable photoluminescence, energy and lighting applications, lanthanide-doped materials are widely utilized in thermoluminescence (TL) due to the unique properties of their partially filled 4f shells. The discrete and stable energy levels of Ln^{3+} ions act as efficient trapping centers, storing radiation-induced energy and releasing it as light upon heating. The glow curve characteristics provide valuable information about trap characteristics and kinetic parameters. Owing to these features, TL materials are extensively applied in radiation dosimetry, particularly in medical dosimetry, cancer radiotherapy etc.

Table1: Representative Rare Earth Activated Materials for Photonics, Energy and Biomedical Applications

Rare Earth Activated Material (Host: Dopant)	**Silent findings**	**Application Area**	**Ref**
LaF_3:Ln^{3+} (Ln =Eu^{3+}, Er^{3+}, Tm^{3+})	Efficient NIR–visible up-conversion; tunable multicolor emission	Photonics	[5]
Y_2O_3 :RE^{3+}	Enhanced photoluminescence	Optoelectronics, LED's	[6]
YAG: Ce^{3+}, Gd^{3+} phosphor and YAG: Ce^{3+}, Gd^{3+} /PMMA nanocomposites	Strong visible emission with good thermal stability	White LEDs, solid-state lighting	[7]
β-$NaYF_4$: Er^{3+}, Yb^{3+}@SiO_2@TiO_2 core–double shell sub-microprisms	Efficient NIR-to-visible upconversion; improved light scattering and charge transfer; significant enhancement in photocurrent density and overall PCE compared to bare TiO_2 photoanode	High-performance dye-sensitized solar cells	[8]
β-$NaGdF_4$: Yb^{3+}, Er^{3+}–mesoporous TiO_2 nanocomposite	Broad-spectrum photon harvesting; paramagnetic and enhanced photocurrent response	DSSCs / solar energy conversion	[9]
Y_2O_3: Er/Au@TiO_2 plasmonic–upconversion composite	Combined plasmonic enhancement and upconversion for superior photon utilization	Enhanced DSSC efficiency	[10]

$BaAlF_5$: Dy^{3+} nanophosphor	Improved TL sensitivity after optimized annealing; linear dose response	Radiotherapy dosimetry (in vivo TLD)	[11]
$NaLi_2PO_4$: Tb^{3+} phosphor	Well-defined glow peak; linear dose response (clinical dose range), stable trapping parameters and reproducibility	Medical radiation dosimetry	[12]

Summary and Future Outlook

Rare-earth-activated materials, owing to their unique 4f electronic structure, exhibit sharp emission bands, long lifetimes, high photostability, and excellent color purity, making them highly promising for optoelectronic devices, energy harvesting systems, and biomedical applications such as bioimaging and radiation dosimetry. Through careful host–dopant engineering and controlled energy transfer processes, their multifunctional performance can be effectively tuned. Future research should focus on enhancing quantum efficiency, minimizing nonradiative losses, improving biocompatibility, and enabling scalable device integration, thereby advancing their role in next-generation sustainable and healthcare technologies.

References

1. C. Feldmann, Nanoscale, 3 (2011) 1947-48.
2. A. Henning, H. Angew., Chemie International Edition, 48 (2009) 3572 – 3582.
3. S. Han, et al., Angew., Chemie International Edition, 53 (2014) 11702-11715.
4. Y. Liu, et al., Nanoscale, 5 (2013) 1369–1384.
5. S. Sivakumar, et al., Journal of American Chemical Society, 127 (2005) 12464–12465.
6. K.N. Venkatachalaiah, et al., Materials Research Bulletin, 94 (2017) 442-455.
7. V. Tucureanu, Journal of Material Science, 50 (2015) 1883–1890.
8. L. Liang, et al., Advanced Materials, 25 (2013) 2174-2180.
9. P. Padhye, et al., RSC Advances, 6 (2016) 53504-53518.
10. F. Meng, et al., Journal of Power Sources, 316 (2016) 207–214.
11. M. S. Bhadane, et al., Journal of Materials Science: Mater. in Electroni., 35 (2024) 1453.
12. P. P. Kulkarni, et al., Journal of Physics and Chemistry of Solids, 210 (2026) 113322.

Al- Doped ZnO and Ni-Doped ZnO Nanostructures and Composites for High-Performance Gas Sensors

Baban P. Gawari

Assistant Professor, Department of Physics, Gokhale Education Society's, Arts, Commerce & Science College, Jawhar, Palghar-401 603, Maharashtra, India

Email: jwracsc123@gmail.com

Article DOI Link: https://zenodo.org/uploads/19787754

DOI: 10.5281/zenodo.19787754

Abstract

Al-doped ZnO (AZO) and Ni-doped ZnO (NZO) based composites are promising materials for high-performance gas sensors due to their enhanced electrical conductivity, increased oxygen vacancy concentration, and improved catalytic activity. Al doping enhances carrier concentration and sensitivity toward reducing gases, while Ni doping improves surface reactivity and selectivity toward oxidizing gases and volatile organic compounds. The formation of composites further boosts sensing performance through heterojunction effects and improved charge transfer, enabling lower detection limits, faster response–recovery times, and reduced operating temperatures. These advanced doped ZnO composites are strong candidates for next-generation environmental and industrial gas sensing applications.

Keywords: ZnO, Gas Sensors, Sensitivity

Introduction

Gas sensing technologies have become a cornerstone of environmental monitoring, industrial safety, medical diagnostics, and homeland security. With rapid urbanization and industrial expansion, there is an increasing need for sensitive, selective, reliable, and low-cost gas sensors capable of detecting toxic and flammable gases at low concentrations. zinc oxide (ZnO) stands out for its unique combination of electrical, optical, and catalytic characteristics. [1-3]. Among MOS materials, zinc oxide (ZnO) stands out because of its excellent electrical and optical characteristics, high surface reactivity, and thermal stability [4–6]. The sensitivity of ZnO-based sensors is primarily governed by surface reactions between adsorbed gas molecules and oxygen species, which modulate the electrical resistance of the material [7,8]. ZnO is a II–VI semiconductor with a wide direct bandgap (~3.37 eV) and large exciton binding energy (~60 meV). Despite the potential of pristine ZnO, challenges remain. Conventional ZnO

sensors often operate at high temperatures (>200 °C), suffer from limited sensitivity at low gas concentrations, and exhibit poor selectivity to specific gases [2,9]. In particular, doping ZnO with elements such as aluminum (Al) and nickel (Ni) has shown significant promise. The inclusion of dopants can influence electrical conductivity, defect levels, surface area, catalytic activity, and thus gas sensing performance [10–12]. This chapter explores the synthesis, properties, sensing mechanisms, and performance enhancements of Al-doped ZnO (AZO) and Ni-doped ZnO (NZO) based composites as active materials for high-performance gas sensors.

Fundamentals of ZnO Gas Sensing

- **Gas Sensing Mechanism**

The gas sensing properties of ZnO are primarily based on surface adsorption–desorption processes and charge transfer between adsorbed gas molecules and the semiconductor. In ambient air, oxygen species (O_2^-, O^-, O^{2-}) adsorb on the ZnO surface by capturing electrons from the conduction band, forming a depletion layer that increases electrical resistance. When reducing gases (e.g., CO, H_2, CH_4) are introduced, they react with chemisorbed oxygen ions, releasing electrons back into ZnO and decreasing resistance. Conversely, oxidizing gases (e.g., NO_2) further extract electrons, increasing resistance. [7,13].

- **Purpose and Effects of Doping**

Doping introduces foreign atoms into the ZnO lattice, altering conductivity, defect density, and surface chemical properties. Al doping, typically substituting Zn^{2+} with Al^{3+}, increases free carrier concentration and can reduce crystallite size, enhancing surface area and gas adsorption [15,16]. Ni doping introduces d-orbital interactions and defect states that modify surface reactivity and catalytic activity, improving sensitivity, especially to certain sulfur-containing gases [17,18]. Composite materials, combining doped ZnO with other metal oxides or catalysts, leverage synergistic effects such as heterojunction formation, increased active sites, and improved electron mobility to further enhance sensor performance [19].

Synthesis and Structural Characteristics

- **Al-Doped ZnO (AZO)/ Ni-Doped ZnO**

Al-doped ZnO (AZO) is achieved by introducing Al^{3+} ions into the ZnO lattice. Synthesis methods include spin coating, sol-gel techniques, sputtering, spray pyrolysis, and hydrothermal methods [20]. Recent work reported high-quality AZO films deposited via spin coating, where Al doping (e.g., ~3 at. % Al) reduced crystallite and grain sizes, enlarged the optical bandgap slightly, and altered surface wettability [21]. These microstructural changes significantly impact gas adsorption and sensor performance. Studies have shown that Al

doping leads to smaller ZnO crystallites due to lattice distortion, increased surface roughness, and greater active surface sites, all beneficial for gas sensing [21,22].

Ni-doped ZnO is synthesized by incorporating Ni ions into the ZnO host lattice using hydrothermal, chemical bath deposition, sol-gel, or spray pyrolysis techniques [17,23]. The Ni ion, with a similar ionic radius to Zn, can substitute at Zn sites without dramatically altering the wurtzite structure but influences defect concentration and surface energy. The optimum Ni concentration often exists, where moderate doping enhances gas response but excessive doping may reduce surface area or degrade crystallinity [17,24]. Emerging reports indicate sponge-like Ni-ZnO thin films exhibit enhanced NO_2 response compared to other transition metals doped ZnO films [25].

Gas Sensing Performance of Al & Ni- Doped ZnO Composites

- **Ethanol and VOC Detection**

Al-doped ZnO has been extensively explored for detection of volatile organic compounds (VOCs), particularly ethanol. Recent work demonstrated that 3 at. % Al-doped ZnO thin films achieved significantly higher responses to ethanol vapor compared to undoped ZnO, with fast response/recovery times and excellent stability for low ethanol concentrations (e.g., 20 ppm) [21]. This improved performance is attributed to greater active surface area, increased oxygen vacancy concentration, and enhanced electron transfer dynamics.

- **Sulfur Gas Detection**

Recent studies on AZO nanoplatelets have shown that Al doping enhances H_2S gas sensing. The optimal operating temperature achieved for peak response was around 300 °C, with Al doping levels significantly influencing response magnitude.

- **Composite Structures**

AZO combined with other metal oxides (e.g., CuO, Co_3O_4) forms heterojunctions that further enhance sensing performance. For instance, Al-ZnO/CuO composites exhibit high selectivity and fast response to ammonia (NH_3) gas even at room temperature due to synergistic effects between n-type AZO and p-type CuO. The heterojunction interfaces facilitate charge separation and intensified modulation of electrical resistance under gas exposure.

- **H_2S and NO_2 Detection**

Ni-ZnO nanostructures show significant promise for detecting sulfur-containing gases. Hydrothermally synthesized Ni-ZnO nanowire arrays exhibited high selectivity and sensitivity toward H_2S, outperforming responses to ethanol, acetone, toluene, and NO_2 at optimized operating temperatures (~250 °C) [17].

The enhanced sensing performance is directly linked to Ni's influence on surface chemistry, increasing active sites for adsorption.
Recent reports also demonstrate that sponge-like Ni-ZnO films enhance NO_2 sensing performance. Doping Ni into ZnO significantly increased sensor response (e.g., response values of ~2.1–6.3 over 10–100 ppm NO_2), with porous morphology contributing to improved gas diffusion and adsorption [25]. These findings indicate Ni doping is particularly effective for oxidizing and sulfur gas detection.

Conclusion

Doping ZnO with Al and Ni has emerged as a powerful strategy to improve the performance of gas sensors by enhancing sensitivity, selectivity, and stability. Al-doped ZnO composites provide increased surface activity and conductivity beneficial for VOC and reducing gas detection, while Ni-doped ZnO composites excel in detecting oxidizing and sulfur gases such as NO_2 and H_2S. Composite heterostructures further amplify sensor performance by leveraging synergistic effects. Tailoring dopant concentration, nanostructure morphology, and composite interfaces are key to optimizing gas sensing behavior. Continued research into room-temperature operation, humidity mitigation, and integration with advanced electronics will support the broad deployment of doped ZnO gas sensors in environmental, industrial, and medical applications.

References

1. Gurlo, A. Metal oxide gas sensors: Sensitivity and influencing factors. Sens. Actuators B Chem. 2016.
2. Yamazoe, N.; Shimanoe, K. Sens. Actuators B Chem. 2009.
3. Korotcenkov, G. Metal oxide sensors: What determines the choice? Mater. Sci. Eng. B 2007.
4. Özgür, Ü. et al. J. Appl. Phys. 2005.
5. Janotti, A.; Van de Walle, C. G. Rep. Prog. Phys. 2009.
6. Wang, Z. L. J. Phys.: Condens. Matter 2004.
7. Barsan, N.; Weimar, U. Conduction model for MOS sensors. J. Electro-ceramics 2001.
8. Xu, C. et al. Mechanisms for gas sensing. Sens. Actuators B Chem. 2018.
9. Neri, G. Doped ZnO for gas sensors. Sens. Actuators B Chem. 2017.
10. Acharya, T. R. et al. Impact of Al doping on ZnO ethanol sensing. Ceram. Int. 2024, 55143–55158.
11. Shewale, R. N. et al. Al-doped ZnO nanoplatelets for H_2S detection. Sci. Rep. 2025.
12. Enhanced H_2S Gas-Sensing Performance of Ni-Doped ZnO Nanowire Arrays. PubMed 2024.

13. Effect of Al doping on NO_2 sensing. Sci. Total Environ. 2022.
14. ZnO gas sensors fundamentals. Sensors 2020.
15. Al doping effects on ZnO properties. Sens. Actuators B Chem. 2018.
16. Al-ZnO/CuO composites. Mater. Sci. Eng. B 2018.
17. Ni doping influence on ZnO. J. Alloys Compd. 2025.
18. Ni doping and sensing optimization. ArXiv 2024.
19. Composite heterostructures for gas sensing. Sens. Actuators B Chem. 2019.
20. AZO synthesis methods review. J. Mater. Chem. 2019.
21. Acharya et al., ethanol sensing enhancements. Ceram. Int. 2024.
22. Al doping effects on ZnO nanostructures. Sensors 2023.
23. Ni-ZnO nanowires for H_2S. PubMed 2024.
24. Porosity and morphology in Ni-doped sensors. Phys. J. 2025.
25. Ni-doped ZnO thin films for NO_2. IJIRSET 2025.

Rare Earth Doped Metal Oxides for Enhancing Gas Sensing Response in $BiFeO_3$ Ferrite

[1]Avinash Ramkishan Gaikwad, [2]Amol Rajendrasing Pardeshi

[1]Vivekanand College, Kolhapur (An Empowered Autonomous Institute)

[2]Dada Patil Mahavidhyalaya Karjat, Dist: Ahilyanagar 414 402

Email: argphysics@gmail.com

Article DOI Link: https://zenodo.org/uploads/19787847

DOI: 10.5281/zenodo.19787847

Abstract

Bismuth ferrite, also known as bismuth iron oxide, has the chemical formula $BiFeO_3$, also known as BFO. It has the characteristics of a multiferroic perovskite structure, which makes it a promising candidate for gas sensor application due to its structural, electrical, and magnetic properties. In this chapter, the application of rare earth (RE) dopants for the development of metal oxide gas sensors based on bismuth iron oxide will be addressed. Specifically, the fundamental properties of bismuth iron oxide, the fundamental properties of gas sensors, and the application of rare earth dopants for the development of gas sensors will be addressed. In addition, the application of lanthanum, erbium, yttrium, and gadolinium dopants will be addressed, based on the recent literature available on the subject matter. In addition, the challenges associated with the application of bismuth iron oxide will be addressed, including the future prospects of the development of gas sensors based on the compound.

Introduction

Bismuth ferrite ($BiFeO_3$) is a lead-free perovskite-type multiferroic material with simultaneous ferroelectric, antiferromagnetic, and piezoelectric properties at room temperature. Its rhombohedral structure with the R3c space group and relatively small band gap (2.2-2.8 eV) enable its application in different fields. In the field of gas sensing, $BiFeO_3$ is a p-type semiconductor where the variation in the electrical resistance is observed after the reaction with the target gas [1-2]

Gas sensors based on metal oxide semiconductors play a vital role in the detection of volatile organic compounds (VOCs), toxic gases, and biomarkers present in exhaled breath. However, the application of $BiFeO_3$ is limited by its low sensitivity, high working temperature, and poor selectivity. Thus, the doping of rare earth elements such as lanthanides and sometimes scandium and yttrium has been found to be a promising approach to overcome the drawbacks associated

with $BiFeO_3$.

This chapter is focused on RE-doped $BiFeO_3$ systems. It is a synthesis of the latest research on the synthesis, performance, and mechanisms of the material. It is focused on the applications for the detection of gases such as CO, acetone, n-butanol, and ethanol [3-6]

Fundamentals of $BiFeO_3$ and Gas Sensing Principles

- **Structure and Properties of $BiFeO_3$**

It has a distorted perovskite structure, with Bi^{3+} at the A site and Fe^{3+} at the B site. The lone pair on the Bi^{3+} contributes to the ferroelectric polarization, and the G-type antiferromagnetism arises from the super exchange between the Fe-O-Fe interactions. The band gap of the material makes it possible for visible light to be absorbed, which can influence gas sensing. When nanostructured, such as nanoparticles and nanofibers, $BiFeO_3$ has a greater surface area, which can be advantageous for gas sensing. Synthesis techniques include sol-gel, hydrothermal, and solid-state reactions [1-7]

- **Gas Sensing Mechanisms in Metal Oxides**

In p-type semiconductors such as $BiFeO_3$, gas sensing occurs through the chemisorption of oxygen from the atmosphere, which forms O_2^-, O^-, and O^{2-}, trapping holes and creating a HAL, thus decreasing resistance. In the presence of a reducing gas, such as CO and VOCs, these gases react with adsorbed oxygen, releasing trapped holes back to the valence band, thus increasing resistance [2].

The Performance Parameters of a Gas Sensor Are

- **Sensitivity/Response:** Change in resistance, typically expressed as Rg / Ra or Ra / Rg, where Rg is resistance in the gas and Ra is resistance in air.
- **Response/Recovery Time:** Time taken to reach 90% of the steady-state value. Selectivity: Ability of the sensor to respond to a particular gas in the presence of interferents.
- **Limit of Detection:** Lowest concentration that can be detected.
- **Operating Temperature:** Temperature at which the sensor is optimized to operate.
- **Stability:** Ability of the sensor to function reliably over a long period of time. Doping helps to improve these parameters [11]

Role of Rare Earth Doping in $BiFeO_3$

Rare earth ions have partially filled 4f orbitals. These replace Bi^{3+} (A-site) due to comparable ionic radii (e.g., La^{3+}: 1.03 Å and Bi^{3+}: 1.03 Å). This doping also stabilizes the perovskite structure, prevents Bi volatility during synthesis, and induces lattice distortions. Some benefits, Oxygen Vacancies: Doping introduces

defects that favour oxygen adsorption. Band Gap Tuning: Reduces the band gap to Favor charge transfer. Morphology Control: Doping results in porous or nanofibrous materials to facilitate better gas diffusion. Ferroelectricity Improvement: Enhances polarization to facilitate charge separation. The synthesis process involves incorporating RE precursors in sol-gel or hydrothermal processes and then annealing [6-10].

Specific Rare Earth Dopants and Their Effects on Gas Sensing

- **Lanthanum (La) Doping**

La-doped $BiFeO_3$, for instance, such as Bi1-x Lax FeO_3, was explored for CO sensing. Doped samples with 8% and 10% La showed faster response times (0.17 s, 0.40 s), as well as increased sensitivity, owing to the presence of oxygen vacancies and phase purity. Working at reduced temperatures, the sensors showed selectivity to NO_2 and NH_3. La-activated $BiFeO_3$ modified ZnO spheres were explored for n-butanol sensing at ppb levels, reaching a response of 8.4 to 10 ppm at 300°C [14]

- **Erbium (Er) Doping**

Er-doped $BiFeO_3$ nanoparticles, synthesized via sole-gel, show enhanced acetone sensing. The doping induces rhombohedral-to-orthorhombic phase transition, reduces particle size (~20-50 nm), and lowers band gap (2.1 eV). Sensitivity reaches ~50 for 100 ppm acetone at 280°C, with response time <10 s and good selectivity over ethanol and formaldehyde. Mechanisms involve increased surface area and defect-mediated adsorption [11-15]

Dopant	**Target Gas**	**Optimal Temp (°C)**	**Response (to conc.)**	**Response/ Recovery Time (s)**	**Key Enhancement Factor**	**Reference Insights**
La (8–15%)	CO	~300	High (fast kinetics)	0.17–0.40	2–5× faster than pristine	Ultra-fast response; phase purity
La-activated	n-Butanol	300	8.4 (10 ppm)	N/A	ppb-level LOD (~50 ppb)	ZnO composite; superior selectivity
Er (10%)	Acetone	280–300	43–50 (100 ppm)	<10	4.8× pristine BFO	Phase transition; band gap reduction

Er (10%)/SnO_2	Ethanol	330	62 (100 ppm)	5/96	2.3× base Er-BFO	p-n heterojunction; oxygen vacancies
Y (3%)	n-Butanol	150	60.2 (100 ppm)	9/47	2–3× pristine; low temp operation	Nanofibers; excellent repeatability
Gd/others	VOCs (general)	RT–200	Enhanced (photocatalysis-linked)	N/A	Improved charge separation	Emerging; multiferroic benefits

Table 1 summarizes performance metrics

- **Yttrium (Y) Doping**

Y-doped $BiFeO_3$ nanofibers show improved performance for n-butanol gas sensing. The response values are 2-3 times higher than those of pure $BiFeO_3$. The LOD is 1 ppm at 250°C. Selectivity is also high for acetone and toluene [8-15]

- **Gadolinium (Gd) Doping**

Doping with Gadolinium improves the photocatalytic activity of $BiFeO_3$. This is related to gas sensing through the help of the photo-assisted mechanism. Gd^{3+} substitution decreases the band gap and improves the charge carrier separation. This improves the VOC degradation and sensing. For sensor applications, Gd-doped $BiFeO_3$ is promising for the detection of humidity and gases; however, the gas sensing data is still emerging [14]

Mechanisms of Enhancement in RE-Doped $BiFeO_3$

- **Defect Engineering**

Oxygen vacancies (V-O) are created through RE doping due to charge compensation. Lattice strain caused by RE^{3+} replacing Bi^{3+} results in defects. These vacancies improve adsorption sites, thereby increasing O_2 chemisorption and reaction with target gases [10].

- **Electronic and Band Structure Modulation**

Doping influences the Fermi level, band gap, and mobility of charge carriers. In Er^{3+}-doped $BiFeO_3$, reduction of the band gap helps in the generation of electron-hole pairs for sensing in ambient conditions [11].

- **Ferroelectric and Multiferroic Coupling**

The ferroelectric polarization in $BiFeO_3$ induces internal fields that separate charge carriers, thereby inhibiting their recombination and increasing sensitivity. This effect is enhanced in RE-doped samples due to increased remanent polarization [12].

Conclusion

Rare earth doping greatly improves the gas sensing properties of $BiFeO_3$ ferrite, which is achieved through defect, electrical, and morphological engineering. The use of La, Er, Y, and Gd dopants ensures that gas sensors based on $BiFeO_3$ ferrite exhibit high sensitivity, low-temperature performance, and gas selectivity, making them critical for various applications. This chapter emphasizes the role of RE-doped $BiFeO_3$ ferrite in improving sensor technology, creating a path towards sustainable and efficient gas sensors.

References

1. Kumar M, et al. Ceram Int. 2021;47:12345-12360.
2. Singh A, et al. J Mater Chem C. 2020;8:15670-15685.
3. Zhang Y, et al. Appl Phys Lett. 2022; 120:082902.
4. Korotcenkov G. Mater Sci Eng B. 2020; 256:114558.
5. Wang C, et al. Sens Actuators B Chem. 2021;329:129119.
6. Li J, et al. J Alloys Compd. 2019;803:25-34.
7. Catalan G, Scott JF. Adv Mater. 2019; 31:1805610.
8. Chen D, et al. Nanomaterials. 2022; 12:2145.
9. Mirzaei A, et al. Chemosensors. 2021; 9:190.
10. Zhao H, et al. J Eur Ceram Soc. 2020;40:3712-3720.
11. Liu X, et al. Sens Actuators B Chem. 2023;375:132850.
12. Patel R, et al. Mater Today Chem. 2022;24:100864.
13. Sharma P, et al. J Mater Sci Mater Electron. 2021; 32:14567-14580.
14. Xu L, et al. ACS Appl Electron Mater. 2022; 4:2234-2245.

Synthesis Route Techniques for the Development of Bio-Derived Carbon Quantum Dots (CQDs)

Nita Shinde, Shraddha Pande

Department of Physics, L.A.D. and Smt. R.P. College for Women, Nagpur 440010, India

Email: nita.shinde2931980@gmail.com

Article DOI Link: https://zenodo.org/uploads/19787940

DOI: 10.5281/zenodo.19787940

Abstract

Bio- derived carbon quantum dots (CQDs) prepared via bottom-up or top -down approach. CQDs synthesized from bottom -up synthesis methods plays an important role to control size and surface properties and hence can be employed in applications such as biomedical, bioimaging applications, sensing, catalyst, solar cell, multicolour LEDs, Waste water treatment etc.

Keywords: Bioderived CQDs. Different methods to synthesize CQDs

Introduction

Carbon Quantum dots (CQDs)are the nanomaterials which have size typically less than the 10 nm, CQDs gathered an attention because of their straightforward synthesis methods, water solubility, non-toxicity, greater light response, chemical stable, huge surface area and functional groups (hydroxyl, carboxyl, amino) influence properties, employed for energy storage, sensing, catalysis, bioimaging applications. These CQDs serve as alternatives for the semiconductor metal-based quantum dots (QDs) and synthetic organic dyes as these materials are toxic and hence cause harmful environmental impact Consequently, CQDs are of great interest due to their strong fluorescence properties and low toxic material property , shows wide applications such as Drug delivery, photocatalysis, optoelectronics, bio-imaging, biomedical uses ,as well as Single electron transistors, solar cells, multicolor LEDs, wastewater treatment etc.

Green Synthesis Methods for the development of CQDs

CQDs can be synthesized via green synthesis methods by using agricultural waste, fruit peel, biomass sources, plant extract, shells, renewable sources, flower extracts, leaves, etc. It helps to reduce our dependence on fossil fuel use of non-renewable energy sources and also helps to convert this waste into valued products. These green raw materials are easily available and found to be a widely

in the nature, these low-cost materials are replacement for the chemicals used in the preparation methods. These CQDs material green synthesis techniques are of great importance because of ease synthesis techniques includes sustainability and renewability. environmentally friendly and sustainable. These green synthesis methods are nontoxic, provides high quantum yield, high sustainability, potential for scale up.

Carbon Quantum Dots (CQDs) can be synthesized via bottom up or top-down synthesis methods. The bottom-up approach is often preferred, as the materials synthesized from bottom-up approach are of low-cost techniques and environment friendly helps in controlling size and ensures uniformity across the particle population. As these bottom-up approach, building structures from atomic or molecular precursors as compared to top-down approach in which larger one cut up to nanoscales are formed leading to improved performance and broader applicability.

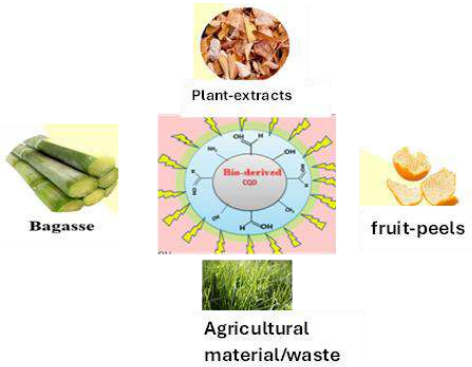

Figure 1: Bioderived CQDs from natural resources

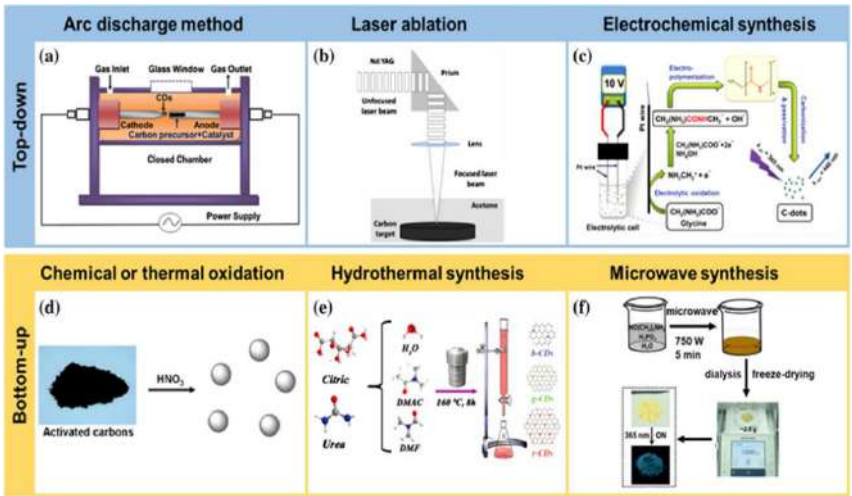

Figure 2: Synthesis of CQDs: Bottom- up and Top- down approach methods

- **Arc Discharge Synthesis Method**

This method is the easy and commonly used for synthesis. This method uses a easy to handle instrument and obtain the required high temp. which is required for the synthesis of CQDs by evaporating the plasma (Wu et al., 2012).'This synthesis method properties as rate of flow, metallic concentration as well as The variations of the process parameters such as flow rate, metal absorption, and compression of gas are the most important to obtain the finest product of carbon nano tubes for this technique '.

- **Laser Ablation Synthesis Method**

Monodispersed, fine and equal size CQDs with high fabrication rates can be synthesized by using this method. Colloidal solution of CQDs can be obtain by laser ablation method by using variety of solvents. The laser refinement and all the initial antecedents found to be the constraints which helps to properties of the product by using this method.

- **Electrochemical Synthesis Method**

The electrochemical synthesis method is of a "top-down" approach. This method is a chemical cutting process of a carbon material such as graphite, carbon nanotube, or carbon fibre electrodes8. The CQDs synthesized from this method not equal in size and need further purification via filtration or require chromatography to synthesize monodispersed carbon quantum dots.

- **Chemical Oxidation Synthesis Method**

Natural materials are treated with the use of chemical oxidants like hydrogen peroxide and oxidizing acids to synthesize CQDs. In this method, the bio waste materials are treated with a chemical oxidant first, then they are carbonized. After filtration and purification, the subsequent CQDs can be obtained.

- **Hydrothermal Synthesis Method**

This method is a bottom-up synthesis method for the preparation of CQDs. In the hydrothermal synthesis method, all the bio- precursors are mixed in a solvent then reaction is carried out in a Teflon-lined autoclave at a very high temperature range. Autoclaves are closed tightly and pressure is applied for the reaction to be carried out to prepare desired product 8,9.

- **Microwave Radiation Synthesis Method**

The rapid synthesis of bio- derived CQDs at low temperature can be possible by using this method using bio- waste as a precursor. CQDs obtain by this method can be used for biomedical applications. This synthesis method offers a significant enhancement in the competencies of reaction as well as saves time.

- **Solvothermal Synthesis Method**

In this synthesis method unlike the hydrothermal method the use of a non-aqueous precursor solution such as benzene, DMF (dimethylformamide),or DMSO (dimethyl sulfoxide), are used to synthesized CQDs instead of organic solvents of water, necessary for the determination of size and shape of the synthesized materials. With this synthesis method, it is able to precisely legalize the size, shapes, and crystallinity of the CQDs.

- **Pyrolysis Synthesis method**

Pyrolysis method is accomplished of changing waste into CQDs. This is a thermal decomposition process. This method is used to synthesize to produce Bio-derived CQDs

References

1. Fang, Xuan-Wei, Chang, Hao, Wu, Tsunghsueh, Yeh, Chen-Hao, Hsiao, Fu-Li, Ko, Tsung-Shine, Hsieh, Chiu-Lan, Wu, Mei-Yao, Lin, Yang-Wei, Sci Rep, 9, 22,2024, 23573- 23583,
2. Praseetha, P.K., Litany, R., Alharbi, H.M. et al., Sci Rep 14, 24435 (2024).
3. Sruti Chattopadhyay, N., Mehrotra, S. & Jain Harpal Singh, Microchemical J. 170,2021.
4. Sharma, V. D. et al. Mater. Today Sustain. Volume 19,2022,100184,2589 – 2347.
5. Liu S, et al. Adv Mater. 2012;24(15): 2037-41.
6. Chu, Xiaohong & Wang, Mingqian & Shi, Shaoze & Sun, Baohong & Song, Qiuxian & Xu, Wang & Shen, Jian & Zhou, Ninglin. (2022).
7. Titus Chinedu Egbosiuba, Ijeoma Jacinta Ani, Blessing Onyinye Okafor, Saheed Mustapha, Jimoh Oladejo Tijani, Chinenye Adaobi Igwegbe, Chukwunonso Chukwuzuloke Okoye, Wisdom Chukwuemeke Ulakpa, Ebuka Emmanuel Ezennajiego, Ambali Saka Abdulkareem, Advanced Nanoscale Materials,2023, 103-141.
8. Anuja Vibhute, Tejaswini Patil, Rutuja Gambhir, Arpita Pandey Tiwari, Applied Surface Science Advances,11, 2022,100311, 2666-5239.
9. Yongqiang Dong, Ruixue Wang, Hao Li, Jingwei Shao, Yuwu Chi, Xiaomei Lin, Guonan Chen,50, 8,2012,2810-2815.
10. Lei Bao, Zhi-Ling Zhang, Zhi-Quan Tian, Li Zhang, Cui Liu, Yi Lin, Baoping Qi, Dai-Wen Pang,Advanced materials, 23, 48, 2011, 5801-5806.
11. S.M. Sayyah, M.M. El-Deeb, S.M. Kamal, R.E. Azooz,J. Appl. Polym. Sci., 112 (6) (2009)
12. Hu Z, Jiao X-Y, Xu L. Microchem J. 2020;154: 104588.
13. Wang J, Wang CF, Chen S. Amphiphilic egg-derived carbon dots: rapid plasma fabrication, pyrolysis process, and multi-color printing patterns.

Angew Chem Int Ed. 2012;51(37):9297–301.
14. Aniruddha Kundu, Jungpyo Lee, Byeongho Park, Chaiti Ray, K. Vijaya Sankar, Wook Sung Kim, Soo Hyun Lee, Il-Joo Cho, Seong Chan Jun, Journal of Colloid and Interface Science, 513,2018,505-514.
15. Su J, et al. J Food Meas Charact. 2023;17: 4565.

Quantum Dot Nanomaterials: Synthesis, Quantum Confinement, and Emerging Applications in Energy Storage, Gas Sensing, and Dosimetry

Kangude Sahadev Hanumant, Khedkar Akanksha Dipak

Rayat Shikshan Sanstha's Dada Patil Mahavidyalaya Karjat, Dist- Ahilyanagar-414402

Email: sahadevkangude72832@gmail.com

Article DOI Link: https://zenodo.org/uploads/19788034

DOI: 10.5281/zenodo.19788034

Abstract

Quantum dots (QDs) are nanometre-scale semiconductor materials whose optical and electronic properties are strongly influenced by the phenomenon of quantum confinement. Their tunable band gap, high surface-to-volume ratio, along with superior electrical conductivity make them promising candidates for advanced technological applications. This chapter discusses the fundamental properties, synthesis methods, and multifunctional applications of quantum dots. Common synthesis techniques like hydrothermal, sol-gel, and chemical co-precipitation are highlighted. The chapter also explores the role of quantum dots in energy storage devices, gas sensing, and radiation dosimetry, emphasizing their ability to enhance electrochemical performance, sensing sensitivity, and radiation detection. Finally, current challenges and future research directions for sustainable and scalable quantum dot technologies are discussed.

Keywords: Quantum Dots (QDs), Energy Storage Devices, Supercapacitors, Gas Sensing & Radiation Dosimetry.

Introduction

Worldwide energy demand crisis is characterized by the growing disparity between energy demand and supply, increasing fuel costs, and environmental problems associated with the extensive use of fossil fuels. Factors such as rapid industrial development, rising population, and accelerated urbanization have further aggravated this challenge worldwide [1]. In this context, advanced nanomaterials have attracted considerable attention for improving energy storage technologies. Among them, quantum dots (QDs) are nano range semiconductor materials that have shown significant potential for enhancing the efficiency of modern energy storage systems, including batteries and supercapacitors. Their distinctive physical and chemical characteristics make them highly suitable for

next-generation energy technologies [2].

Different types of quantum dot materials have been investigated for energy storage applications. These include carbon-based QDs, silicon QDs, and metal or metal-oxide QDs such as ZnO and TiO_2. Furthermore, chalcogenide quantum dots including CdS, CdSe, MoS_2, and WS_2, as well as MXene-derived QDs such as Ti_3C_2, have demonstrated remarkable potential because of their superior electrochemical behavior and improved charge storage capability [3].

Among the different nanomaterials investigated, carbon quantum dots (CQDs) are considered attractive because of their environmentally benign nature, efficient electrical transport properties, and high stability. Their nanoscale structure, large specific surface area, and the presence of abundant surface functional groups significantly enhance their electrochemical behavior. These properties enable CQDs to improve electrical conductivity, increase active surface sites, and promote rapid ion transport within electrode materials. Consequently, they bring about higher energy density, enhanced cycle durability and superior device efficiency in modern energy-storage systems. As the demand for sustainable energy solutions increases, supercapacitors have evolved from basic backup power units to advanced systems used in grid storage, energy harvesting, and regenerative braking [4].

Quantum dots also exhibit a large surface-to-volume ratio, offering many active sites for electrochemical reactions and thereby improves charge storage capability [5]. Additionally, their tunable band gap and superior electrical conductivity facilitate efficient charge transfer processes in batteries and supercapacitors. The extremely small size of these nanomaterials also shortens ion diffusion paths, resulting in faster charging and discharging rates [6].

To obtain quantum dots with controlled size, morphology, and physicochemical properties, several synthesis approaches have been developed. Commonly used methods like the hydrothermal synthesis, sol-gel, and chemical precipitation techniques. In the sol–gel method, precursor materials experience hydrolysis and condensation reactions to form a gel framework, which is subsequently dried and calcined to produce quantum dots with high purity and uniform particle size. This technique is frequently employed for the preparation of TiO_2 and ZnO quantum dots [7]. The hydrothermal or solvothermal method involves carrying out the reaction in a sealed autoclave at elevated temperature and pressure, allowing controlled crystal growth and improved crystallinity. This approach is widely applied for synthesizing carbon quantum dots and various metal oxide quantum dots [8]. This method is relatively simple, economical, and suitable for High-scale production, and it is often used for synthesizing metal sulfide and oxide quantum dots such as CdS and CdSe [9].

Quantum Confinement and Applications

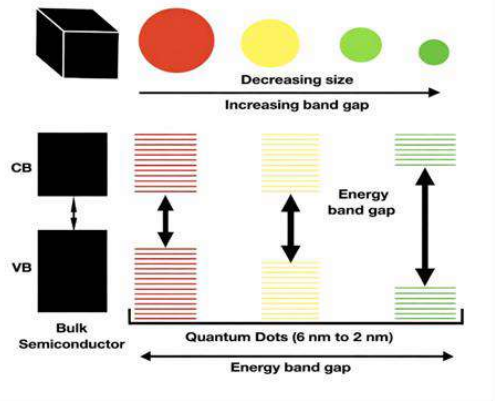

Fig. a. Quantum Confinement [10].

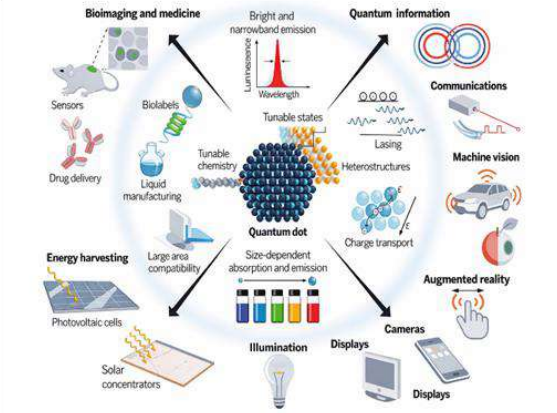

Fig. b. Application of QD [11].

Quantum dots are core–shell semiconductor nanostructures whose properties are strongly influenced by the quantum confinement effect when their size becomes less than the exciton Bohr radius. Under this condition, the electronic energy levels become discrete, resulting in size-dependent band gaps. Smaller quantum dots exhibit larger band gaps and larger energy levels compared to higher ones. Consequently, quantum dots exhibit adjustable optical and electronic properties, which enable their application in various technological fields. [10].

- **Applications in Energy Storage Devices**

Quantum dots enhance energy storage performance by providing high surface area and short ion diffusion pathways, which improve electrochemical kinetics. In supercapacitors, they increase capacitance and energy density through abundant active sites. In lithium-ion batteries, QDs improve conductivity, structural stability, and cycle life, especially when combined with nanomaterials like graphene [12].

- **Applications in Gas Sensing**

Quantum dots enable highly sensitive gas detection due to their tunable electronic properties and large surface area. Gas adsorption induces measurable changes in electrical or optical signals via charge transfer mechanisms. QD-based sensors offer fast response, room-temperature operation, and high selectivity, especially with surface functionalization [13].

- **Applications in Dosimetry**

Quantum dots are effective in radiation dosimetry due to their radiation-dependent photoluminescence behavior. They allow precise, real-time measurement of radiation doses with high sensitivity. Due to their small dimensions and tunable optical characteristics, they are suitable for use in

medical radiotherapy, environmental monitoring, and nuclear safety fields [14].

Challenges and Future Scope

Although quantum dots offer significant advantages in energy storage, sensing, and dosimetry, several challenges remain. Certain heavy metal quantum dots, such as CdS and CdSe, may cause environmental and health risks because of their toxicity. Achieving large-scale synthesis with uniform size, controlled morphology, and long-term stability is also difficult. Future research should emphasize the development of eco-friendly quantum dots, particularly carbon- and silicon-based materials, along with eco-friendly synthesis approaches and hybrid nanostructures to improve efficiency and enable real technological applications.

Conclusion

Quantum dots are widely recognized as important nanomaterials owing to their size-related optical, electronic, and electrochemical features. Their high surface area, tunable band gap, and efficient electrical conductivity enable their use in applications such as energy storage devices, gas sensing, and radiation dosimetry. Various synthesis methods, like as hydrothermal, sol-gel , and chemical precipitation techniques, enable the controlled preparation of quantum dots with desirable characteristics. Despite existing challenges related to toxicity and large-scale production, continued research on eco-friendly materials and advanced synthesis strategies is expected to further expand the practical applications of quantum dots in modern nanotechnology and sustainable energy systems.

References

1. Farghali, M., Osman, A. I., Mohamed, I. M. A., et al. (2023). Strategies to save energy in the context of the energy crisis: A review. Environmental Chemistry Letters, 21, 2003–2039.
2. Efros, A. L., & Brus, L. E. (2015). Nanocrystal quantum dots. Annual Review of Materials Research, 45, 1–27.
3. Zhang, Y., Li, X., & Wang, H. (2022). Advances in quantum dot nanomaterials. Nano Energy, 90, 106–115.
4. Zhang, Y., Liu, X., Wang, S., & Li, H. (2023). Carbon quantum dots for advanced supercapacitor applications: Progress and challenges. Journal of Energy Storage, 62, 106997.
5. Kumar, S., Gupta, R., & Singh, A. (2023). Emerging nanomaterials for energy conversion and storage applications. Materials Research Express, 10(4), 042001.
6. Gupta, R., Kumar, S., & Sharma, P. (2022). Quantum dots for next-generation energy storage devices. Carbon Nanomaterials, 8(3), 160–175.

7. Brinker, C. J., & Scherer, G. W. (1990). Sol–gel science: The physics and chemistry of sol–gel processing. Academic Press
8. Wang, Y., & Hu, A. (2014). Carbon quantum dots: synthesis, properties and applications. Journal of Materials Chemistry C, 2(34), 6921–6939.
9. Murray, C. B., Norris, D. J., & Bawendi, M. G. (1993). Synthesis and characterization of nearly monodisperse CdE (E = S, Se, Te) semiconductor nanocrystallites. Journal of the American Chemical Society, 115(19), 8706–8715
10. Quantum dots: an overview of synthesis, properties, and applications Kushagra Agarwal, Himanshu Rai and Sandip Mondal Department of Electrical Engineering, Indian Institute of Technology Bombay, Mumbai 400076, India
11. García de Arquer, F. P., Talapin, D. V., Klimov, V. I., Arakawa, Y., Bayer, M., & Sargent, E. H. (2021). Semiconductor quantum dots: Technological progress and future challenges. Science, 373(6555), eaaz8541.
12. Chen, L., Wang, X., & Zhang, Y. (2022). Quantum dots for electrochemical energy storage applications: Progress and perspectives. Nanomaterials, 12(21), 3814.
13. Zhang, J., Liu, X., & Neri, G. (2018). Nanostructured materials for room-temperature gas sensors. Advanced Materials, 30(36), 1705265.
14. García-Torres, J., Gómez, L., & González, R. (2019). Quantum dots for radiation dosimetry applications: A review. Radiation Physics and Chemistry, 159, 40–47.

Quantum Dots: Fundamentals and Applications

Preethi. A. Nikam

Department Of Physics,Tuljaram Chaturchand College, Baramati

Email: drpreethinikam@gmail.com

Article DOI Link: https://zenodo.org/uploads/19788114

DOI: 10.5281/zenodo.19788114

Abstract

In this ever-changing world, the technology has given countless boons to the humanity by making devices sustainable and energy efficient. Quantum dots have opened the doors of technology that was hidden for a while. Quantum dots (QDs) are semiconductor nanocrystals that reveal distinctive optical and electronic properties due to the quantum confinement effect. QDs have size-dependent optical and electronic behavior, which allows tuning of the band gap energy and emission wavelength by controlling the particle size during reaction. Quantum dots demonstrate remarkable properties such as high photoluminescence quantum yield, narrow emission spectra, broad absorption bands, and excellent photostability. These characteristics make them highly attractive for applications in optoelectronic devices, biological imaging, solar cells, light-emitting diodes, sensors, and quantum computing technologies. This Chapter discusses about the fundamentals, principle and applications.

Keywords: Quantum Dots, Quantum Confinement, Exciton dynamics

Introduction

The rapid evolution of nanotechnology has led to the reduction of the dimensions of materials upto the scale of nanometers (1–100 nm), which significantly changes the physical and chemical properties of the materials. Such nanoparticles (NPs), exhibit exceptional properties which have enabled major breakthroughs in various fields [1,2]. Quantum dots (QDs) are one of the most diverse classes of nanoparticles, and is basically semiconductor nanocrystals of size ranging between 2 to 10 nm in diameter. These have discrete energy levels and not continuous energy bands as e--h+ are confined in all three spatial directions [3]. Such QDs are referred to as Artificial Atoms [4]. Alexei Ekimov first observed the shift in optical absorption as a function of particle size [5]. Independently, Louis Brus observed similar behavior in colloidal cadmium sulfide systems [6]. The fundamental characteristics of QDs which make them outstanding NPs are high surface to volume ratio and Quantum mechanical effects [7]. Further developments in the synthesis process and surface engineering will expand the

usage of QDs in advanced next generation devices, as nanoparticles and quantum dots have proven to be reliable materials.

Synthesis of Quantum Dots

Both physical and chemical methods are used to synthesise Quantum dots (QDs) under controlled conditions. The most commonly used method is the colloidal hot-injection method in which size-controlled nucleation and growth is enabled. The compositional uniformity is achieved by sol–gel method via hydrolysis and condensation reactions. Hydrothermal synthesis produces highly crystalline QDs at high temperature and pressure in autoclaves. For optoelectronic devices chemical vapor deposition (CVD) and Molecular beam epitaxy (MBE) are best suited as these methods enable epitaxial growth of QDs on substrates. In applications where the thickness must be precise, SILAR (Successive Ionic Layer Adsorption and Reaction) technique is used as it allows layer-by-layer growth for thickness control.In addition to the above methods, microwave-assisted synthesis provides rapid, energy-efficient production with narrow size distribution [8].

Underlying Mechanisms of Quantum Dots:

- **Quantum Confinement Effect:** In Quantum dots there is confinement of motion of electrons and holes in all three spatial dimensions.The quantum confinement effect takes place when the particle size becomes comparable to or smaller than the exciton Bohr radius and as a result the continuous energy bands of bulk semiconductors break into discrete energy levels, as the particle size. Thus, the electrons in QDs occupy quantized energy states [8].
- **Exciton Formation:** When a photon is absorbed by QD,then photon excites an electron from the valence band to the conduction band. Thus, a hole is left behind in the valence band. This electron and hole together form a bound pair called exciton. As the Carriers are spatially confined, the exciton energy levels become discrete [9].
- **Radiative Recombination:** After excitation, the electron relaxes from the conduction band to the valence band and it combines with the hole. The energy difference between these states is released as a photon. Since the bandgap depends on particle size, just by controlling the size of QD, the emission wavelength can be tuned [9].

QD Size	Bandgap Energy	Emission Color
Small	Large	Blue
Medium	Moderate	Green
Large	Small	Red

- **Surface Effect:** Since the QDs have large surface-to-volume ratio, many atoms lie on the surface. And this greatly influences the emission efficiency and stability [8,9].

Classification of Quantum Dots

Category	Type	Examples	Key Features	Refs.
Based on Composition Category	II–VI Semiconductor QDs	Cadmium Selenide, Cadmium Sulfide	High quantum yield, size-tunable emission	[2]
	III–V Semiconductor QDs	Indium Phosphide, Indium Arsenide	Lower toxicity alternative to Cd-based QDs	[10]
	IV–VI Semiconductor QDs	Lead Sulfide, Lead Selenide	Near-infrared (NIR) emission	[11]
	Carbon Quantum Dots (CQDs)	Carbon-based nanodots	Biocompatible, low toxicity	[12]
	Graphene Quantum Dots (GQDs)	Graphene fragments	High conductivity, edge-state emission	[13]
	Perovskite QDs	Cesium Lead Bromide	Narrow emission, high color purity	[14]
Based on Structure	Core-only QDs	Bare semiconductor core	Surface defects influence emission	[2]
	Core–Shell QDs	CdSe/ZnS	Improved stability, enhanced quantum yield	[15]
	Doped QDs	Mn-, Cu-doped QDs	Modified optical/magnetic properties	[16]
Based on Dimensionality	0D QDs	Fully confined nanocrystals	Discrete energy levels	[2]
Based on Synthesis	Top–Down QDs	Lithographically defined QDs	Precise size control	[10]
	Bottom–Up QDs	Colloidal synthesis	Scalable, solution-processable	[2]

Based on Optical Behavior	Fluorescent QDs	Visible-emitting QDs	Size-dependent Photoluminescence	[2]
	Near-Infrared QDs	Pb-based QDs	Deep tissue imaging	[11]
	Upconversion QDs	Rare-earth doped QDs	Anti-Stokes emission	[11]

Applications of Quantum Dots

Quantum dots (QDs) being a versatile nanomaterial with properties like size-tunable bandgap, high photoluminescence quantum yield, and excellent photostability, it has wide-range of applications such as (i)Optoelectronics:The narrow emission bandwidth and color purity of QDs makes it suitable for applications like light-emitting diodes (QLEDs), lasers, and display technologies. Efficiency and brightness is improved by their tunable emission enables precise control of red, green, and blue outputs. (ii)Photovoltaics: In QDs better utilization of solar energy and solar cell performance is achieved through multiple exciton generation and broad spectral absorption. (iii)Biomedical field: Since long-term imaging of cells and tissues is possible due to the strong and stable fluorescence of QDs. They are applied in bioimaging, biosensing, and targeted drug delivery. Thus, proving to be a superior alternative to traditional organic dyes. Surface functionalization enables bioconjugation with antibodies or biomolecules for selective detection of proteins and pathogens. (iv)Photodetectors and sensors: QDs have high absorption coefficient and rapid charge transfer which improves sensitivity and makes them applicable for chemical and gas sensing applications. (v)Quantum computing and photonics: Semiconductor QDs function as single-photon emitters and qubits due to their discrete energy levels and excitonic properties. (vi)Photocatalysis and environmental remediation: QDs facilitates pollutant degradation under visible light irradiation. Their adjustable band structure improves redox efficiency and charge separation [9].

Future Scope

Having the unique properties, QDs have proved to be the promising candidates for next-generation energy, biomedical, environmental, and quantum technologies.Continued development of highly efficient QDs will further improve the performance of Optoelectronic devices. Future studies are required to focus on improving charge transport and stability of devices that enables renewable energy conversion. The development of non-toxic and environmentally friendly QDs is the need of the hour in biomedical field. Several challenges like large-scale synthesis, long-term stability, toxicity issues, and integration into commercial devices must be addressed.

References

1. Gleiter, H. Nanostructured materials: Basic concepts and microstructure. Acta Materialia, 48 (2000) 1–29.
2. Alivisatos, A.P. Semiconductor clusters, nanocrystals, and quantum dots. Science, 271 (1996) 933–937.
3. Brus, L.E. Electron–electron and electron-hole interactions in small semiconductor crystallites. Journal of Chemical Physics, 80 (1984) 4403–4409.
4. Bimberg, D., Grundmann, M., Ledentsov, N.N. Quantum Dot Heterostructures. Wiley, 1999.
5. Ekimov, A.I., Onushchenko, A.A. Quantum size effect in semiconductor microcrystals. JETP Letters, 34 (1981) 345–349.
6. Brus, L.E. A simple model for the ionization potential, electron affinity, and aqueous redox potentials of small semiconductor crystallites. Journal of Chemical Physics, 79 (1983) 5566–5571.
7. Roduner, E. Size matters: Why nanomaterials are different. Chemical Society Reviews, 35 (2006) 583–592
8. G. A. Ozin and A. C. Arsenault, Nanochemistry: A Chemical Approach to Nanomaterials. Cambridge, U.K.: RSC Publishing, 2009.
9. A. L. Rogach, Semiconductor Nanocrystals and Quantum Dots. New York, NY, USA: Marcel Dekker, 2004.
10. R. Xie et al., “Synthesis and characterization of highly luminescent InP nanocrystals,” J. Am. Chem. Soc., vol. 127, pp. 7480–7488, 2005.
11. M. A. Hines and G. D. Scholes, “Colloidal PbS nanocrystals,” Adv. Mater., vol. 15, pp. 1844–1849, 2003.
12. S. N. Baker and G. A. Baker, “Luminescent carbon nanodots,” Angew. Chem. Int. Ed., vol. 49, pp. 6726–6744, 2010.
13. X. Sun et al., “Graphene quantum dots,” J. Mater. Chem. C, vol. 1, pp. 3277–3292, 2013.
14. L. Protesescu et al., “Nanocrystals of $CsPbX_3$ perovskites,” Nano Lett., vol. 15, pp. 3692–3696, 2015.
15. B. O. Dabbousi et al., “CdSe/ZnS core–shell quantum dots,” J. Phys. Chem. B, vol. 101, pp. 9463–9475, 1997.
16. D. J. Norris et al., “Doped nanocrystals,” Science, vol. 291, pp. 2390–2392, 2001.

Structural and Optical Properties of NiO and Co_3O_4 for Energy and Sensor Applications: A Short Review

Vaishnavi. K. Raut, Rutuja. S. Malave

Department of Physics, Dada Patil Mahavidyalaya Karjat, Dist. Ahilyanagar-414402

Email: rautvaishnavi123456@gmail.com

Article DOI Link: https://zenodo.org/uploads/19788223

DOI: 10.5281/zenodo.19788223

Abstract

Semiconductor-based gas sensors play an important role in modern technology for the detection of harmful and toxic gases. Among different metal oxide semiconductors, nickel oxide (NiO) and cobalt oxide (Co_3O_4) have attracted considerable attention due to their remarkable structural, optical including catalytic properties. NiO is a chemically stable p-type semiconductor widely used in batteries, photocatalysis, electrochromic devices, and gas sensing systems. Co_3O_4 is a mixed-valence oxide that exhibits strong surface catalytic activity, which enhances gas adsorption and surface reactions. A variety of analytical methods, including X-ray diffraction (XRD), scanning electron microscopy (SEM), Fourier transform infrared (FTIR) spectroscopy, and UV–visible spectroscopy, are widely employed to examine the structural and optical characteristics of these materials. These techniques help to determine crystallite size, morphology, and optical band gap. Various nanostructures of NiO and Co_3O_4 such as nanoparticles, nanowires, and nanofibers, have shown promising performance in sensing and energy-related applications. Therefore, these materials are considered potential candidates for future smart sensing devices and energy storage technologies.

Keywords: Gas sensors, p-type semiconductor, Mixed-valence oxide, Gas adsorption, Energy storage devices, Nanostructures, Nanoparticles, Nanowires.

Introduction

Rapid technological development has increased the demand for reliable gas sensing systems for environmental monitoring, industrial safety, and healthcare applications. Semiconductor-based gas sensors are widely used because of their greater sensitivity, quick response, simple operation, and easy integration with electronic systems. These sensors are capable of detecting harmful gases such as liquefied petroleum gas (LPG), carbon monoxide (CO), and nitrogen dioxide (NO_2).

Metal oxide semiconductors are commonly used as sensing materials because their electrical properties change when gas molecules interact with their surface. Nickel oxide (NiO) is one of the most widely studied p-type metal oxide semiconductors. It possesses good chemical stability, excellent optical properties, and relatively low cost. NiO generally crystallizes in a cubic structure and exhibits good sensitivity toward reducing gases. Because of these characteristics, NiO has been explored for applications such as gas sensors, batteries, photocatalysis, and electrochromic devices [1].

Cobalt oxide (Co_3O_4) is another important transition metal oxide that has received significant attention in recent years. It is a mixed-valence oxide containing both Co^{2+} and Co^{3+} ions and crystallizes in a cubic spinel structure. Co_3O_4 exhibits p-type semiconducting behavior and strong catalytic activity due to its oxygen-rich surface. These properties make it suitable for applications such as gas sensing, electrochemical devices, catalysis, and energy storage systems [2].

At the nanoscale, the performance of metal oxide semiconductors improves significantly due to the increase in surface area and active sites available for gas adsorption. Nanostructures such as nanoparticles, nanowires, nanorods, and nanofibers provide enhanced sensitivity and faster response time compared with bulk materials. Therefore, NiO and Co_3O_4 nanostructures are considered promising materials for advanced sensing and energy-related technologies.

Characterization Methods

- **Structural Characterization**

The results show that the particles are spherical, and some particles have stuck together to form nanoclusters. According to SEM nanoparticles is about 24 nm. The crystallinity can be determined by looking at the particle size from SEM. If it is a single crystal (monocrystalline), the size is small, but if there are many small crystals (polycrystalline), the structure is larger and more complex [3].

The XRD of the nanoparticles was performed to check their crystal type, purity, and size. The metal oxide nanoparticles used are pure. Co3O4 has a face-centered cubic crystal structure, while the others have a rhombohedral crystal structure. The average crystallite size of the nanoparticles was determined using the Debye-Scherrer equation [4].

- **FTIR:** FTIR spectroscopy is widely employed to determine the functional groups present in various materials.
- **UV-vis Spectroscopy:** UV-vis spectroscopy is a simple method used to study materials. In this technique, light is passed through a sample and the amount of light absorbed is measured. This helps to understand the size, structure, and concentration of nanoparticles [5].

Optical Characterization

The UV-visible absorption spectrum of NiO nanoparticles absorption wavelength depends on the particle size; smaller particles have shorter absorption wavelengths. The main absorption edge of NiO nanoparticles appears at 235 nm, while for bulk NiO it is at 340 nm. This shift happens due to the quantum confinement effect.

With the help of Tauc method, the energy band gap of Nickel Oxide nanoparticles was calculated. This confirms that the synthesized NiO particles are truly nanosized. Also, smaller particles have a larger band gap, meaning the band gap increases as the particle size decreases [6].

The light absorption behavior of the synthesized cobalt oxide nanofibers was analyzed using UV-visible absorption spectroscopy. In semiconductor materials, reducing the particle size can lead to changes in optical behavior due to the quantum effect. For Co3O4, two distinct band gaps were observed. The first band occurs because of energy transfer between O2- and Co2+ ions. Overall, the light absorption properties of Co3O4 nanoparticles are mainly influenced by the size of the particles [7].

Energy and sensor applications of NiO and CoO

Nickel oxide is an important semiconductor material with a variety of technological applications. Because of its good chemical stability and electrochemical properties, NiO is widely used in photocatalysis, batteries, electrochromic devices, and chemical gas sensors. It is also used in the anode layer of solid oxide fuel cells and as a cathode material in lithium-ion batteries. NiO nanostructures such as nanowires and nanofibers are being actively studied for advanced sensing and energy storage applications. In addition, NiO can act as a catalyst and has applications in optical filters, alkaline battery electrodes, and gas sensors for detecting gases such as carbon monoxide, hydrogen, and formaldehyde [8].

Cobalt oxide (Co_3O_4) is also widely used in energy-related applications because of its excellent catalytic and electrochemical properties. Co_3O_4 thin films are used in electrochromic devices, which can change color when an electric voltage is applied. In addition, cobalt oxide nanostructures are explored for use in solar cells, supercapacitors, and lithium-ion batteries. Due to its high catalytic activity and good electrical conductivity, Co_3O_4 is considered a promising material for improving the performance of modern energy storage systems [9]..

Conclusion

Nickel oxide (NiO) and cobalt oxide (Co_3O_4) are important metal oxide semiconductors that exhibit excellent structural, electrical, and optical properties. NiO is a stable p-type semiconductor with a cubic crystal structure and shows

good sensitivity toward reducing gases. Because of its favorable properties, it has been widely applied in gas sensors, batteries, electrochromic devices, and catalytic systems. On the other hand, Co_3O_4 is a mixed-valence oxide with a cubic spinel structure that shows strong catalytic activity and good electrochemical performance. These characteristics make it suitable for applications in gas sensing, catalysis, and energy storage devices. The nanoscale forms of these materials provide enhanced surface area and improved performance, making them promising candidates for future sensing technologies and energy applications.

References

1. Nurfani, E., Grace, G., Darmawan, M. Y., Marlina, R., Jatmika, J., Rinovian, A., &Rianjanu, A. (2025). Structural, optical, and electrical properties of Cu-doped NiO films synthesized by spray pyrolysis for potential gas sensing applications. arXiv. https://arxiv.org/abs/2509.241977
2. Mohammed, H. R. A., Hasan, N. B., &Shinen, M. H. (2025). Structural, morphological and optical properties of $(NiO)_{1-x}(Co_3O_4)_x$ composite thin films prepared by chemical spray pyrolysis technique. Revue des Composites et des MatériauxAvancés – Journal of Composite and Advanced Materials, 35(2), 367–373. https://doi.org/10.18280/rcma.350218
3. Rahdar, A., Aliahmad, M., & Azizi, Y. (2015). NiO nanoparticles: Synthesis and characterization. Journal of Nano-Structures, 5, 145–151
4. Tian, K., Baskaran, K., & Tiwari, A. (2018). Nonenzymatic glucose sensing using metal oxides – Comparison of CuO, Co_3O_4, and NiO. Vacuum, 155, 696–701. https://doi.org/10.1016/j.vacuum.2018.06.060
5. UV-vis Spectroscopy - an overview | ScienceDirect Topics https://share.google/bG6KqeNrx5g3F7Bvu
6. Danjumma, S. G., Abubakar, Y., & Suleiman, S. (2019). Nickel oxide (NiO) devices and applications: A review. International Journal of Engineering Research & Technology (IJERT), 8(4), 1–7.
7. Drasovean, R., Condurache-Bota, S., &Tigau, N. (2010). Structural and electrical characterization of cobalt oxide semiconductors. Journal of Science and Arts, 10(2), 379–384
8. Deshpande, M. P., Patel, K. N., Gujarati, V. P., Patel, K., & Chaki, S. H. (2016). Structural, thermal and optical properties of nickel oxide (NiO) nanoparticles synthesized by chemical precipitation method. Advanced Materials Research, 1141, 65–71. https://doi.org/10.4028/www.scientific.net/AMR.1141.65
9. Barakat, N. A. M., Khil, M. S., Sheikh, F. A., & Kim, H. Y. (2008). Synthesis and optical properties of two cobalt oxides (CoO and Co_3O_4) nanofibers produced by electrospinning process. Journal of Physical Chemistry C, 112(32), 12225–12233. https://doi.org/10.1021/jp8027353

Role of Nanotechnology in Advanced Physics Research

Rani. S. Gaikwad, Manjushri S. Mandlik

Department of Physics, Rayat Shikshan Sanstha's Dada Patil Mahavidyalaya Karjat,

Dist- Ahilyanagar-414402

Email: ranivarat555@gmail.com

Article DOI Link: https://zenodo.org/uploads/19788357

DOI: 10.5281/zenodo.19788357

Abstract

Nanotechnology is emerging fiel of science that studies materials at a very tiny scale known as the nanometrically, it is usually between 1 to 100 nanometers. When materials are reduced to this size, their physical properties can change significantly compared to their larger forms. These changes happen because of quantum effect and the large surface area of tiny particles. Researchers use different nanomaterial like as nanoparticles, nanowires, carbon nanofibers, and quantum dots for study electrical, optical, and magnetic properties. This field also helps in the progress of advanced technology. nanotechnology provides new opportunities to explore physical processes and design innovative systems. Because of these advantages, nanotechnology has become a important tool in modern physics research and technological progress.

Keywords: Nanotechnology, Nanoparticals, scale 1 to 100nm,

Introduction

A nonotechnology is commonly used in different areas of physics. It plays a important role in the progress of nanoelectronics, nano scale sensors, nanophotonics, and energy system such as advanced batteries and solar cells. These technologies help create high performance and efficient electronic and optical tools. Therefore, nanotechnology has become an essential tool for modern physics research and technological development. In advanced physics research, scientists' study different nanostructures such as nanoparticles, nanowires, nanotubes, and quantum dots to understand the behavior of matter at nanoscale dimensions. These nanostructures help researchers explore important physical phenomena like electron transport, optical response, magnetic behavior, and energy transfer. Understanding these effects is very important for developing modern technologies such as nanoelectronics, photonic devices, and advanced sensors. Therefore, theoretical concepts in nanotechnology help physicists explain how materials behave at extremely small scales and how these properties

can be used in scientific research and technological applications [1][2].

Theory

Nanotechnology studies materials and structures at extremely small, typically ranging from 1 to 100 nanometers scale. At this extremely small scale, materials exhibit unique physical, chemical, and mechanical properties that vary greatly compared to bulk materials [3]. Those changes are primarily because of quantum mechanical effects and high area to volume ratio of nanostructures. Understanding these nanoscale phenomena is essential in advanced physics research, as they govern the behavior of electrons, photons, and atoms in confined systems [4]. The following section discusses the key theoretical concepts of nanotechnology that form the foundation for modern applications in nanoelectronics, nanophotonics, and advanced material science. The following points are included in the role of nanotechnology in physics research. These topics greatly help in understanding nanotechnology in physics research.

- **Nanoscale Physics Fundamentals**

In the nanoscale, the conventional laws of physics often need modifications to account for quantum behavior. Materials exhibit new mechanical, electrical, and optical properties as their dimensions approach a few nanometers [5]. The enhancement of the surface area-to-volume ratio enhances surface energy, which significantly alters chemical reactivity and structural stability [6]. These fundamental nanoscale properties provide the basis for designing novel materials with controlled behavior. Nanoscale systems also allow scientists to study phenomena such as tunneling, ballistic transport, and quantum interference, which are crucial for understanding advanced physical processes [7].

- **Quantum Confinement Effect**

Quantum restrictions effect is one of the central concepts in nanotechnology. Whenever the dimensions of a material become close to the de Broglie wavelength of electrons, the motion of charge carrier is confined to a limited space. This, unlike the continuous energy bands in bulk materials [8]. Quantum confinement is confinement results in discrete energy levels evident in various nanostructures namely, quantum dots, nanowires and quantum wells, where the optical and electronic properties can be altered through size and shape [9]. For instance, the color of light emitted by quantum dots depents on their size, which is utilized in optoelectronic devices, display technologies, and biomedical imaging [10,11].

- **Developing Nanoelectronics**

Nanoelectronics is focuses on the design of electronic devices at the using nanoscale materials and architectures. As traditional semiconductor devices

approach their physical scaling limits, nanotechnology provides alternative solutions by enabling the fabrication of optimized electronic component with reduced size and enhancement performance.[12]. Materials such as grapheme and carbon nanotubes display show outstanding electrical conductivity and mechanical strength. Graphene, composed of a single atomic layer of carbon in a hexagonal lattice, allows extremely high electron mobility, making it suitable for high-speed transistors and logic circuits [13]. Carbon nanotubes can function as show either metallic or semiconducting behaviour depending on their atomic configuration, allowing their use in nanoscale sensors, memory devices, and integrated circuits [14].

Fig. 2 Developing nanoelectrons [15]

- **Exploring Nanophotonics**

The nanoelectronics is defined as the application of nanotechnology in electronic components. Nanophotonics studies the hoe light behaves at the nanoscale and its contact with nanostructured materials. At this scale, light can be confined, guided, and manipulated in ways not possible with conventional optical systems [16]. An outstanding phenomenon is surface collective resonance, where free electrons on the surface of metallic nanoparticles oscillate collectively in response to incident light, producing enhanced local electromagnetic fields [17]. These effects are widely applied in high-sensitivity optical sensors, imaging, and nanoscale photonic devices. Nanophotonics also encompasses photonic crystals and nanoscale lasers, which enable precise control of light propagation and integration into advanced optical circuits [18].

- **Fabricating Advanced Nanomaterials and Applications**

Fabrication of advanced nanomaterials is central to modern research in nanotechnology. Materials including graphene, carbon nanotubes along with metal nanoparticles, and semiconductor nanocrystals display unique electrical, optical and mechanical properties that help them to ideal to advanced physics research [19]. These materials are also applied in energy-related technologies, including solar cells, batteries, and supercapacitors, due to their ability to improve light absorption, energy storage, and charge transport [20]. Additionally,

nanomaterials are extensively used in nanosensors for detecting chemical and biological molecules at very low concentrations, making them valuable in medical diagnostics, environmental monitoring, and industrial application [21].

References

1. C. P. Poole Jr. and F. J. Owens, Introduction to Nanotechnology, Wiley-Interscience, 2003.
2. B. Bhushan, Springer Handbook of Nanotechnology, Springer, 2017.
3. C. Dupas, P. Houdy, and M. Lahmani, Nanoscience: Nanotechnologies and Nanophysics, Springer, 2007.
4. G. Cao and Y. Wang, Nanostructures and Nanomaterials, World Scientific, 2011.
5. C. Kittel, Introduction to Solid State Physics, Wiley, 2005.
6. M. Sattler, Handbook of Nanophysics, CRC Press, 2010.
7. S. Datta, Quantum Transport: Atom to Transistor, Cambridge University Press, 2005.
8. A. P. Alivisatos, "Semiconductor Nanocrystals and Quantum Dots," Science, 1996.
9. P. Avouris, "Carbon Nanotube Electronics," Chemical Physics, 2002.
10. R. Waser, Nanoelectronics and Information Technology, Wiley-VCH, 2012.
11. Aravnd B.S. july 11, 2020
12. A. K. Geim and K. S. Novoselov, "The Rise of Graphene," Nature Materials, 2007.
13. L. Novotny and B. Hecht, Principles of Nano-Optics, Cambridge University Press, 2012.
14. S. A. Maier, Plasmonics: Fundamentals and Applications, Springer, 2007.
15. J. D. Joannopoulos, Photonic Crystals: Molding the Flow of Light, Princeton University Press, 2008.
16. Dr. L.amulmurgan march 2011
17. M. A. Green, Solar Cells: Operating Principles, Prentice Hall, 1982.
18. B. Dunn, H. Kamath, and J.-M. Tarascon, "Electrical Energy Storage for the Grid," Science, 2011.
19. N. J. Tao, "Nanotechnology and Sensors," Nature Nanotechnology, 2006.
20. C. Joachim et al., "Electronics Using Hybrid Molecular and Nanostructures," Nature, 2000.
21. H. Dai, "Carbon Nanotubes: Synthesis, Integration, and Properties," Accounts of Chemical Research, 2002.

Review on MoS2/rGO Functional Nanocomposites for Enhance Hydrogen Evolution Reaction

[1]B. S. Maharnavar, [2]Supriya P. Salunkhe

[1]Department of Physics, Rayat Shikshan Sanstha's Dada Patil Mahavidyalaya Karjat, Dist- Ahilyanagar (MS) India -414402

[2]Bharati Vidyapeeth's College of Eninnering for Women, Pune (MS), India-411043

Email: balbhim02@gmail.com

Article DOI Link: https://zenodo.org/uploads/19788489

DOI: 10.5281/zenodo.19788489

Abstract

The growing demand for sustainable and carbon-neutral energy sources has intensified research on hydrogen production technologies. Electrochemical water splitting has emerged as a promising method for generating clean hydrogen, particularly when powered by renewable energy. However, the high cost and scarcity of noble metal catalysts such as platinum limit their large-scale application. In this context, molybdenum disulfide (MoS_2) has attracted considerable attention as an efficient and low-cost alternative catalyst for the hydrogen evolution reaction (HER). Due to its layered two-dimensional structure, high surface area, and abundant catalytic edge sites, MoS_2 exhibits promising electrocatalytic and photocatalytic properties. This chapter discusses the important functional characteristics of MoS_2 and highlights various synthesis strategies for MoS_2-based functional nanocomposites, including hydrothermal, solvothermal, chemical vapor deposition, and exfoliation methods. The influence of synthesis routes on morphology, defect formation, and crystal phase is also examined. Furthermore, structural and morphological characterization techniques such as X-ray diffraction (XRD) and field emission scanning electron microscopy (FESEM) are discussed to understand the relationship between nanostructure and catalytic performance. The chapter highlights the potential of MoS_2 functional nanocomposites as cost-effective catalysts for renewable hydrogen production and future energy applications

Keywords: MoS2, Nanocomposites, Hydrogen Energy, electrocatalytic materials.

Introduction

The rapid depletion of fossil fuel resources and growing environmental concerns have accelerated the search for renewable and carbon-neutral energy carriers.

Hydrogen energy has emerged as a promising solution due to its high gravimetric energy density and zero carbon emission during utilization. Electrochemical water splitting represents one of the most sustainable approaches for hydrogen production when powered by renewable electricity sources [1]. Water electrolysis involves two half reactions: hydrogen evolution reaction (HER) at the cathode and oxygen evolution reaction (OER) at the anode. Platinum-based catalysts exhibit superior HER activity but remain economically prohibitive for large-scale deployment. Therefore, developing cost-effective alternatives has become a major research priority [2]. Two-dimensional molybdenum disulfide (MoS_2) has gained considerable interest as a potential replacement for noble metal catalysts due to its layered structure analogous to graphene. Among its polymorphs, the metallic 1T phase demonstrates superior conductivity compared to semiconducting 2H-MoS_2, enabling enhanced electrocatalytic performance [3]. Recent investigations have shown that catalytic activity mainly originates from exposed edge sites rather than basal planes. Consequently, strategies such as defect engineering, heteroatom doping, and interface engineering are widely adopted to maximize active sites and optimize hydrogen adsorption energy [4]. Integration with carbon materials, metal oxides, MXenes, and transition metal chalcogenides improves electrical conductivity and structural stability. For example, MoS_2 heterostructures exhibit synergistic electronic interactions that enhance reaction kinetics and charge transfer efficiency during HER [5].

Figure 1: Important Functional Properties of MoS_2 in Photocatalysis

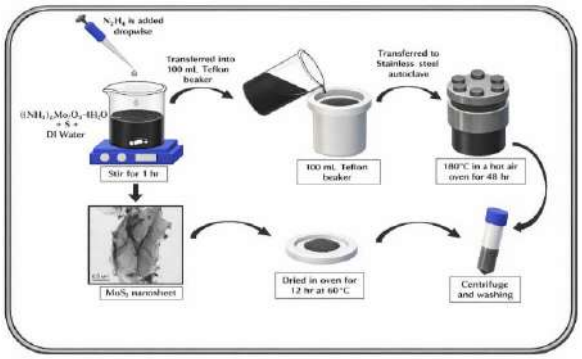

Figure 2: schematic illustration of synthesis of MoS_2 by the hydrothermal method [7].

Additionally, photocatalytic hydrogen generation has attracted attention through semiconductor coupling strategies. MoS_2-based Z-scheme heterojunctions enable efficient charge separation and improved solar-to-hydrogen conversion efficiency [6]. Therefore, MoS_2 functional nanocomposites represent a promising pathway toward scalable renewable hydrogen generation technologies. The essential characteristics of MoS_2 such as high adsorption ability, rapid charge carrier transport, simple synthesis process, and its ability to form composites with

different photocatalysts. These combined properties improve its overall photocatalytic efficiency and practical applicability it shows in Fig.1.

- **Synthetic Routes for MoS_2-Based Functional Nanocomposites**

The electrocatalytic performance of Molybdenum disulfide (MoS_2)-based functional nanocomposites strongly depends on the synthesis route, as morphology, defect density, and crystal phase significantly affect electrochemical activity. Hydrothermal and solvothermal methods(fig.2) are widely used due to their simplicity and scalability, typically employing ammonium molybdate with thiourea or thioacetamide at 180 °C to produce flower-like nanosheets or hierarchical structures with high surface area; incorporation of graphene oxide or metal oxides during synthesis prevents restacking and promotes uniform heterostructure formation [7], and MoS_2@VS_2 nanocomposites prepared hydrothermally exhibit enhanced HER kinetics due to improved conductivity and synergistic interfacial coupling [8]. Chemical vapor deposition (CVD) enables precise control over thickness and crystallinity through sulfurization of molybdenum oxide precursors, allowing phase engineering beneficial for electrocatalysis [9]. Exfoliation methods, including liquid-phase exfoliation and lithium intercalation, produce ultrathin nanosheets with increased exposed edge sites, while hybridization with reduced graphene oxide enhances electron transport and HER efficiency [10]. Furthermore, transition metal doping (Co, Ni, Fe) and heterostructure engineering with sulphides, carbides, or oxides modulate electronic structure and promote bifunctional HER/OER activity, with recent studies emphasizing support integration strategies to improve long-term electrolysis stability [11-12].

- **Structural and Morphological study of MoS_2 Nanocomposites**

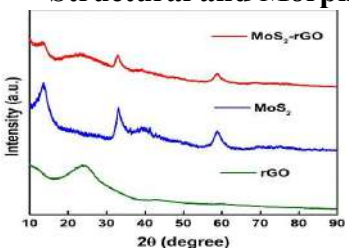

igure 3 X Ray Diffraction (XRD) ›attern of rGO, MoS2 and Mos2-rGO nanocomposites [13]

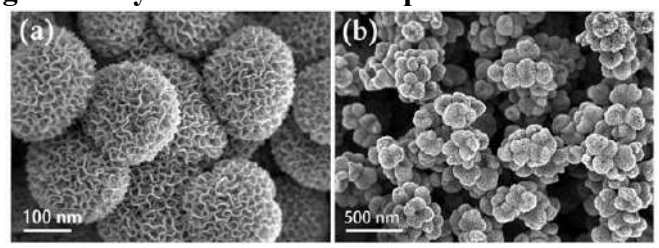

Figure 4: FESEM images of COFE-Nanoflower Structure of 100 nm and 500 nm [14]

Characterization techniques play a critical role in correlating structural properties with catalytic performance. XRD spectra confirming the crystalline structure of MoS_2 and the successful formation of the MoS_2–rGO composite. Characteristic MoS_2 peaks appear around ~14°, ~33°, and ~58°, while rGO shows a broad peak near ~24°, indicating reduced graphene oxide structure. The composite pattern contains features of both materials, confirming successful integration fig. 3 shows

(13). The nanoflower morphology of CoFe–MoS_2 enhances water splitting performance by providing a high surface area with abundant exposed edge active sites for HER and OER. The porous and interconnected nanosheet structure improves electrolyte contact, facilitates fast electron and ion transport, and enables easy release of generated gas bubbles (H_2 and O_2), thereby reducing overpotential and increasing overall electrocatalytic efficiency in fig.4 shows. (14).

- **Water Splitting Applications of MoS_2 Functional Nanocomposites**

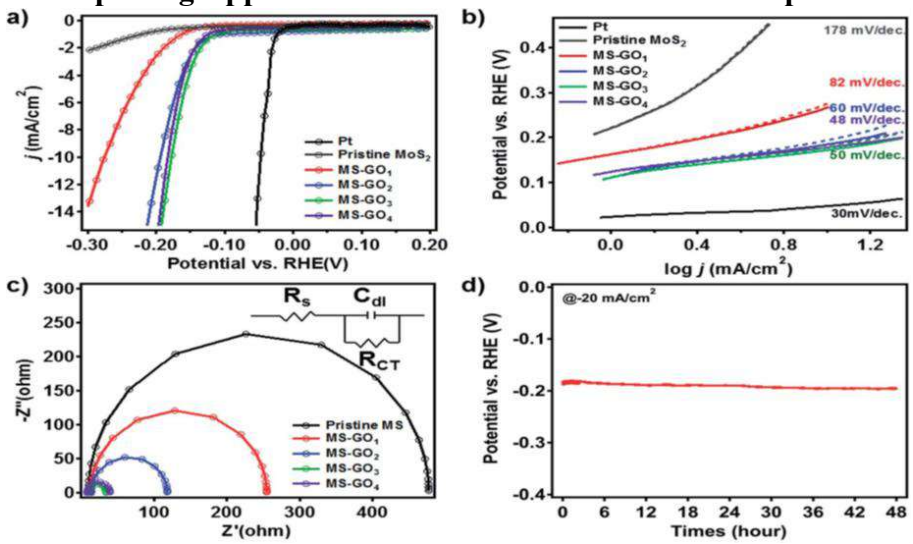

Fig.5 Electrochemical characterizations of pristine MoS2 and MoS2/rGO hybrids [15].

The MoS_2/rGO hybrids were tested for hydrogen production using glassy carbon electrodes. Compared to pure MoS_2, the hybrids showed much better performance, starting the reaction at lower voltages (onset potential) and producing higher current densities[fig]. Among the samples, MS-GO3 showed (a) the best results with the lowest onset potential (–0.147 V) and high current density (–24.4 mA cm^{-2}). The Tafel slope, which indicates how fast the reaction occurs, was also lower for the hybrids, meaning faster reaction rates(b). These hybrids had low charge transfer resistance and high double-layer capacitance, showing good conductivity and large active surface area(c). Durability tests showed that MS-GO4 and MS-GO3 remained stable for a long time, maintaining performance even after 48 hours and 1000 cycles(d). Overall, the right ratio of MoS_2 to rGO improves activity, conductivity, and stability, making these hybrids excellent HER catalysts [15].

Conclusions

MoS_2-based functional nanocomposites are promising materials for hydrogen production through water splitting. Their layered structure, active edge sites, and ability to form hybrids with conductive materials make them a good alternative to

costly noble metal catalysts. The hydrothermal synthesis method provides controlled morphology and high surface area of MoS_2 nanomaterials, which significantly improves their catalytic performance for hydrogen evolution reactions. MoS_2/rGO hybrids show improved electrocatalytic performance due to better conductivity, larger surface area, and strong interactions between components. These materials exhibit lower onset potential, higher current density, faster reaction kinetics, and good long-term stability. Therefore, MoS_2 nanocomposites are attractive low-cost catalysts for efficient and sustainable hydrogen generation.

References

1. Roger, I., Shipman, M., & Symes, M. (2017). Nature Reviews Chemistry, 1, 0003.
2. Seh, Z. W., et al. (2017). Combining theory and experiment in electrocatalysis. Science, 355, eaad4998.
3. Tripathi, P., Singh, D., Pathak, A., Verma, A. K., Sinha, A. S. K., & Singh, S. (2025). Journal of Materials Chemistry A, 13, 39603–39659.
4. Liu, C., Li, X., Liu, Z., Zhang, L., Jiang, S., & Jiao, T. (2025). Catalysts, 15, 520.
5. Pujar, M. S., & Padasalagi, A. (2025). ACS Applied Materials & Interfaces, 17(31), 44053–44072.
6. Sharma, R., et al. (2025). Journal of Water Process Engineering, 71, 107404.
7. Bricha, M., Belmamouni, Y., Essassi, E. M., Ferreira, J. M. F., & Mabrouk, K. E. (2012 Journal of Nanoscience and Nanotechnology, 12(10), 8042–8049.
8. Singh, R., et al. (2024). ACS Applied Energy Materials, 7, 1324.
9. Kumar, A., et al. (2025). Applied Surface Science, 679, 161104.
10. Aggarwal, R., Saini, D., Mitra, R., Sonkar, S. K., Sonker, A. K., & Westman, G. (2024). Langmuir, 40(19), 9855–9872.
11. Chen, W., et al. (2022). Journal of Energy Chemistry, 75, 16.
12. Hanslin, S. Ø., Jónsson, H., & Akola, J. (2024). ChemPhysChem, 25(20), e202400349.
13. Senthilkumar, R., Ramakrishnan, S., Balu, M., Ramamurthy, P. C., Kumaresan, D., & Kothurkar, N. K. (2018). Journal of Solid-State Electrochemistry, 22, 3331–3341.
14. Li, X., Song, Y., Huang, Y., Zhang, J., Wu, S., Zhang, W., Wang, J., & Zhang, X. (2025). Molecules, 30(11), 2343.
15. Lee, J. E., Jung, J., Ko, T. Y., Kim, S., Kim, S.-I., Nah, J., Ryu, S., Nam, K. T., & Lee, M. H. (2017). Nanoscale, 9(2), 710–718

Recent Advances in $NiFe_2O_4$ Electrocatalysts for Hydrogen and Oxygen Evolution Reaction

[1]Anna S. Dhawale, [2]Pratik S. Patil, [1]Balbhim S. Maharnavar

[1]Department of Physics Rayat Shikshan Sanstha's Dada Patil Mahavidyalaya Karjat, Dist- Ahilyanagar (MS) India -414402

[2]Deapartment of Physics, Shankarao Jawale Patil Senior College Lohara, Dharashiv (MS) India-413608

Email: annadhawale22@gmail.com

Article DOI Link: https://zenodo.org/uploads/19788635

DOI: 10.5281/zenodo.19788635

Abstract

Hydrogen is considered a clean & sustainable energy source for future energy systems. Electrochemical water splitting offers an environmentally friendly approach for hydrogen generation; however, However, its overall efficiency is often constrained by the slow kinetics of the oxygen evolution reaction (OER) and hydrogen evolution reaction (HER), necessitating the development of cost-effective and high-performance electrocatalysts. Nickel ferrite ($NiFe_2O_4$), a spinel-structured transition metal oxide, has emerged as a promising bifunctional catalyst because of its excellent electrical conductivity, chemical stability, and abundant active sites. The presence of Ni and Fe ions enhances catalytic activity, while strategies such as doping, nanostructuring, and composite formation further improve its electrocatalytic performance for water-splitting applications.

Keyword: $NiFe_2O_4$, Electrocatalyst, Water Splitting, Hydrogen Evolution Reaction (HER), Oxygen Evolution Reaction (OER).

Introduction

High demand for energy and the environmental problems associated with fossil fuel consumption have accelerated the search for sustainable and clean energy sources. Conventional fuels coal, petroleum, and Natural gas utilization is recognized as a significant source of greenhouse gas emissions, thereby contributing to environmental degradation. As a result, the development of renewable and environmentally friendly energy technologies has become an important research focus in recent years. Among the various alternatives, hydrogen has emerged as a promising energy carrier because it produces only water as a by-product during combustion and possesses high gravimetric energy

density. Therefore, hydrogen is widely considered a key component in future clean energy systems [1]. Electrochemical water splitting is one of the attractive methods for hydrogen production, especially when powered by renewable energy sources such as solar or wind energy. In this process, water molecules are split into hydrogen and oxygen through two half-reactions known as the hydrogen evolution reaction (HER) and the oxygen evolution reaction (OER). Although this technique is environmentally friendly, the efficiency of water splitting is limited by the slow reaction kinetics and high energy barriers associated with these electrochemical processes. Consequently, efficient electrocatalysts are required to accelerate the reactions and reduce the required overpotential [2].

In this context, nickel ferrite ($NiFe_2O_4$) has gained attention due to its spinel structure, chemical robustness, and promising electrochemical behavior. The presence of nickel and iron ions in the lattice provides multiple active sites that can enhance catalytic activity and improve charge transfer during electrochemical reactions. In addition, structural modification strategies such as nanostructuring, doping, and composite formation can further enhance the electrocatalytic performance of $NiFe_2O_4$. Therefore, $NiFe_2O_4$-based materials are considered promising bifunctional catalysts for efficient hydrogen & oxygen evolution in water-splitting systems [3].

Nickel Ferrite for Oxygen Evolution Reaction

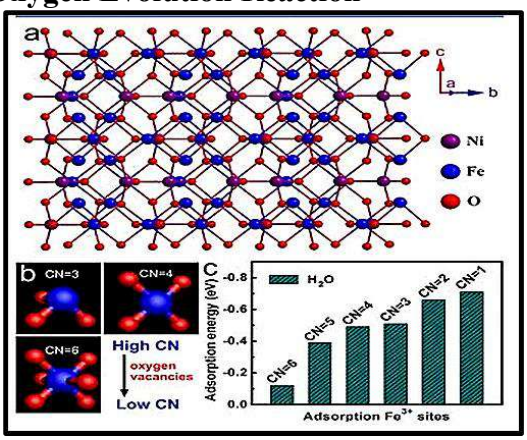

Figure 1. Schematic representation of the OER mechanism on $NiFe_2O_4$ catalyst surface (adapted from Ref. 8).

Oxygen evolution reaction (OER) is a key half-reaction in electrochemical water splitting for hydrogen production. However, OER is kinetically slow and requires efficient electrocatalysts to improve its performance. The reaction involves a four-electron and four-proton transfer process to produce oxygen from water [4]. In acidic media, the reaction proceeds as $2H_2O \rightarrow O_2 + 4H^+ + 4e^-$, while in alkaline media it occurs as $4OH^- \rightarrow O_2 + 2H_2O + 4e^-$. One major challenge in OER is the formation of the O–O bond, which increases the reaction energy

barrier [5]. In spinel ferrite catalysts such as $NiFe_2O_4$, OER mainly follows two mechanisms, the adsorbate evolution mechanism (AEM) and the lattice oxygen mechanism (LOM) [6]. In the AEM pathway, oxygen evolves through adsorbed intermediates on the catalyst surface, while in LOM lattice oxygen directly participates in oxygen formation. Among the metal sites, Fe sites act as active catalytic centers that facilitate O–O bond formation and enhance OER efficiency [7]. The diagram illustrates the crystal structure of $NiFe_2O_4$ with surface-exposed (400) facets where Ni, Fe, and O atoms form a spinel lattice. It also shows Fe^{3+} atoms with different coordination numbers formed due to oxygen vacancies on the surface. Fe sites with lower coordination numbers strongly adsorb H_2O molecules, making them highly active for the OER process [8].

Nickel Ferrite for Hydrogen Evolution Reaction

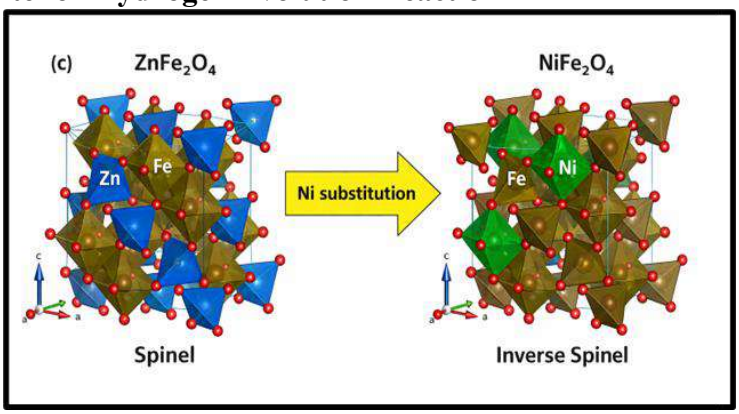

Figure 2. Structural transformation from $ZnFe_2O_4$ to $NiFe_2O_4$. [adapted from Ref. 12].

Nickel ferrite ($NiFe_2O_4$) has emerged as an effective electrocatalyst for the hydrogen evolution reaction (HER) and related water-splitting processes. It is often regarded as a bifunctional catalyst due to its capability to facilitate both the oxygen evolution reaction (OER) and oxygen reduction reaction (ORR) within electrochemical systems. In such processes, catalysts are essential for improving reaction kinetics and minimizing energy losses. Consequently, transition metal–based materials such as $NiFe_2O_4$ are being explored as economical and sustainable alternatives [9]. The spinel structure of $NiFe_2O_4$ provides abundant active sites along with favorable redox characteristics, which contribute to enhanced catalytic activity [10]. Furthermore, coupling $NiFe_2O_4$ with conductive materials such as $MoSe_2$ nanosheets can improve charge transport and increase the availability of active sites. This synergistic interaction leads to better catalytic performance in water-splitting reactions, along with improved conductivity and structural stability, which are important for long-term operation. In addition to catalysis, $NiFe_2O_4$-based materials also find applications in energy storage systems, including fuel cells and rechargeable metal–air batteries. Owing to these

advantages, $NiFe_2O_4$-based bifunctional catalysts are considered promising for sustainable energy conversion technologies [11]. It is also noteworthy that substituting Ni in place of Zn in $ZnFe_2O_4$ induces a transition from a normal spinel to an inverse spinel structure. This change involves redistribution of cations within the lattice, which can further enhance the catalytic properties of the material [12].

Table 1. Comparison of electrocatalytic performance of $NiFe_2O_4$-based catalysts for HER and OER.

Catalyst	*Reac -tion*	*Over potential (mV)*	*Current Density (mA cm⁻²)*	*Tafel Slope (mV dec⁻¹)*	*Electrolyte*	*Ref.*
$NiFe_2O_4$	OER	300	10	60	1 M KOH	13
$NiFe_2O_4$/Phosphorene	OER	243	10	39	1 M KOH	14
$NiFe_2O_4/MoSe_2$	HER	210	10	85	1 M KOH	15
Zn-doped $NiFe_2O_4$	OER	270	10	50	1 M KOH	16

Conclusion

Electrochemical water splitting is increasingly recognized as a viable and sustainable route for hydrogen generation. However, its efficiency is largely governed by the activity of electrocatalysts involved in HER and OER. Nickel ferrite ($NiFe_2O_4$) has emerged as a promising candidate due to its low cost, structural stability, and favorable catalytic properties. Its spinel framework offers multiple active sites that facilitate charge transfer and improve overall reaction efficiency, while Fe ions contribute to enhanced OER kinetics.

Moreover, approaches such as doping and compositional modification can further improve conductivity and catalytic behavior, leading to reduced overpotential and faster reaction rates. Considering these advantages, $NiFe_2O_4$-based materials provide a cost-effective alternative to noble metal catalysts. Further optimization of their structure and composition is expected to advance their performance in sustainable hydrogen production systems.

References

1. Majeed et al. (2024). Materials Chemistry and Physics, 325, 129682.
2. Kubisztal et al. (2024). International Journal of Hydrogen Energy, 56, 912–923.
3. Khan et al. (2024). ACS Applied Energy Materials, 7, 4960–4974.
4. Taylor et al. (2020). ACS Applied Energy Materials, 3, 387–400.
5. Liu et al. (2024). Journal of Environmental Chemical Engineering.

6. Li et al. (2024). Applied Catalysis B: Environment and Energy, 355, 124116.
7. Avcı et al. (2022). ACS Catalysis, 12, 9058–9073.
8. Yang et al. (2017). ACS Catalysis, 7, 5557–5564.
9. Li et al. (2024). Ceramics International, 50, 34060–34069.
10. Sebastian et al. (2024). ACS Applied Energy Materials, 7, 8635–8647.
11. Saravanakumar et al. (2021). Energy & Fuels, 35, 5372–5382.
12. Roy et al. (2021). Electrochimica Acta, 389, 138771.
13. Li, X., et al. (2024). Small, 20, 2308941.
14. Zhao, Y., et al. (2024). Journal of Alloys and Compounds, 982, 173639.
15. Wang, W., et al. (2024). Nanotechnology, 35, 315401.
16. Zhang, X., et al. (2024). Journal of Colloid and Interface Science, 661, 123–132.

Comparison between Metal Oxide (MO), Graphene Oxide (GO), Carbon Nanotube (CNT), and Polymer-Based Gas Sensors

Vishal Kashinath Pandit

F.E. Department, Adsul Technical Campus, Ahilyanagar-414005

Email: vishalpandit20@gmail.com

Article DOI Link: https://zenodo.org/uploads/19788828

DOI: 10.5281/zenodo.19788828

Abstract

Gas sensors provide continuous monitoring of toxic, flammable, and hazardous gases in industrial facilities, automotive systems, environmental monitoring stations, medical diagnostics, homeland security, and wearable health devices. They are crucial parts of contemporary smart infrastructure. Sensing technologies that provide high sensitivity, selectivity, low power consumption, quick response, and long-term stability are in great demand due to the increased exposure to hazardous and volatile gases brought on by growing urbanization and industrialization. Metal oxide (MO) semiconductors, graphene oxide (GO)-based materials, carbon nanotubes (CNTs), and polymer-based systems are some of the most extensively studied and commercially used sensing materials. The unique electrical properties, surface chemistries, fabrication techniques, and performance traits of each material class dictate their appropriateness for various applications.

Metal Oxide Gas Sensors

The most developed and well-established sensing technique is metal oxide gas sensors. Tin oxide (SnO_2), zinc oxide (ZnO), tungsten oxide (WO_3), titanium dioxide (TiO_2), and indium oxide (InO_3) are common semiconducting oxides. Chemiresistance is the primary mechanism by which these materials function. Ionized oxygen species are created when oxygen molecules adsorb onto the oxide surface at high temperatures, usually between 200°C and 400°C, and take electrons from the n-type semiconductor's conduction band. Electrical resistance rises as a result of this electron depletion layer. Electrons are liberated back into the conduction band when reducing gases like CO, H_2, or NH_3 react with the adsorbed oxygen, lowering resistance.

On the other hand, oxidizing gasses such as NO_2 raise resistance even more. The sensing signal is the change in resistance. MO sensors are prized for their great sensitivity, quick reaction time, robustness, and suitability for mass production. Because they must run at high temperatures, they use a lot of power and require microheaters. Additionally, they have poor selectivity, interference from

humidity, and slow signal drift over time. [1-3]

Graphene Oxide-Based Sensors

A RT substitute based on 2D CNT is provided by GO based sensors. GO has a large number of oxygen functional groups, including hydroxyl, epoxy, and carboxyl groups, which improve gas molecule adsorption and introduce fault sites. Charge transfer interactions between adsorbed gas species and the conductive network are the main mechanism of sensing. Carrier concentration and electrical conductivity are altered when gases like NH_3, NO_2, CO_2, or H_2S interact with GO. GO devices are appealing on the contrast less power than MO sensors and work with flexible substrates. Despite these benefits, GO sensors have drawbacks such as shorter recovery times for heavily adsorbed gases, unpredictability in material production, and susceptibility to dampness. [4] Improvements are still needed in the field of long-term environmental stability.

Carbon Nanotube Gas Sensors

The benefits of carbon nanomaterials are extended into quasi-one-dimensional structures via gas sensors based on carbon nanotubes. Single-walled (SWCNTs) and multi-walled (MWCNTs) carbon nanotubes (CNTs) are cylindrical tubes made from rolled graphene sheets. They have huge specific surface areas, high aspect ratios, and remarkable electrical conductivity. Charge transfer effects, Schottky barrier modulation at metal–CNT contacts, and variations in contact resistance are commonly involved in gas sensing in CNTs. Measurable conductance variations result from adsorbed gas molecules shifting the Fermi level and changing the carrier concentration.

CNT sensors have minimal power consumption, quick response and recovery, and operate at room temperature. Their mechanical adaptability facilitates incorporation into portable and wearable technology. However, the process can be complicated, frequently requiring careful electrode alignment, purification, dispersion control, and chemical vapor deposition growth. Reproducibility and material cost are still issues, and performance may be impacted by humidity interference unless surface functionalization is used to increase selectivity. [5,6]

Polymer-Based Gas Sensors

Another significant category is polymer-based gas sensors, especially those that use conducting polymers like PEDOT: PSS, Polypyrrole(PPy), and Polyaniline (PANI). Protonation and deprotonation reactions, redox processes, charge transfer, and physical swelling of the polymer matrix upon gas absorption are examples of gas sensing methods. Molecular imprinting and chemical functionalization methods can improve selectivity toward particular analytes. Recovery times may be slower for certain gases, and temperature variations can influence baseline conductivity. Comparative study reveals clear performance

differences between these technologies. GO sensors are similarly highly sensitive at room temperature, whereas MO sensors produce powerful responses but require higher operating temperatures. Polymer sensors provide adequate sensitivity for many practical applications, although they may not achieve ultra-trace detection levels. MO sensors have the highest power consumption due to heating requirements, whereas GO, CNT, and polymer sensors function at ambient temperatures, making them appropriate for portable and battery-powered systems. [7-9]

Selectivity varies significantly: polymers have configurable chemical selectivity, MO sensors frequently use noble metal doping, while CNT and GO devices rely on surface functionalization techniques. In terms of stability, MO sensors have the longest working lifetime, especially in severe environments, whereas polymers and GO can degrade with time. Fabrication complexity is lowest for polymers and GO materials, intermediate for MO sensors with proven industrial processes, and greatest for CNT-based devices that need controlled nanostructure synthesis. Recent research has shifted toward hybrid and composite sensors, which combine complimentary material benefits. MO/CNT composites, which reduce operating temperature while increasing sensitivity, GO/polymer hybrids, which increase flexibility and adsorption selectivity, CNT/MO heterojunctions, which allow for synergistic charge transfer, and polymer-coated CNT systems, which improve dispersion and durability. Such hybrid techniques strive to concurrently increase sensitivity, selectivity, stability, and power efficiency. Advanced technologies for improving sensor array performance include noble metal doping, molecular imprinting, nanostructuring, and artificial intelligence-assisted pattern recognition.[10]

Table. Comparative analysis of Gas Sensing materials

Material	**Cost**	**Sensitivity Level**	**Temperature**	**Selectivity**	**Speed**	**Power Requirement**	**Stability**	**Flexibility**	**Humidity Effect**	**Mechanical Strength**
MO	Low	High (ppm level)	High (200–400°C)	Low (needs doping)	Fast	High	Excellent	No	High	High
GO	Moderate	High (ppm–ppb)	Room temperature	Moderate	Moderate	Low	Moderate	Yes	High	Moderate
CNT	High	Very High (ppb)	Room temperature	Low without functionalization	Fast	Very Low	Good	Yes	Moderate	Very High
Polymer	Low	Moderate to High	Room temperature	Good (tunable chemistry)	Moderate to slow	Low	Moderate to Low	Yes	High	Moderate

Applications

Material selection is greatly influenced by application requirements. MO sensors remain the ideal choice for industrial safety and extreme environmental situations due to their durability and reliability. Wearable health monitoring and breath analysis favor CNT, GO, and polymer sensors due to their room temperature functioning and versatility. Environmental air quality monitoring frequently leverages MO and CNT technologies for high sensitivity, whereas smart home and IoT applications favor low-power GO and polymer systems. Emerging developments include printed flexible sensors, self-powered platforms, AI-assisted gas detection, and nanostructured MO materials that can operate at low temperatures.

Conclusion

Finally, MO, GO, CNT and polymer-based gas sensors offer diverse but complimentary technological methods. MO sensors dominate commercial applications because of their endurance and mature manufacture, although they require more power. GO sensors enable low-power, room-temperature sensing, but they require more stability. CNT sensors offer ultra-high sensitivity and low power consumption, but cost and reproducibility remain issues. Polymer-based sensors provide versatility, low cost, and chemical tunability, however they have long-term stability problems. The future of gas sensing is in hybrid nanocomposite systems that combine the strength of MO, the sensitivity of CNTs, the surface functionality of GO, and the flexibility of polymers to provide advanced, application-specific sensing platforms for next-generation smart environments.

References

1. Patrick T Moseley Meas. Sci. Technol. 28 (2017) 082001,
2. Ananya Dey, Materials Science and Engineering: B, 229, (2018),206-217
3. N. Barsan et al., Sensors and Actuators B: Chemical, 121-1, (2007), 18-35
4. Christian Thomsen et al. Proceedings of SPIE - The International Society for Optical Engineering 108(1970) 115-234,
5. M. Mittal, et al. Sensors and Actuators B: Chemical,203, (2014), 349-362,
6. Dajing Chen, et al. Sensors, 11-7, (2011) 6509-6516
7. Arunima Verma, Sensors and Actuators Reports, 5, (2023), 100143
8. Shanlei Guo, ACS Appl. Mater. Interfaces (2026), XXXX,
9. Vishal Pandit et al. ES General, 3 (2024), 1058
10. Vishal Pandit et al. AIP Conf. Proc. 3139, (2024) 020006

Semiconductor Devices

Shital Gawade, Shweta Patil

Assistant Professor, Department of Electronics, Tuljaram Chaturchand College,

Baramati, Pune, Maharashtra

Email: shitalgawade29@gmail.com

Article DOI Link: https://zenodo.org/uploads/19788891

DOI: 10.5281/zenodo.19788891

Abstract

Semiconductor devices play vital role in advanced technologies and has immense importance in applied physics. Applied physics deals with theory, practical knowledge essential for study of different properties of semiconductors like optical, material and electrical. Advanced technologies involve smartphones, computers, Internet of Things, quantum computing, AI technologies and renewable energy and many more, increases the requirement of advanced semiconductor devices. Also these devices are foundation of largest electronics industries in the word. The given chapter analyzes the structure, principle, emerging technologies, semiconductor technologies, research and future trends of semiconductor devices in above domain.

Keywords: BJT, MOSFET, fabrication, AI, IoT, photolithography, nanoelectronics, biomedical, etching.

Introduction

As we know, solid state materials categorized in insulators, conductors and semiconductors depending on the property electric conductivity. Semiconductors having two types: Intrinsic semiconductors, Extrinsic semiconductors. When impurities are added to intrinsic semiconductors, extrinsic semiconductors are formed. Semiconductors have conductivity between conductors and insulators, sensitive to energy band gap, impurity doping, temperature and magnetic field. Based on doping atoms, semiconductors further divided into n- type semiconductors due to donor impurities and p-type semiconductors due to acceptor impurities with carrier concentration, electrons and holes respectively.

Semiconductor Devices

A p–n junction is a basic element in modern electronics and semiconductor devices. It forms the foundation of PN junction diodes, are widely used in rectification, switching, wave shaping circuits and voltage regulation. Different types of diodes include rectifier diodes, Zener diodes, photodiodes, Schottky

diodes, varactor diodes and LEDs. Special diodes such as IMPATT diodes and tunnel diodes are used in microwave oscillators, amplifiers, radar systems and satellite communication, operating in the GHz to THz frequency range. Another important semiconductor device is the Bipolar Junction Transistor (BJT), which consists of two p–n junctions that different functional regions are created within a single crystal. BJTs are used for amplification, high-speed switching and power applications, where current flow due to both carriers. To overcome this, Heterojunction Bipolar Transistors (HBTs) are developed using two different semiconductor materials with highly doped base to achieve better high-frequency performance.

The MOSFET is a voltage-controlled semiconductor device in which the gate is insulated from the channel by an oxide layer. It has high input resistance, fast switching speed and low power consumption, so it is widely used in switching circuits, amplifiers, memories, microprocessors and CMOS logic gates. Thyristor has PNPN structure with three junctions and can handle high voltage and current. It is commonly used in power electronics, switching circuits, lighting control, home appliances and industrial power systems.

Emerging Semiconductor Devices

Light Emitting Diode (LED) is a semiconductor device that emits light in all directions when current passes through it. It operates on the principal electroluminescence, occurs in a forward biased p–n junction diode. The colour of light depends on semiconductor material used and band gap energy. LED is made up of compound semiconductors for different colours such as Gallium Arsenide (GaAs) for Red, Gallium Phosphide (GaP) for Green, Gallium Nitride (GaN) for Blue. LEDs operates at low voltage (1.8V–3.3V), low power consumption, narrow-spectrum emission determined by direct bandgap of semiconductor material. Fast response times for optical communication and has high quantum efficiency.

Applications

Energy-efficient solid-state lighting for smart applications, High-speed optical communication systems (Li-Fi technology). In medical phototherapy, biomedical diagnostic instruments, wearable electronics. Infrared LEDs for remote sensing, security systems. Automotive lighting in electric, autonomous vehicles.

Organic Light Emitting Diode (OLED) is advanced display technology where each individual pixel produces its own light when exposed to electric current. It is advanced form of LED in which the emissive electroluminescent layer is made of organic compounds. It is a device made of some immensely fine layers of organic semiconductor materials placed between two conducting electrodes anode and cathode on a supporting surface called substrate. The total thickness of

these layers is very small, usually between 100 and 500 nanometers. In OLED, each pixel produces its own light as it is self-emissive. It provides excellent picture quality with high contrast ratios and bright colors. OLED panels are thin, light weight, flexible, foldable. Generally, consume less power, when displaying dark images, as pixels are turned off. OLEDs applicable in Smartphone displays, Smart TVs, Wearable electronics, foldable and Transparent displays.

LASER (Light Amplification by Stimulated Emission of Radiation) produces highly monochromic, coherent and parallel directional beam of light. The development of laser is most supreme achievements in applied physics and has led to revolutionary advancements in science and engineering. Their extremely high intensity makes them suitable for material ablation, cutting, and welding applications. High-power lasers are widely used in applied physics and engineering for precision cutting, welding, drilling, cleaning through fast, non-contact processing. Also enable advanced manufacturing techniques like laser 3D printing, support sub-micron measurements in optical metrology, and improve material durability through surface engineering processes such as cladding and hardening. A silicon p–n junction diode is used in solar cell. While silicon is dominant, some thin-film solar cells use materials like Cadmium Telluride (CdTe) or Gallium Arsenide (GaAs). For optoelectronics and renewable energy, they are crucial in applied physics. Applications are Space-Based Power Systems, residential Power Generation, solar glass facades, Agrivoltaics, PV-Silicon Tandem Cells, Advanced Energy Storage systems.

Semiconductors have major role in nanoelectronics, integrated circuits, VLSI technology, biomedical devices, sensors and AI systems. Nano-electronics deals with nanometer dimensions and quantum behavior given by classical physics. Examples are FinFET, improve control on gate terminal, carbon nanotubes and graphene devices provide high flexibility. Wearable electronics where MoS2 and WS2, 2-D materials are used.

Semiconductors used in the Electric vehicle (EV) development. Power electronics devices provide electricity in EV by using different converter circuits, to minimize power consumption. Semiconductor devices have wide range applications in biomedical as biosensors, gluco sensors, IR temperature sensors, Micro-Electro-Mechanical Systems (MEMS) sensors, ECG systems, senses biomolecules in human being with great sensitivity. Development of semiconductors demonstrates in IoT in connecting different devices with internet, in wireless communication for data acquisition and control.

Fabrication Techniques

Fabrication techniques convert raw semiconductors into integrated circuits (realized product). The core technologies involved crystal growth, float zone process, lithography, etching, wafer preparation, diffusion, epitaxial growth, film

formation (CVD, thermal oxidation) and metallization. In wafer preparation, pure silicon transforms into sliced, polished and form base wafer. This technique is front end fabrication technology. The crystals formed are used in HPHV devices. The process in which single crystal film, has high quality is deposited on the substrate wafer called film deposition technique. This includes chemical-vapors unwanted material. Plasma etching involves ionize gases in vacuum chamber to unmask materials and use for precise, high resolution. Silicon Etching, Silicon Dioxide Etching, Silicon Nitride, Polysilicon Etching, Aluminum Etching, and Gallium Arsenide Etching are types of wet etching.

Future Scope

In future, there is continue great development and innovation in semiconductor technologies and to increase the efficiency of electronics devices, invention of new materials such as graphene, 2D other materials, 3D stacked integrated circuits by researchers. Combination of semiconductors and AI take forefront in embedded technologies, healthcare, AI algorithms etc. In future, semiconductors form the foundation of nanoelectronics, sustainable energy, power electronics, optoelectronics devices, and quantum mechanics.

Conclusion

Semiconductor devices show a strong co-ordination between applied physics and innovation. From basic semiconductor devices to modern quantum devices, semiconductors have transformed modern life. Amalgamation of semiconductors into emerging trends such as Nano-electronics, Artificial Intellegence, IoT, sustainable energy and biomedical ensures continued global relevance. The future of semiconductor devices exists in inventiveness, simplification, renewability and smart system integration. For students and investigators in applied physics, technologies in semiconductor provides immense academic, commercial and research prospects, making it most versatile and powerful fields of the study in this Era.

References

1. S. M. Sze and K. K. Ng, Physics of Semiconductor Devices, John Wiley & Sons.
2. S. M. Sze and M. K. Lee, Semiconductor Physics and Devices: An Indian Adaptation, Wiley India.
3. B. G. Streetman and S. Banerjee, Solid State Electronic Devices, Pearson Education.
4. D. A. Neamen, Semiconductor Physics and Devices, McGraw-Hill Education.
5. R. F. Pierret, Semiconductor Device Fundamentals. Addison-Wesley.

6. M. N. Yoder, “Wide bandgap semiconductor materials and devices,” IEEE Trans. Electron Devices, vol. 43, 1996.
7. S. Lu, “A systematic analysis of wide band gap semiconductors used in power electronics,” Appl. Comput. Eng., 2024.
8. I. A. Khramtsov and D. Yu. Fedyanin, “Superinjection of holes in homojunction diodes based on wide-bandgap semiconductors,” arXiv preprint, 2019.
9. Q. Li et al., “Room-temperature printing of ultrathin quasi-2D GaN semiconductor via liquid metal gallium surface-confined nitridation reaction,” arXiv preprint, 2022.
10. M. Si et al., “A ferroelectric semiconductor field-effect transistor,” arXiv preprint, 2018.
11. J. Kim et al., “Observation of tunable bandgap and anisotropic Dirac semimetal state in black phosphorus,” Nat. Phys., 2015.
12. D. Jena et al., “Emerging nitride semiconductor materials for future electronic and photonic devices,” Proc. IEEE / arXiv, 2019.

LaB_6-Coated Silicon Nanowire Heterostructure for High-Performance Field Emitters

Amol Deore, Sachin Potdar, Niteshkumar Yadav

Applied Sciences & Humanities, School of Computing, MIT Art, Design and Technology University, Pune, Maharashtra, India

Email: amol.deore@mituniversity.edu.in

Article DOI Link: https://zenodo.org/uploads/19788980

DOI: 10.5281/zenodo.19788980

Abstract

One-dimensional (1D) materials are playing a crucial role in field emitter devices (e.g., vacuum microelectronic applications) because of their height-to-tip radius ratio, well vertical aligned morphology, and virtuous separation between two successive emitters. 1D silicon nanowires (Si-NWs) exhibit a lower turn-on field and a lower current density due to a higher work function (Φ). However, Lanthanum Hexaboride (LaB_6) shows a low work function, superior chemical and thermal properties, and offers an effective Φ modification engineering technique. We can modify the electronic structural behaviors using a simple method to coat LaB_6 onto Si-NWs. In this scenario, Si-NWs act as the backbone of LaB6 coating, and LaB6 itself acts as 1D emitters. In this book chapter, we have discussed the LaB6/Si heterostructure arrays emitters fabrication mechanism, the electron tunneling mechanism by Fowler–Nordheim (F-N) theory, the thin coating Sn film on Si substrate, the screening effects due to two successive emitters, and emission stability. Emission behavior is interpreted from both theoretical and experimental perspectives, and significant structural factors influencing performance are investigated. Reduced turn-on fields and increased current density are obtained by combining the intrinsic emissive properties of LaB6 with the geometric field enhancement from Si-NWs. Scalability, reliability issues, and prospects for device integration in sophisticated vacuum electronic systems are covered.

Keywords: Silicon Nanowires, Lanthanum Hexaboride, Heterostructure, Field Emission, Fowler–Nordheim Theory, HFCVD, Work Function

Introduction

Applying a strong electric field, the bending of the barrier height of the potential well occurs, and due to the image potential triangular shape becomes a smooth surface, then electrons are tunneled out from the emitters. This phenomenon is

established by Fowler–Nordheim and it is also called the F-N theory [4]. Field emission is very appealing for small and energy-efficient vacuum electronic devices like field emission displays, X-ray sources, microwave amplifiers, and electron microscopy systems because it functions well at room temperature in contrast to thermionic emission, which needs high temperatures [3].

Nanostructured materials such as Si-NWs eliminate the disadvantages of planar emitters by concentrating the electric fields at their sharp ends and enhancing the local electric field by geometric amplification [5]. The tip radius and nanowire aspect ratio have a significant impact on the field enhancement factor (β). However, the work function of bare silicon is about 4.15 eV, which limits the emission current density that can be achieved and raises the operating voltage requirements. One such common cathode material is LaB6, with a low work function (2.6 eV), a high melting point, high electric conductivity, and resistance to oxidation and ion bombardment [6, 7]. This heterostructure exhibits better electron emission characteristics through a combination of a geometric field enhancement and a reduction in height of the surface barrier with the coating of Si-NWs with LaB6. Experimental studies have demonstrated significant increases in current density and turn-on fields of less than 2 V/mm2 compared with bare Si-NWs [1,2,7].

Field Emission Mechanism

Fowler–Nordheim tunneling theory governs the electron emission behavior of LaB6/Si heterostructures [4]. The emission current density (J) is expressed as:

$$J = A(\beta E)^{2} \exp[-B\varphi^{(3/2)}/(\beta E)] \quad (1)$$

Here, φ: work function of the emitting surface, β : field enhancement factor, and E : applied macroscopic electric field. β is a very crucial parameter related to the h J = A(βE)² exp[-Bφ^(3/2)/(βE)] (1)eight-to-tip radius ratio of the emitters. The maximum emission current density depends on the φ parameter, and it can be modified by LaB6 coating on Si-NWs.

However, the maximum J value and lower turn-on field depend on multiple parameters such as tip radius and overall coating of lower φ material, which modify β values. Additionally, high-density emitters experience a local electric field (Elocal) interaction over the tip called the screening effect, which can reduce the Elocal experienced by individual emitters. Hence, to improve the emission current density and lower turn-on values, are only possible by optimizing the thickness over nanowires, and the minimal tip radius (aspect ratio) of nanowires.

Fabrication Methodology

LaB6/Si arrays fabrication entails a regulated multi-step synthesis pathway in

order to achieve uniformity. Nanowire development and conformal coating. The substrate is then a polished silicon which is cleansed with standard. RCA processes to eliminate organic and oxide pollution. A thin Sn catalyst film (typically 5–10 nm) is deposited by thermal evaporation. The thickness of this catalyst layer directly influences the size distribution of catalyst droplets formed during subsequent thermal treatment. The Sn-coated substrate undergoes hydrogen annealing, causing the continuous film to dewet into nanoscale droplets. These droplets act as nucleation centers for nanowire growth. This substrate is then placed into the HFCVD device, and SiH4 breaks down around the hot filament. The catalyst droplets are supplied with silicon atoms, which favors the growth of nanowires via a VLS pathway to form vertically aligned arrays of Si-NW. To form the heterostructure, LaB_6 is deposited over the nanowire forest using electron-beam evaporation. Well-improved coating thickness (~ 5–20 nm) on Si-NWs effectively modify the surface φ [1].

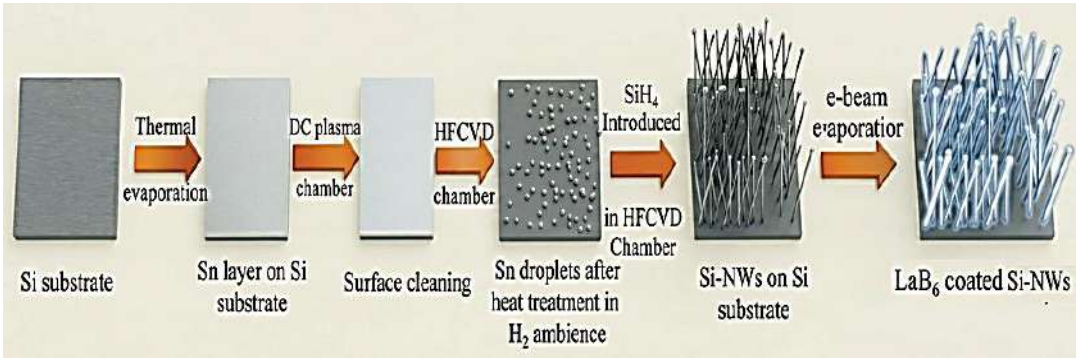

Figure: Schematic representation of the synthesis of LaB6-coated Si-NWs array

Field Emission Performance Analysis

From the measurement point of view, field emission comportment is based on the turn-on values, maximum J value, F-N behavior, and current stability. The minimum field required to tunnel the electrons from emitters is called the turn-on field. Emission current density at moderate fields is markedly enhanced due to the combined effect of geometric field concentration and reduced work function. Properly optimized heterostructures exhibit orders-of-magnitude higher current density than uncoated nanowires. Fowler–Nordheim plots typically display strong linearity over a broad field range, confirming tunneling-dominated emission behavior. A decrease in FN slope following coating shows an effective work-function decrease without loss of high eight values.

Constant current operation stability reflects the protective effect of LaB6. The coating is chemically robust, which reduces ion bombardment damage and surface oxidation, causing less current fluctuation and a longer lifespan of the device.

Comparative Field Emission Study of e-Beam Evaporated LaB_6 Heterostructures

Emitter type	Coating Method	Turn-on Field [V/μm]	Maximum current density and applied field	Ref.
20 nm LaB_6/Si Nanowire Array	E-beam Evaporation	1.2	2.76 mA/cm² ~ 2.7 V/μm	[1]
50 nm LaB_6/Si Nanowire Array	E-beam Evaporation	1.6	2.23 mA/cm² ~ 2.7 V/μm	[1]
LaB_6/Si-tip Field Emitter Array	E-beam Evaporation	~ 3.5	75 μA ~ 1500 V	[8]
LaB_6 Spindt-type FEA on Si	E-beam Evaporation	60	5.58 mA ~ 145 V	[9]
LaB_6 hat-coated Si Nanopillars	E-beam Evaporation	~ 2.5	458 mA/cm² ~ 850 V	[10]

Future Scope and Applications

The next-generation studies should aim at the enhancement of LaB6/Si interface engineering to reduce the contact resistance and increase carrier transport. Emission efficiency may also be enhanced by detailed studies on band alignment. Uniformity of the fabrication process of wafer-level and large-area integration is an important goal. LaB6/Si heterostructures are highly promising in gated triode applications in field emission displays, microwave amplification systems, as well as small-scale X-ray sources. They are thermal and chemically stable, thus can withstand extreme operational environments. Further improvements in thickness regulation, array design, and interface design will make these heterostructures next-generation electron emitters.

References

1. A. Deore, K. Jagtap, O. Bhorade, and M. A. More, “Thickness dependent field emission study of LaB_6 coated Si nanowire arrays,” J. Vac. Sci. Technol. B, vol. 41, no. 2, p. 022806, 2023.
2. A. Deore, “In-situ growth of silicon nanowires array and its field emission behavior,” Mater. Sci. Semicond. Process., vol. 125, p. 105623, 2021.
3. C. A. Spindt, “A thin-film field-emission cathode,” J. Appl. Phys., vol. 39, no. 7, pp. 3504–3505, 1968.
4. R. H. Fowler and L. Nordheim, “Electron emission in intense electric fields,” Proc. R. Soc. A, vol. 119, no. 781, pp. 173–181, 1928.
5. V. T. Binh et al., “Electron field emission from nanomaterials,” Appl. Phys. Lett., vol. 73, no. 21, pp. 3052–3054, 1998.
6. M. A. Gesley and L. W. Swanson, “Spectral analysis of fiel
7. d emission noise from LaB_6,” Phys. Rev. B, vol. 30, no. 3, pp. 162–170, 1984. M. A. More, D. S. Joag, and R. G. Forbes, “Field electron emission

from nanomaterials," in Encyclopedia of Nanotechnology. Cham, Switzerland: Springer, 2015.
8. X. Wang et al., "Field emission characteristics of lanthanum hexaboride coated silicon field emitters," Vacuum, vol. 82, no. 2, 2007.
9. X. Wang et al., "Formation of extremely high current density LaB_6 field emission arrays via e-beam deposition," Appl. Phys. Lett., vol. 93, no. 9, p. 093503, 2008.
10. X. Wang et al., "High-performance field emission from LaB_6 hat-coated silicon nanopillar arrays prepared by microsphere lithography," J. Phys. D: Appl. Phys., vol. 55, no. 17, 2018.

Detecting and Managing Micro-Bending Effects in Optical Fiber Networks: A State-of-the-Art Review

Mhaske Mangal K., Kakade Pravin R., Kangude Sahadev H.

Department of Physics Rayat Shikshan Sanstha's Dada Patil Mahavidyalaya Karjat,

Dist- Ahilyanagar-414402

Email: mhaskemangal78@gmail.com

Article DOI Link: https://zenodo.org/uploads/19789075

DOI: 10.5281/zenodo.19789075

Abstract

In contemporary communication networks, optical fiber technology serves as a key platform, enabling long-distance, high-bandwidth data transfer with minimal loss and excellent immunity to electromagnetic disturbances. With the rapid expansion of optical-fiber infrastructure in telecommunications, power grids, and industrial manufacturing, maintaining the reliability and structural integrity of fiber cables has become increasingly vital. Mechanical stress, environmental factors, and accidental damage can introduce structural defects, leading to signal attenuation. Among various loss mechanisms, micro-bending-induced optical loss is particularly significant, as even minor mechanical perturbations can cause substantial degradation in signal integrity. This review explores the fundamentals of optical fiber communication, the physics of bending-induced losses, and the critical role of network monitoring. Key techniques like Optical Time-Domain Reflectometry (OTDR), interferometric sensing, and Fiber Bragg Grating (FBG) sensors are evaluated. Emerging trends in micro-bending-based sensing and cost-effective monitoring strategies are also highlighted, offering insights into enhancing the resilience and efficiency of optical fiber networks.

Keywords: Optical Fiber, Cable Monitoring, OTDR, FBG, Sensors.

Introduction

The rapid advancement of digital communication technologies has led to a growing need for high-speed and dependable data transmission systems. Traditional communication media, such as copper cables, are constrained by several drawbacks, including significant signal attenuation, restricted bandwidth, and vulnerability to electromagnetic interference. Optical fiber communication systems have largely replaced traditional transmission technologies because they provide higher bandwidth, lower transmission losses, and greater data security [1,2].

Optical fibers carry information using light signals, which are produced by optical sources like laser diodes or light-emitting diodes (LEDs). These optical signals travel through the fiber core and are converted back into electrical signals at the receiving end using photodetectors. Because optical fibers operate at extremely high carrier frequencies, they can support significantly higher data transmission rates compared with conventional electrical communication systems [2].

Dense wavelength division multiplexing (DWDM), a sophisticated multiplexing technology used in modern optical networks, enables the simultaneous transmission of many signals of various wavelengths across a single fiber. That enhances the capacity of communication networks and supports high-speed data transmission required for internet services, cloud computing, and multimedia applications [3].

As optical fiber networks expand in scale and complication, maintaining their operational reliability has become a major challenge. Mechanical stress, temperature variations, and environmental conditions can cause structural changes in optical fibers that affect signal propagation. Continuous monitoring of fiber cables is therefore necessary to detect potential faults and ensure steady communication [4].

Fundamentals of Optical Fiber Communication

A cylindrical dielectric waveguide that uses the total internal reflection concept to direct light is called an optical fiber. The core, cladding, and protective coating are the three main parts of the fiber. The cladding, which surrounds the core and has a slightly lower refractive index, ensures that light stays contained within the core during propagation. The core is the central area where light propagates. [5].

It classified into two categories: single-mode fibers and multimode fibers. Single-mode fibers support only one propagation mode and are commonly used for long-distance communication due to their low attenuation and minimal signal dispersion. Multimode fibers allow multiple propagation modes and are used in short-distance communication systems.[6]

Importance of Fiber-Optic Cable Monitoring

Optical fibers may experience mechanical stress during installation or operation. Environmental factors such as temperature fluctuations, vibrations, and external pressure can also influence fiber performance. Damage to optical fibers can result in signal attenuation, data loss, and reduced network reliability. In critical applications such as energy grids, defines communication networks, and large data centres, failure of optical fiber links can lead to serious economic and operational consequences [7].

It should be capable of identifying faults at an early stage and determining the location of damage along the fiber length. Consequently, there is growing interest in developing simple and cost-effective monitoring techniques based on variations in optical parameters such as transmitted power and scattering losses [8].

Bending Loss in Optical Fibers

Bending of optical fibers is one of the major causes of signal attenuation. When a fiber is bent, part of the optical power propagating through the core may escape into the cladding or surrounding environment, resulting in transmission loss. Bending losses are generally categorized into macro bending loss and micro bending loss.

- **Macro Bending Loss**

Macro bending occurs when an optical fiber is bent with a relatively large radius, typically due to improper cable routing during installation. If the bending radius becomes smaller than a critical value, the optical field spreads beyond the core boundary and leaks into the cladding, leading to signal attenuation [9].

- **Micro Bending Loss**

Micro bending refers to microscopic distortions along the fiber axis caused by external mechanical pressure or structural variations in the fiber. These small perturbations change the propagation characteristics of light inside the fiber and cause coupling between guided modes and radiation modes [10]. However, even minor microbands can lead to noticeable signal attenuation in long-distance fiber networks. Theoretical and experimental studies have shown that micro bending losses depend on fiber design, coating materials, and external mechanical stress [11].

Monitoring Techniques for Optical Fiber Networks

- **Optical Time-Domain Reflectometry (OTDR)**

It is among the most popular methods for identifying problems in optical fiber networks. In this method, short optical pulses are launched into the fiber, and the backscattered light is measured as a function of time. By analysing the returned signal, it is possible to determine attenuation along the fiber and identify the location of faults such as bending losses [12]. Although OTDR provides accurate fault detection, the equipment required is relatively expensive and may not be suitable for continuous monitoring of large-scale fiber networks.

- **Interferometric Fiber Sensors**

Interferometric sensors detect changes in the phase of optical signals caused by mechanical strain or environmental disturbances. These sensors are extremely

sensitive and capable of detecting very small variations in optical path length [13]. However, interferometric systems require exact alignment and technologically advanced instrumentation, which may limit their practical performance.

- **Fiber Bragg Grating Sensors (FBG)**

For evaluating structural health, Fiber Bragg Grating (FBG) sensors are commonly utilized. They are created by introducing periodic refractive index variations in the fiber core. Broadband light passing through the fiber reflects a specific wavelength from the grating. Mechanical strain or temperature changes shift this reflected wavelength, enabling precise measurement of environmental effects on the fiber[14].

- **Micro Bending-Based Sensors**

Micro bending sensors utilize controlled microbands in optical fibers to detect variations in optical power caused by mechanical pressure. When external stress is applied, the resulting microbands cause light to leak from the core, reducing the transmitted optical power.

These sensors are relatively simple, inexpensive, and suitable for distributed monitoring applications [15].

Conclusion

Optical fiber communication is a cornerstone of modern information systems, offering high bandwidth, low attenuation, and immunity to electromagnetic interference. As fiber-optic networks expand across telecommunications, industrial automation, and energy sectors, ensuring their reliability and structural integrity has become essential. Mechanical stress and environmental factors often induce bending losses, degrading signal quality and network performance. Monitoring techniques are therefore vital for early fault detection and maintenance. Micro-bending-based sensing provides a simple, cost-effective approach to detect mechanical disturbances in optical fibers. While advanced methods such as OTDR, interferometric sensors, and fiber Bragg gratings deliver high accuracy, their complexity and cost limit large-scale deployment. Ongoing research into micro-bending-induced loss and affordable sensing technologies will significantly enhance the reliability of optical fiber networks.

References

1. G. Keiser, Optical Fiber Communications, McGraw-Hill, 2010.
2. G. P. Agrawal, Fiber-Optic Communication Systems, Wiley, 2012.
3. B. Culshaw and A. Kersey, “Fiber-optic sensing: A historical perspective,” J. Lightwave Technol., 2008.

4. R. M. Measures, Structural Monitoring with Fiber Optic Technology, Academic Press, 2001.
5. D. Gloger, “Weakly guiding fibers,” Applied Optics, 1972.
6. J. Sakai and T. Kimura, “Bending loss of propagation modes in optical fibers,” IEEE J. Quantum Electronics, 1979.
7. J. D. Murphy et al., “The influence of motion and stress on optical fibers,” Applied Optics, 2013.
8. B. Lee, “Review of the present status of optical fiber sensors,” Optical Fiber Technology, 2003.
9. D. Marcuse, “Curvature loss formula for optical fibers,” JOSA, 1976.
10. K. Petermann, “Upper and lower bounds for microbending loss in single-mode fibers,” IEEE JQE, 1982.
11. X. Jin and F. Payne, “Numerical investigation of microbending loss in optical fibers,” J. Lightwave Technol., 2016.
12. A. Nakamura et al., “Highly sensitive detection of microbending in single-mode fibers,” Optics Express, 2017.
13. B. Culshaw, “Optical fiber sensor technologies,” J. Lightwave Technol., 2004.
14. A. Othonos and K. Kalli, Fiber Bragg Gratings, Artech House, 1999.
15. B. Zhang et al., “Embedded fiber-optic microbend sensor for pressure measurement,” Sensors and Actuators A, 2006.

Emerging Semiconductor Materials for High-Performance Optoelectronic Applications

Kangude Sahadev H., Pawar Pratik R., Mhaske Mangal K.

Department of Physics Rayat Shikshan Sanstha's Dada Patil Mahavidyalaya Karjat, Dist- Ahilyanagar-414402

Email: sahadevkangude7283@gmail.com

Article DOI Link: https://zenodo.org/uploads/19789162

DOI: 10.5281/zenodo.19789162

Abstract

Semiconductor materials play a fundamental role in modern optoelectronic technologies by enabling efficient interaction between electrical signals and optical radiation. Their key properties, including band-gap energy, carrier mobility, recombination mechanisms, and optical absorption, strongly influence device performance. Conventional semiconductors such as silicon and germanium have been widely used in electronic and photonic devices due to their stability and compatibility with established fabrication technologies. In contrast, III–V semiconductor materials such as GaAs, GaN, and InP offer superior optical efficiency for high-performance optoelectronic applications. Recently, emerging materials such as two-dimensional semiconductors, quantum dots, and hybrid perovskites are gaining considerable interest because of their tunable band structures and strong light–matter interactions.

Keywords: Optoelectronics, Semiconductor materials, Gallium nitride, Perovskites, Quantum dots, Photodetectors.

Introduction

Optoelectronics has developed into a dynamic field of modern electronics centered on light–matter interactions within electronic materials. Devices operating on these principles are extensively employed in optical communication, display technologies, imaging systems, sensing platforms, and renewable energy applications [1]. The performance of these devices largely depends on semiconductor materials, whose electronic properties enable efficient conversion between electrical energy and optical signals. The functioning of optoelectronic devices is based on fundamental physical processes such as photon absorption, generation of charge carriers, and radiative recombination. Upon interaction with light, photons possessing adequate energy excite electrons to transition from the valence band to the conduction band, thereby generating electron–hole pairs. Carrier recombination can emit energy in the form of light, serving as the

fundamental mechanism for components such as LEDs and semiconductor laser systems [2]. The selection of semiconductor materials plays a critical role in determining efficiency, stability, and performance of optoelectronic systems. Key material parameters, including band-gap energy, carrier mobility, carrier lifetime, and optical absorption coefficient, determine device behavior. Conventional semiconductors such as silicon have dominated the electronics industry for several decades. However, compound semiconductors including gallium arsenide and gallium nitride are extensively utilized in high-performance optoelectronic applications because of their direct band gaps and excellent optical characteristics [3]. Recent advancements in materials science have enabled the emergence of various semiconductor systems, including two-dimensional materials, nanostructured semiconductors, and hybrid perovskite materials. These emerging materials exhibit unique optical and electronic properties that enable next-generation optoelectronic technologies such as flexible devices, high-speed photodetectors, and highly efficient solar cells [4].

Fundamental Principles of Semiconductor Optoelectronics

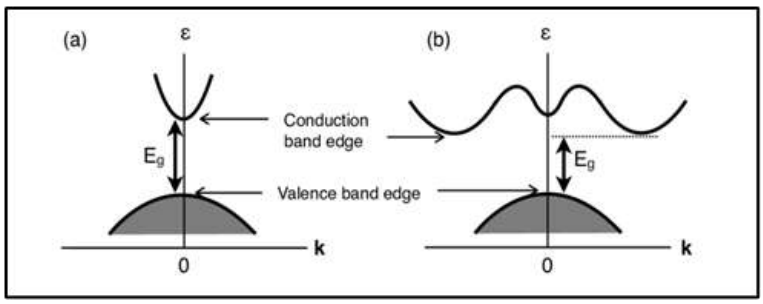

Fig. 1. Schematic energy band representations for (a) a direct band-gap semiconductor and (b) an indirect band-gap semiconductor, highlighting electron–hole recombination processes. [Ref. 5].

Semiconductors possess a characteristic distinct electronic band structure comprising a valence band and a conduction band separated by an energy gap that regulates the photon energies a material can effectively absorb or emit, thereby controlling the wavelength of light in optoelectronic processes [5]. When light with sufficient energy interacts with the material, electrons are excited to the conduction band and their recombination with holes can release energy as photons, producing light emission.

Semiconductor materials can be categorized into direct and indirect band-gap types according to their electronic band structure. In direct band-gap semiconductors, electrons recombine directly with holes without momentum change, enabling efficient photon emission, and materials such as gallium arsenide and indium phosphide are widely used in LEDs and laser diodes [6].

In contrast, indirect band-gap semiconductors such as silicon require the assistance of lattice vibrations (phonons) during recombination, which reduces their light emission efficiency but still allows effective operation in photodetectors and photovoltaic devices.

Elemental Semiconductor Materials

- **Silicon**

Silicon is the most widely used semiconductor due to its abundance, chemical stability, and mature fabrication technology, and its indirect band gap of about 1.12 eV makes it suitable for photovoltaic and photodetection applications but less efficient for light emission [7]. Silicon-based solar cells dominate the global photovoltaic market due to their reliability, mature manufacturing processes, and low cost, while silicon photonics enables the integration of optical components onto silicon-based platforms for high-speed optical communication [8].

- **Germanium**

Germanium is another group-IV semiconductor that exhibits higher carrier mobility than silicon. It has a band gap of approximately 0.67 eV, which enables strong absorption in the infrared region and makes it suitable for infrared photodetectors and optical communication devices [9].

- **Carbon (Diamond)**

Diamond is considered a wide band-gap semiconductor, with an energy gap of about 5.5 eV. with excellent thermal conductivity and chemical stability, and advances in chemical vapor deposition have enabled high-quality diamond films for next-generation electronic and optoelectronic devices [10].

Compound Semiconductor Materials

- **Gallium Arsenide (GaAs)**

Gallium arsenide (GaAs) represents a highly significant compound semiconductor employed in optoelectronic devices. It exhibits a direct band gap of nearly 1.42 eV along with high electron mobility, enabling efficient light emission and fast electronic response [11]. GaAs finds extensive application in optoelectronic systems including light-emitting diodes (LEDs), semiconductor lasers, and high-efficiency photovoltaic cells.

- **Gallium Nitride**

Gallium nitride (GaN) is considered a wide band-gap semiconductor, with an energy gap of about 3.4 eV that has significantly advanced solid-state lighting technologies by enabling the generation of blue and ultraviolet light for modern LED systems [12], GaN-based devices also exhibit high thermal stability and can

operate under high-voltage conditions, making them suitable for both optoelectronic and power electronic applications.

- **Indium Phosphide (InP)**

Indium phosphide (InP) represents a significant III–V semiconductor widely utilized in optoelectronic devices operating at wavelengths suitable for fiber-optic communication systems [13]. InP-based lasers and photodetectors are extensively used in high-speed optical communication networks.

Emerging Semiconductor Materials

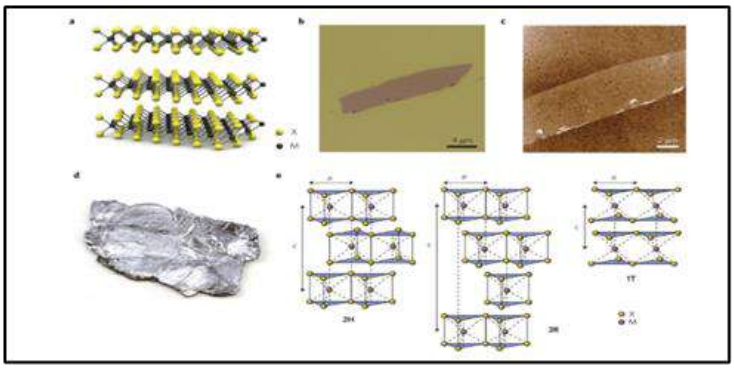

Figure 2. Structure and microscopy images of two-dimensional transition metal dichalcogenide (TMD) materials showing layered atomic structure and different crystal phases. (Ref. 14).

Recent research has focused on new classes of semiconductor materials that offer improved optical properties and enhanced device flexibility. Two-dimensional materials, particularly transition metal dichalcogenides (MoS_2 and WS_2), exhibit strong light–matter interactions and tunable band gaps, making them promising for next-generation optoelectronic devices [14].

Another emerging class of materials is metal halide perovskites, which have demonstrated excellent performance in photovoltaic cells and light-emitting devices due to their high absorption coefficients & tunable band gaps [15]. Nanostructured semiconductors, particularly quantum dots, exhibit strong size-dependent optical properties and have been widely investigated for applications in display technologies, photodetectors, and advanced optoelectronic devices [16].

Applications of Semiconductor Optoelectronics

Semiconductor optoelectronic devices have numerous applications in modern technology. Light-emitting diodes and semiconductor lasers are widely used in display systems and optical communication networks. Photodetectors are employed in imaging, environmental monitoring, and biomedical sensing, while semiconductor solar cells convert sunlight into electrical energy for renewable

power generation [17].

Conclusion

Semiconductor materials have enabled remarkable advancements in optoelectronic technologies over the past several decades. Traditional materials such as silicon and germanium continue to play important roles in electronics and photonics, while compound semiconductors provide superior optical performance for light-emitting and communication devices. Emerging materials including two-dimensional semiconductors and perovskites offer new opportunities for developing flexible, high-efficiency optoelectronic systems. Continued research in semiconductor materials and device fabrication techniques is expected to drive further progress in optoelectronic technologies.

References

1. Zhang, Y., Li, X., & Chen, J. (2023). Journal of Energy Storage, 58, 106345.
2. Zou, J., Zhang, S., & Tang, X. (2024). Photonics, 11, 1014.
3. Shin, H., et al. (2024). Nature Communications, 15, 8125.
4. Abbas, K., et al. (2024). Microsystems & Nanoengineering, 10, 81.
5. Sze, S. M., & Ng, K. K. (2007). Physics of semiconductor devices (3rd ed.). Wiley.
6. Agrawal, G. P. (2012). Semiconductor lasers and optical communication systems. IEEE Press.
7. Green, M. A. (2023). Progress in Photovoltaics, 31, 3–15.
8. Thomson, D., et al. (2024). Journal of Optics, 26, 073003.
9. Liu, J., et al. (2023). Nature Photonics.
10. Isberg, J., et al. (2023). Advanced Materials.
11. Wang, J., et al. (2024). Nano Letters, 24, 12111–12117.
12. Li, B., et al. (2024). Nature Reviews Electrical Engineering, 1, 412–425.
13. Almeida, G., et al. (2023Nature Reviews Materials, 8, 742–758.
14. Wang, Q. H., et al. (2024). Nature Nanotechnology.
15. Aftab, S., et al. (2024). Journal of Materials Chemistry C, 12, 17789–17801.
16. Houtepen, A. J., et al. (2025). Nature Reviews Methods Primers, 5, 42.
17. Abbas, K., et al. (2024). Microsystems & Nanoengineering, 10, 81.

Sensors and Technology: Materials, Mechanisms, and Future

Priyanka Godase

Prof. C.N.R. Rao Research Laboratory, Department of Physics, T.C. College,

Baramati, (413102)

Email: go483182@gmail.com

Article DOI Link: https://zenodo.org/uploads/19789260

DOI: 10.5281/zenodo.19789260

Abstract

Sensors form the backbone of modern technological systems by enabling the detection and quantification of physical, chemical, and biological parameters. Contemporary sensors are no longer standalone mechanical devices; they are miniaturized, highly sensitive systems integrated with the Internet of Things (IoT), micro- and nano-electromechanical systems (MEMS/NEMS), nanostructured materials, and artificial intelligence. A wide range of materials are employed in sensor fabrication, including semiconductors, metal oxides, piezoelectric ceramics, conductive polymers, graphene, and biomolecular components. Advanced synthesis and fabrication techniques such as sol–gel processing, chemical and physical vapor deposition (CVD/PVD), hydrothermal synthesis, electrochemical deposition, and additive manufacturing allow precise control over material properties and device architecture. Modern sensors play a critical role in healthcare diagnostics, environmental monitoring, industrial automation, smart infrastructure, and autonomous systems. Future developments are focused on wireless connectivity, real-time health monitoring, self-powered devices, and intelligent data processing, positioning sensors at the core of next-generation smart technologies.

Keywords: Sensors; MEMS/NEMS; Artificial Intelligence; Smart Systems; Industry 4.0.

Introduction

A sensor is a device designed to detect variations in physical, chemical, or biological parameters and convert them into measurable electrical signals. These signals enable monitoring, regulation, automation, and decision-making across diverse technological systems [1,2]. The evolution of sensing technology traces back to early scientific instruments such as thermometers and barometers in the seventeenth century. A major milestone occurred in 1883 with Warren Johnson's invention of the electric thermostat, marking the transition from purely

mechanical measurement tools to electrically responsive sensing devices [3]. During the mid-twentieth century, advances in electronics and materials science led to the development of semiconductor-based and ultrasonic sensors, significantly improving sensitivity, reliability, and miniaturization. In the twenty-first century, sensors have become integral components of intelligent systems, operating within interconnected networks such as the Internet of Things (IoT). They are embedded within micro- and nano-electromechanical systems (MEMS and NEMS) and increasingly incorporate artificial intelligence for data interpretation and predictive analysis. These advancements underpin emerging technological frameworks including Industry 4.0, smart cities, and digital healthcare [4].

Material selection plays a central role in determining sensor performance. Semiconductor materials such as silicon and gallium arsenide are foundational in electronic and MEMS-based devices due to their well-controlled electrical properties. Metal oxides including ZnO, SnO_2, and TiO_2 are widely used in gas and chemical sensing applications because of their surface reactivity and high sensitivity to environmental changes. Piezoelectric ceramics, particularly lead zirconate titanate (PZT), are employed in pressure and vibration sensing owing to their ability to generate electrical signals under mechanical stress [5]. Flexible and biocompatible polymers are increasingly utilized in wearable and implantable devices, enabling continuous physiological monitoring. Nanostructured materials such as graphene and carbon nanotubes enhance sensor performance by providing high surface-to-volume ratios, superior electrical conductivity, and rapid response characteristics [6]. In biomedical diagnostics, biosensors incorporate biologically active elements enzymes, antibodies, nucleic acids, and other biomolecules to achieve highly selective detection of analytes [7]. Fabrication techniques are equally important in tailoring sensor functionality. Thin-film deposition methods, including chemical vapor deposition (CVD), physical vapor deposition (PVD), and sputtering, enable controlled formation of functional layers. Electrochemical deposition is commonly used for coating and functionalization, while additive manufacturing and 3D printing technologies allow the fabrication of flexible and customized sensing platforms [8].

This paper presents a comprehensive overview of sensor materials, operating principles, fabrication strategies, and integration into smart systems, emphasizing their expanding role in advanced technological applications.

Types of Sensors

Sensors are embedded in everyday systems and industrial infrastructure, operating continuously to enhance safety, efficiency, and comfort. Their applications span domestic appliances, transportation, healthcare, security, and environmental monitoring.

- **Temperature Sensors**

These devices monitor thermal variations in environments and systems. They regulate climate control units, refrigeration systems, automotive engines, and industrial processes, ensuring optimal operational conditions and preventing overheating.

- **Pressure Sensors**

Pressure-sensitive devices measure force per unit area in gases or liquids. They are essential in automotive tire pressure monitoring systems, industrial machinery, hydraulic systems, and household appliances to maintain safety and performance stability.

- **Proximity Sensors**

Designed to detect the presence or absence of nearby objects without physical contact, proximity sensors are used in smartphones, automatic doors, robotics, and parking assistance systems.

- **Motion Sensors**

These sensors identify movement within a defined area and are widely deployed in security systems, smart lighting, surveillance infrastructure, and interactive gaming platforms.

- **Light Sensors**

Light-dependent sensors measure illumination intensity and adjust system responses accordingly. Applications include automatic brightness control in electronic displays, adaptive street lighting, and solar energy optimization.

- **Humidity Sensors**

Humidity sensors determine moisture content in air, playing a critical role in weather monitoring, agricultural management, HVAC systems, and controlled storage environments.

- **Gas Sensors**

Gas detection systems identify hazardous or combustible gases in residential, industrial, and automotive settings, contributing significantly to environmental safety and occupational health.

- **Biometric Sensors**

These sensors authenticate identity through physiological characteristics such as fingerprints, facial features, or iris patterns. They are central to modern security systems, mobile devices, and access control technologies.

Table 1: Synthesis Methods, Material Systems, Sensitivity, and Applications of Sensor Technologies

Synthesis Method	**Material Used**	**Sensor Type**	**Typical Sensitivity / LOD**	**Key Applications**
Sol–Gel Method	TiO_2, ZnO, WO_3, SnO_2	Metal oxide gas sensor	ppm–ppb	Gas sensing & environmental monitoring
Hydrothermal / Solvothermal	ZnO, TiO_2, MoS_2	Gas & biosensors	ppb	Toxic gas detection, glucose sensing
Chemical Vapor Deposition (CVD)	Graphene, CNTs, MoS_2	Nano-electronic sensors	ppb–ppt	Ultra-sensitive gas sensors, biosensors
Physical Vapor Deposition (PVD) / Sputtering	Thin films of ZnO, SnO_2, ITO	Resistive & optical sensors	ppm–ppb	Humidity, gas, photodetectors
Electrochemical Deposition	Au, Pt nanoparticles, Conducting polymers	Electrochemical biosensors	µM–nM (nM–pM LOD)	Glucose sensors, pathogen detection
Spray Pyrolysis	SnO_2, WO_3, TiO_2 thin films	Gas sensors	ppm	Industrial gas monitoring
Screen Printing	Carbon ink, Graphene oxide	Disposable biosensors	µM–nM	Point-of-care diagnostics
Electrospinning	Polymer nanofibers, ZnO composite fibers	Flexible gas sensors	ppb	Wearable environmental sensors
Microwave-Assisted Synthesis	Metal oxide nanoparticles	Gas sensors	ppb	Rapid synthesis for air quality sensors
Lithography (MEMS Fabrication)	Silicon, SiO_2	Pressure, capacitive sensors	High precision (fF resolution)	Automotive, aerospace pressure sensing
Laser Ablation	Metal nanoparticles (Au, Ag)	Plasmonic sensors	nM–pM	Chemical & biomolecule detection
Self-Assembly	CNT networks, Graphene sheets	Flexible nano-sensors	ppb–ppt	Wearable electronics

Future and scope

Next-generation sensors will combine intelligence, autonomy, and seamless wireless connectivity to support distributed and edge-based computing systems [9]. By processing data closer to the source, these devices will reduce latency and enhance reliability in real-time industrial operations. In manufacturing, advanced sensors will enable predictive maintenance through continuous monitoring of vibration, temperature, pressure, and acoustic signals, allowing early fault detection and minimizing downtime. Wireless sensor networks will extend monitoring to remote, hazardous, and inaccessible environments, including aerospace and offshore platforms [10]. The evolution of sensor materials and fabrication techniques has significantly improved sensitivity, durability, and application-specific performance. Integrated with artificial intelligence and networked infrastructures, modern sensors now function as intelligent decision-support nodes rather than simple measurement tools. Future development will emphasize energy efficiency, miniaturization, sustainability, and scalable production. As industries advance toward automation and digitalization, sensors will remain fundamental to ensuring operational safety, efficiency, and adaptive system performance.

References

1. Mehrotra, P. Journal of Oral Biology and Craniofacial Research (2016), 6, 153–159,
2. Kumar, K.; Sharma, A.; Tripathi, S.L. In Electronic devices, circuits, and systems for biomedical applications; Elsevier, (2021) 177–195.
3. Lawlor, C. PhD Thesis, Institute of Art, Design Technology, 2024.
4. Mandić, V.; Panžić, I.; Bafti, A.; Radovanović-Perić, F.; Pavić, L. In Biotechnology and Human Enhancement; De Sio, L., Turmus, E.K., Eds.; NATO Science for Peace and Security Series A: Chemistry and Biology; Springer Netherlands: Dordrecht, (2025); pp. 111–143.
5. Mehmood, Z.; Haneef, I.; Udrea, F. Microsyst Technol (2020), 26, 2751–2766
6. Erdem, Ö.; Derin, E.; Zeibi Shirejini, S.; Sagdic, K.; Yilmaz, E.G.; Yildiz, S.; Akceoglu, G.A.; Adv Materials Technologies (2022).
7. Erdem, Ö.; Derin, E.; Zeibi Shirejini, S.; Sagdic, K.; Yilmaz, E.G.; Yildiz, S.; Akceoglu, G.A.; Inci, F. Adv Materials Technologies (2022.
8. Liu, Y.; Wang, H.; Zhao, W.; Zhang, M.; Qin, H.; Xie, Y. Flexible, Sensors (2018), 18, 645.
9. Ficili, I.; Giacobbe, M.; Tricomi, G.; Puliafito, A. Sensors (2025), 25, 1763.
10. Rashvand, H.F.; Abedi, A. In Wireless Sensor Systems for Extreme Environments; Rashvand, H.F., Abedi, A., Eds.; Wiley, (2017) 1–19.

Topological Magnetic Materials for Low-Power Spintronic Applications

Jawale Rhushikesh Sanjay

Department of Physics, Jamkhed Mahavidyalaya Jamkhed, Dist-Ahilyanagar-413201

Email: rhushikeshjawale5@gmail.com

Article DOI Link: https://zenodo.org/uploads/19789340

DOI: 10.5281/zenodo.19789340

Abstract

Topological magnetism offers a route to energy-efficient spintronic devices by stabilizing magnetic states through geometry and symmetry rather than large magnetic fields. When spin–orbit coupling, exchange, and broken inversion symmetry cooperate, nanoscale textures such as skyrmions and chiral domain walls can be created, moved, and detected with lower current density than conventional magnetization dynamics. In parallel, magnetic topological insulators and Weyl semimetals provide band-structure topology that links charge transport to magnetization via Berry curvature, enabling distinctive Hall signals and efficient spin–orbit torques. This paper reviews real-space and momentum-space topology, summarizes representative performance metrics reported in the literature, and discusses how topological stabilization can reduce write energy and improve endurance. Key challenges include room-temperature stability, defect-mediated pinning, and scalable materials integration, with an outlook toward low-power memories, oscillators, and logic based on topological magnetic states.

Keywords: Berry curvature, SOT, DM, Band-topological platforms, spintronic technology

Introduction

Spintronics encodes and manipulates information using the electron's spin in addition to its charge. Spin-transfer torque (STT) and spin–orbit torque (SOT) have enabled technologies such as magnetic tunnel junctions and spin-torque MRAM, but further reductions in switching current and improved scalability remain central goals. Topological magnetic materials provide an alternative. Here, "topology" denotes properties robust to smooth deformations: in real space, nontrivial winding of the magnetization stabilizes textures such as skyrmions; in reciprocal space, Berry curvature yields quantized or enhanced transport responses. Both forms can couple strongly to electrical currents, lowering

thresholds for motion or switching. Because low-power operation is essential for edge devices and high-density memories, understanding how topological magnetism can be engineered is timely.

This paper surveys key classes of topological magnetic materials relevant to low-power spintronics and organizes their principles into (i) real-space topology (skyrmions and chiral domain walls) and (ii) band topology (magnetic topological insulators and Weyl semimetals). We then discuss representative results from the literature and extract materials and device design rules.

Background

Topological textures arise when competing interactions favor noncollinear magnetization. In chiral magnets with broken inversion symmetry, the Dzyaloshinskii–Moriya interaction (DMI) competes with exchange and anisotropy, favoring spirals and skyrmions. Interfacial DMI at heavy-metal/ferromagnet interfaces can similarly stabilize Néel-type skyrmions in ultrathin films, which are attractive for CMOS-compatible stacks. The small size of skyrmions (from a few to hundreds of nanometers) and their ability to move under spin torques motivates skyrmion "racetrack" concepts.

Band topology enters when spin–orbit coupling reshapes the electronic structure, producing Berry curvature and topological invariants. In magnetic topological insulators, time-reversal symmetry is broken by magnetism, enabling phenomena such as the quantum anomalous Hall effect (QAH) and chiral edge conduction. In magnetic Weyl semimetals, Weyl nodes act as sources and sinks of Berry curvature, leading to large anomalous Hall effects and current-induced torques. These properties can provide efficient electrical readout and new pathways for writing magnetic states.

From a device perspective, low power is achieved by reducing (a) the critical current for switching or motion, (b) the required pulse duration, and (c) energy losses from pinning and stochasticity. Topological stabilization can lower the write threshold and improve tolerance to moderate disorder, but strong inhomogeneity can also create pinning sites that offset these gains. Therefore, materials design and interface engineering are as important as the topological concept itself.

Theory

Real-space topology is commonly characterized by the skyrmion number, an integer that counts how many times the magnetization wraps the unit sphere. For a continuous magnetization field $\mathbf{m}(x, y)$, the topological charge is $N = (1/4\pi) \int \mathbf{m} \cdot (\partial_x \mathbf{m} \times \partial_y \mathbf{m})\, dx\, dy$. Nonzero N implies that the texture cannot be unwound without creating a singularity, supporting metastability. Dynamics under currents can be described by the Landau–Lifshitz–Gilbert equation augmented with

STT/SOT terms, while a reduced Thiele equation captures the motion of a rigid skyrmion and predicts both longitudinal drift and a transverse skyrmion Hall angle.

Interfacial DMI favors Néel skyrmions with a fixed chirality. The characteristic length scale is set by the ratio of exchange stiffness to DMI strength, and perpendicular anisotropy and dipolar interactions tune the diameter and stability window. In multilayers, repeating heavy-metal/ferromagnet stacks can enhance stability and device compatibility, but also modifies dipolar coupling and current flow.

An intrinsic anomalous Hall conductivity can be written as an integral of $\Omega(k)$ over occupied states. In magnetic topological insulators, exchange gaps in Dirac surface states can yield quantized Hall conductance at low temperatures. In magnetic Weyl semimetals, Weyl nodes act as sources and sinks of Berry curvature, often giving large anomalous Hall effects at higher temperature. Efficient spin–orbit torques arise when a charge current generates a spin accumulation (via spin Hall or Edelstein mechanisms) that exerts a torque on a nearby ferromagnet; torque efficiency depends on interfacial transparency and magnetic damping, directly impacting switching energy.

Results & Discussion

Representative literature illustrates why topological magnetic materials are promising for low-power devices. In bulk chiral magnets such as MnSi, current-driven skyrmion motion has been reported at threshold current densities on the order of 10^6 A/m^2, far below typical values for metallic domain-wall motion. In sputtered multilayers (for example, Pt/Co/Ir-based stacks), room-temperature skyrmions can be nucleated and driven by SOT, with current densities commonly in the 10^{10}–10^{11} A/m^2 range. While higher than in bulk crystals, these values are compatible with thin-film processing and can be reduced by optimizing damping, DMI, and current delivery.

Low-power operation requires deterministic writing and reliable readout. Skyrmion creation using localized pulses, nanoconstrictions, or voltage-controlled anisotropy has been explored to lower energy per event. The skyrmion Hall effect, which can drive skyrmions toward device edges, remains a challenge; strategies include antiferromagnetically coupled multilayers or ferrimagnets to reduce the net gyrotropic term.

Band-topological platforms provide complementary advantages. The quantum anomalous Hall effect in magnetically doped $(Bi,Sb)_2Te_3$ films demonstrates chiral edge channels and quantized Hall resistance, suggesting ultra-low-loss interconnects and sensitive magnetic readout. Although many demonstrations require cryogenic temperatures, materials progress is pushing operating temperatures upward. Magnetic Weyl semimetals and related materials can

exhibit large anomalous Hall angles and strong current-induced torques, offering another route to efficient SOT switching when integrated with ferromagnets.
Across platforms, integration is decisive. Device stacks must combine strong spin–orbit coupling, controlled anisotropy, low damping, and defect management. Pinning from grain boundaries and interfacial roughness can offset topological advantages, making uniformity critical for large arrays. Thermal stability (often targeting roughly 40–60 kBT for long retention) constrains the minimum texture size. Overall, topology can lower the effective switching pathway, but practical power gains require co-optimization of materials, patterning, and drive schemes.

Conclusion and Future Scope

Topological magnetic materials expand the spintronics design space by offering states and transport responses that are robust and strongly coupled to electrical currents. Real-space textures such as skyrmions and chiral domain walls can, in favorable materials, move at low thresholds and enable dense, reconfigurable information carriers. Momentum-space topology in magnetic topological insulators and Weyl semimetals provides efficient charge–spin interconversion and distinctive Hall signatures that can support low-loss interconnects and sensitive readout.
Future progress toward low-power applications hinges on four priorities. (1) Room-temperature, field-free stabilization of nanoscale textures with tight size distributions for scalable memory. (2) Reduced pinning and stochasticity through interface control and defect engineering to improve endurance and uniformity. (3) CMOS-compatible integration while maintaining clean interfaces and stable materials. (4) Circuit designs that exploit analog dynamics for oscillators and neuromorphic computing, where ultra-low energy per operation is possible without strict binary switching. With coordinated advances in materials discovery and device engineering, topological magnetism is well positioned to enable next-generation low-power spintronic technologies.

References

1. Žutić, I., Fabian, J., & Das Sarma, S. (2004). Spintronics: Fundamentals and applications. Reviews of Modern Physics, 76(2), 323–410.
2. Fert, A. (2008). Nobel lecture: Origin, development, and future of spintronics. Reviews of Modern Physics, 80(4), 1517–1530.
3. Nagaosa, N., & Tokura, Y. (2013). Topological properties and dynamics of magnetic skyrmions. Nature Nanotechnology, 8(12), 899–911.
4. Jonietz, F., Mühlbauer, S., Pfleiderer, C., Neubauer, A., Münzer, W., Bauer, A., Adams, T., Georgii, R., Böni, P., Duine, R. A., Everschor, K., Garst, M., & Rosch, A. (2010). Spin transfer torques in MnSi at ultralow current

densities. Science, 330(6011), 1648–1651.
5. Armitage, N. P., Mele, E. J., & Vishwanath, A. (2018). Weyl and Dirac semimetals in three-dimensional solids. Reviews of Modern Physics, 90(1), 015001.
6. Tokura, Y., Yasuda, K., & Tsukazaki, A. (2019). Magnetic topological insulators. Nature Reviews Physics, 1, 126–143.

An overview of Density Functional Theory

[1]Vipul S. Ghemud, [2]Kishor Gavhane

[1]Department of Physics, BJS's Arts, Science & Commerce College, Pune 412207, India

[2]Department of Physics, Savitribai Phule Pune University, Pune 411007, India.

Email: vipul.ghemud@gmail.com

Article DOI Link: https://zenodo.org/uploads/19789419

DOI: 10.5281/zenodo.19789419

Abstract

Density Functional Theory (DFT) has emerged as one of the most powerful theoretical frameworks for investigating the electronic structure of atoms, molecules, and condensed matter systems. This chapter presents a concise overview of the historical development and fundamental concepts underlying DFT. The discussion begins with the Born–Oppenheimer approximation, which simplifies the many-body quantum mechanical problem by separating nuclear and electronic motions. The early attempt to describe many-electron systems using electron density as the fundamental variable, introduced in the Thomas–Fermi model, is then discussed. The theoretical foundation of modern DFT is established through the Hohenberg–Kohn theorems and the Kohn–Sham formulation, which enable practical computational implementations. Finally, commonly used approximations and computational approaches, including pseudopotentials and plane-wave methods, are briefly described. This chapter provides a conceptual framework for understanding the application of DFT in modern materials science and condensed matter physics.

Introduction

A rigorous quantum mechanical description of a physical system must explicitly consider the indistinguishability of identical particles. As a consequence, any physically measurable quantity must remain invariant under the exchange of identical particles. This principle forms the basis for the quantum mechanical treatment of electrons in atoms, molecules, and solids.

In general, a physical system such as an atom, molecule, cluster, thin film, or bulk material can be regarded as a collection of electrons (N) and atomic nuclei (P) interacting via electrostatic Coulombic forces. The complete quantum mechanical description of such a system is provided by the many-body Hamiltonian given in equation (1), which contains contributions from the kinetic energies of the nuclei and electrons, along with the Coulomb interactions among

all charged particles.

$$\hat{H} = -\frac{\hbar^2}{2}\sum_{I=1}^{P}\frac{1}{M_I}\vec{\nabla}_I^2 - \frac{\hbar^2}{2m_e}\sum_{i=1}^{N}\vec{\nabla}_i^2 + e^2\sum_{i=1}^{N}\sum_{j=i+1}^{N}\frac{1}{|\vec{r}_i - \vec{r}_j|} + e^2\sum_{I=1}^{P}\sum_{J=I+1}^{P}\frac{Z_I Z_J}{|\vec{R}_I - \vec{R}_J|} \pm e^2\sum_{I=1}^{P}\sum_{i=1}^{N}\frac{Z_I}{|\vec{R}_I - \vec{r}_i|} \quad (1)$$

Where, the terms correspond to kinetic energy of nuclei, kinetic energy of electrons, electron-electron interactions, nucleus-nucleus interactions, and electron-nuclear pair interactions respectively.

In principle, solving non-relativistic time-independent Schrödinger equation can be used to study all physical properties of any system. Each electron experiences Coulomb repulsion from all other electrons. These interdependencies lead to strongly coupled equations containing two-body interaction operators, making exact solutions feasible only for the simplest systems such as hydrogen-like atoms.

Consequently, theoretical approaches capable of providing accurate approximations are essential for practical calculations involving many-electron systems.

Born-Oppenheimer Approximation

One of the most important simplifications in quantum mechanics of many-body systems is the Born–Oppenheimer approximation [1]. This approximation exploits the large mass difference between atomic nuclei and electrons. Since nuclei are orders of magnitude heavier than electrons, electrons move way to faster than nucleus. Thus, the nuclei can be considered fixed during the electronic calculation. The total wavefunction can therefore be expressed as a product of electronic and nuclear wavefunctions viz.

$$\Psi\left(\{\vec{r}_i\},\{\vec{R}_I\}\right) = \psi^{\{\vec{R}_I\}}(\{\vec{r}_i\})\Phi\left(\{\vec{R}_I\}\right)$$

Within this approximation, the Schrödinger equation is solved for obtaining electronic energy as a function of nuclear positions, by considering a fixed nuclear configuration. This energy defines the Born–Oppenheimer potential energy surface, which governs the motion of the nuclei. Although the Born–Oppenheimer approximation significantly reduces the many-body problem, solving the electronic Schrödinger equation still is computationally demanding due to electron–electron interactions. Further theoretical developments are therefore required.

Thomas – Fermi Model

An important step toward simplifying the many-electron problem was proposed independently by L. H. Thomas [2] and E. Fermi [3] in the late 1920s. In their

approach they considered kinetic, correlation and exchange energy contributions to be same as those of homogeneous electron gas with same electronic density. This theory of considering the inhomogeneous system to be locally homogeneous proved to be sensible for kinetic energy of condensed phases, but seemed very crude for atomic and molecular systems since the atomic shell structure is absent, density profile diverges at the nucleus and the total energies are very poorly predicted.

While the Thomas–Fermi model successfully captured some qualitative features of condensed matter systems, it exhibited several limitations. For example, it failed to reproduce atomic shell structures, predicted inaccurate total energies, and produced unphysical behaviour of the electron density near the nucleus. Despite these shortcomings, the model introduced the density-based description of electronic systems, which later became the cornerstone of present-day density functional theory.

Hohenberg-Kohn Theorems

Extending the Thomas-Fermi model, to treat the electronic density as the basic variable, Hohenberg and Kohn (H-K) provided a theory with a firm mathematical and theoretical footing via two theorems, describing that ground-state properties can be exactly determined by its ground-state charge-density distribution [4]. Their formulation is based on two fundamental theorems.

First Hohenberg–Kohn theorem states that the external potential acting on an interacting electron system is uniquely determined by the ground-state electron density, apart from an additive constant.

Second Hohenberg–Kohn theorem states among all possible electron densities that correspond to the correct number of electrons, the density that minimizes the total energy functional corresponds to the true ground-state density.

These theorems establish electron density as the central variable in the description of many-electron systems. Furthermore, the excited states and dynamic processes can also be studied by expanding this formalism to time-dependent DFT (TDDFT).

Density Functional Theory

Although the Hohenberg–Kohn theorems provided a conceptual framework for density-based approaches, they did not provide a practical method for computing the electron density. This difficulty was resolved by Kohn and Sham, who replaced the real interacting system with a non-interacting system with same ground-state density. The total energy of the system is given by,

$$E_{KS}[\rho] = T_0[\rho] + \int \rho(\vec{r})\hat{V}_{ext}(\vec{r})d\vec{r} + \frac{1}{2}\int\int \frac{\rho(\vec{r})\rho(\vec{r}')}{|\vec{r}-\vec{r}'|}d\vec{r}d\vec{r}' + \tilde{E}_{XC}[\rho] \qquad (2)$$

Here, $\tilde{E}$_XC [ρ] is the exchange-correlation contributions of interacting particles

system not included anywhere before.

The effective Kohn-Sham potential (V_KS) is defined as the sum of V_ext, V_XC and V_H depending on the density and indirectly on the orbitals, with

$$V_{XC}[\rho] = \frac{\delta \tilde{E}_{XC}[\rho]}{\delta \rho(\vec{r})} \quad (3)$$

Hence, these equations need to be solved self-consistently by confirming that the reference potential and the obtained solution coincide via,

$$\rho(\vec{r}) = \sum_{i=1}^{N} |\emptyset_i(\vec{r})|^2 \quad (4)$$

In practice, we consider a trial density ρ_t (r ⃗) along with external potential and solve Kohn-Sham equations resulting in new set of wavefunctions giving rise to new density and corresponding potential. This process is continued till the input and output densities match within a certain given accuracy. Once this is achieved, we say that self-consistency is achieved, as shown in Figure 1.

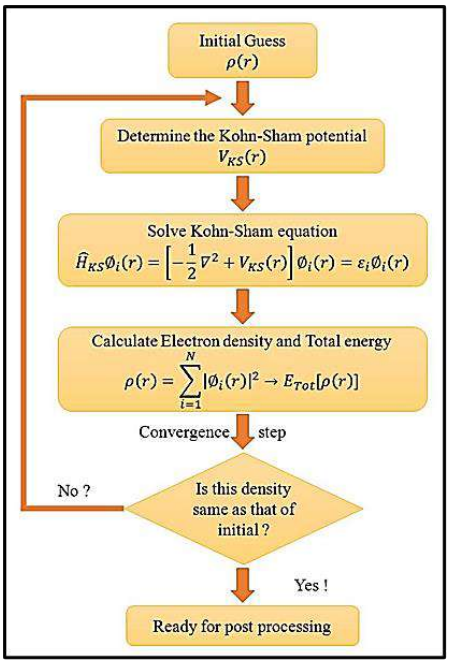

Figure 1 Flowchart for self-consistency during computational calculations.

The approximations categorizing exchange–correlation functionals according to their increasing accuracy and complexity are often organized within the conceptual framework known as Jacob's ladder.

Pseudopotential Method

In practical electronic structure calculations, explicitly treating all electrons in an atom can be computationally expensive. The pseudopotential method provides an efficient solution by introducing effective potential that mimics the Coulombic

nuclear potential and the core electronic contributions, and acts only on valence electrons [7-8].

The resulting pseudo-wavefunctions are smoother and free from rapid oscillations near the nucleus. As a consequence, they can be represented using fewer basis functions, which significantly reduces the computational effort required for calculations. Pseudopotentials therefore play a crucial role in enabling large-scale simulations of materials using plane-wave based DFT methods.

DFT for Computational Studies

The Quantum Espresso (QE) [9] and Vienna Ab initio Simulation Package [10], better known as VASP, packages implementing density functional theory (DFT) are widely used for performing ab-initio electronic-structure calculations and material modeling. These packages are based on plane wave basis sets and use pseudo-potential method for simulation purpose. The QE is an open-source software developed by numerous groups from all over the world for better performance and develop advanced features for exploring material properties. The basic calculation consists of plane-wave self-consistent formalism (PWscf) followed by post-processing methods. The VASP is not open-source software, but works in a similar way. The method of implementing DFT using plane-wave basis sets is same in both the packages. The ion-electron interactions are described by ultrasoft Vanderbilt or projector-augmented wave pseudopotentials, reducing plane-waves required to describe the system, effectively reducing the computing time. Performing the calculations in parallel reduces huge computing time with limited resources.

References

1. M. Born and R. Oppenheimer, Ann. d. Phys. 389 (1927) 457.
2. L. H. Thomas, Math. Proc. Camb. Phil. Soc. 23 (1926) 542.
3. E. Fermi, Zeits Fur. Physik. 48 (1928) 73.
4. P. Hohenberg and W. Kohn, Phys. Rev. 136 (1964) B864.
5. W. Kohn and L. J. Sham, Phys. Rev. 140 (1965) A1133.
6. M. C. Payne, M. P. Teter, D. C. Allan, T. A. Arias, J. D. Joannopoulos, Rev. Mod. Phys. 64 (1992) 1045.
7. J. C. Phillips and L. Kleinman, Phys. Rev. 116 (1959) 287.
8. J. C. Phillips, Phys. Rev. 112 (1958) 685.
9. http://www.quantum-espresso.org.
10. G. Kresse and J. Hafner, Phys. Rev. B. 47 (1993) 558.

Density Functional Theory: From Basics to Modern Approaches

Jayashri Waghmode, Shubhangi Bhosale, Vijay Mohite, Ramchandra Sapkal

Prof. C. N. R. Rao Research Laboratory, Department of Physics, Tuljaram Chaturchand College of Arts, Science and Commerce, Baramati (413102)

Email:

Article DOI Link: https://zenodo.org/uploads/19789521

DOI: 10.5281/zenodo.19789521

Abstract

Density Functional Theory (DFT) has become one of the most important tools in materials science and modern chemistry. Over the past few decades, improvements in methods, algorithms and computer power have made DFT a reliable way to study how electrons behave in molecules and solids. This chapter gives a clear overview of the main ideas behind DFT, the different types of approximations used to make calculations possible and the basic steps needed to apply it in practice. We also include examples that show how DFT helps to solve real problems in chemistry, physics such as predicting how molecules react or understanding the properties of new materials. These case studies highlight both the strengths of DFT like its efficiency and wide range of uses. By connecting DFT to the broader field of quantum mechanics, the chapter aims to give readers a solid understanding of how it works, why it is useful and how it continues to outline research in science and technology.

Keywords: DFT; Kohn–Sham equations; LDA; GGA; TD-DFT

Introduction

Density Functional Theory (DFT) is one of the most widely used method in quantum mechanics for studying how electrons behave in atoms, molecules and materials. Instead of working with the very complicated wavefunctions used in traditional approaches, DFT focuses on electron density. This change makes it possible to study systems with many interacting particles more efficiently, while still giving accurate results. The foundations of DFT were developed by Walter Kohn, whose groundbreaking work earned him the Nobel Prize in Chemistry in 1998. His ideas provided a practical way to solve problems involving many electrons and offered a powerful alternative to older quantum chemistry methods. Today, DFT is central to research in chemistry, physics and materials science because it combines reasonable computational cost with reliable accuracy.

DFT is used to explore a wide range of properties such as how molecules react, how materials behave and how they conduct electricity or interact with light. Because of this versatility, it has become a key tool for understanding matter at the quantum level and for designing new functional materials.
This chapter introduces the basic principles of quantum mechanics. It explains the challenges of many-particle systems and how DFT addresses them to enable efficient and accurate study of complex electronic structures.

Theoretical Framework
Density Functional Theory (DFT) describes many-electron systems using electron density instead of the complex wavefunction. The Kohn–Sham formalism simplifies this by modeling non-interacting electrons that reproduce the same density as the real system.
The total energy functional in the Kohn–Sham formalism is expressed as:

$$E[\rho] = T_s[\rho] + V_{ext}[\rho] + J[\rho] + E_{xc}[\rho]$$

The exchange–correlation functional E_xc [ρ]is not known exactly and must be approximated.

Exchange Correlation Approximations
In DFT, the main challenge is the exchange–correlation term, which captures quantum electron interactions but has no exact form. It is approximated using methods like the Local Density Approximation (LDA), based on local electron density, and the more accurate Generalized Gradient Approximation (GGA), which also includes density variations in space.
Several approximations have been developed to estimate E_xc [ρ]:

- **Local Density Approximation (LDA):** The Local Density Approximation (LDA) assumes the exchange–correlation energy depends only on the local electron density and works well for slowly varying systems. It is the simplest functional, based on known analytic exchange energy and parameterized correlation energy of a homogeneous electron gas.

$$E_{xc}^{LDA}(\rho) \int = \int \in_{xc}(\bar{r}, \rho(\bar{r}))\, \rho(\bar{r})\, d\bar{r}$$

∈xc ($\bar{r}$, ρ ($\bar{r}$))=Energy per electron for homogeneous electron gas of density ρ(r)

- **Generalized Gradient Approximation (GGA):** Incorporates the gradient of the density, improving accuracy for molecular and surface systems. Popular GGA functionals include PBE and PW91.

i. **Hybrid Functionals:** Combine a portion of exact exchange from Hartree–Fock theory with GGA. B3LYP is widely used in quantum chemistry.

ii. **Meta-GGA and Beyond:** Include higher-order terms or kinetic energy density for enhanced accuracy.

Computational Implementation

DFT calculations are typically performed using basis sets (e.g., plane waves or Gaussian functions) and involve solving the Kohn–Sham equations iteratively via a self-consistent field (SCF) procedure. Widely used software packages include:

- **Vienna Ab initio Simulation Package (VASP):** Vienna Ab initio Simulation Package (VASP) is a program for studying materials at the atomic level, especially crystals with repeating structures. It models electrons using plane waves and simplifies electron–ion interactions with pseudopotentials or the PAW method. It can compute electronic structure, total energy, atomic forces, and stress, and supports advanced methods like hybrid functionals, the GW approximation, and molecular dynamics. In short, it serves as a virtual lab for exploring material behavior at the quantum level.
- **Quantum ESPRESSO:** Quantum ESPRESSO is a free program for studying materials at the atomic level. Based on DFT, it uses plane waves and pseudopotentials to simplify calculations and can handle both periodic (crystals) and non-periodic systems (molecules, surfaces). It computes ground-state energy, optimizes structures, and studies vibrations and phonons, while also supporting advanced methods like many-body perturbation theory and time-dependent DFT. Its open-source, modular design allows easy customization and extension.
- **Gaussian:** Gaussian is a widely used program for studying molecules using quantum mechanics. It includes methods like Hartree–Fock, post-HF approaches (MP2, coupled-cluster), and DFT to calculate energies, optimized structures, vibrational frequencies, reaction pathways, and spectroscopic properties. By solving the Schrödinger equation with Gaussian-type basis functions, it enables efficient computations. It is widely used to study reaction mechanisms, thermochemistry, transition states, solvent effects, and excited states (TD-DFT), making it a versatile tool in computational chemistry.

Applications

- **Physics:** Calculating band structures, magnetic properties and superconductivity properties theoretically.

Band Structure

Example: For silicon, DFT predicts an indirect band gap between the valence band maximum at Γ and the conduction band minimum near X. Although LDA/GGA underestimate the gap, they accurately capture dispersion relations and effective masses. Band structures are commonly computed using plane-wave

codes like Vienna Ab initio Simulation Package or Quantum ESPRESSO. A DFT band structure for vanadium oxide (VO) is shown in Figure 1.

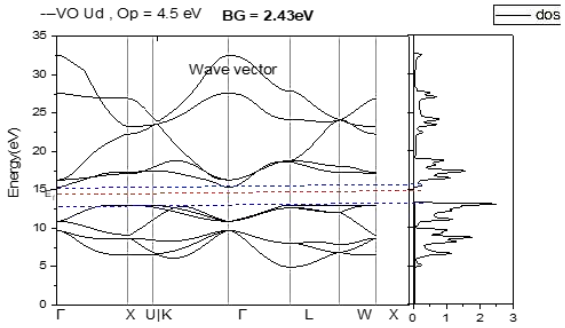

Figure 1. Band gap structure using DFT for vanadium oxide (VO)

DFT also gives the calculation of magnetic moments and exchange interactions, DFT describes ground-state electronic properties, superconductivity requires treatment of electron–phonon coupling.

- **Materials Science:** Designing catalysts, semiconductors and energy storage materials. Semiconductor Design. DFT predicts band structures, density of states (DOS), effective masses and defect energetics, which are critical for semiconductor engineering. Figure 2. shows DOS file of vanadium oxide (VO)

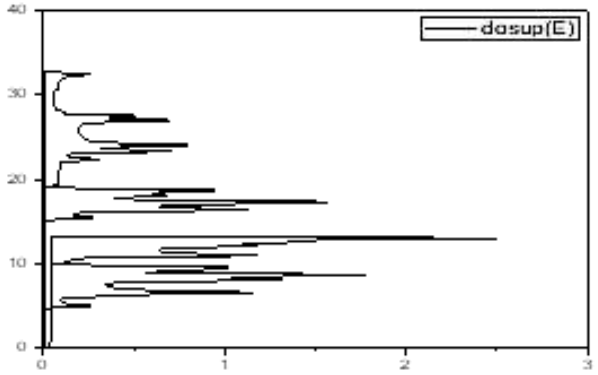

Figure 2. DOS file of vanadium oxide (VO)

Example: In silicon, DFT band structure calculations capture its indirect band gap and electronic dispersion. For semiconductors like GaN, DFT evaluates how dopants (e.g., Mg, Si) affect electronic structure and carrier concentration, with hybrid functionals (e.g., HSE06) improving band gap accuracy. This predictive power helps design materials for photovoltaics, LEDs, and microelectronics before experiments. DFT also computes adsorption energies, reaction intermediates, and activation barriers, and is widely used in electrochemistry to study ion diffusion, redox potentials, stability, and phase changes—such as

modeling lithium-ion diffusion in battery electrodes.

- **Chemistry:** Predicting molecular geometries, reaction energies and spectroscopic properties

Reaction Energies: DFT computes reaction energies (ΔE or ΔG) from the difference in total electronic energies between reactants and products.
Example: For the hydrogenation of ethene: $C_2H_4 + H_2 \rightarrow C_2H_6$

DFT can calculate the electronic energies of reactants and product and the energy difference provides the reaction enthalpy. With appropriate functionals and basis sets, predicted reaction energies often agree with experimental thermochemical data within a few kcal/mol.

Advantages
- Efficient scaling with system size
- Broad applicability to molecules and solids
- Good balance between computational cost and accuracy

Limitations
- Accuracy depends on the chosen functional
- Poor treatment of van der Waals interactions and dispersion forces
- Inadequate for strongly correlated systems (e.g., transition metal oxides)

Recent Developments

Recent Advances Include
- **Time-Dependent DFT (TDDFT):** Extends DFT to excited states and time-dependent phenomena
- **Dispersion-Corrected Functionals:** Improve predictions for molecular crystals and biomolecules
- **Machine Learning Functionals:** Use data-driven approaches to design new exchange–correlation models

Conclusion
DFT allows researchers to predict properties like conductivity, magnetism and chemical reactivity with good accuracy, even for systems containing hundreds or thousands of atoms. Scientists keep developing better functionals, inventing faster algorithms and now even combining DFT with machine learning. DFT will be a powerful tool for discovering new materials, designing drugs and solving big challenges in energy and technology. The calculation of a wide range of molecular properties with DFT allows a close connection between theory and experiment and often leads to important clues about the geometric, electronic and

spectroscopic properties of the systems being studied. By using DFT we compute the structral, optical, morphological properties theoretically. Thus, we compare these properties to the experimental results in material science, that why it plays a vital role.

References

1. Hohenberg, P., & Kohn, W. (1964). Inhomogeneous Electron Gas. Physical Review, 136(3B), B864–B871. https://doi.org/10.1103/PhysRev.136.B864 (doi.org in Bing)
2. Kohn, W., & Sham, L. J. (1965). Self-Consistent Equations Including Exchange and Correlation Effects. Physical Review, 140(4A), A1133–A1138. https://doi.org/10.1103/PhysRev.140.A1133 (doi.org in Bing)
3. Perdew, J. P., Burke, K., &Ernzerhof, M. (1996). Generalized Gradient Approximation Made Simple. Physical Review Letters, 77(18), 3865–3868. https://doi.org/10.1103/PhysRevLett.77.3865 (doi.org in Bing)
4. Becke, A. D. (1993). Density-functional thermochemistry. III. The role of exact exchange. The Journal of Chemical Physics, 98(7), 5648–5652. https://doi.org/10.1063/1.464913
5. Giannozzi, P., et al. (2009). Quantum ESPRESSO: a modular and open-source software project for quantum simulations of materials. Journal of Physics: Condensed Matter, 21(39), 395502. https://doi.org/10.1088/0953-8984/21/39/395502 (doi.org in Bing)
6. Kresse, G., &Furthmüller, J. (1996). Efficient iterative schemes for ab initio total-energy calculations using a plane-wave basis set. Physical Review B, 54(16), 11169–11186. https://doi.org/10.1103/PhysRevB.54.11169 (doi.org in Bing)
7. M. F. M. Taib, M. K. Yaakob, F. W. Badrudin, T. I. T. Kudin, O. H. Hassan, M. Z. A. Yahya, First-principles calculation of the structural, elastic, electronic and lattice dynamics of GeTiO2, Ferroelectrics, 452, 122–128 (2013).
8. M. F. M. Taib, M. K. Yaakob, F. W. Badrudin, M. S. A. Rasiman, T. I. T. Kudin, O. H. Hassan, M. Z. A. Yahya, First-principles comparative study of the electronic and optical properties of tetragonal (P4mm) ATiO2 (A = Pb, Sn, Ge), Integr. Ferroelectr., 155, 23–32 (2014).
9. M. F. M. Taib, M. K. Yaakob, F. W. Badrudin, M. S. A. Rasiman, T. I. T. Kudin, O. H. Hassan, M. Z. A. Yahya, First-principles comparative study of the electronic and optical properties of tetragonal (P4mm) ATiO2 (A = Pb, Sn, Ge), Integr. Ferroelectr., 155, 23–32 (2014).
10. G. Prandini, A. Marrazzo, I. E. Castelli, N. Mounet, N. Marzari, Precision and efficiency in solid-state pseudopotential calculations, npjComput. Mater., 4, 72 (2018).
11. K. F. Garrity, J. W. Bennett, K. M. Rabe, D. Vanderbilt, Pseudopotentials for high-throughput DFT calculations, Comput. Mater. Sci., 81, 446 (2014).

Theoretical Study of Quantum Tunneling in Semiconductor Devices

[1]Rhushikesh S. Jawale, [2]Bharti D. Pawar

[1]Assistant Professor, Department of Physics, Jamkhed Mahavidyalaya Jamkhed, District Ahilyanagar (MS)

[2]Student, Department of Physics, Jamkhed Mahavidyalaya Jamkhed, District Ahilyanagar (MS)

Email: rhushikeshjawale5@gmail.com

Article DOI Link: https://zenodo.org/uploads/19789676

DOI: 10.5281/zenodo.19789676

Abstract

Quantum tunneling is one of the most important quantum-mechanical effects used in modern electronics. Although classical physics predicts that a particle with energy lower than a barrier cannot cross it, quantum theory shows that there is still a finite probability of penetration through a thin barrier. This principle explains the operation of tunnel diodes, resonant tunneling structures, scanning tunneling systems, flash memory devices, and many leakage processes found in scaled transistors. The present paper gives a theoretical study of quantum tunneling in semiconductor devices using a simple analytical approach based on barrier width, barrier height, carrier effective mass, and applied electric field. The discussion is focused on how tunnelling probability changes with device dimensions and why this effect becomes stronger as semiconductor structures move to the nanometer scale. The paper also compares useful tunneling with unwanted tunneling leakage and explains why this phenomenon is both a design challenge and an engineering opportunity. Theoretical results show that thinner barriers and lower effective mass strongly increase transmission probability, leading to faster switching in some special devices but also higher off-state current in conventional transistors. This study highlights the continued importance of quantum tunneling in semiconductor research and design.

Introduction

Semiconductor devices are the foundation of modern communication, computing, sensing, and power systems. For many years, their behavior could be explained largely by classical ideas such as drift, diffusion, and standard energy band theory. However, when device dimensions are reduced to the nanometer range, quantum effects begin to play a direct role in charge transport. Among these

effects, quantum tunneling is especially significant because it allows electrons or holes to pass through a potential barrier even when their energy is lower than the barrier height. This behavior is impossible in classical mechanics, but it is a natural consequence of the wave nature of matter.

In practical semiconductor engineering, tunneling can be useful or harmful. It is useful in devices such as the Esaki tunnel diode, where tunneling creates negative differential resistance and enables high-speed operation (Esaki, 1958). It is also central to resonant tunneling devices and charge storage mechanisms in memory technologies. At the same time, tunneling can create gate leakage, junction leakage, and reliability problems in highly scaled MOSFETs and thin-oxide structures (Sze & Ng, 2006). Therefore, a theoretical understanding of this effect is essential for device design.

Background

Quantum tunneling arises from the Schrödinger equation, where a particle's wave function penetrates and decays within a potential barrier instead of vanishing at its edge. The transmitted wave gives a finite probability (its square) of crossing the barrier, so even classically forbidden regions can allow current if the barrier is sufficiently thin.

Historically, tunneling became important in semiconductor physics after the development of heavily doped p-n junctions. Esaki showed that narrow junctions in germanium could support tunneling current, creating the tunnel diode (Esaki, 1958). Later, tunneling through artificial superlattices and thin barriers led to resonant tunneling concepts (Tsu & Esaki, 1973). In present-day devices, tunneling is strongly linked with nanoscale dimensions, high electric fields, and ultra-thin dielectric layers. It is also influenced by band alignment, effective mass, and interface quality. Therefore, tunneling is not only a basic quantum concept but also a practical issue in semiconductor technology (Ferry, 2000; Lundstrom, 2000).

Methodology

This paper follows a theoretical and analytical method rather than an experimental one. The discussion begins with a one-dimensional rectangular energy barrier model, which is commonly used to explain direct tunneling in semiconductors. A carrier with energy E is incident on a barrier of height V0 and width a, where $V_0 > E$. Under these conditions, the transmission probability can be approximated by an exponential expression. The model captures the main dependence of tunneling on barrier shape and material parameters.

A simplified Wentzel-Kramers-Brillouin (WKB) approach is used to interpret the effect of changing barrier width, barrier height, and carrier effective mass. The analysis is qualitative but physically meaningful. Barrier width represents the

thickness of depletion or oxide regions, barrier height represents the energy separation that the carrier must penetrate, and effective mass represents how the carrier responds to the crystal environment. Theoretical comparison is then made between ordinary transport, where carriers go over the barrier, and tunneling transport, where carriers pass through it. This method helps explain why scaling down device size makes tunneling more important even when the barrier material remains unchanged.

$$T \approx \exp(-2\kappa a)$$

$$\kappa = \sqrt{[2m^*(V_0 - E)]} / \hbar$$

Results & Discussion

The analysis shows that tunneling probability is highly sensitive to barrier width: even a slight reduction greatly increases transmission due to the exponential decay of the wave inside the barrier. As a result, nanometer-scale oxides and junctions in semiconductor devices can exhibit significant tunneling current, making this effect unavoidable with continued miniaturization.

Barrier height is the second key factor: higher barriers reduce transmission, while lower ones increase it. In real materials, this depends on band structure, doping, oxide type, and interface quality. Thus, material selection is crucial, with approaches like high-k dielectrics and optimized gate stacks used to control leakage while maintaining device performance.

The third result concerns effective mass. A lower carrier effective mass increases tunneling probability because the carrier behaves more like a delocalized quantum wave. Materials with smaller effective mass may therefore show stronger tunneling for the same barrier geometry. This is one reason why device behavior differs from one semiconductor system to another.

This relation shows that tunneling depends exponentially on the product of decay constant and barrier width. The decay constant itself depends on effective mass and the difference between barrier height and carrier energy. Therefore, width, mass, and energy separation all act together.

From a device point of view, the same quantum effect can lead to opposite outcomes. In tunnel diodes, strong tunneling is desirable because it produces high-speed response and a region of negative differential resistance that is useful in oscillators and switching circuits. In flash memory, tunneling helps move charge through thin oxide layers during write and erase operations. In contrast, for modern MOSFETs, direct gate tunneling and band-to-band tunneling can increase standby power loss and reduce efficiency. Thus, tunneling must be enhanced or suppressed depending on the purpose of the device.

A further important point is that tunneling cannot be fully understood by geometry alone. Real devices include non-ideal interfaces, trap states, image-

force barrier lowering, and field-induced barrier deformation. Under a high electric field, a triangular barrier may form, leading to Fowler-Nordheim tunneling instead of simple direct tunneling. Even so, the basic theoretical lesson remains the same: the smaller and thinner the structure, the more dominant quantum transport becomes. This is why classical-only modeling becomes insufficient for deeply scaled semiconductor devices.

Conclusion

Quantum tunneling is a fundamental phenomenon that strongly influences the behavior of semiconductor devices, especially at reduced dimensions. This theoretical study shows that tunneling probability rises sharply when barrier width decreases, barrier height decreases, or carrier effective mass becomes smaller. These trends explain both the useful operation of special devices such as tunnel diodes and the undesired leakage found in ultra-scaled transistors. The study also shows that quantum tunneling is not simply a correction to classical transport; in many nanoscale structures it becomes a primary conduction mechanism.

Future Scope

Future work can extend this study by using numerical simulations for realistic barrier shapes, multi-layer semiconductor systems, and temperature-dependent effects. Additional research may also focus on tunneling in two-dimensional materials, quantum wells, and low-power device architectures. A better understanding of tunneling will help engineers design semiconductor components that balance speed, memory performance, and energy efficiency in next-generation electronics.

References

1. Datta, S. (1995). Electronic transport in mesoscopic systems. Cambridge University Press.
2. Esaki, L. (1958). New phenomenon in narrow germanium p-n junctions. Physical Review, 109(2), 603-604. https://doi.org/10.1103/PhysRev.109.603
3. Ferry, D. K. (2000). Transport in nanostructures. Cambridge University Press.
4. Lundstrom, M. (2000). Fundamentals of carrier transport (2nd ed.). Cambridge University Press.
5. Sze, S. M., & Ng, K. K. (2006). Physics of semiconductor devices (3rd ed.). John Wiley & Sons.
6. Tsu, R., & Esaki, L. (1973). Tunneling in a finite superlattice. Applied Physics Letters, 22(11), 562-564. https://doi.org/10.1063/1.1654509

Theoretical Study of Galaxy Rotation Curves and Implications for Gravity

[1]Rhushikesh S. Jawale, [2]Sandesh M. Avhad

[1]Assistant Professor, Department of Physics, Jamkhed Mahavidyalaya Jamkhed, District Ahilyanagar (MS)

[2]Student, Department of Physics, Jamkhed Mahavidyalaya Jamkhed, District Ahilyanagar (MS)

Email: rhushikeshjawale5@gmail.com

Article DOI Link: https://zenodo.org/uploads/19789817

DOI: 10.5281/zenodo.19789817

Abstract

Galaxy rotation curves test how mass and gravity behave on kiloparsec scales. Many disks show nearly flat outer velocities that are too high to be explained by visible stars and gas alone. This paper summarizes a theoretical modeling approach in two frameworks: standard gravity with a dark matter halo and low-acceleration modified-gravity phenomenology. We outline baryonic mass modeling, discuss common halo profiles and fit degeneracies, and highlight robust qualitative outcomes such as flat outer curves and baryonic scaling relations. We then explain why rotation curves by themselves rarely provide a unique verdict on gravity and identify complementary observables—especially lensing and satellite dynamics—that can break degeneracies.

Introduction

If galactic mass followed light, the circular speed v(r) should decline outside the bright disk, roughly as v ∝ r^(-1/2). Instead, H I and optical measurements often remain roughly constant over large radii (Rubin, Ford, & Thonnard, 1980; Sofue & Rubin, 2001). The discrepancy can be interpreted as evidence for an extended, non-luminous mass component (dark matter) or as a breakdown of the Newtonian mapping between baryons and gravity in weak fields (Milgrom, 1983).

Here we present a compact theoretical study of how rotation curves are modeled and what conclusions are robust to reasonable changes in assumptions. The focus is on transparent ingredients, fit degeneracies, and implications for gravity that survive common observational uncertainties.

Background

In Newtonian gravity, v(r)^2 = G M(<r)/r. For a thin baryonic disk, the enclosed mass M(<r) grows quickly in the inner region and then saturates, so v(r) should peak and fall. Flat outer curves imply M(<r) continuing to rise with r, i.e., a mass distribution more extended than the light.

The dark matter interpretation introduces a halo surrounding the baryons. A common parametric form is the Navarro-Frenk-White (NFW) profile, motivated by collisionless simulations (Navarro, Frenk, & White, 1997). Cored profiles (e.g., pseudo-isothermal halos) are often used when inner data favor shallow slopes, particularly in dwarfs. Inferring halo structure is complicated by uncertainties in stellar mass-to-light ratios and by systematics such as inclination errors and non-circular motions.

Modified-gravity phenomenology instead links outer dynamics to baryons through an acceleration scale a0. In MOND-like models, the low-acceleration limit g ≈ sqrt (gN a0) yields approximately flat outer speeds and the scaling v^4 ∝ Mb, where Mb is the total baryonic mass (Milgrom, 1983; McGaugh, 2005). Relativistic extensions were proposed to address lensing and cosmology constraints (Bekenstein, 2004), but rotation curves remain a central test bed.

Methodology

We model the predicted circular speed as the quadrature sum of contributions from the stellar disk, bulge (if present), gas, and an additional component or effective-gravity term. Stellar contributions are derived from the surface-brightness profile multiplied by a mass-to-light ratio (M/L); the gas term is computed from the H I surface density (with a correction for helium). Disk contributions are calculated using standard thin-disk expressions or numerical integration when needed.

For dark matter, the additional term is computed from a halo density profile through the enclosed halo mass. We consider NFW and cored pseudo-isothermal halos and fit parameters by minimizing chi-square between model and observed velocities, propagating uncertainties from measurement error, distance, and inclination.

For modified gravity, we compute the Newtonian baryonic acceleration gN(r) from the baryonic model and infer the effective acceleration g(r) using an interpolation function with scale a0. The predicted speed follows from v(r) = sqrt(r g(r)). We treat (M/L) as a nuisance parameter with plausible priors and use diagnostics such as the outer flat speed and the relation between gobs = v^2/r and gN across radii.

To reduce bias, we also consider standard corrections that are often necessary in practice. In gas-rich dwarfs and outer disks, pressure support can lower the observed rotation speed relative to the true circular speed (asymmetric-drift

correction). Radio beam smearing can artificially flatten the inner rise if angular resolution is limited, and small inclination errors can systematically rescale velocities. In applications, these effects are handled by using high-resolution data where available, propagating distance and inclination uncertainties, and testing whether inferred parameters remain stable under reasonable systematics variations.

Result & Discussion

The key theoretical requirement for flat outer rotation curves is straightforward: either the gravitating mass must keep increasing with radius or the effective gravitational response must strengthen relative to Newtonian expectations in the outer, low-acceleration region. In halo models, flatness typically arises once the halo contribution dominates beyond the optical disk; both NFW and cored halos can reproduce the outer shape over common radial ranges.

Fits consistently reveal degeneracies. A higher stellar (M/L) reduces the halo needed in the inner galaxy, while a lower (M/L) pushes the halo to contribute earlier; this can mimic differences between cusps and cores. Low-mass galaxies often prefer shallower inner profiles than simple collisionless cusps, which may reflect baryonic feedback reshaping the inner potential, but it can also be read as a challenge to overly rigid halo parameterizations.

Modified-gravity fits tend to reproduce outer curves with fewer shape parameters because the asymptotic behavior is tied to baryonic mass. They naturally yield the baryonic Tully-Fisher relation (Tully & Fisher, 1977; McGaugh, 2005) and are consistent with the observed tight correlation between gobs and gN (often discussed as a radial acceleration relation). In standard gravity, the same regularities can emerge if galaxy formation couples baryons and halo structure through feedback and angular-momentum exchange.

Therefore, rotation curves alone rarely provide a unique verdict on gravity. The clearest gravity tests combine kinematics with observables that respond differently to matter and to the gravitational law, including weak/strong lensing, satellite dynamics, and multi-tracer measurements that quantify pressure support and non-circular motions.

Conclusion and Future Scope

Rotation curves robustly show that outer galactic dynamics exceed what luminous matter predicts under naive Newtonian expectations. Both dark matter halos in standard gravity and low-acceleration modified-gravity prescriptions can reproduce the primary kinematic signatures, but each relies on assumptions that must be checked with independent evidence.

Future work should prioritize joint analyses that reduce baryonic mass uncertainties and directly compare kinematics with lensing on the same systems.

Higher-resolution H I mapping, integral-field spectroscopy, improved stellar-population constraints on (M/L), and simulations that quantify feedback-driven halo response can all sharpen inferences. These steps can clarify whether galaxy-scale discrepancies are best explained by unseen matter, modified gravity, or a hybrid description.

References

1. Bekenstein, J. D. (2004). Relativistic gravitation theory for the modified Newtonian dynamics paradigm. Physical Review D, 70(8), 083509.
2. McGaugh, S. S. (2005). The baryonic Tully-Fisher relation of galaxies with extended rotation curves and the stellar mass of rotating galaxies. The Astrophysical Journal, 632(2), 859-871.
3. Milgrom, M. (1983). A modification of the Newtonian dynamics as a possible alternative to the hidden mass hypothesis. The Astrophysical Journal, 270, 365-370.
4. Navarro, J. F., Frenk, C. S., & White, S. D. M. (1997). A universal density profile from hierarchical clustering. The Astrophysical Journal, 490(2), 493-508.
5. Rubin, V. C., Ford, W. K., & Thonnard, N. (1980). Rotational properties of 21 Sc galaxies with a large range of luminosities and radii. The Astrophysical Journal, 238, 471-487.
6. Sofue, Y., & Rubin, V. (2001). Rotation curves of spiral galaxies. Annual Review of Astronomy and Astrophysics, 39, 137-174.
7. Tully, R. B., & Fisher, J. R. (1977). A new method of determining distances to galaxies. Astronomy and Astrophysics, 54, 661-673.

Plant-Mediated Silver Nanoparticles: Sustainable Synthesis and Biomedical Applications

Mhaske Mangal K., Kangude Sahadev H., Maharnavar Balbhim S

Assistant Department of Physics Rayat Shikshan Sanstha's Dada Patil Mahavidyalaya Karjat, Dist- Ahilyanagar-414402

Email: mhaskemangal78@gmail.com

Article DOI Link: https://zenodo.org/uploads/19789921

DOI: 10.5281/zenodo.19789921

Abstract

Silver nanoparticles (AgNPs) are famous for their antimicrobial, catalytic, and biomedical properties. Traditional preparation methods often involve the use of toxic reagents, high power consumption, and expensive setups, contributing to environmental risks and health problems. Green fabrication methods utilizing plant extracts offer a safer, affordable, and environmentally responsible solution. Plant phytochemicals like flavonoids, phenolics, terpenoids, proteins play a dual role as reducing and stabilizing agents in converting silver ions to their nanoparticle state. The prepared AgNPs are studied using various techniques like UV–Vis spectroscopy, XRD, TEM/SEM, FTIR, and DLS to confirm formation, morphology, and stability. These nanoparticles exhibit strong antibacterial, antifungal, and antiviral activities, with applications in medicine, wound healing, environmental remediation, biosensing, and agriculture.

Keywords: Silver Nanoparticles, Green Synthesis, Antimicrobial, Environmental remediation.

Introduction

Historically, silver has been widely used for its antimicrobial properties. With nanotechnology, its effectiveness has improved through silver nanoparticles (AgNPs), which, due to their small size and large surface area, show strong antibacterial, antifungal, antiviral, and anti-inflammatory activities useful in medicine, pharmaceuticals, environmental science, and agriculture [1,2]. Conventional synthesis methods (physical and chemical) can produce uniform nanoparticles but require costly equipment, high energy, and toxic chemicals, posing environmental and health risks [3].

To overcome these issues, green synthesis methods have gained attention. These use natural sources like plants, microorganisms, and biomolecules as reducing and stabilizing agents. Plant-based synthesis is especially popular because it is

simple, cost-effective, and eco-friendly [4]. Plant extracts contain bioactive compounds (flavonoids, phenolics, terpenes, alkaloids) that reduce Ag^{+} to Ag^{0} and stabilize nanoparticles, preventing aggregation [5]. This method operates under mild conditions without toxic chemicals, making it suitable for large-scale production [6].

Medicinal plants such as Azadirachta indica, Ocimum sanctum, Curcuma longa, Camellia sinensis, and Aloe vera are commonly used. Nanoparticle properties (size, shape, stability) depend on factors like plant type, extract composition, temperature, pH, and time [7]. These green-synthesized AgNPs have applications in pollution control, biosensing, catalysis, agriculture, and biomedicine, making plant-mediated synthesis a rapidly growing area of research [8].

This chapter covers green synthesis of plant-based AgNPs, their preparation methods, characterization, and key biomedical applications.

Synthesis of Silver Nanoparticles Using Plant Extracts

Biosynthesis of silver nanoparticles (AgNPs) using plant extracts is often called green or biological synthesis. This method has received notable interest due to its sustainable and green properties, simplicity, and affordability. In this approach, plant extracts act as both r acting as reducing and stabilizing agents, avoiding the use of toxic chemicals commonly employed in conventional nanoparticle preparation methods [9].

Silver nanoparticles are produced by first preparing a plant extract from washed, dried, and cut plant parts (leaves, flowers, bark, or roots). The material is boiled or soaked in water to obtain phytochemical-rich extract (flavonoids, phenolics, terpenoids, alkaloids, proteins, carbohydrates), which acts as a natural reducing and stabilizing agent. When mixed with silver nitrate ($AgNO_3$), these compounds reduce Ag^{+} to Ag^{0}, forming nanoparticles, indicated by a color change from pale yellow to brown due to surface plasmon resonance [10,11].

Plants such as Azadirachta indica, Ocimum sanctum, Curcuma longa, and Aloe vera are commonly used for eco-friendly synthesis [12–14]. Factors like silver nitrate concentration, extract amount, pH, temperature, and reaction time affect nanoparticle size and stability [15]. Thus, plant-based synthesis is a simple, efficient, and environmentally friendly method for producing AgNPs.

Applications of AgNPs

Antimicrobial Applications

Silver nanoparticles (AgNPs) exhibit strong antibacterial, antifungal, and antiviral activity. They attach to microbial cell membranes, causing damage and increasing permeability. They also release Ag^+ ions and generate reactive oxygen species (ROS), which disrupt cellular functions and damage proteins, lipids, and DNA, ultimately leading to cell death [16].

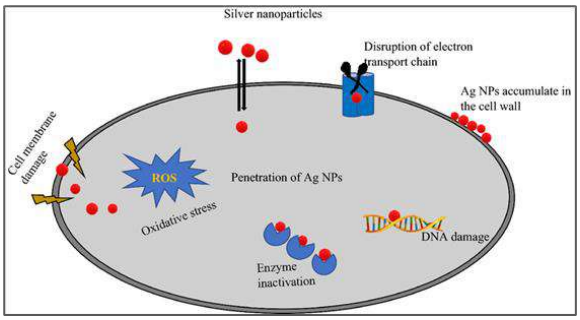

Figure 3.1 Visual schematic of the antimicrobial mechanism of AgNPs showing membrane disruption, Ag^+ ion release, ROS generation, and intracellular damage leading to microbial cell death [16].

Wound Healing and Biomedical Applications

Silver nanoparticles (AgNPs) enhance wound healing by preventing infection and reducing inflammation. They are used in creams, gels, and dressings to promote tissue regeneration and protect against pathogens. They also show potential in anticancer therapy and drug delivery systems. [17].

Environmental Remediation

AgNPs are used in water filtration and pollutant removal due to their antimicrobial and catalytic properties. They help eliminate microorganisms and degrade organic pollutants, including toxic dyes, supporting environmental sustainability. [18].

Biosensing and Diagnostic Uses

AgNPs possess unique optical and electronic properties, enabling their use in biosensors to detect pathogens, biomolecules, and toxins. Their strong surface plasmon resonance improves detection sensitivity, making them useful in medical diagnostics, food safety, and environmental monitoring. [19].

Conclusion

Plant-based synthesis of AgNPs offers a simple, resource-saving and budget-friendly alternative to ordinary routes. The resulting AgNPs demonstrate significant antimicrobial and biomedical potential. With increasing demand for

sustainable nanotechnology, Plant-based green fabrication method represents a promising process for large-scale synthesis of nanoparticle and Various uses.

References

1. Rai M., Yadav A., Gade A. 2009. Silver nanoparticles as a new generation of antimicrobials. Biotechnology Advances.
2. Akhter M. S. et al. 2024. Green synthesis of silver nanoparticles and their biomedical applications. Heliyon.
3. Iravani S. 2011. Green synthesis of metal nanoparticles using plants. Green Chemistry.
4. Ahmed S., Ahmad M., Swami B. L., Ikram S. 2016. A review on plants extracts mediated synthesis of silver nanoparticles. Journal of Advanced Research.
5. Fares A. et al. 2024. Applications of silver nanoparticles in agriculture and plant science. Planta.
6. Mittal A. K., Chisti Y., Banerjee U. C. 2013. Synthesis of metallic nanoparticles using plant extracts. Biotechnology Advances.
7. Shankar S. S. et al. 2004. Biological synthesis of triangular silver nanoparticles. Nature Materials.
8. Singh P. et al. 2018. Biological synthesis of nanoparticles from plants and microorganisms. Trends in Biotechnology.
9. Shahzadi S. et al. 2025. Green synthesis of silver nanoparticles using plant extracts. RSC Advances.
10. BalaKumaran M. et al. 2024. Plant mediated synthesis of silver nanoparticles. UP Journal of Zoology.
11. Nkosi N. et al. 2024. Characterization of green synthesized silver nanoparticles. Bioengineering.
12. Prabhu S., Poulose E. K. 2012. Silver nanoparticles: mechanism of antimicrobial action. International Nano Letters.
13. Rajak K. K. et al. 2023. Synthesis of silver nanoparticles using Curcuma longa.
14. Chandran S. P. et al. 2006. Synthesis of gold and silver nanoparticles using Aloe vera.
15. Song J. Y., Kim B. S. 2009. Rapid biological synthesis of silver nanoparticles using plant extracts.
16. Sameena, V. P., & Thoppil, J. E. (2022). Green synthesis of silver nanoparticles from Euphorbia hirta and its biological activities. South African Journal of Botany.
17. Jangid H., Singh S., Kashyap P., et al. 2024. Advancing biomedical applications: antimicrobial, anticancer, and wound healing roles of silver nanoparticles. Frontiers in Pharmacology.
18. Shahzadi S., Fatima S., Ain Q., et al. 2025. Green synthesis of silver nanoparticles using plant extracts and their environmental applications. RSC Advances.
19. Eker F., Duman H., Akdaşçi E., et al. 2024. Silver nanoparticles in therapeutics and advanced applications. Nanomaterials.

Role of Nanotechnology in Environmental Protection and Sustainability

Rani S. Gaikwad

Department of Physics, Rayat Shikshan Sanstha's Dada Patil Mahavidyalaya Karjat, Dist- Ahilyanagar-414402

Email: ranivarat555@gmail.com

Article DOI Link: https://zenodo.org/uploads/19790015

DOI: 10.5281/zenodo.19790015

Abstract

Environmental pollution and depletion of natural resources have become serious global concerns. To address these problems, advanced scientific technologies are required. Nanotechnology is one of the emerging fields that offers effective solutions for environmental protection and sustainable development. Nanomaterials possess unique properties such as very small size, large surface area, and high chemical reactivity. Because of these properties, they can interact efficiently with pollutants and help remove harmful substances from the environment. Nanotechnology is widely used in water purification, air pollution control, soil remediation, renewable energy systems, and environmental monitoring. These technologies often perform better than traditional methods and require less energy and fewer chemicals.

Keywords: Pollution, Global concern, Nanotechnology, Nanomaterials, Renewable

Introduction

Environmental pollution has increased significantly in recent years due to industrial growth, urbanization, and population increase. Large amounts of pollutants are released into air, water, and soil from industries, and agricultural activities. [1]. Nanotechnology is a branch of science and engineering that deals with materials at a very small scale, usually between 1 and 100 nanometers. At this nanoscale, materials show different physical and chemical properties compared to their larger forms. These unique properties make nanomaterials very useful for environmental applications such as removing pollutants, detecting harmful substances, and improving energy systems [2]. Researchers have developed different types of nanomaterials including metal nanoparticles, metal oxide nanoparticles, carbon nanotubes, and graphene-based materials. These materials can help remove contaminants from water and air, clean polluted soil,

and improve renewable energy technologies [3]. Because of these advantages, nanotechnology is becoming an important tool for solving environmental problems. It helps improve pollution control methods and supports sustainable use of natural resources [4]

Theory and Applications of Nanotechnology in Environmental Protection

- **Properties of Nanomaterials**

Nanomaterials have unique properties due to their extremely small size, especially a high surface area-to-volume ratio, which enhances interaction with chemicals and pollutants [5]. They also exhibit high reactivity and strong adsorption, enabling them to capture, degrade, or transform harmful substances. Common types include metal nanoparticles, metal oxides, carbon nanotubes, graphene, and nanocomposites, which are widely used in filtration, catalysis, sensing, and energy devices for environmental protection [6].

- **Nanotechnology in Water Purification**

Nanotechnology plays a vital role in water purification. Clean water is essential, yet many sources are contaminated by industrial waste, agricultural chemicals, and sewage, introducing heavy metals, organic pollutants, and microorganisms. Nanotechnology offers efficient solutions to remove these contaminants. Silver nanoparticles are widely used for their strong antimicrobial properties, while titanium dioxide nanoparticles act as photocatalysts to break down organic pollutants under light [7,8]. In addition, nanofiltration membranes and carbon nanotube filters effectively remove dissolved pollutants, heavy metals, and microbes. These technologies improve water treatment efficiency while reducing energy use and chemical consumption [9].

- **Nanotechnology in Air Pollution Control**

Air pollution is a major environmental problem caused by vehicle emissions, industrial activities, and burning of fossil fuels. Pollutants such as particulate matter, nitrogen oxides, and sulfur dioxide can cause respiratory diseases and environmental damage.Nanotechnology offers effective solutions for controlling air pollution. Nanofiber filters and carbon nanotube-based filters are capable of trapping very small particles from the air [10]. Nanocatalysts are also used in emission control systems such as catalytic converters. These catalysts help convert harmful gases into less harmful substances through chemical reactions. For example, toxic gases like carbon monoxide can be converted into carbon dioxide, which is less harmful to the environment [11]. These technologies help improve air quality and reduce harmful emissions.

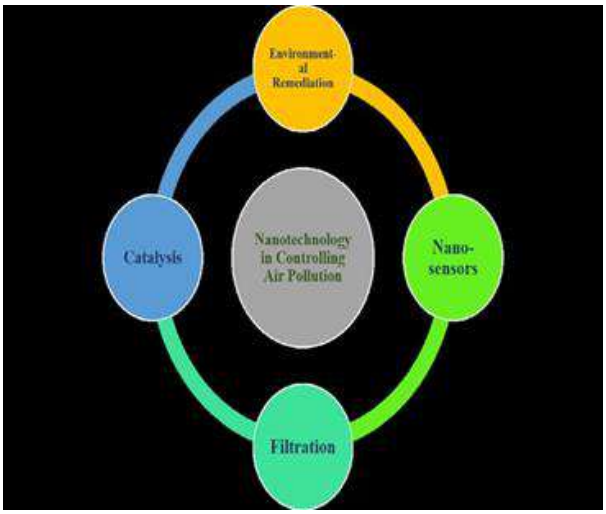

Figure 2: Air pollution control with the help of nanotechnology [11]

- **Soil Remediation Using Nanotechnology**

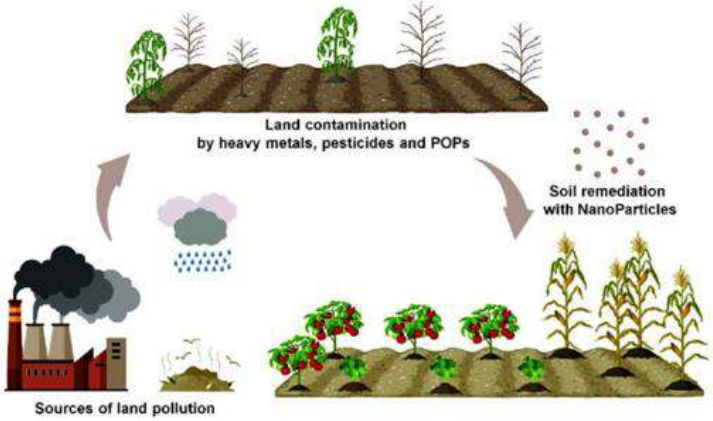

Figure 3: Soil remediation with nanoparticles. [12]

Nanotechnology in soil remediation is often called nanoremediation. It uses engineered nanoparticles to degrade or remove organic pollutionts are heavy metals from soil and ground water. Soil pollution occurs when harmful substances such as heavy metals, pesticides, and industrial chemicals accumulate in soil. This pollution affects plant growth, food safety, and ecosystem health. Nanotechnology can be used to clean contaminated soil through a process known as soil remediation. One commonly used material is nanoscale zero-valent iron. These nanoparticles can react with harmful substances and convert them into less harmful compounds [12]. Because nanoparticles are very small, they can move easily through soil pores and reach contaminated areas more effectively than larger materials. This makes the remediation process faste and more efficient

- **Nanotechnology in Renewable Energy**

Renewable energy technologies are important for reducing environmental pollution and dependence on fossil fuels. Nanotechnology helps improve the performance of renewable energy systems such as solar cells, fuel cells, and energy storage devices. Nanomaterials are used in solar panels to improve light absorption and increase electricity generation. They are also used in fuel cells to enhance energy conversion efficiency [13]. In addition, nanotechnology plays an important role in developing advanced batteries and supercapacitors. Nanostructured materials improve energy storage capacity and increase battery life [14]. These technologies support sustainable energy production and help decrease greenhouse gas emissions.[15]

- **Nanotechnology in Nanosensors and Monitoring**

Nanosensors are emerging as promising devices for improving energy conversion, utilization, and storage in solar cells. With dimensions around 100 nm, they offer high sensitivity and are transforming fields like healthcare, environmental monitoring, and sensor networks. They are especially important for detecting environmental pollution, as nanomaterial-based sensors can identify trace amounts of heavy metals in water, toxic gases in air, and harmful chemicals in soil with high sensitivity and rapid response [16]. Integrated with wireless and smart systems, nanosensors enable real-time monitoring. They are typically made from nanoparticles or nanowires.

- **Environmental Risks of Nanotechnology**

Although nanotechnology provides many environmental benefits, there are also concerns about the possible risks of nanoparticles. Some nanoparticles may have toxic effects on living organisms if they accumulate in the environment.Therefore, it is important to study the environmental and health impacts of nanomaterials before using them on a large scale. Researchers are now focusing on developing eco-friendly nanomaterials through green nanotechnology approaches [17]

Conclusion

Nanotechnology has become an important tool for environmental protection and sustainable development. The unique properties of nanomaterials make them highly effective for removing pollutants from water, air, and soil. Nanotechnology also improves renewable energy systems and environmental monitoring technologies.Compared to traditional methods, nanotechnology-based solutions often provide higher efficiency and better performance. However, careful evaluation of environmental and health risks is necessary for safe application.With continued research and responsible use, nanotechnology has the potential to play a major role in solving environmental problems and supporting

sustainable development in the future.

References

1. Bhushan, B. (2017). Springer handbook of nanotechnology. Springer.
2. Poole, C. P., & Owens, F. (2003). Introduction to nanotechnology. Wiley.
3. Rao, C. N. R., Müller, A., & Cheetham, A. (2004). The chemistry of nanomaterials. Wiley-VCH.
4. Kumar, C. S. S. R. (2018). Nanomaterials for environmental protection. Wiley.
5. Cao, G. (2004). Nanostructures and nanomaterials. Imperial College Press.
6. Wang, Z. L. (2013). Nanostructures for environmental applications. Advanced Materials.
7. Qu, X., Alvarez, P., & Li, Q. (2013). Nanotechnology in water treatment. Water Research.
8. Fujishima, A., & Zhang, X. (2006). Titanium dioxide photocatalysis. Surface Science Reports.
9. Shannon, M. A., et al. (2008). Water purification technologies. Nature.
10. Cao, G. (2011). Nanomaterials in air filtration.
11. Abhishek soni, department of chemical engineering, maulana azad national itstittute of technology, Bhopal
12. Somorjai, G., & Li, Y. (2010). Surface chemistry and catalysis. Wiley.
13. Zhang, W. (2003). Nanoscale iron for environmental remediation. Journal of Nanoparticle Research.
14. Zhou, X., & Liu, J. (2016). Nanomaterials for renewable energy. Nano Energy. And Rehman Q Khan A.D.khan A.d noman Ali, . absorbtion of solar energy using a plasmonic nanoparticals based solar cell.
15. Tarascon, J. M., & Armand, M. (2001). Lithium battery technologies. Nature.
16. Aragay, G., Pons, J., & Merkoçi, A. (2011). Nanomaterial-based sensors. Chemical Reviews.
17. Klaine, S. J., et al. (2008). Nanomaterials in the environment. Environmental Toxicology and Chemistry.

Solar Energy Materials and Their Role in Sustainable Development

Shinde Pranjali M., Kangude Sahadev H.

Department of Physics Rayat Shikshan Sanstha's Dada Patil Mahavidyalaya Karjat,

Dist- Ahilyanagar-414402

Email: smachindra74@gmail.com

Article DOI Link: https://zenodo.org/uploads/19790599

DOI: 10.5281/zenodo.19790599

Abstract

Solar energy is often described as clean and sustainable, but this statement becomes meaningful only when the materials used in solar systems are examined carefully. The performance, durability, environmental impact, and economic feasibility of photovoltaic systems are strongly dependent on the materials involved in light absorption and charge transport. This chapter discusses major categories of solar energy materials with a focus on their long-term sustainability rather than only efficiency. It evaluates material extraction, processing, toxicity, scarcity, and end-of-life management, and argues that true sustainable development depends not only on renewable electricity production but also on responsible material engineering.

Keywords: Solar Energy Materials, Photovoltaic Technology, Sustainable Development, Emerging Photovoltaic Materials, Renewable Energy Systems.

Introduction

The continuous growth in global energy demand, coupled with increasing concerns over environmental pollution, has led to a strong requirement for sustainable and renewable energy sources. Conventional fossil fuels, particularly coal, oil, and natural gas, play a significant role in greenhouse gas emissions and the progression of climate change [1]. Within this framework, solar energy is recognized as a highly promising renewable resource capable of fulfilling future energy requirements while mitigating environmental effects. Photovoltaic energy is broadly recognized as a clean and sustainable alternative because it is abundant, renewable, and capable of producing electricity without direct carbon emissions during operation [2]. Photovoltaic (PV) technology is the most common method used to convert solar energy into electricity. The overall performance and reliability of photovoltaic systems are strongly governed by the materials utilized in solar cell fabrication, particularly semiconductor materials

play a key role in light absorption and charge carrier generation transport. Conventional solar panels are manufactured using materials such as crystalline silicon, metals, dopants, polymers, and glass. However, the extraction, purification, and processing of these materials involve mining activities, chemical treatments, transportation, and energy-intensive manufacturing processes. Therefore, the sustainability of solar energy systems must be evaluated not only in terms of electricity generation but also through the lifecycle impacts of the materials used in their production [3].

Recent advances in material science have led to the development of several new photovoltaic materials, including thin-film semiconductors, perovskite materials, and organic photovoltaic systems. These emerging materials aim to reduce manufacturing costs, improve efficiency, and minimize environmental impact. Understanding the role of these solar energy materials is essential for developing sustainable photovoltaic technologies that can support long-term global energy transition and sustainable development [4].

Solar Energy Materials

- **Silicon: Reliable but Energy Intensive**

Silicon remains the most widely used material in photovoltaic technology because of its stable crystal structure and well-established electronic properties. Crystalline silicon solar cells account for over 90% of global photovoltaic production due to their reliability and mature manufacturing infrastructure. Nevertheless, the fabrication of solar-grade silicon requires energy-demanding processes such as high-temperature purification and wafer processing, which contribute to increased manufacturing cost and embodied energy. However, silicon solar panels typically operate for more than 25 years and generate substantially more energy during their lifetime than is consumed during their production [5].

- **Thin-Film Materials**

Thin-film photovoltaic technologies use very thin semiconductor layers deposited on supporting substrates, which significantly reduces material consumption compared with conventional silicon wafer cells. Commonly utilized thin-film materials comprise cadmium telluride (CdTe) and copper indium gallium selenide (CIGS). These systems generally require less energy during manufacturing and show lower life-cycle environmental impacts. The greenhouse gas emissions from thin-film solar electricity are about 20 g CO_2/kWh, far lower than fossil-fuel power generation. However, the use of scarce elements such as tellurium and indium highlights the need for efficient recycling and resource management [6].

- **Perovskite Materials**

Perovskite solar cells are promising next-generation photovoltaics due to their rapidly improving efficiency and low-temperature fabrication. They can be produced using solution or vapor methods, reducing energy use, material consumption, and costs compared to silicon cells, while offering shorter energy payback times. However, challenges remain, including poor long-term stability and environmental concerns, as they are sensitive to moisture, heat, and light and often contain lead [7].

- **Organic and Emerging Materials**

Organic photovoltaic (OPV) cells employ carbon-based materials and exhibit benefits including mechanical flexibility, low weight, and compatibility with low-temperature fabrication processes. Semiconducting polymers generally act as donor materials, while fullerene derivatives like PCBM function as electron acceptors. OPVs can be fabricated on flexible substrates such as polyethylene terephthalate (PET) through roll-to-roll techniques. Nanomaterials including quantum dots and graphene may enhance performance, but issues related to stability, durability, and recyclability still require improvement [8].

Solar Materials and Sustainable Development

Solar energy materials are vital for sustainable development, enabling clean power generation and reducing environmental impact. Photovoltaic systems produce electricity without greenhouse gas emissions, lowering reliance on fossil fuels and helping mitigate climate change. They also support economic growth by creating jobs in manufacturing, installation, maintenance, and research. However, true sustainability depends on responsible material management, including recycling and life cycle assessment [9].

Organic photovoltaic (OPV) technologies are emerging as next-generation solar systems due to their lightweight, flexible design and potential for low-cost production. They use organic semiconductors like conjugated polymers and small molecules for light absorption and charge transport. Unlike silicon cells, OPVs can be produced using low-temperature, solution-based methods such as printing and coating, reducing energy use. Their compatibility with flexible substrates allows portable and adaptable devices, though improving stability, lifespan, and eco-friendly materials remains crucial [10].

Applications of Organic Photovoltaic Systems

Organic photovoltaic (OPV) materials are valuable for sustainable solar energy due to their flexibility, lightweight nature, and low-temperature fabrication. They can be used in building-integrated photovoltaics, wearable devices, indoor energy systems, and semi-transparent solar windows. Unlike rigid silicon panels, OPVs can be made on flexible substrates, allowing use on curved and lightweight

surfaces. Their compatibility with roll-to-roll manufacturing enables large-scale, low-energy production. They also perform well in low-light conditions, making them suitable for powering IoT devices and smart sensors [11].

Conclusion and Future Scope

Photovoltaic materials are essential for sustainable energy, enabling clean electricity generation. While crystalline silicon dominates due to its stability and mature technology, emerging materials like thin films, perovskites, and organic photovoltaics offer higher efficiency, lower material use, and flexible designs. However, sustainability depends on eco-friendly material sourcing, low-energy manufacturing, and effective recycling. Future research should focus on greener materials, improved stability, and circular lifecycle design to ensure solar technologies support a sustainable, low-carbon future.

References

1. REN21. (2023). Renewables 2023 global status report. REN21 Secretariat.
2. Ellabban, O., Abu-Rub, H., & Blaabjerg, F. (2014). Renewable and Sustainable Energy Reviews, 39, 748–764.
3. Peter, L. M. (2018).. Journal of Materials Chemistry A, 6(38), 18633–18639.
4. Green, M. A., Dunlop, E. D., Hohl-Ebinger, J., Yoshita, M., Kopidakis, N., & Hao, X. (2020). Progress in Photovoltaics: Research and Applications, 28(7), 629–638.
5. Goetzberger, A., Hebling, C., & Schock, H. W. (2006). Photovoltaic materials, history, status and outlook. Materials Science and Engineering: B, 74(1–3), 1–11.
6. Fthenakis, V. (2009). Sustainability of photovoltaics: The case for thin-film solar cells. Renewable and Sustainable Energy Reviews, 13(9), 2746–2750.
7. Li, C., et al. (2021). Sustainability in perovskite solar cells. ACS Applied Materials & Interfaces, 13(5), 6226–6237.
8. Liu, X., et al. (2022). Advanced materials for emerging photovoltaic systems: Environmental hotspots in the production and end-of-life phase of organic, dye-sensitized, perovskite, and quantum dots solar cells. Sustainable Materials and Technologies, 31, e00501.
9. Zhao, X., Ren, L., & Wu, Y. (2022). Solar energy technology and its roles in sustainable development. Clean Energy, 6(3), 476–488.
10. Brabec, C. J., Distler, A., Du, X., Egelhaaf, H. J., Hauch, J., Heeney, M., & Scherf, U. (2020). Organic photovoltaics: Materials, device physics, and manufacturing technologies. Advanced Energy Materials, 10(13), 1902847.
11. Kalowekamo, J., & Baker, E. (2009). Estimating the manufacturing cost of purely organic solar cells. Solar Energy, 83(8), 1224–1231.

Applications of Artificial Intelligence in Physics: From Materials Discovery to Particle Detection

Kangude Sahadev H., Dhawale Ganesh

Department of Physics Rayat Shikshan Sanstha's Dada Patil Mahavidyalaya Karjat,

Dist- Ahilyanagar-414402

Email: sahadevkangude7283@gmail.com

Article DOI Link: https://zenodo.org/uploads/19790756

DOI: 10.5281/zenodo.19790756

Abstract

Artificial intelligence (AI) is transforming modern physics by providing advanced computational tools to analyze complex systems and massive datasets. This chapter reviews key applications of AI, including machine learning for accelerated materials discovery, physics-informed neural networks (PINNs) for solving differential equations while enforcing fundamental physical laws, and AI-driven particle detection in high-energy physics experiments. These methods enhance researchers' ability to predict properties, uncover patterns, and process large-scale experimental data efficiently. Despite challenges such as model interpretability, data availability, and computational demands, AI integration with traditional physics techniques offers promising avenues for accelerating scientific discovery and deepening understanding of the physical universe.

Keywords: Artificial Intelligence, Machine Learning, Physics-Informed Neural Networks (PINNs), Materials Discovery, High-Energy Particle Detection.

Introduction

Artificial Intelligence (AI) has become a powerful tool in modern scientific research. Over the past decade, methods such as machine learning, deep learning, and neural network models have been widely adopted in many scientific domains. Physics, in particular, has experienced significant progress through the use of AI-based computational techniques. Contemporary physics experiments and simulations generate enormous amounts of data, creating a strong demand for advanced analytical approaches that can efficiently process complex datasets and reveal meaningful patterns [1]. Conventional approaches in physics research are mainly based on theoretical analysis, computational modeling, and experimental observations. Although these methods play a fundamental role in understanding physical phenomena, they may become challenging when applied to highly complex systems or large-scale datasets. In this context, artificial intelligence

provides advanced data-driven techniques capable of identifying hidden patterns, predicting material or physical properties, and supporting faster scientific advancements [2]. Artificial intelligence has found important applications in several branches of physics, including materials science, particle physics, astrophysics, and computational modeling. In materials research, machine learning models can estimate the properties of new compounds even before laboratory synthesis is carried out. In high-energy physics, deep learning methods assist researchers in detecting and classifying particle interactions generated in large experimental setups such as the Large Hadron Collider. These examples highlight that AI does not replace traditional physics principles; instead, it strengthens researchers' ability to analyze complex systems and solve scientific problems more effectively [3].

This chapter explores the expanding impact of artificial intelligence on contemporary physics research. It highlights three key areas where AI has made significant contributions: the use of machine learning for discovering new materials, the application of physics-informed neural networks to model and solve complex physical systems, and AI-driven methods for detecting particles in high-energy physics experiments.

Fundamentals of Artificial Intelligence and Machine Learning

Artificial intelligence (AI) refers to computer systems designed to perform tasks that typically require human intelligence, such as pattern recognition, data analysis, prediction, and decision-making. A key subset of AI, machine learning (ML), enables systems to improve performance by learning from data without explicit programming for each task [4].

ML techniques help identify relationships between inputs and outputs, allowing models to detect patterns and make predictions on new data. Common methods include regression, decision trees, support vector machines, and neural networks. Deep learning, an advanced form of ML, uses multilayered neural networks to extract complex features from large datasets, making it especially effective for image analysis, signal processing, and large-scale data tasks. In physics, ML supports data analysis, accelerates simulations, and reveals patterns in complex systems, contributing to the emerging field of AI-driven physics [5].

Machine Learning in Materials Discovery

Developing materials with enhanced physical and chemical properties is a key goal in materials science and condensed matter physics. Traditional methods based on laboratory experiments and computational modelling are often time-consuming and resource-intensive. Recently, artificial intelligence and machine learning have accelerated this process by predicting material properties from existing datasets. By analyzing large-scale materials databases, ML models can

identify relationships between atomic structure, composition, and properties such as band gap, conductivity, thermal stability, and mechanical strength, helping researchers prioritize promising candidates before synthesis [6]. Public materials databases have significantly advanced AI-driven research by providing extensive experimental and computational data. When combined with machine learning, these datasets enable rapid screening of materials for applications in energy storage, electronics, and renewable energy systems [7]. For example, ML has been used to identify high-performance electrode materials for batteries and supercapacitors, as well as perovskite compounds for solar cells. These advances demonstrate how AI can reduce the time and cost of materials discovery compared to traditional approaches [8].

Physics-Informed Neural Networks

Physics-informed neural networks (PINNs) represent a novel computational strategy that combines machine learning with established physical principles. Unlike traditional neural networks that rely purely on data, PINNs embed governing physical equations into the training process, ensuring that model outputs adhere to known scientific laws. Many physical systems—including heat transfer, fluid flow, electromagnetic phenomena, and quantum processes—are described by partial differential equations, which can be computationally intensive to solve using standard numerical methods. PINNs overcome this challenge by training neural networks to approximate solutions while simultaneously enforcing the relevant physical constraints through the loss function. This methodology not only reduces computational demands but has also been successfully applied in fields such as fluid dynamics, plasma physics, and thermal modeling, even when experimental data are scarce [9].

Artificial Intelligence in Particle Detection

Experiments in high-energy physics produce massive volumes of data that demand advanced analytical techniques. Particle detectors capture millions of collision events every second, making it challenging to extract significant interactions from the raw data. In this context, artificial intelligence has emerged as an effective approach for processing and interpreting these large experimental datasets [10].

Machine learning methods are extensively employed to categorize particle interactions and separate significant signals from background noise. In particular, deep learning approaches—such as convolutional neural networks—have been used to analyze images from particle detectors and track particle trajectories. These models are capable of detecting intricate patterns in detector data with high precision [11].

Artificial intelligence has become an essential tool in contemporary particle

physics experiments, including those carried out at the Large Hadron Collider, where vast amounts of data are generated from proton–proton collisions. Machine learning techniques assist researchers in identifying rare events, categorizing particle types, and processing collision data efficiently. Similar AI-driven approaches are also employed in neutrino and cosmic-ray experiments to enhance detection accuracy and automate the analysis of large-scale datasets [12].

Conclusion

Artificial intelligence is transforming contemporary physics research by providing advanced computational tools capable of handling complex systems and massive datasets. Machine learning approaches have accelerated the discovery of new materials by allowing researchers to estimate their properties prior to laboratory synthesis. Physics-informed neural networks offer novel strategies for solving differential equations while ensuring that fundamental physical laws are respected. In high-energy physics, AI-driven particle detection methods have enhanced the speed and accuracy of analyzing experimental data.

While challenges such as the interpretability of models and limited availability of training data persist, combining artificial intelligence with traditional physics approaches opens exciting avenues for future investigations. As AI technologies continue to develop, they are expected to play an increasingly central role in deepening our understanding of the physical world.

References

1. Suresh, R., et al. (2024). Frontiers in Physics, 12, 1322162.
2. Karniadakis, G. E., et al. (2021). Nature Reviews Physics, 3(6), 422–440.
3. Carleo, G., et al. (2019). Reviews of Modern Physics, 91(4), 045002.
4. Ren, Z., et al. (2025). Applied Sciences, 15(14), 8092.
5. Zhang, Y., et al. (2023). Computers, 12(5), 91.
6. Schmidt, J., et al. (2019). Nature Reviews Materials, 4(4), 241–258.
7. Merchant, A., et al. (2023). Nature, 624, 80–85.
8. Wang, A. Y. T., et al. (2022). Chemistry of Materials, 34(8), 3335–3366.
9. Cuomo, S., et al. (2022). Journal of Scientific Computing, 92(3), 88.
10. Yang, Z., et al. (2023). Engineering, 23(4), 40–55.
11. Albertsson, K., et al. (2022). Journal of Physics: Conference Series, 2438, 012104.
12. Mondal, S., et al. (2024). European Physical Journal Special Topics, 233, 2657–2686.

Manchester System in Brachytherapy Cervical Implant

[1]Sujata D Kolhatkar, [2]Vikas D Kolhatkar, [1]Shivani Padwal

[1]Department of Medical Physics, DY Patil college, Kolhapur

[2]Department of Physics, Dada Patil Mahavidyalaya, Karjat, Dist: Ahilyanagar 414402

Email: vikaskolhatkar1@gmail.com

Article DOI Link: https://zenodo.org/uploads/19790921

DOI: 10.5281/zenodo.19790921

Abstract

The Manchester system, also known as the Pateracer-Parker system, was developed at Christie Hospital as one of the earliest standardized brachytherapy dosimetry systems. It was initially designed for interstitial implants, introducing concepts such as as uniform source distribution, central plane, and basal dose to achieve homogeneous dose delivery within the target volume. Later, it was adapted for intracavltary treatment of carcinoma cervix, where dose is prescribed to Point A and Point B is used to estimate pelvic wall dose. The system originally used radium sources and later cesium, producing a characteristic pear-shaped isodose distribution, based on two-dimensional radiographic planning, it laid the foundation for modern image guided brachytherapy techniques.

Introduction

Brachytherapy is a internal radiation therapy which treat cancer by placing radioactive sources directly inside or next to a tumor. Basically, there are two type of brachytherapy one is high dose rate brachytherapy in which use temporary involve the cathetors or needles into the target area to deliver high dose radiation in few minutes. The amount of dose which is deliver during that procedure 12 Gy/h. So high dose brachytherapy is used to treat cervical, prostate, breast, skin, oesophagal and head & neck cancer. Another one is low dose rate brachytherapy where a targeted cancer cells are treated by placing radioactive sources (seeds or wires) directly in to or next to a tumor for a prolonge period, typically days or permenantly. It delivers Continuous radiation usually 0.4 to 2 Gy/h. (LDR is primarily used for prostate cancer, brain tumors and gynocological treatment). This type of treatment is basically used to destroy to cancer cells while sparing healthy tissue, which is not the Case in all the others type of radiation treatments.

History

The manchester system was developed at christie hospital as one of the earliest

standardized branchytherapy dosemetry system.It is named after the Holt-radium institute in manchester, England where it was developed in 1913s by Raltson Paterson and Herbert Parker. It was initially designed for interstitial implants, introducing concepts such as uniform source distribution, central plane and basal dose to achieve homogeneous dose delivery within the target volume. Later it was adopted for intracavitory treatment of carcinoma cervix where dose prescribed point A and point B is used to estimate pelvic wall dose. The system originally used radium sources and later cesium producing a characteristic isodose distribution based on two-dimensional radiographic planning. It led the Foundation for modern image guided brachytherapy image.

The treatment uses radium 226 source, whose half-life is 1600 years later it is replaced by Cesium 137 or irridium 192 because radium produces radon gas which was creating excess of pressure on the applicators. The half-life of cesium is 30.17 years and irridium 73.83 days. The applicators made up of stainless steel, tungsten for shielding, plastic or nylon.

Brachytherapy treatment involves point wise dose distribution in which point an important point which is 2 cm superior from the external cervical OS. (i.e. os is outer opening to the vagina) and 2 cm away from central tandem. A central tandem refers to a centrally placed applicator used in medical brachytherapy. Ovoids are small egg shaped, hollow holders, to deliver high dose targeted radiation. Point A is where uterine, artery crosses the ureter and Point B is 3 cm laterally away from point A. It is point which represents lymph node area. In this process we insert the applicator inside the cervix then we apply the source through the applicator. First, it will go to one of the ovoids then it goes the central tandem then it goes to the another ovaid, respectively. The source loading intensity is non-uniform but the dose distribution is uniform. Depending upon each individual angle of inclination of tandem varies 15 degree/30 degree /45 degree / etc. A manchester is point based dosimetry in which, a pear shape isodose distribution takes place. The source loading in this system takes place in such a way that Ra equivalent of dose loading by each ovoid and typically tandem loading 10 to 15 mg Ra equivalent, so the dose ratio is tandem ovoid is equivalent to 2:1.

The characteristics of the dose distribution are high central dose, rapid full of laterally means the energy of the source decreases rapidly, steep gradient protecting bladder and rectum. Typically, the tolerance level of organ at risk is 80 to 90 Gy for bladder and 70 to 75 Gy to rectum. Tolerance in radiotherapy refers to the maximum radiation dose healthy tissue can receive before sever damage occurs.

We can check position of the source after loading by using a device which is called as autoradiograph. Autoradiograph is a device which works on the mechanism in which a Sample is placed in direct contact with a photograph

emulsion (i.e. a highly sensitive, gelatin-based Coating contains suspended silver halide crystal typically silver bromide applied to films). So, when it is exposed to light triggers a chemical reaction on the silver halide crystal forming latent image. It is necessary to check that the unit will position the source with millimeter accuracy at predetermined program, positions along treatment applicators.

Advantages of these systems is, it is a standardized system it means that the parameter such as distance between the central tandem and ovoid remains the same for all the patients simple dose prescription which means that as the radioactive material have inherent property to emit the radiation so we do not need to generate it which is not the case in teletherapy. It gives the good clinical outcome, the dose can reproduce easily. Now the limitations are it is based on 2D radiographs. MRI is the 3D radiograph which gives high exposure radiation to the patient so we avoid it mostly, no individual anatomy is considered as the same applicator used the all patient, no volumetric dose assesment, cannot evaluate OAR (organ at risk) dose precisely.

TG-43 report is set of formalism and data published by American Association of Physicist in medicine (AAPM) which provides the standard method for calculating the absorb dose distribution around the brachytherapy sources. The original formalism of TG-43 was done in 1995. TG-43 U1 is a 2004 American Association of Physicist in Medicine (AAPM) updated protocols for brachytherapy dosimetry, TG-43UISI 2007 suppliment to the 2004 AAPM TG-43U1 report that provides updated dosimetry parameters for Specific newly available low energy brachytherapy sources. The advantage of TG-43 is implitation in TPS (Treatment Planning system) universally accepted protocals it ensures consistent dose delivery across the clinical Centers. limitations TG-43 are no applicator attenuation, No patient specific geometry. The modern improvement which overcomes the TG-43 limitation is adjustment of model base dose calculation algorithms (MDCA) has been developed.

Conclusion

The Manchester system of brachytherapy developed 1930s revolutionized cervical cancer treatment by introducing standardized loading rules and dose specifications to 'point A', it ensured consistent radiation dosing minimized vaginal necrosis and allowed for reproducible treatment, remaining a corner stone Gynacological oncology particularly in low dose rate (LDR) and later high dose rate (HDR)

References

1. IAEA students and teachers .pdf
2. F.M Khan

Advanced Electrode Materials and Charge Storage Mechanisms in Energy Storage Systems

Prathamesh B. Dahivade, Balkrishna J. Lokhande

Lab of Electrochemical Studies, School of Physical Sciences, Punyashlok Ahilyadevi Holkar Solapur University, Solapur, MH, India. 413255.

Email: bjlokhande@yahoo.com

Article DOI Link: https://zenodo.org/uploads/19791011

DOI: 10.5281/zenodo.19791011

Abstract

Advanced electrode materials are the key components in next-generation energy storage systems. Transition metal oxides, conducting polymers, and carbon nanomaterials are some of the examples that control electrochemical performance. This chapter summarizes major developments between 2020 and 2025 with an emphasis on mechanistic insights into charge storage through operando techniques such as X-ray absorption spectroscopy, in-situ Raman spectroscopy, and time-resolved X-ray diffraction. Transition metal oxides usually show pseudocapacitive behaviour via surface redox reactions and intercalation mechanisms while carbon nanomaterials essentially give electric double-layer capacitance with high-rate capability. Conducting polymers add extra redox-active functionality but need structural stabilization. The balance between Faradaic and non-Faradaic processes is discussed along with performance trade-offs and sustainability considerations for rational electrode design for advanced supercapacitors and battery-type systems.

Keywords: Electrode materials; charge storage mechanisms; pseudocapacitance; operando characterization; energy storage systems

Introduction

The global transition toward sustainable energy technologies has significantly accelerated research on advanced electrochemical energy storage systems, including supercapacitors, lithium-ion batteries, sodium-ion batteries, and hybrid capacitive devices for renewable integration, electric mobility, grid stabilization, and portable electronics. Among all components, electrode materials are the most critical, as they directly determine energy density, power density, cycling stability, safety, and cost-effectiveness. Electrochemical performance depends on charge storage mechanisms occurring at the electrode–electrolyte interface and within the bulk structure of active materials.

Transition metal oxides such as MnO_2, V_2O_5, NiO, and Co_3O_4 are widely studied due to their reversible multivalent redox reactions, which enable high theoretical capacitance; however, their low conductivity and structural instability often require nano structuring or composite engineering. Carbon-based nanomaterials including graphene, carbon nanotubes, and activated carbon store charge mainly through electric double-layer capacitance, offering high power density and long cycle life. Conducting polymers like PANI, PPy, and PEDOT combine electronic conductivity with pseudocapacitive behaviour for flexible and lightweight devices as shown in fig.1. Recent advances (2020–2025) emphasize pseudocapacitive mechanisms, operando characterization techniques, and sustainable synthesis approaches, integrating mechanistic understanding with environmentally responsible electrode design.

Literature Review (2020-2025)

- **Transition Metal Oxide Electrodes**

Transition metal oxides are widely studied for pseudocapacitors due to multiple oxidation states and high theoretical capacity. MnO_2 on activated carbon delivers >500 F g^{-1} via Mn^{3+}/Mn^{4+} redox and reversible cation intercalation, enhanced by nanostructuring. Ternary $NiO/V_2O_5/MnO_2$ systems reach ~600 F g^{-1} through improved conductivity and redox synergy. Multicationic oxides like iron tungstate and WO_3 nanosheets enable efficient intercalation pseudocapacitance. Ni–Co oxides and MOF-derived $MnNi_2O_4$ exceed 1000 F g^{-1} due to high porosity and active sites. However, low conductivity and structural degradation necessitate composite engineering for stable high-rate performance [11].

- **Conducting Polymer Electrodes**

Conducting polymers serve as substitutes for electrodes that are flexible and light in weight. The process through which charges are stored within these materials happens due to reversible doping and dedoping accompanied by redox transitions through conjugated backbones. In this case, PANI changes form by proton-coupled redox transformations while PPy operates through anion exchange; on the other hand, PEDOT possesses relatively better electrochemical stability. However, volumetric expansion and contraction during cycling result in mechanical degradation leading to fading capacitance over time. Therefore, recent studies focus on polymer–carbon or polymer–oxide composites that can enhance conductivity as well as structural integrity for longer stability instead of using them as standalone electrodes.

- **Electrodes of Carbon Nanomaterials**

Carbon nanomaterials dominate commercial supercapacitors due to high-rate capability and durability through electric double-layer capacitance (EDLC), enabling excellent cycle life without Faradaic reactions. Graphene delivers 230–

405 F g^{-1}, while nitrogen doping enhances wettability and adds pseudocapacitance. Activated carbon remains cost-effective and scalable, with MnO_2/activated carbon composites reaching ~557 F g^{-1}. CNTs improve conductivity and mechanical strength, especially in CNT/graphene hybrids. Biomass-derived carbons (mango peel, coconut shell, rice husk) support circular economy principles. MXene–carbon hybrids integrate redox-active carbides with carbon frameworks for advanced supercapacitors and sodium-ion batteries.

- **Understanding Charge Storage Mechanisms**

Advances in electrochemical kinetics and operando diagnostics clarify charge-storage mechanisms. Battery-type materials exhibit diffusion-controlled Faradaic plateaus, while EDLC shows linear voltage–charge behaviour. Pseudocapacitance includes underpotential deposition, surface redox, and fast intercalation with minimal lattice strain. Capacitance-dominated sodium storage and interfacial water-assisted desolvation highlight ion transport and structural stability importance.

Operando Characterization Breakthroughs

Operando techniques provide real-time insight into electrochemical processes. XANES and EXAFS monitor oxidation state and coordination changes, revealing reversible Fe and W redox in $FeWO_4$. In-situ XRD distinguishes pseudocapacitive and battery-type behavior via phase evolution. Operando Raman tracks bonding changes, while TEM observes nanoscale morphology and degradation. Combined with DFT, these tools enable multiscale mechanistic understanding [17].

Methodology and Technological Framework

- **Material Synthesis Routes**

Synthesis routes control crystallinity, morphology, and electrochemical performance. Metal oxides are prepared via hydrothermal, sol-gel, coprecipitation, electrodeposition, or microwave methods. MOF-derived strategies yield porous structures. Carbon materials arise from CVD, activation, or biomass pyrolysis. Composite electrodes require optimized mass loading and thickness for efficient transport [11,12].

- **Operando Characterization Techniques**

Operando XAS uses synchrotron radiation to view changes in oxidation state and local structure during cycling. XANES can see valence shifts; EXAFS gives bond distances and coordination numbers. In-situ XRD tracks phase transitions as well as lattice strain. Changes in vibration can be seen by Raman spectroscopy; D/G bands in carbon are one example, plus variations in metal–oxygen bonding. Mass

changes during insertion of ions into the material (and desolation) are measurable with an electrochemical quartz crystal microbalance [1,15].

- **Mechanistic Analysis Methods**

The power-law relation distinguishes capacitive ($b \approx 1$) from diffusion-controlled processes ($b \approx 0.5$). Current separation quantifies relative contributions ($i = k_1v + k_2v^{1/2}$). Coupling electrochemical analysis with operando techniques and computational modelling enables comprehensive mechanistic interpretation [15,16,17].

Results and Discussion

Transition metal oxides deliver 500–1000 F g^{-1} via pseudocapacitive redox but face diffusion limits and lattice strain. Carbon nanomaterials offer 200–400 F g^{-1} with superior rate capability and stability; nitrogen doping enhances wettability and pseudocapacitance. Composites improve conductivity, voltage window, stability, and sustainability through biomass-derived carbons [3][12][13].

Future Scope and Research Directions

Future research targets hierarchical oxide–carbon–polymer composites and intercalation pseudocapacitive materials like Nb_2O_5 and MoO_3 to bridge battery–capacitor behaviour. Operando tools, AI-driven discovery, lifecycle assessment, and digital twin modeling will guide sustainable optimization [14,16].

Conclusion

Electrode materials govern energy storage performance. Metal oxides deliver high pseudocapacitance, while carbon nanomaterials ensure rapid, durable cycling. Composites integrate both benefits. Operando studies guide future scalable, cost-effective, and sustainable supercapacitor and battery development.

References

1. J. Patra et al., "Understanding the charge storage mechanism of supercapacitors: in situ/operando spectroscopic approaches and theoretical investigations," Journal of Materials Chemistry A, 9, 45, 25852–25891, 2021.
2. A. Mohite et al., "Metal oxide-based nanocomposites as advanced electrode materials for enhancing electrochemical performance of supercapacitors: A comprehensive review," Materials Today: Proceedings, 2024.
3. A. G. Olabi et al., "Carbon-based materials for supercapacitors: Recent progress, challenges and barriers," Batteries, 9, 1, 19, 2022.
4. A. Meena et al., "Green supercapacitors: review and perspectives on sustainable template-free synthesis of metal and metal oxide nanoparticles," Journal of Energy Storage, 52, 104882, 2022.
5. P. Kour et al., "MnO_2 nanorod loaded activated carbon for high performance

supercapacitors," Journal of Alloys and Compounds, 922, 164834, 2022.
6. Y. Wang et al., "Symmetric supercapacitors composed of ternary metal oxides ($NiO/V_2O_5/MnO_2$) nanoribbon electrodes with high energy storage performance," Chemical Engineering Journal, 427, 131804, 2021.
7. N. Goubard-Bretesché et al., "Unveiling pseudocapacitive charge storage behavior in $FeWO_4$ electrode material by operando X-ray absorption spectroscopy," Small, 16, 33,2002855, 2020.
8. Y. Wang et al., "Two-dimensional WO_3 nanosheets for high-performance electrochromic supercapacitors," Advanced Materials Interfaces, 2020.
9. Y. Wang et al., "A novel layered WO_3 derived from an ion etching engineering for ultrafast proton storage in frozen electrolyte," Advanced Functional Materials, 33, 10, 2211491, 2023.
10. M. S. Vidhya et al., "Nickel–cobalt hydroxide: a positive electrode for supercapacitor applications," RSC Advances, 10, 33, 19410–19418, 2020.
11. L. Mengdi et al., "Metal-organic framework-derived porous $MnNi_2O_4$ micro flower as an advanced electrode material for high-performance supercapacitors," Journal of Alloys and Compounds, 851, 153546, 2020.
12. R. Muruganantham et al., "Biomass feedstock of waste mango-peel-derived porous hard carbon for sustainable high-performance lithium-ion energy storage devices," Energy & Fuels, 35, 14,11316–11327, 2021.
13. H. Ji et al., "Cellulose-derived nanostructures as sustainable biomass for supercapacitors: A review," Polymers,14,1,169, 2022.
14. Y. Zhao et al., "Intercalation pseudocapacitance in 2D $VS_2/Ti_3C_2T_x$ MXene hybrids for all-climate and long-cycle sodium-ion batteries," Advanced Functional Materials, 33,38, 2307794, 2023.
15. W. Xiong et al., "Mg-doped $Na_4Fe_3(PO_4)_2(P_2O_7)/C$ composite with enhanced intercalation pseudocapacitance for ultra-stable and high-rate sodium-ion storage," Advanced Functional Materials,32, 52, 2211257, 2022.
16. Y. Wang et al., "Interlayer confined water enabled pseudocapacitive sodium-ion storage in nonaqueous electrolyte," ACS Nano,17, 22, 22622–22631, 2023.
17. J. S. Weaving et al., "Elucidating the sodiation mechanism in hard carbon by operando Raman spectroscopy," ACS Applied Energy Materials, 3, 7, 7474–7484, 2020.

Carbon Nanostructures for Green Energy Applications: Electrical Conductivity, Charge Transport, and Energy Storage Mechanisms

Prajakta S. More, Sampada D. Karpe

Department of Physics, Dada Patil Mahavidyalaya, Karjat, Dist – Ahilyanagar, 414 402

Email: sainathmore2020@gmail.com

Article DOI Link: https://zenodo.org/uploads/19791115

DOI: 10.5281/zenodo.19791115

Abstract

Carbon nanostructures are extremely small carbon materials such as carbon nanotubes, graphene, and fullerenes. These materials are good conductors of electricity and have a large surface area. Because of these features, they are very useful in green energy technologies. Their tiny structure allows electric charge to move easily, which improves the flow of electrons in energy devices. This helps the devices work more efficiently. Their shape and surface properties also make it easier for ions to move and allow more energy to be stored. For this reason, carbon nanostructures are widely used in supercapacitors, lithium-ion batteries, and fuel cells. The structure of carbon nanomaterials and the movement of charge influence electrical conductivity and energy storage. It also explains different ways, such as material combinations and design methods to improve the performance of these energy devices. Different charge storage and chemical energy storage are discussed to show how green energy systems can become more efficient, more powerful, and more durable.

Keywords: Electrical Conductivity, Charge Transport, Energy storage mechanisms.

Introduction

Carbon is an important and versatile element because it can form different types of bonds with varying strengths. It has four valence electrons that can arrange in sp, sp^2, and sp^3 bonding patterns, leading to different forms called allotropes, such as diamond, graphite, and amorphous carbon.

In addition to natural forms, scientists have created artificial carbon materials like graphene, fullerenes, carbon nanotubes, and carbon fibers [1]. These carbon-based nanostructures have unique mechanical, thermal, optical, and chemical properties, making them useful in nano-electronics, nano-composites, and nano-

medicine. Their large surface area and tiny pores help in energy generation, storage, and transfer. One-dimensional nanostructures like nanowires are gaining attention for applications such as flat-panel displays [2]. Carbon nanomaterials also have high electrical conductivity and strong structures, allowing faster movement of electrons and ions, which improves energy device performance.

Renewable energy is clean and comes from natural sources, but in 2013 it contributed only 10% of total energy and remains costly. As fossil fuels become scarce and expensive, the use of renewable energy is expected to increase [3].

Carbon Nanostructures Types

- **Graphene**

Graphene is a very thin sheet made of only one layer of carbon atoms arranged in a flat structure. The carbon atoms in graphene are joined by strong sp^2 bonds. Graphene is known as the basic material from which different forms of carbon are made.

- 0-D structures like round buckyballs.
- 1-D structures like carbon nanotubes.
- 3-D structures like graphite, which is formed by stacking many graphene layers on top of each other.

People have been studying two-dimensional graphite for many years. It is used to understand other carbon materials. [1,4]

- **Carbon Dots and Fullerenes**

Fullerenes are round, cage-like molecules made entirely of carbon. The most stable forms are C_{60} and C_{70}, which is why they are widely used in medicine and industry [5]. Carbon dots (CDs) are extremely small carbon particles, less than 10 nanometers in size, with unique optical, electrical, and chemical properties.

- **Carbon Nanotubes (CNTs)**

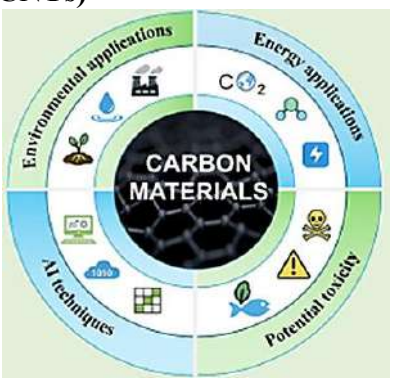

Diagram: Carbon Materials [6]

Carbon nanotubes (CNTs) are tiny tube-like structures that are very special. They were discovered in 1991. CNTs are very strong, can absorb materials, work as catalysts, conduct electricity, and can also transfer information. Their ability to

absorb lightappears in certain regions (UV, visible, NIR), which happens because of changes in their electrons' energy. [6]

Electrical Conductivity and Charge Transport:

- **Electrical Conductivity**

The electrical conductivity of fullerenes is very low (10^{-12} S m^{-1}), so they act like insulators and are not good at carrying electricity. This limits their use in rechargeable batteries. But if –OH groups are added, their conductivity improves (from 10^{-4} to 10^{-2} S m^{-1}). Also, adding some metal atoms to fullerenes can increase their conductivity even more. [1,7]

- **Charge Transport**

Charge transport in carbon stores charge because ions stick to the electrode and then come off. Because of this, the graph looks like a rectangleand a triangle. EDLS usually hold less charge [7]

- **Influence of Structural Defects**

Defects and functional groups can increase or decrease electrical flow because they change the charge density and trap charge in some places.

Energy Storage Mechanisms

- **Li/Na-ion Batteries**

Carbon materials are commonly used as anodes in lithium-ion and sodium-ion batteries because they allow electricity to flow easily and can react well with ions. In lithium-ion batteries, lithium ions enter the graphite structure and form a stable compound called LiC6, which gives the battery around 370 mAh g^{-1} of capacity. In sodium-ion batteries, carbon stores sodium ions by attracting them to its surface and filling the tiny pores inside the carbon structure. [8]

- **Supercapacitors**

Electrochemical capacitors were earlier called by different names, like ultracapacitors or power capacitors. But today, they are called supercapacitors. NEC company gave this name in 1971 for their device [3].

- **Microbial Fuel Cells**

Microbial fuel cells (MFCs) are a promising technology that can generate electricity using organic materials. With ongoing global issues like limited land, energy shortages, water scarcity, and climate change, both scientists and industry experts are very optimistic about its potential. [5]

Green Energy Devices

- Green energy devices that can store a lot of energy and deliver high power are

very important today. They are used in portable gadgets, self-powered or remote sensors, and different types of vehicles.

- Compared to batteries and pseudocapacitors, electrostatic supercapacitors can charge and discharge very quickly, give high power, and last a long time.
- Carbon-based electrodes are popular because they conduct electricity well, have a large surface area, and are lightweight. [9]

Future Directions and Challenges

There is an increasing need to find sustainable ways to store energy and use resources efficiently. Some plants have the ability to hold nutrients, store water, and release them slowly when needed. Because of these abilities, Studying plants can provide useful ideas for developing better systems for energy storage and resource management. [10]

Future Directions

- Improve carbon for faster charge transfer
- Make materials cheap and eco-friendly
- Use models to understand charge/ion movement
- Reuse old materials

Challenges

- Hard to scale from lab to real devices.
- Hard to control size and quality.
- Conductivity drops in real devices.

Conclusion

Graphene, carbon nanotubes, and porous carbon are very useful for storing green energy. They conduct electricity easily, charge moves well, and energy stores efficiently. Their surface is large and like a network, so devices work better. They give more energy and last longer in things like supercapacitors and batteries.

References

1. Kuhar, A. (2025). Int. J. Sci. Res. Eng. Trends, 11(2), 2580–2592.
2. P. R., et al. (2011). IEEE Conference Proceedings.
3. Notarianni, M., et al. (2016). Beilstein J. Nanotechnol., 7, 149–196.
4. Rustamaji, H., et al. (2025). Future Batteries, 5, 100028.
5. Lawal, A. T. (2025). Carbon Trends, 19, 100470.
6. Sun, Z., et al. (2025). Sustainable Carbon Materials, 1, e007.
7. Merum, D., & Kang, M. (2025). Adv. Ind. Eng. Chem., 1, 26.
8. Kong, D., et al. (2023). Energy Mater. Devices, 1, 9370017.
9. Wei, J., et al. (2020). ACS Appl. Energy Mater., 3, 3530–3540.
10. Gautam, K., et al. (2025). Scientific Reports, 15, 11506

Sodium-Ion Batteries: A Mini Review

Pranjal J. Kapare, Mahesh S. Bhadane

Department of Physics, Rayat Shikshan Sanstha's Dada Patil Mahavidyalaya Karjat,

Dist-Ahilyanagar-414402

Email: pranjalj.kapare@gmail.com

Article DOI Link: https://zenodo.org/uploads/19791199

DOI: 10.5281/zenodo.19791199

Abstract

Sodium-ion batteries (SIBs) offer a sustainable, cost-effective alternative to lithium-ion batteries for large-scale energy storage, leveraging abundant sodium resources and compatible manufacturing. This chapter reviews key cathode and anode materials, synthesis approaches, sodiation/desodiation mechanisms, performance properties, and distinctive features. Recent innovations address challenges like lower energy density and kinetics, positioning SIBs for grid applications and beyond. Emerging solutions highlight commercialization pathways, with projections for widespread adoption in stationary storage by the late 2020s.

Keywords: SIBs, Charge–Discharge Mechanism, Electrode-Materials, Batteries.

Introduction

Energy underpins modern society; however, the rapid depletion of fossil fuels such as coal and petroleum, along with their contribution to climate change, necessitates sustainable alternatives. The United Nations Sustainable Development Goals advocate renewable energy sources like solar and wind power. Yet, their intermittent and weather-dependent nature creates fluctuations between energy generation and demand, highlighting the need for efficient storage systems [1,2]. Among available technologies, including pumped hydro, hydrogen storage, and supercapacitors, batteries stand out due to their high energy density, operational flexibility, and scalability from portable electronics to grid-level applications.

Battery technology has evolved systematically from the Voltaic pile to lead–acid, nickel–cadmium (Ni–Cd), nickel–metal hydride (Ni–MH), and lithium-ion batteries (LIBs). Although LIBs dominate owing to superior performance, concerns over lithium scarcity, cost, and safety persist [3]. Sodium-ion batteries (SIBs) emerge as a cost-effective and sustainable alternative, despite lower energy density caused by larger Na^+ ions [4].

Structure of Sodium-ion Batteries

The figure represents the structural components and working mechanism of a sodium-ion battery (SIB). The system consists of a cathode, electrolyte, and anode connected through an external circuit for electron (e^-) flow. The cathode includes sodium-containing materials such as layered oxides, polyanionic compounds, alkali-rich phases, and amorphous structures, which reversibly store Na^+ ions. The electrolyte contains sodium salts (e.g., $NaPF_6$, $NaClO_4$, NaTFSI, NaFSI) dissolved in organic solvents like EC, DMC, PC, FEC, or glymes, enabling ionic conduction while preventing electron transfer. The anode commonly comprises hard carbon, alloying/conversion materials, TiO_2, or $Na_2Ti_3O_7$. During charging, Na^+ ions migrate from the cathode to the anode, while electrons flow through the external circuit. During discharge, the process reverses, generating electrical energy through reversible sodium-ion shuttling and redox reactions at both electrodes. [5].

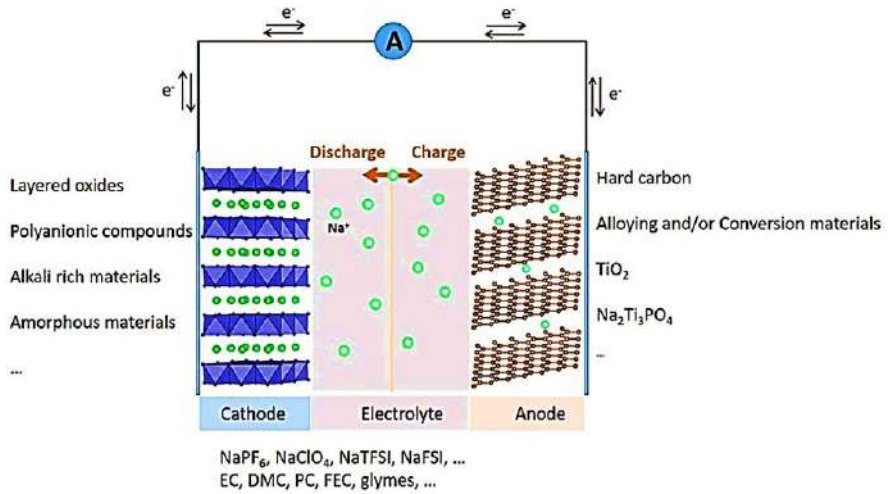

Fig. 1: Schematic image of Na-ion Battery System. (reproduced with permission from ref. 5, copyright 2020, John Wiley & Sons)

Materials of Sodium-ion

Sodium-ion battery performance strongly depends on electrode materials. Layered oxides and polyanionic compounds provide stable cathodic frameworks, while Prussian blue offers open channels for rapid Na^+ transport. Hard carbon remains the most practical anode due to structural disorder accommodating larger Na^+ ions. Alloying materials such as Sn and Sb deliver high capacity but require volume-change control. Continuous material optimization is essential for enhancing electrochemical stability and energy density.

Table 1: Representative cathode and anode materials for sodium-ion batteries (SIBs), key electrochemical features, and corresponding literature references.

Sr. No.	Material	Electrode Type	Key Feature	Ref.
1.	$NaMnO_2$	Cathode	steady cycling performance	[6]
2.	$Na_3V_2(PO_4)_3$	Cathode	Fast Na^+ diffusion (NASICON type)	[7]
3.	$NaFePO_4$	Cathode	Thermal stability	[8]
4.	Prussian Blue ($KFe^{3+}Fe^{2+}(CN)_6$)	Cathode	large-scale energy storage system	[9]
5.	Hard Carbon	Anode	High reversible capacity	[10]
6.	NTO-based	Anode	enhanced electrochemical performance	[11]
7.	Sn (Tin)	Anode	High capacity (alloying)	[12]
8.	Sb (Antimony)	Anode	High energy density	[13]

Working Mechanism of Sodium-Ion Batteries

Sodium-ion batteries (SIBs) function through a reversible sodium-ion shuttling mechanism involving intercalation and deintercalation reactions at both electrodes. During charging, Na^+ ions are extracted (deintercalated) from the cathode host structure through an oxidation reaction and migrate through the electrolyte toward the anode. Simultaneously, electrons flow through the external circuit to maintain electrical neutrality. The sodium ions are then inserted (intercalated) into the anode material, commonly hard carbon.

The general electrochemical reactions can be expressed as:

Cathode: $Na_xMO_2 \rightleftharpoons Na_{x-}yMO_2 + yNa^+ + ye^-$

Anode (hard carbon): $C + yNa^+ + ye^- \rightleftharpoons Na_\gamma C$

During discharge, the process reverses, generating electrical energy via reduction at the cathode and oxidation at the anode. Although SIBs share a similar mechanism with lithium-ion batteries, the larger ionic radius of Na^+ results in slower diffusion kinetics and increased structural strain in electrode materials, influencing capacity, rate performance, and cycling stability.

Advantages and Challenges

Sodium-ion batteries offer numerous advantages that make them smart for next-generation energy storage. Sodium is naturally abundant and widely available, which reduces dependence on limited resources and lowers raw material costs compared to lithium-based systems. As a result, the overall manufacturing cost of sodium-ion batteries is relatively low. These batteries also reduce reliance on rare

and critical elements and are particularly suitable for large-scale energy storage applications. In addition, sodium-ion systems provide safer operation with lower fire risk and exhibit good thermal stability. The use of aluminum as a current collector for both electrodes further decreases cost. Moreover, sodium resources are environmentally sustainable, making these batteries suitable for renewable energy storage such as solar and wind power.

However, several challenges remain. Sodium-ion batteries generally have lower energy density than lithium-ion batteries. The larger ionic radius of Na^+ slows ion diffusion within electrode materials. Some anode materials also experience volume expansion during cycling, leading to structural degradation over repeated charge–discharge processes. Furthermore, the availability of stable, high-performance cathode materials is still limited, and electrolyte stability issues can affect battery cycle life and safety.

Recent Advances and Applications of Sodium-Ion Batteries

Significant progress has been made in the development of sodium-ion batteries through continuous improvements in materials and cell design. Recent research has focused on advanced cathode materials such as layered oxides, polyanionic compounds, and Prussian blue analogues, which offer better structural stability and improved sodium storage capacity. On the anode side, hard carbon materials with optimized pore structures have shown promising performance for efficient Na^+ storage. In addition, electrolyte engineering has been widely explored to enhance ionic conductivity and stabilize the solid electrolyte interphase (SEI), which is essential for long-term cycling stability. The use of nanostructured electrode materials helps shorten sodium-ion diffusion pathways, thereby improving rate capability. Furthermore, strategies such as surface coating and elemental doping have been applied to enhance electrode stability and extend battery life.

Due to these advancements, sodium-ion batteries are being considered for several practical applications, including grid-scale energy storage, integration with renewable energy sources such as solar and wind power, low-cost electric mobility solutions, and backup power systems, portable electronic devices.

Conclusion and Future Perspectives

Sodium-ion batteries (SIBs) are emerging as a promising alternative to lithium-ion batteries for sustainable and large-scale energy storage. Their major advantages include the natural abundance of sodium, low cost, and improved safety. Although significant progress has been made in developing cathode and anode materials, challenges such as lower energy density, slower ion diffusion, and long-term cycling stability remain. Future research should focus on designing advanced electrode materials, optimizing electrolytes, and improving structural

stability to enhance overall battery performance. With continued technological advancements and material innovations, sodium-ion batteries have strong potential for practical applications in grid storage, renewable energy integration, and next-generation energy systems.

References

1. Y. Haldorai, (2022). Energy storage for renewable integration. Journal of Energy Storage. Elsevier.
2. E. Fekete. et al. (2023). Renewable energy intermittency solutions. Renewable Energy Reviews. Elsevier.
3. J. Chen et al. (2022). Lithium-ion battery safety issues. Journal of Power Sources. Elsevier.
4. R. Dorau et al. (2024). Sodium abundance advantages. Nature Energy. Springer Nature.
5. Yasin Emre Durmus et al., Adv. Energy Mater. 2020, 10, 2000089.
6. Komaba S. et al., (2011) Electrochemical Na insertion and solid electrolyte interphase for hard-carbon electrodes, Adv. Funct. Mater., 21, 3859–3867.
7. X. Zeng, (2020) Research Progress on Na3V2(PO4)3 Cathode Material of Sodium Ion Battery. Sec. Electrochemistry, Volume 8.
8. B. Ellis et al., (2007) A multifunctional 3.5 V iron-based phosphate cathode, Nat. Mater., 6, 749–753.
9. Wessells, C., Huggins, R. & Cui, Y. (2011), Copper hexacyanoferrate battery electrodes with long cycle life and high power. Nat Commun 2, 550.
10. D. A. Stevens, J. R. Dahn, (2000) High-capacity anode materials for rechargeable sodium-ion batteries," J. Electrochem. Soc.,147, 1271–1273.
11. W. P. U. S. Wickramarathna, (2026) DOI: 10.1039/D5YA00317B (Review Article) Energy Adv., Advance Article.
12. Matthew D. L. Garayt et al 2024 J. Electrochem. Soc. 171 070523.
13. Mater. Chem. Front., 2018,2, 437-455.

NiAl LDH Based Nanocomposites for Supercapacitor Application: Review

[1]Hemant K. Suryawanshi, [2]Amol R. Pardeshi

[1]Department of Physics, VPMK's Arvind (Appasaheb) Bhanushali College, Kinahvali 421 403.

[2]Department of Physics, Dada Patil Mahavidyalaya, Karjat, Dist: Ahilyanagar 414 402

Email: amolrp111@gmail.com

Article DOI Link: https://zenodo.org/uploads/19791308

DOI: 10.5281/zenodo.19791308

Abstract

The growing need for efficient and sustainable energy storage technologies has driven extensive research toward the development of high-performance electrode materials for supercapacitors. Among various candidates, nickel-aluminum layered double hydroxides (NiAl-LDHs) have emerged as promising materials owing to their notable redox behavior, high surface area, and favorable electrochemical performance. This chapter focuses on the preparation of NiAl-LDH-based nanocomposites through a hydrothermal synthesis route and examines their structural features, surface morphology, and electrochemical behavior for energy storage applications. Structural analysis confirms the formation of layered double hydroxide phases, while morphological studies reveal nanosheet-type structures with high surface accessibility. Electrochemical measurements indicate strong pseudocapacitive behavior and good charge storage capability. A comparative study with previously reported NiAl-LDH based materials further highlights their potential as efficient electrode materials for supercapacitor applications.

Keywords: NiAl LDH Nanocomposite, Hydrothermal Method Supercapacitor.

Introduction

Rapid increasing economies, energy storage and environmental pollution due to high use of fossil fuels create more serious problem in current scenario which demand the renewable energy storage devices. The developing the clean – renewable energy of most effective for this problem of energy shortage and solution for environmental pollution. There are many energy sources such as solar energy, wind energy, ocean energy, and geothermal energy which limited by their geographical distribution and require energy conversion and storage

technologies. At present, energy storage devices such as batteries, fuel cell and supercapacitors have attracted wide attention, but supercapacitor is considering most promising energy storage technology due to high power density, safety, fast charge/discharge rate and long cyclic life [1-3].

Electrode material used in supercapacitor are play most promising role for electrochemical performance, Metal hydroxide metal compound, especially nickel-based composite has hotspot in field in recent time, due to their redox reaction active sites and high theoretical capacitance. NiAl LDH based nanocomposite are synthesized via many methods such as co-precipitation method, hydrothermal method, solvothermal method, sol-gel method and spray pyrolysis method but hydrothermal method is most safe, and provide high specific capacitance. NiAl LDH based nanocomposite provides the highly conductive and flexibility due to carbon composition, Nickel are bivalent metal cation and aluminum is trivalent metal cation which widely applied in supercapacitor, due to owing their battery- type characteristics, high redox activity, large surface area [4-6]. This chapter studies the synthesis mechanism, structural, morphological and electrochemical studies of NiAl LDH based nanocomposite for supercapacitor application.

Synthesis Approach of NiAl LDH Based Nanocomposite

NiAl LDH was synthesized using the hydrothermal method with nickel nitrate hexahydrate, anhydrous aluminum nitrate, ammonium fluoride, urea/hexamine, and distilled water. The solution was stirred for 30 minutes until completely dissolved, then transferred to an autoclave and heated at 120 °C for 24 hours. The product was filtered and dried at 60 °C overnight.

For the nanocomposite, materials were mixed during the stirring step and then subjected to the same hydrothermal process for a specific reaction time [4–7]. Figures 1(a) and 1(b) show the hydrothermal synthesis approach for NiAl LDH-based nanocomposites with improved electrochemical performance.

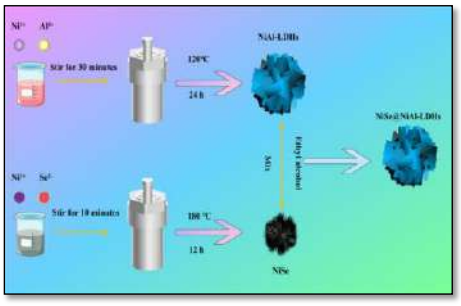

Fig. 1 a: Preparation of NiSe, NiAl – LDH and NiSe@NiAl - LDH via hydrothermal Method [4]

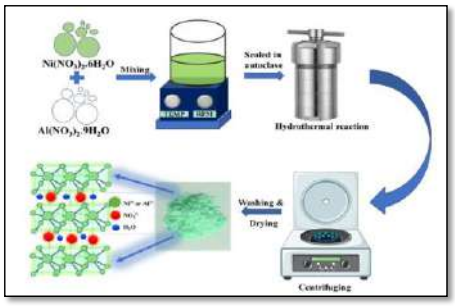

Fig. 1b: Hydrothermal Process of NiAl – LDH [7].

Structural, Morphological, and electrochemical studies

- **Structural and Morphological Studies**

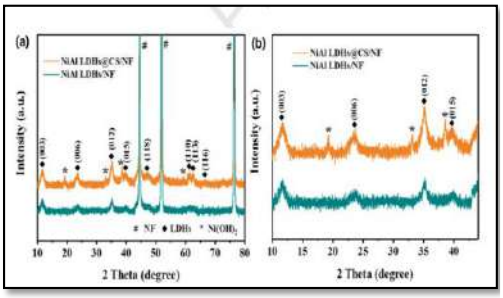

Fig. 2a: XRD of NiAl LDHs/NF and NiAl LDHs@CS/NF [6].

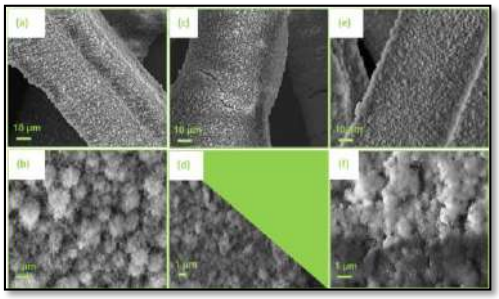

Fig. 2b) (a,b) NiFe LDHs@CS/NF, (c,d) NiCr LDHs@CS/NF, and NiAl LDHs@CS/NF [6].

The crystal structure of NiFe LDHs/NF, NiFe LDHs@CS/NF, NiCr LDHs/NF, NiCr LDHs@CS/NF, NiAl LDHs/NF, and NiAl LDHs@CS/NF was examined by X-ray diffraction. As shown in Fig. 2a, NiAl LDHs exhibit higher crystallinity than NiFe LDHs and NiCr LDHs under identical synthesis conditions. The diffraction peaks at 11.7°, 23.6°, 35.1°, 39.7°, 47.3°, 61.2°, 62.6°, and 66.5° correspond to the typical LDH planes (JCPDS No. 15-0087). Additional weak peaks related to $Ni(OH)_2$ are also observed. Because the materials were grown on nickel foam (NF), the LDH peaks appear relatively weak; therefore, the XRD pattern in the range of 10–44° is enlarged in Fig. 2a. In contrast, NiFe LDHs@CS/NF and NiCr LDHs@CS/NF show poorly defined peaks due to their lower crystallinity [6].

SEM analysis (Fig. 2b) reveals that the morphology varies with the type of trivalent metal ion. NiFe LDHs/NF (Fig. 2(a,b)) shows an interconnected nanowire-like structure, whereas NiFe LDHs@CS/NF consists of nanosheets distributed on carbon spheres (~400 nm). The carbon spheres formed during hydrothermal carbonization of glucose and influence the growth of LDH nanosheets, producing a pom-pom-like structure. For NiCr samples, thin nanosheets cover the NF and CS/NF surfaces forming NiCr LDHs/NF (Fig. 2(c, d)) and NiCr LDHs@CS/NF (Fig. 2(c, d)). In contrast, NiAl LDHs/NF and NiAl LDHs@CS/NF (Fig. 2(e, f)) show similar morphologies with densely interconnected nanosheets uniformly deposited on the substrates [6].

Electrochemical Studies

The electrochemical properties of Ni–LDH electrodes were studied using cyclic voltammetry (CV) and galvanostatic charge–discharge (GCD). The CV curves (Fig. 3a) for NiAl-LDH-120, NiAl-LDH-160, and NiAl-LDH-200 at 5 mV s^{-1} show clear redox peaks, indicating that charge storage is mainly due to Faradaic reactions at the LDH surface. GCD results (Fig. 3b) further confirm their capacitive behavior. NiAl-LDH-160 and NiAl-LDH-200 show a discharge

plateau near 0.25 V (vs. Ag/AgCl), consistent with the CV results. At 1 A g^{-1}, they exhibit specific capacitances of 1578 F g^{-1} and 1454 F g^{-1}, respectively, while NiAl-LDH-120 shows a lower value of 1212 F g^{-1}. The rate performance (Fig. 3c) was tested from 1–20 A g^{-1}. At 20 A g^{-1}, NiAl-LDH-160 and NiAl-LDH-200 retain 884 F g^{-1} (56%) and 744 F g^{-1} (51%), respectively, while NiAl-LDH-120 performs worse. Electrochemical impedance spectroscopy (EIS) was used to study charge transfer behavior. The Nyquist plots (Fig. 3d), recorded from 100 kHz to 0.01 Hz, were analyzed using an equivalent circuit model [9].

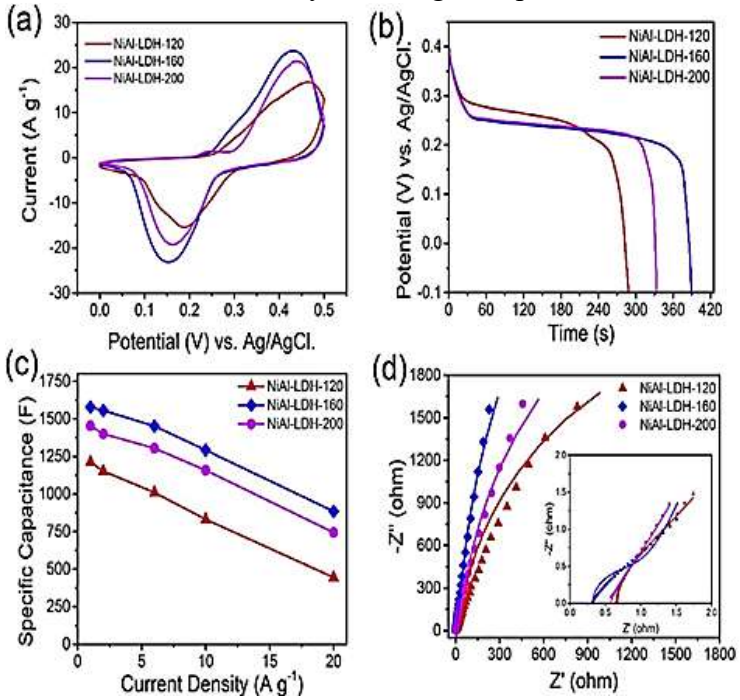

Fig. 3: Fig. 3: Electrochemical characterization: (a) CV curves at 5 mV s^{-1}; (b) GCD curves at 2 A g^{-1}; (c) rate capability at 1–20 A g^{-1}; (d) Nyquist plots [9].

Comparative study of NiAl LDH Based Nanocomposite

Electrode Material	*Electrolyte Solution (KOH)*	*Specific Capacitance F/g*	*Energy Density (Wh/kg)*	*Power Density (W/kg)*	*Retention per cycle*	*Ref.*
CMF@NiAl-LDH	1 M	1667	45.2	170	105.4% after 2000	01
CNTs/NiAl – LDH	-	694	-	-	92% after 3000	02
NiAl – LDH	6 M	1285.2	50	0.37 kW/kg	80 % after 5000	03
NiSe@NiAl – LDH	6 M	1972.7	30.8	955	79.9 % after 5000	04

rGO/NiAl LDH	6 M	1148	35.75 mWh/cm^3	1.01 W/cm^3	83.2 % after 10000	05
NiAl – LDH	1 M	923	216	5200	91 % after 10000	07
NiAl – LDH/MnO_2	6 M	1127	17.8	7899.6	90.1 % after 10000	08
NiAl - LDH	6 M	1578	20	0.75 kW/kg	93.75 % after 10000	09
NiAl – LDH-NF/GNS	6 M	165.6 C/g	31.5	400	80 % after 5000	10
NiAl LDH – rGO	2 M	1.42 C/cm^2	0.22 mWh/cm^2	4.5 mW/cm^2	-	11

Conclusion

NiAl-LDH based nanocomposites were successfully prepared using a hydrothermal synthesis method and evaluated as electrode materials for supercapacitors. Structural and morphological analyses confirmed the formation of layered structures with nanosheet morphology that provides a large active surface area. Electrochemical studies demonstrated good pseudocapacitive behavior, efficient charge transfer, and promising energy storage performance. The results suggest that NiAl-LDH based nanocomposites are promising candidates for advanced supercapacitor applications and can contribute to the development and sustainable energy storage devices.

References

1. Jing Xu et. al. Journal of Alloys and Compounds 787 (2019) 27e35.
2. Caihui Bai et. al. Journal of Colloid and Interface Science 480 (2016) 57–62
3. Zhouliang Tan et. al. Eneryg Fuels 2020, 34, 89.9 – 8946.
4. Jie He et. al. Journal of Alloys and Compounds 1054 (2026) 186345
5. Lei Li et. al chemical engineering j.S1385-8947(18)30737-X
6. Min Li et. al. Electrochemical Acta 2020 0013-4686(20)31057-4
7. Raman Duddi et. al. Hybrid Advances 8 (2025) 100372
8. Wenwen Zheng et. al. Journal of Alloys and Compounds 2018 0925-8388
9. Wencong Wang et. al. chemical engineering journal 338 (2018) 55-61
10. Luojiang Zhang et. al. international journal of hydrogen energy xxx (2016) 1e11
11. Jiuli Chang et. al. Applied surface science 538 (2021) 148106

Recent Advances in Multifunctional Polymer–Metal Oxide Nanocomposites for Gas Sensing and Energy Storage Applications

[1]Kailas Namdevrao Warale, [2]Avinash Ramkishan Gaikwad

[1]Bhimthadi Education Society's Late K.G.Kataria College Daund, Pune

[2]Vivekanand College, Kolhapur (An Empowered Autonomous Institute)

Email:

Article DOI Link: https://zenodo.org/uploads/19791443

DOI: 10.5281/zenodo.19791443

Abstract

The development of multifunctional nanomaterials has greatly advanced sensing and energy storage technologies. Among them, polymer–metal oxide nanocomposites have gained attention due to the combination of high electrical conductivity and flexibility of polymers with the thermal stability, catalytic activity, and semiconducting nature of metal oxides. This synergy enables low-cost, high-performance materials for various applications. Due to interfacial charge transfer and heterojunction formation, these nanocomposites exhibit improved sensitivity, selectivity, and lower operating temperature in gas sensing. In energy applications such as supercapacitors and lithium-ion batteries, they provide enhanced charge storage, excellent cyclic stability, and fast ion diffusion. Their multifunctional nature makes them highly suitable for integrated smart systems that combine sensing and energy storage capabilities.

Keywords: Polymer–metal oxide nanocomposites, Gas sensors, Supercapacitors, Charge transport, Hybrid nanomaterials, Energy storage.

Introduction

Research on materials for energy storage and environmental monitoring has increased due to the demand for sustainable technology [1]. Renewable systems require efficient batteries and supercapacitors, while pollution monitoring needs low-cost, sensitive sensors. Conventional materials often face issues like high cost, poor conductivity, slow kinetics, or structural instability. Metal oxides offer durability and catalytic activity but have low conductivity, whereas conducting polymers provide high conductivity and tunable redox properties but limited stability [2]. Nanoscale polymer–metal oxide composites combine these advantages, improving charge transport and multifunctional performance [3].

Literature Review

Over the past decade, hybrid nanocomposites have advanced significantly for multifunctional applications. Conducting polymers such as polyaniline (PANI), polypyrrole (PPy), and PEDOT are intrinsically conducting polymers with high conductivity, stability, and easy synthesis, widely used in gas sensing and energy storage due to their π-electron–based charge transport [1]. Combining these polymers with metal oxides (ZnO, SnO_2, NiO, MnO_2, CoO_4, VO_2) integrates conductivity, chemical stability, and catalytic activity, thereby enhancing sensing and energy storage performance [2,3].

- **Hybrid Nanocomposites for Gas Sensing**

Polymer–metal oxide nanocomposites overcome the limitations of single-component sensors through synergistic effects such as heterojunction formation, improved charge transfer, and increased active surface sites, leading to major advancements in the past decade [4]. Nanohybrids like PANI/ZnO and PPy/SnO_2 show enhanced sensitivity toward NH_3, NO_2, ethanol, and VOCs at room temperature due to efficient charge modulation during gas adsorption. Compared with pristine materials, they provide faster response, better selectivity, and lower operating temperatures, though issues like humidity instability and baseline drift remain [2]. The incorporation of graphene and noble metals (Pd, Pt) further improves conductivity and catalytic selectivity, while p–n heterojunctions at interfaces amplify resistance changes during gas exposure.

- **Hybrid Nanocomposites for Energy Storage**

CP–MO hybrids have emerged as high-performance electrodes for supercapacitors and batteries. While polymers guarantee conductivity and pseudocapacitance, metal oxides offer redox activity and stability [5]. High capacitance, superior cycling, and improved energy density are provided by composites such as PANI–NiO, PANI–Co_3O_4, PEDOT/Co_3O_4, and vanadium oxide hybrids [2,6,7].

By combining electric double-layer and pseudocapacitive effects—where metal oxides offer redox activity and polymers facilitate quick charge transfer—PANI/MnO_2 and PPy/NiO nanocomposites demonstrate high capacitance [8]. Ferrite-polymer composites are versatile. Optimization depends on morphological control, heterojunction engineering, and nanoarchitecture even though sensing and storing processes are different.

Materials and Theoretical Background

- **Structural Characteristics**

Conducting polymers and semiconducting metal oxide nanostructures are combined in polymer-metal oxide nanocomposites to produce synergistic electrical and electrochemical characteristics. They usually create layered

heterostructures that improve carrier modulation, embedded nanoparticle matrices that offer conductive routes and flexibility, core-shell structures that improve interfacial charge transfer, and porous frameworks that allow gas diffusion and ion transport [9,10]. Band alignment, mobility, and adsorption behavior are always regulated by nanoscale interfaces.

- **Charge Transport Mechanism**

While metal oxides show band conduction with adsorption-dependent carrier density [9], conducting polymers carry charge via polarons and bipolarons by hopping conduction [11]. Together, they create a p–n heterojunction, which modifies conductivity by forming a depletion barrier. Gas sensing and electrochemical energy storage capabilities are improved by this combination [11].

Mechanisms

- **Gas Sensing Mechanism**

An electron depletion layer that increases resistance is formed when oxygen adsorbs on the metal oxide surface in air and grabs electrons ($O_2 + e^- \rightarrow O_2^-$). Trapped electrons are released back into the conduction band when exposed to reducing gases (Gas + $O^- \rightarrow$ oxidized products + e^-), which reduces the depletion width and interfacial barrier. Measurable resistance variations for gas detection are produced by this carrier modulation via surface adsorption and p–n heterojunction processes [8].

- **Energy Storage Mechanism**

Combining EDLC at the oxide–electrolyte interface with pseudocapacitive redox reactions of the polymer backbone results in super capacitive behavior in polymer–metal oxide nanocomposites. Charge storage is improved by reversible doping–dedoping and oxide surface redox processes, and electron transport, ion diffusion, capacitance, rate capability, and cycling stability are all improved by nanoscale interfaces [12].

Applications

Polymer–metal oxide nanocomposites are widely used in smart systems, batteries, supercapacitors, and gas sensing. They are suitable for portable monitoring devices due to their ability to detect hazardous gases such as NH_3, NO_2, CO, and VOCs with high sensitivity and fast room-temperature response via efficient charge transfer [13]. In supercapacitors, synergistic redox and surface charge storage mechanisms enable high capacitance, rapid charge–discharge, and excellent cycling stability, supporting flexible devices [14]. In lithium-ion batteries, they enhance rate performance by improving electrode stability and ion diffusion [15]. These hybrids also enable integrated sensing–

energy storage platforms for wearable technology and the Internet of Things.

Challenges and Future Scope

Polymer–metal oxide nanocomposites have practical limitations despite advancements. Overoxidation and exposure to the environment cause conducting polymers to break down, decreasing their stability and conductivity. Humidity affects the selectivity of gas detection, and electrochemical cycling causes mechanical stress and material degradation. Consistent morphology and scalable, economical manufacture are still difficult to achieve [16]. Green synthesis, sophisticated manufacturing (such as 3D printing and flexible substrates), AI-assisted sensing, magnetic polymer–ferrite systems, and self-powered platforms incorporating energy harvesting for autonomous operation should be the focus of future study [17].

Conclusion

Polymer-metal oxide nanocomposites are a flexible family of multifunctional materials that can be used for both energy storage and environmental monitoring. Electrical conductivity, catalytic activity, and structural stability are all improved by the cooperative combination of metal oxides with conducting polymers. Interfacial charge transfer and heterojunction creation greatly increase sensitivity and selectivity in gas sensing applications. High capacitance and cyclic stability are achieved in energy storage systems by combining electric double-layer and pseudocapacitive processes.

Commercialization is anticipated to be facilitated by ongoing developments in nanostructure engineering and materials optimization, notwithstanding obstacles pertaining to durability and large-scale production. These nanocomposites' versatility makes them attractive options for smart and sustainable technology of the future.

References

1. Zegebreal, L. T. (2023). Sensors and Actuators A: Physical. https://doi.org/10.1016/j.sna.2023.114472
2. Oladele I. Oet al., (2024). RSC Advances. https://doi.org/10.1039/d4ra08601e
3. M. Akhtar et al., (2025). RSC Advances. https://doi.org/10.1039/D5RA01821H
4. Lemma Tirfie Zegebreal et al., (2023). Sensors and Actuators A: Physical. https://doi.org/10.1016/j.sna.2023.114472
5. Pranoti H. Patil et al., (2022). Journal of Composites Science, 6(12), 363. https://doi.org/10.3390/jcs6120363
6. Batistalang Myrthong et al., (2025). Journal of Energy Storage. https://doi.org/10.1016/j.est.2025.116182

7. Snook, G. A., Kao, P., & Best, A. S. (2011). Journal of Power Sources, 196(1), 1–12. https://doi.org/10.1016/j.jpowsour.2010.06.084
8. Wang, Y., Song, Y., & Xia, Y. (2016). Chemical Society Reviews, 45, 5925–5950. https://doi.org/10.1039/C5CS00580A
9. Jian Zhang et al., (2017). Physical Chemistry Chemical Physics. https://doi.org/10.1039/C6CP07799D
10. Bai, H., & Shi, G. (2007). Sensors, 7(3), 267–307. https://doi.org/10.3390/s7030267
11. Barsan, N., & Weimar, U. (2001). Journal of Electroceramics, 7, 143–167. https://doi.org/10.1023/A:1014405811371
12. Zhang, J., Liu, X., Neri, G., & Pinna, N. (2016). Advanced Materials, 28(5), 795–831. https://doi.org/10.1002/adma.201503825
13. Dey, A. (2018). Materials Science and Engineering B, 229, 206–217. https://doi.org/10.1016/j.mseb.2017.12.036
14. Javed, M., Mehmood, U., Ahmad, I., & Kim, K.-H. (2023). Sensors and Actuators A: Physical, 359, 114472. https://doi.org/10.1016/j.sna.2023.114472
15. Tundwal, A., Kumar, H., Binoj, B. J., Sharma, R., Kumari, R., Dhayal, A., … & Kumar, P. (2024). RSC Advances, 14, 9406–9439. https://doi.org/10.1039/D3RA08312H
16. Ma, et al. (2025). Renewable and Sustainable Energy Reviews. https://doi.org/10.1016/j.rser.2025.115982
17. Valle, M., & Esfahani, S. (2021). Advanced Functional Materials, 31(1), 2006739. https://doi.org/10.1002/adfm.202006739

Lithium-Ion Batteries in Clean Energy Technologies: A Mini Review

Rohini Bhagwat Shendkar, Mahesh S. Bhadane

Department of Physics, Rayat Shikshan Sanstha's Dada Patil Mahavidyalaya Karjat, Dist-Ahilyanagar-414402

Email: shendkarrohini742@gmai.com

Article DOI Link: https://zenodo.org/uploads/19791568

DOI: 10.5281/zenodo.19791568

Abstract

Lithium-ion batteries are extensively used in modern energy storage systems. The power portable electronics such as mobile phones, laptops, and electric vehicles and renewable energy storage for solar and wind power. These batteries provide high energy density, long lasting life, and fast charging capability. A typical lithium-ion battery comprises four main components: i) anode, ii) cathode, iii) electrolyte, and iv) separator. They function via the reversible inter-electrode movement of lithium ions during charge–discharge cycles. Proper recycling and responsible use of raw materials are essential to reduce environmental impact.

Keywords: Lithium-Ion Batteries, Energy Storage Devices, Electrode Materials

Introduction

Lithium-ion batteries are one of the most important modern energy storage technologies and are essential for environmental sustainability. As demand for clean energy grows, efficient storage systems are needed to ensure a stable electricity supply. These rechargeable devices store and release energy through reversible redox reactions involving the movement of Li^+ ions between the anode and cathode. A typical lithium-ion battery includes four key components: anode, cathode, electrolyte, and separator, where the electrolyte enables ion transport and the separator prevents electrical contact while allowing ionic movement.

Due to their high energy density, low weight, and long lifespan, lithium-ion batteries are widely used in portable electronics such as smartphones, laptops, and tablets. They are also crucial in electric vehicles, offering high efficiency and fast charging, and are increasingly used in renewable energy systems to store solar and wind power, ensuring continuous energy supply during low-generation periods [1]. A major benefit of lithium-ion batteries is their role in reducing environmental pollution and greenhouse gas emissions by lowering dependence on fossil fuels like coal and diesel, thereby supporting the shift toward

sustainable energy. Ongoing research focuses on improving electrode materials, electrochemical stability, safety, and battery lifespan [2]. Advances in nanostructured electrodes, material design, and battery management systems have further improved performance and reliability, enabling large-scale energy storage and next-generation applications [3].

Structure of Lithium-ion Battery

Figure 1 presents a schematic representation of the operating principle of a lithium-ion battery under charging and discharging conditions. The system is composed of four essential elements: the anode, cathode, electrolyte, and separator. The separator, positioned between the electrodes, inhibits direct electrical contact while still permitting the transport of lithium ions (Li^+) through the electrolyte medium.

During charging, the application of an external power supply drives lithium ions from the cathode toward the anode via the electrolyte. Simultaneously, electrons (e^-) migrate through the external circuit in the same direction. These lithium ions are accommodated within the anode structure through an intercalation mechanism.

In the discharging stage, the direction of ion movement is reversed. Lithium ions migrate back to the cathode through the electrolyte, while electrons flow through the external circuit, delivering energy to the connected load (illustrated as a bulb). This bidirectional transport of Li^+ ions between the electrodes forms the basis of energy storage and release in lithium-ion battery systems.

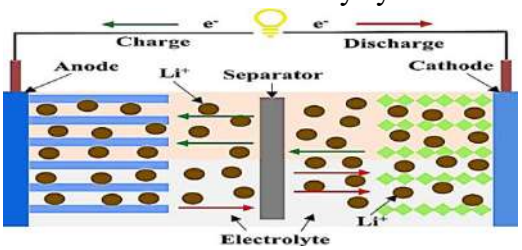

Fig. 1: Schematic illustration of the charge–discharge mechanism in a lithium-ion battery showing the movement of Li^+ ions through the electrolyte and electron flow through the external circuit between the anode and cathode.

Materials of Lithium-Ion Batteries

The performance of lithium-ion batteries strongly depends on the materials used in their electrodes and electrolyte. The cathode is typically made from lithium-based metal oxides such as $LiCoO_2$, $LiFePO_4$, $LiMn_2O_4$, and NMC ($LiNiMnCoO_2$), which provide high energy density and stable electrochemical performance. The anode is commonly composed of graphite, which can reversibly intercalate lithium ions within its layered structure. In recent years, alternative anode materials such as silicon-based compounds and lithium titanate

($Li_4Ti_5O_{12}$) have been investigated to improve capacity and cycling stability.
The electrolyte generally consists of lithium salts (e.g., $LiPF_6$) dissolved in organic solvents that allow lithium-ion transport between the electrodes. A porous separator, usually made of polyethylene (PE) or polypropylene (PP), prevents short circuits while permitting ion movement. The selection and optimization of these materials play a crucial role in determining the energy density, safety, and cycle life of lithium-ion batteries.

Table: Common Materials Used in Lithium-Ion Batteries

Component	Material	Key Properties	Application	Ref.
Anode	Graphite	High stability, good cycle life	Commercial Li-ion batteries	4
Anode	Silicon	Very high theoretical capacity (~4200 mAh g^{-1})	Next-generation high-capacity batteries	5
Cathode	$LiCoO_2$	High energy density, stable layered structure	Mobile phones, laptops	6
Cathode	$LiFePO_4$	Excellent thermal stability and safety	Electric vehicles, grid storage	7
Cathode	$LiMn_2O_4$	Low cost, good thermal stability	Power tools, EV batteries	8
Electrolyte	$LiPF_6$ in carbonate solvents	High ionic conductivity	Commercial Li-ion batteries	9
Separator	Polyethylene / Polypropylene	Prevents short circuit, allows ion flow	Battery safety component	10

Advantages and Limitations of Lithium-Ion Batteries

Lithium-ion batteries offer numerous advantages compared with traditional rechargeable batteries. One of the most significant benefits is high energy density, which allows them to store a huge amount of energy in a compact size. They also demonstrate long cycle life and relatively low self-discharge rates. Additionally, these batteries demonstrate high efficiency in various fields such as portable electronics, electric vehicles, and renewable energy storage. Their ability to support clean energy technologies has made them an essential component of modern sustainable energy infrastructure.

Despite these advantages, some limitations still exist. The extraction of lithium and other raw materials can have environmental impacts if not managed properly. Furthermore, lithium-ion batteries may pose safety risks under extreme conditions such as overheating, overcharging, or physical damage. Recycling

technologies and improved battery management systems are therefore necessary to minimize environmental impact and ensure safe operation.

Future Research Directions

Despite their widespread success, lithium-ion batteries still require continuous improvement to meet future energy demands. Research efforts are increasingly focused on designing new electrode materials that can deliver higher capacity, improved structural stability, and longer operational life. For example, silicon-based anodes and high-energy cathode materials are being explored to enhance overall battery performance. Another important research area involves the development of safer electrolyte systems, particularly solid-state electrolytes, which can minimize leakage, improve safety, and increase thermal stability.

In addition, sustainable recycling technologies are needed to recover valuable metals such as lithium, cobalt, and nickel from spent batteries while reducing environmental impact. Advances in battery management systems, rapid-charging techniques, and thermal control strategies are also essential for improving reliability and efficiency. Continued progress in electrochemistry, nanomaterials, and energy engineering will support the development of next-generation lithium-ion batteries for electric vehicles, portable electronics, and large-scale renewable energy storage systems.

Conclusion

Lithium-ion batteries are now recognized as a key technology for energy storage in contemporary society. Their combination of high energy density, extended service life, and adaptability to renewable energy integration makes them highly suitable for applications such as portable electronics, electric transportation, and grid-level energy storage. Ongoing advancements in electrode materials, electrolyte formulations, and cell design are anticipated to significantly improve their performance, safety, and long-term sustainability.

References

1. Liu J. et al., Energy Storage Materials, 2021, 34, 563–585.
2. Li M. et al., Advanced Materials, 2020, 32, 1901998.
3. Zhang X. et al., Journal of Energy Chemistry, 2022, 64, 546–563.
4. J-M Tarascon & M. Armand, 2001, Nature, 414, 359–367.
5. M. N. Obrovac & V. L. Chevrier, 2014, Chemical Reviews, 114, 11444–11502.
6. K. Mizushima et al., 1980, Materials Research Bulletin, 15, 783–789,
7. Padhi et al., 1997, Journal of the Electrochemical Society, 144, 1188–1194.
8. Thackeray et al., 1983, Materials Research Bulletin, 18, 461–472
9. Xu, 2004, Chemical Reviews, 104, 4303–4418.

Photocatalysts for Energy and Environmental Sustainability

[1]Tahenish K. Mujawar, [2]Amol R. Pardeshi

[1]Department of Physics, New Art's, Commerce and Science College, Parner. Dist. Ahilyanagar – 414 302.

[2]Department of Physics, Dada Patil Mahavidyalaya, Karjat, Dist: Ahilyanagar – 414 402.

Email: mujawartahenish@gmail.com

Article DOI Link: https://zenodo.org/uploads/19791713

DOI: 10.5281/zenodo.19791713

Abstract

This chapter introduces the fundamentals of photocatalysts and their role in the development of sustainable technologies. It explains the basic principles, mechanisms and working of photocatalysts for hydrogen generation. It also explores the different types of photocatalysts, including their characteristics and features at both the nanoscale and microscale. The methods of synthesis and the importance of green synthesis compared to other conventional routes are discussed in detail. In addition, this chapter discusses key parameters reported in the literature, including photocatalyst reusability and stability, factors affecting photocatalytic performance, and the need for advanced strategies to enhance efficiency for energy production and environmentally friendly technology development.

Keywords: Photocatalyst, sustainable technologies, nanoscale, microscale, green synthesis.

Introduction

Over the past two decades, global efforts have focused on developing sustainable technologies to protect the environment and maintain ecological balance. Rapid population growth and rising market demand, especially in developing countries, have driven the expansion of industries and the need for low-cost production and recycling. In this context, photocatalysis has emerged as a promising and sustainable solution to environmental challenges, gaining attention for its potential in water splitting to produce clean hydrogen energy [1,2].

Titanium dioxide (TiO_2) is widely studied for its strong photoresponse, high chemical and thermal stability, low toxicity, and cost-effectiveness. However, its practical use is limited by a wide band gap (3.2 eV for anatase), restricting activity to UV light, and rapid electron–hole recombination, which reduces

efficiency [3]. To address these issues, strategies such as band gap modification and forming hybrid systems have been explored. In particular, combining TiO_2 with graphene-based materials enhances charge transport and reduces recombination due to graphene's high electron mobility. Various TiO_2-based composites with materials like rGO, CdS, WO_3, $BiVO_4$, and ZnO have been reported. This chapter discusses the principles, mechanisms, synthesis methods, and factors affecting photocatalysis [4].

Principles and Mechanism of Photocatalysis

Fig 1. Represent the photocatalytic process is based on the absorption of light by photocatalyst for which metal oxide semiconductors are preferable because of their suitability for the formation of electron-hole pair creation in the conduction band (CB) & the valence band (VB) [5]. Thus, during the absorption of light electrons in the VB are excited into the CB where they form electron and hole pairs. There are two photochemical reactions that involve the photoinduced electrons and holes which are continuously generated.

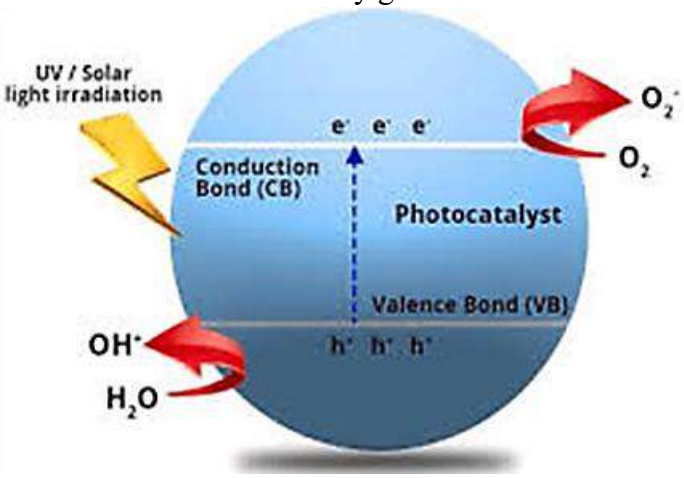

Figure 1. The photocatalytic mechanism under UV/solar irradiation [1].

The following steps are followed during the photocatalytic process:

Step I: The generation of hole/ electron pair

Step II: The separation of charge carriers and their diffusion towards the electrode surface.

Step III: Photooxidation and reduction reactions take place at surface of the photocatalyst

Synthesis Methods

Fig. 2. show the different synthesis methods for preparing photocatalytic materials

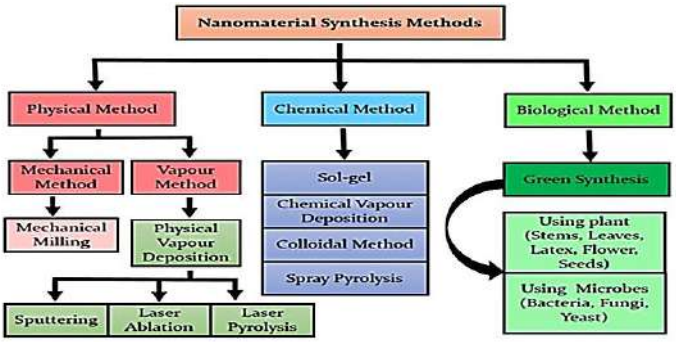

Figure 2. Methods used for the synthesis of photocatalytic materials [1].

Factors affecting photocatalytic activity

- **The Bandgap**

Wide bandgap semiconductor photocatalysts have been assigned more importance due to their use in environment friendly wastewater treatment processes. Among the different types of oxides, ZnO and TiO_2 are the most promising materials; they have been studied many times because of their characteristics, such as high chemical stability, low cost and nontoxic nature [6,7]. However, Large Bandgap semiconductors can absorb only light in the UV region and are unable to absorb visible light.

- **Particle Size**

The shape and size of a material can affect its photocatalytic performancer. In bulk materials, the atomic orbitals overlap, producing bands with a small energy gap as compared to those of nanomaterials. tiny particles usually have a high area and show higher adsorption performance that help to initiate the interaction between the catalyst and the reactants.

- **Doping**

Doping elements into a different host material is the most common strategy for improving the performance of metal-oxide semiconductor [8]. It can affect many parameters, such as the particle size, bandgap, binding energy, lattice defects and other associated properties.

Strategies for boosting photocatalytic efficiency

In the last few years, many researchers have made concerted efforts to design and develop new energy efficient photocatalysts which are better at harvesting the maximum component of the solar spectrum, generating large number of charge carriers and providing large numbers of carriers and providing catalytic sites to support effective photocatalytic process [7].

Applications

Due to globalization in the industrial sector, issues related to energy and the environment are becoming more serious. Now a days water and air pollution are hot topics due to their adverse effects on human health. To control and resolve these issues, there is a need to adopt sustainable technology for the betterment of mankind.

The scope of photocatalysts in energy and environmental sustainability is discussed below.

- **Energy Sustainability**

In the last few decades, many countries have used fossil fuels such as coal, oil and agricultural waste products to generate electricity in power plants to fulfil the demand for energy in all sectors; such fossil fuel uses have made a major contribution to air, water and soil pollution all over the world

- **Environmental Sustainability**

In recent water pollution from industrial waste has been a very serious global issue. Contamination due to heavy metals. The energy efficient photocatalysis process has great potential to remove and degrade organic pollutants naturally using solar energy.

Conclusion and Future Prospects

Photocatalysis is a low-cost, energy-efficient, and eco-friendly approach to address environmental and energy challenges. There is strong demand for visible-light-active metal oxide photocatalysts for hydrogen production and wastewater treatment, but large-scale application remains underdeveloped. Future research should focus on advancing sustainable, sunlight-driven technologies. Although photocatalysis has significant potential, key challenges include improving efficiency, material quality, and reactor performance for large-scale use.

References

1. T. Hisatomi and K. Domen, Nature Catalysis, vol. 2, pp. 387–399, 2019.
2. J. Kosco et al., Nature Materials, vol. 19, pp. 559–565, 2020.
3. X. Meng, S. Wang, C. Zhang, C. Dong, R. Li, B. Li, Q. Wang, and Y. Ding, ACS Catalysis, vol. 12, pp. 10115–10126, 2022.
4. J. Serafin, E. Kusiak-Nejman, A. Wanag, A. W. Morawski, and J. Llorca, Journal of Catalysis, 2017.
5. Y. Zheng, L. Zheng, Y. Zhan, X. Lin, Q. Zheng, and K. Wei, Inorganic Chemistry, vol. 46, pp. 6980–6986, 2007.
6. H. B. Wu and X. W. D. Lou, Advanced Materials, vol. 24, pp. 2567–2571, 2012.
7. J. Serafin, E. Kusiak-Nejman, A. Wanag, A. W. Morawski, and J. Llorca, Applied Surface Science, 2018.
8. J. Serafin, E. Kusiak-Nejman, A. Wanag, A. W. Morawski, and J. Llorca, International Journal of Hydrogen Energy, 2017.

Supercapacitor: Fundamentals and Charge Storage Mechanism

Amol R. Pardeshi, Nilesh R. Kawade

Dada Patil Mahavidyalaya, Karjat, Dist: Ahilyanagar 414 402

Email: amolrp111@gmail.com

Article DOI Link: https://zenodo.org/uploads/19791794

DOI: 10.5281/zenodo.19791794

Abstract

The rapid growth of renewable energy technologies has intensified the need for efficient and sustainable energy storage systems. In this context, electrochemical energy storage devices with high performance and reliability are receiving increasing attention. Among the available technologies, supercapacitors have gained significant interest because of their exceptional power density, fast charging-discharging capability, long operational lifetime, and environmentally friendly nature. This chapter provides an overview of the fundamental principles governing supercapacitor technology. It discusses the major categories of supercapacitors, including electrochemical double-layer capacitors (EDLCs), pseudocapacitors, and hybrid supercapacitors. The mechanisms responsible for energy storage in these systems are explored in detail. These include the electrostatic charge accumulation at the electrode–electrolyte interface in EDLCs, rapid and reversible faradaic redox reactions in pseudocapacitors, and the combination of both mechanisms in hybrid devices. In addition, key electrochemical performance indicators such as specific capacitance, energy density, power density, and cycling stability are analyzed and compared across different types of supercapacitors. Through this discussion, the chapter establishes a fundamental understanding of how charge storage behavior influences device performance and highlights important considerations for the development of advanced supercapacitor systems for future energy storage applications.

Keywords: Supercapacitor, EDLCs, Pseudocapacitor, Hybrid Supercapacitor

Introduction

The rapid depletion of fossil fuel resources, coupled with accelerated population growth, climate change, and the continuously rising global energy demand, has amplified the demand for efficient and sustainable energy storage devices. The effective integration of renewable energy sources into modern energy systems depends critically on the availability of reliable energy storage devices capable of delivering both high performance and long-term stability. Among existing

technologies, lithium-ion batteries which widely recognized as prominent energy storage systems due to their high energy density and established commercial viability. However, their relatively limited power density and slower charge-discharge rates restrict their performance in applications requiring rapid energy delivery [1-2].

To address these limitations, supercapacitors have gained prominence as complementary energy storage. Supercapacitors are capable of storing significantly higher energy than conventional dielectric capacitors while delivering much higher power density than batteries. Owing to their fast charge-discharge capability, high cyclic life, operational safety, and environmentally benign characteristics, supercapacitors have attracted considerable attention for diverse applications, including hybrid electric vehicles, microelectronic systems, smartwatches, backup power units, and other portable electronic devices [3-4].

In recent years, supercapacitors have gained substantial importance because they link the performance the intermediate space between capacitors and batteries, offering enhanced energy density compared to capacitors and superior power density compared to batteries, along with excellent cycling stability and eco-friendly operation [5]. This chapter presents a comprehensive overview of supercapacitors, focusing on their fundamental principles and the underlying charge storage mechanisms that govern their performance

Fundamentals of Supercapacitor

Supercapacitor have unique properties as compare to electrolyte capacitor and batteries, its has 100-time greater energy density, also as compare to other energy storage devices supercapacitor have fast charge discharge mechanism [3]. Supercapacitor Supercapacitors are commonly divided into three main categories: electrochemical double-layer capacitors (EDLCs), pseudocapacitors, and hybrid supercapacitors.

- **Electrochemical Double-Layered Capacitor (EDLCs):** it is consisting two electrode which separated by distance, which cause to change the capacitance of capacitor. The electric double layer forms due to the rearrangement of charges at the electrode-electrolyte interface. In this system, energy storage occurs through electrostatic charge accumulation without involving redox reactions or charge transfer across the interface. However, this model was later considered incomplete because it does not account for the thermal motion and diffusion of ions in the electrolyte solution. [3,8].
- **Pseudocapacitor:** Pseudocapacitors store energy through reversible faradaic charge transfer reactions that occur at the interface between the electrode and the electrolyte. These rapid and reversible electrochemical processes enable pseudocapacitors to deliver higher capacitance and greater energy density compared with electrochemical double-layer capacitors (EDLCs). However,

the involvement of faradaic reactions during the charging and discharging processes generally results in lower power density. In addition, repeated redox reactions can lead to reduced cycle life and limited mechanical stability of the electrode materials. The mechanisms responsible for pseudocapacitance are typically categorized into three types: underpotential deposition, redox pseudocapacitance, and intercalation pseudocapacitance [3,8].

- **Hybrid Supercapacitor:** Hybrid supercapacitor eliminated many limitations of EDLCs and Pseudocapacitor. Hybrid supercapacitor represents the middle ground between two batteries, which consisting carbon-based capacitive electrode paired with either a lithium-modified electrode or another faradaic electrode. pseudocapacitor. In hybrid supercapacitor, cathode is intercalated with faradaic reaction, while anode is intercalated with non-faradaic reaction which is provides higher energy density, power density without affecting cyclic stability. Hybrid supercapacitor is combination of EDLCs and Pseudocapactive electrode for positive and negative electrode fig. 1 (a,b,c,d): represent the nature of the EDLCs, Pseudocapacitor, Battery and Hybrid supercapacitor [3,8].

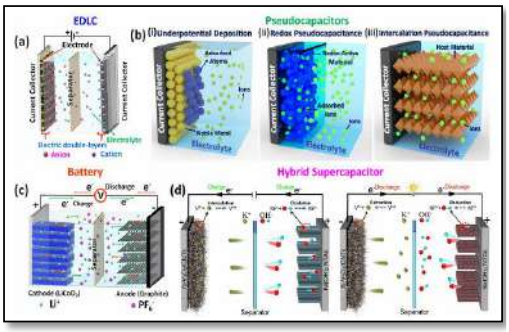

Fig. 1: a) EDLC b) Pseudocapacitor and its three-subdivision c) Battery d) Hybrid Supercapacitor [6].

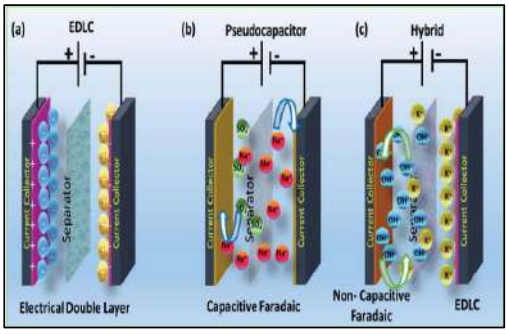

Fig. 2: Charge Storage Mechanism of Supercapacitor [2].

Charge Storage Mechanism of Supercapacitor

Charge storage behavior of supercapacitors can be broadly divided into three distinct categories: (i) capacitive non-faradaic processes occurring in electric double-layer capacitors (EDLCs), (ii) capacitive faradaic processes associated with pseudocapacitors, and (iii) non-capacitive faradaic processes typically observed in hybrid supercapacitor systems.

In electric double-layer capacitors, energy storage is governed by a non-faradaic mechanism. When an external voltage is applied during charging and discharging, an electric double layer develops at the interface between the electrode and the electrolyte. This double layer arises from the electrostatic attraction between the charged electrode surface and oppositely charged

electrolyte ions, leading to reversible ion adsorption and desorption without any charge transfer across the interface. Since no redox reactions are involved, the process is highly reversible and enables rapid energy delivery, resulting in high power density (Fig. 2a) [2,7,9].

In contrast, pseudocapacitors store energy through rapid and reversible faradaic reactions occurring at or near the electrode surface. The charge storage process involves surface redox reactions, ion intercalation-de-intercalation, doping-de-doping, and electrosorption phenomena. Unlike EDLCs, these processes involve charge transfer between the electrode and electrolyte, producing characteristic redox features in electrochemical measurements (Fig. 2b). Owing to these faradaic contributions, pseudocapacitors generally exhibit higher specific capacitance and energy density compared to EDLCs, as the storage mechanism is not limited to purely electrostatic charge accumulation [2,7,9].

The third category involves non-capacitive faradaic processes, commonly represented by hybrid supercapacitors. These systems typically combine a high-power EDLC-type electrode (often serving as the negative electrode) with a battery-type electrode possessing high energy density (generally used as the positive electrode). This configuration integrates both non-faradaic and faradaic charge storage mechanisms within a single device (Fig. 2c). As a result, hybrid supercapacitors achieve improved energy density relative to conventional EDLCs while maintaining enhanced power capability and cycling stability through the synergistic contribution of both mechanisms [2,7,9].

Comparative study of charge storage mechanism for EDLCs, Pseudocapacitor and hybrid supercapacitor are represented in table 1.

Table 1: Typical quantitative performance range of different energy storage mechanism [10].

Energy Storage Mechanism	*Electrode Material*	*Typical Charge Storage Feature*	*Specific Capacitance (F/g)*	*Energy Density (Wh/kg)*	*Power Density (W/kg)*	*Cycle Life*
EDLC	Activated carbon, graphene, carbon nanotubes.	Electric double-layer adsorption	100 - 300	3 – 30	10^3 -10^5	More than 10^4
Pseudocapacitor	Conducting polymers, transition metal oxides, MXene, MOFs/COFs	Surface redox pseudocapacitance surface + intercalation pseudocapacitance	100 - 2000	10 – 50	10^3-10^4	10^3-10^4
Hybrid Supercapacitor	Capacitor + battery-type electrode	EDLC + Pseudocapacitance	-	20 – 150	10^3-10^4	10^3-10^5

Conclusion

Supercapacitors are important electrochemical energy storage devices that operate between traditional capacitors and rechargeable batteries in terms of performance. Their high-power output, fast charge-discharge behavior, and long service life make them suitable for a wide range of modern technologies such as portable electronics, electric vehicles, and emergency power systems. This chapter discussed the basic operating concepts of supercapacitors and described the major charge storage mechanisms associated with electrochemical double-layer capacitors, pseudocapacitors, and hybrid systems. EDLCs store energy through electrostatic ion accumulation at the electrode-electrolyte interface, providing excellent power capability and cycling stability. Pseudocapacitors utilize rapid surface redox reactions to achieve higher capacitance and energy density. Hybrid supercapacitors integrate these mechanisms to balance energy and power performance. Overall, improvements in electrode materials, electrolytes, and device design will continue to enhance the efficiency and practical applications of supercapacitor technologies in future energy storage systems.

References

1. Mutawara Mahmood Baig et. al. Journal of Electroanalytical Chemistry 904 (2022) 115920.
2. Nilimapriyadarsini Swain et. al. J. Mater. Chem. A,2021,9, 25286.
3. Mayank Pandey et. al. Sustainable Energy Fuels, 2025, 9,6380.
4. Sajjad Gharanli et. al. Journal of Energy Storage 122 (2025) 116509.
5. Yonggang Wang et. al. Chem. Soc. Rev., 2016, 45, 5925.
6. Nargish Parvin et. al. J. Mater. Chem. A,2025,13, 24320.
7. S.M. Sultan Mahmud Rahat et. al. Journal of Energy Storage 73 (2023) 108847.
8. Elumalai Dhandapani et. al. Journal of Energy Storage 52 (2022) 104937.
9. Chandu V. V. Muralee Gopi et. al. Mater. Horiz., 2025, 12, 4092.
10. Chenyu Du et. al. Journal of Alloys and Compounds 1054 (2026) 186363

Graphene Oxide/Reduced Graphene Oxide: Methods and Nanocomposite for Supercapacitor Application

Amol R. Pardeshi, Priti R. Pardeshi

Dada Patil Mahavidyalaya, Karjat, Dist: Ahilyanagar 414 402

Email: amolrp111@gmail.com

Article DOI Link: https://zenodo.org/uploads/19791888

DOI: 10.5281/zenodo.19791888

Abstract

The growing demand for sustainable and high-performance energy storage systems has intensified research on advanced electrode materials for next-generation supercapacitors. Among various carbon-based materials, graphene oxide (GO) and reduced graphene oxide (rGO) have emerged as highly promising candidates owing to their two-dimensional structure, large surface area, tunable surface chemistry, and favorable electrochemical characteristics. This chapter presents a comprehensive overview of the synthesis methodologies of GO and rGO, including the modified Hummers' oxidation process and environmentally benign phytochemical reduction approaches. Furthermore, the preparation of graphene-derived nanocomposites through hydrothermal and related techniques is discussed, highlighting their structural and functional advantages. Particular emphasis is placed on the integration of GO/rGO with metal oxides, bimetallic nanoparticles, sulfides, and conducting polymers to enhance charge storage performance.

Keywords: GO, rGO, Supercapacitors; Nanocomposites, Hydrothermal synthesis, Hummers' method, Electrochemical performance.

Introduction

Now day's clean energy source is highly demanded due to high use of fossil fuels and increasing concerns about the environmental issues, clean and highly efficient energy storage devices are demanded [1]. Supercapacitor device has highly significant for this problem due to potential to store high energy for instantaneous applications and highly promising alternative for batteries due to unique features, including high life span, rapid charging capability, recent studied found that supercapacitor exhibits excellent electrochemical properties for high energy density (Ed) and high-power density (Pd) due to graphene-based materials. Graphene (GO) and reduced Graphene Oxide (rGO) have attention due to their surface modifications, non-toxicity, and other surface parameters [2-3]. In

addition, supercapacitor exhibits high charging – discharging process with competence to become a potential candidate for various consumer devices (e.g. Laptop, Mobile, Electronics devices etc.) [4]. Also, supercapacitor work as bridge bap between batteries which have low power density and capacitor which has law energy density. supercapacitor is categorized into three types – Electrical Double Layered Capacitor (EDLC) which has energy storage process by collection of ions among the electrode material and electrolyte, Pseudo-capacitor (PCs) which referred redox reaction in charge-storage mechanism and hybrid supercapacitor which exhibits on energy storage process as well as redox reaction [5].

Graphene Oxide have unique properties due to two-dimension structure which allowing to manipulated into different dimensional forms such as fullerene (0 D), carbon nanotubes (1 D) and graphite (3D). Graphene Oxide contain oxygen-containing functional groups, imparting unique properties such as hydrophilicity and chemical reactivity. Graphene oxide, rGO and its composite can be synthesized using many different methods such as modified hummers method, hydrothermal method, Sol- gel method [6-7, 24]. Currently, researchers are mostly focusing on asymmetric capacitor fabrication with carbonaceous negative electrode and metal oxide/conducting material based positive electrode for higher energy density with excellent cyclic stability [8]. There are many different material which made up by different method and deliver high energy and power density with carbon material (GO and rGO) [9-13]. This chapter reveals methodology of GO/rGO and its roll in supercapacitor application with its nanocomposite due to iconic surface properties.

Methods

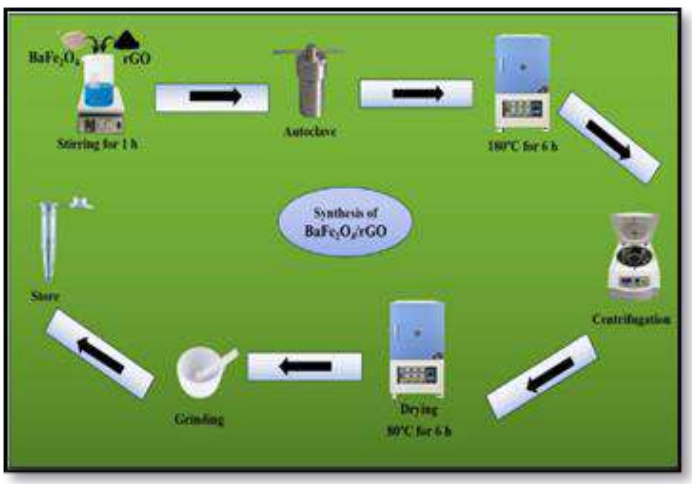

Fig. 1: Schematic Demonstration of BaFe2O4/rGO Nanocomposite via hydrothermal Method [3].

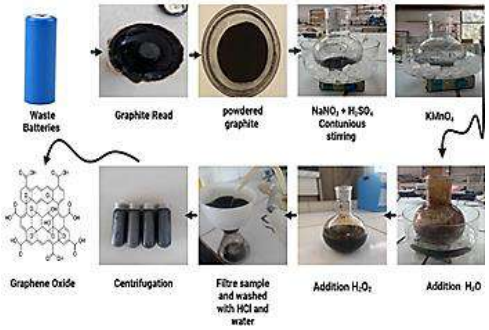

Fig. 2: Synthesis of Graphene Oxide using Hummer's Method [12].

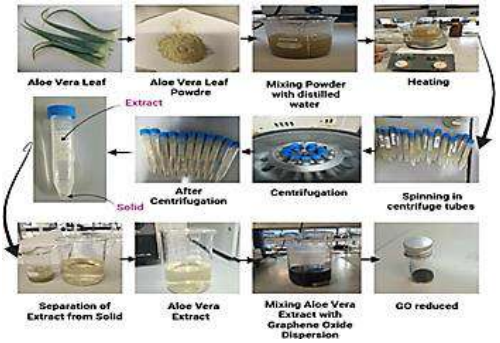

Fig. 3: Synthesis of Reduced Graphene Oxide using Aloe Vera Extraction [12].

rGO was prepared by Hummers' Method then prepare the nanocomposite of BaFe2O4/rGO nanocomposite Fig, 1, where rGO framework give high conductivity, charge transfer kinetics and electrochemical stability [3]. Synthesis process of Graphene Oxide via Hummer's Method using recycled batteries, in this process, 1 g of graphite was dispersed in 25 mL concentrated H_2SO_4 containing 1 g $NaNO_3$ under ice-bath conditions to regulate heat evolution. Subsequently, 5 g $KMnO_4$ was added gradually with continuous stirring to promote controlled oxidation and prevent excessive exothermicity. The reaction was maintained at low temperature and stirred for 8 h to ensure sufficient oxidation and interlayer modification. After oxidation, 10 mL H_2O_2 was introduced to terminate the reaction and reduce residual permanganate species to MnO_2, accompanied by a color transition to yellow. The product was purified by washing with 5% HCl solution to remove metallic impurities, followed by repeated rinsing with deionized water until neutral pH was achieved Fig, 2 [12]. Reduced graphene oxide (rGO) was synthesized via a phytochemical reduction route using extract derived from Aloe vera leaves. Fresh leaves were washed, comminated, and extracted in distilled water (1:5 w/v), followed by thermal treatment at 60 ± 2 °C for 1 h under continuous stirring to promote the release of bioactive reducing constituents. The extract was filtered prior to use. For reduction, 100 mg of graphene oxide (GO) was dispersed in 30 mL demineralized water and ultrasonicated for 30 min to obtain a homogeneous suspension. The plant extract (0.1 g mL^{-1}) was then added dropwise, and the mixture was refluxed at 80–100 °C for 6–12 h. Phytochemical species facilitated the reduction of oxygenated functional groups, as indicated by a color change from brown to black. The product was recovered by centrifugation, washed repeatedly with hot demineralized water, and dried at 60 ± 2 °C to obtain rGO powder fig. 3 [12].

GO, rGO based Nanocomposite

The formation of GO/rGO-based nanocomposites has been pursued as a rational materials engineering approach. Coupling graphene derivatives with electroactive species such as transition-metal oxides, sulfides, hydroxides, or intrinsically conducting polymers generates cooperative effects that enhance electron transport, increase accessible active sites, and facilitate efficient ion diffusion. These hybrid systems integrate electric double-layer charge storage with reversible faradaic processes, thereby improving specific capacitance, rate performance, and cycling durability. Accordingly, the deliberate structural design and compositional optimization of graphene-centered nanocomposites remain pivotal for the development of advanced supercapacitor technologies [2].

Comparative study of GO/rGO based nanocomposite given in below table

Sr. No.	**Nanocomposite**	**Specific Capacitance C_s (Fg^{-1})**	**Energy Density ($Whkg^{-1}$)**	**Power Density ($kWkg^{-1}$)**	**Ref.**
01	MoS_2 – Polypyrrole	1942	12.9	15.0	01
02	$BaFe_2O_4$/rGO	1498.673	54.693	0.256	03
03	Ag – Ni /rGO	897	80	0.400	04
04	$NaFeO_2$/rGO	1221.97	33.75	0.223	05
05	$MnFe_2O_4$ -rGO	750	27.7	0.750	07
06	rGO/$BiVO_4$	151	33.7	8.0	08
07	ZrO_2/rGO	210.58	33.57	6.3	13
08	In (OH)3/rGO	251.34 mA hg^{-1}	-	-	14
09	GO	147	14.90	0.242	15
10	rGO/TiO_2	156	7.8	1.6	16
11	rGO	176.5 F cm^{-1}	-	-	17
12	PZ – rGO	374 μFg^{-1}	-	-	18
13	N-rGO/Mn_3O_4	345	12	22.5	19
14	ZnO/SnO_2 – rGO	128.43	212.36	1.44	20
15	NHCS/GF_x	367 F cm^{-1}	24.99 mW	822 mW	21

			cm^{-3}	cm^{-3}	
16	rGO/α Fe_2O_3/TiO_2	646.5	-	-	22

Conclusion

Graphene oxide (GO) and reduced graphene oxide (rGO) are promising materials for supercapacitor applications due to their high surface area, tunable surface functionality, and favorable electrochemical properties. Although individual graphene derivatives face challenges such as agglomeration and limited conductivity (in GO), these limitations can be effectively addressed through nanocomposite formation. The incorporation of metal oxides, nanoparticles, and conducting polymers with GO/rGO creates synergistic effects that enhance charge storage capacity, electrical conductivity, and cycling stability. Therefore, rational design and controlled synthesis of GO/rGO-based nanocomposites play a crucial role in developing high-performance and sustainable supercapacitor devices for future energy storage technologies.

References

1. Jin Hao et al., ACS Appl. Nano Mater., 2021, 4, 1330–1339.
2. Suveksha Tamang et al., J. Alloys Compd., 2023, 947, 169588.
3. Haifa A. Alyousef et al., Eur. Phys. J. B, 2025, 98, 243.
4. Madhurya Chandel et al., ACS Appl. Electron. Mater., 2019, 1, 1215–1224.
5. Ghulam Elyas et al., J. Inorg. Organomet. Polym. Mater., 2025.
6. Rahul S. Nikam et al., Next Mater., 2025, 7, 100626.
7. Priyanka Makkar et al., ACS Appl. Energy Mater., 2020, 3, 2653–2664.
8. Santosh S. et al., ACS Appl. Mater. Interfaces, 2016, 8, 31602–31610.
9. Khira Z. Riahi et al., J. Mol. Struct., 2020, 1216, 128304.
10. Wei-Ting Chang et al., J. Power Sources, 2019, 414, 86–95.
11. Rui Yuan et al., Colloids Surf. A, 2018, 547, 56–63.
12. Soukaina El Bourachdi et al., Surf. Interfaces, 2025, 73, 107524.
13. Suveksha Tamang et al., Chem. Data Collect., 2025, 60, 101207.
14. Venkatesha Narayanaswamy et al., J. Power Sources, 2025, 653, 237739.
15. Vijay Prajapati et al., J. Chem. Inorg. Mater., 2026, 8, 100135.
16. Ritesh Kumar et al., Microchem. J., 2025, 219, 115940.
17. Viet Hung Pham et al., J. Phys. Chem. C, 2016, 120, 5353–5360.
18. G.K. Ayyadurai et al., J. Mol. Struct., 2025, 1337, 142247.
19. Katlego Makgopa et al., ACS Omega, 2021, 6, 31421–31434.
20. Suganya Govindasamy et al., J. Organomet. Chem., 2025, 1041, 123842.
21. Xianghui Yu et al., ACS Appl. Nano Mater., 2025, 8, 1935–1943.
22. K.D. Jagtap et al., Electrochim. Acta, 2025, 543, 147474.

NiCo Layered Double Hydroxide (NiCo-LDH) Based Nanocomposites: Hydrothermal Synthesis and Electrochemical Energy Storage Applications

Vaishnavi S. Sabale, Amol R. Pardeshi

Dada Patil Mahavidyalaya, Karjat, Dist: Ahilyanagar 414 402

Email: amolrp111@gmail.com

Article DOI Link: https://zenodo.org/uploads/19791972

DOI: 10.5281/zenodo.19791972

Abstract

Growing global demand for effective and sustainable energy storage device has accelerated research on advanced electrode materials with high electrochemical performance. Nickel-cobalt layered double hydroxide (NiCo-LDH) promising pseudocapacitive material due to multiple oxidation states, compositional tunability, and high charge storage capability. This chapter systematically discusses the hydrothermal synthesis of NiCo-LDH-based nanocomposites and their electrochemical characteristics for hybrid supercapacitor applications. The hydrothermal method enables controlled crystal growth, uniform morphology, and strong interfacial interaction between active materials and conductive substrates. Furthermore, the integration of NiCo-LDH with carbonaceous materials and other functional components significantly enhances electrical conductivity, structural stability, and ion diffusion kinetics. Electrochemical investigations demonstrate improved reversibility, favorable rate capability, and long-term cycling durability.

Keywords: NiCo-LDH, Layered Double Hydroxides, Hydrothermal synthesis, Electrochemical energy storage.

Introduction

The excessive use of fossil fuels has led to environmental pollution & accelerated climate change. With rapid industrialization and economic expansion, the demand for advanced energy storage systems possessing high energy density, high power density, rapid charge-discharge capability, long cycle life, low cost, and environmental compatibility have significantly increased [1-4]. Therefore, the development of sustainable electrochemical energy storage devices has become a research priority. Among the commercially available technologies, lithium-ion batteries represent one of the most mature and widely utilized systems. However, despite their high energy density, lithium-ion batteries suffer

from inherent limitations, including limited cycle life, capacity degradation, safety concerns, and relatively slow charge-discharge kinetics. These drawbacks restrict their applicability in high-power and rapid energy delivery systems. In contrast, supercapacitors (SCs) have attracted considerable attention owing to their superior power density, extended cycling stability, fast charge-discharge characteristics, low maintenance requirements, and environmentally benign nature. Nevertheless, symmetric SCs often exhibit limited energy density due to intrinsic conductivity constraints, while asymmetric supercapacitors have been developed to overcome this limitation and enhance overall energy density [5-7]. Charge storage in supercapacitors generally occurs through two primary mechanisms, leading to their classification as electric double-layer capacitors (EDLCs) and pseudocapacitors. In EDLCs, energy storage arises from the electrostatic accumulation of ions at the interface between the electrode surface and the electrolyte, forming an electrical double layer. This process involves reversible ion adsorption and desorption without charge transfer, which enables fast charge–discharge behavior, high power capability, and excellent cycling stability. Nevertheless, EDLCs typically exhibit limited specific capacitance due to the absence of Faradaic reactions. In contrast, pseudocapacitors store energy through rapid and reversible Faradaic redox processes that occur at or near the electrode surface. These surface or near-surface electrochemical reactions contribute additional charge storage, resulting in considerably higher specific capacitance compared with purely electrostatic EDLC systems. [8-10].

Various metal hydroxides, Ni $(OH)_2$, Co $(OH)_2$, and bimetallic Nickel-Cobalt Layered Double Hydroxide (NiCo-LDH) have been extensively investigated as electrode materials. These materials store energy primarily through reversible redox processes involving multiple oxidation states of transition metal ions. Compared to monometallic hydroxides, NiCo-LDH demonstrates superior electrochemical performance due to the synergistic interaction between nickel and cobalt species. This synergism enhances electrical conductivity, increases electroactive surface area, improves hydrophilicity, and enables more efficient utilization of uniformly distributed transition metal active sites. Consequently, NiCo-LDH exhibits higher specific capacitance, improved energy density, and enhanced overall electrochemical performance [11-14].

In this chapter, emphasis is placed on the hydrothermal synthesis of NiCo-LDH-based nanocomposites and their electrochemical behavior for advanced energy storage applications.

Hydrothermal Synthesis Approach for NiCo-LDH Nanocomposites

During the synthesis of the NiCo LDH/MnO_2/PPy/g-C_3N_4 nanocomposite, hexamethylenetetramine (HMTA) hydrolyzes in water to gradually generate hydroxide (OH^-) ions. These hydroxide ions react with Ni^{2+} and Co^{2+} ions to form

nickel and cobalt hydroxide precursors. Meanwhile, dissolved oxygen partially oxidizes Co^{2+} to Co^{3+}, which facilitates the formation of a mixed metal layered double hydroxide (NiCo LDH). The resulting hydroxide units subsequently self-assemble into nanoflower-like NiCo LDH structures that act as a framework for the incorporation of MnO_2, PPy, and g-C_3N_4, producing the final nanocomposite, which represented in fig. 1 [10].

Fig. 1: Hydrothermal Approach to prepare NiCo LDH based Nanocomposites [10].

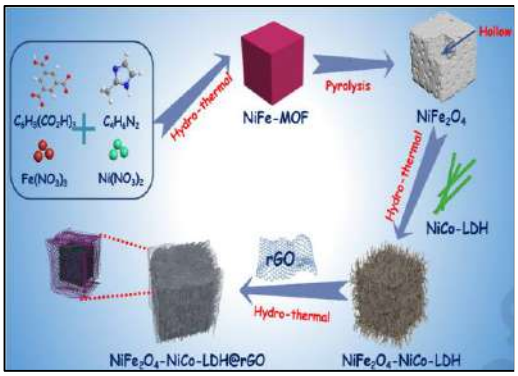

Fig. 2: Fabrication of $NiFe_2O_4$ – NiCo – LDH @rGO [11].

Synthesis of $NiFe_2O_4$ – NiCo – LDH/rGO are represented in Fig. 2. which include the pyrolysis of NiFe-MOF and two - step hydrothermal reaction [11]. A NiCo-based nanocomposite electrode was synthesized using a hydrothermal approach. A carbon cloth (2 × 4 cm^2) substrate was first cleaned by sequential ultrasonication in acetone, ethanol, and distilled water for 30 min each. An aqueous solution containing nickel nitrate, cobalt nitrate, sodium dodecyl sulfate, and urea was prepared in a mixed water/ethanol solvent and stirred at room temperature to obtain a homogeneous precursor solution. The cleaned carbon cloth and precursor solution were then placed in a Teflon-lined autoclave and heated at 110 °C for 10 h. After natural cooling, the obtained material was washed with deionized water and dried under vacuum at 60 °C. The dried precursor was subsequently phosphorized using NaH_2PO_2 at 300 °C for 2 h under an argon atmosphere, producing the final CC/NiCoP electrode with a mass loading of approximately 1.1 mg cm^{-2} [11].

Electrochemical measurements were conducted in a three-electrode configuration using the synthesized electrode as the working electrode, Hg/HgO as the reference electrode, and platinum foil as the counter electrode. Cyclic voltammetry was recorded within a potential window of 0.1–0.7 V at different scan rates fig. 3a., while galvanostatic charge-discharge tests were performed at current densities ranging from 1 to 10 A g^{-1}. The GCD curves exhibited distinct potential plateaus and good symmetry, indicating typical battery-type behavior and high coulombic efficiency of the electrode material.

Electrochemical Performance of NiCo-LDH Nanocomposites

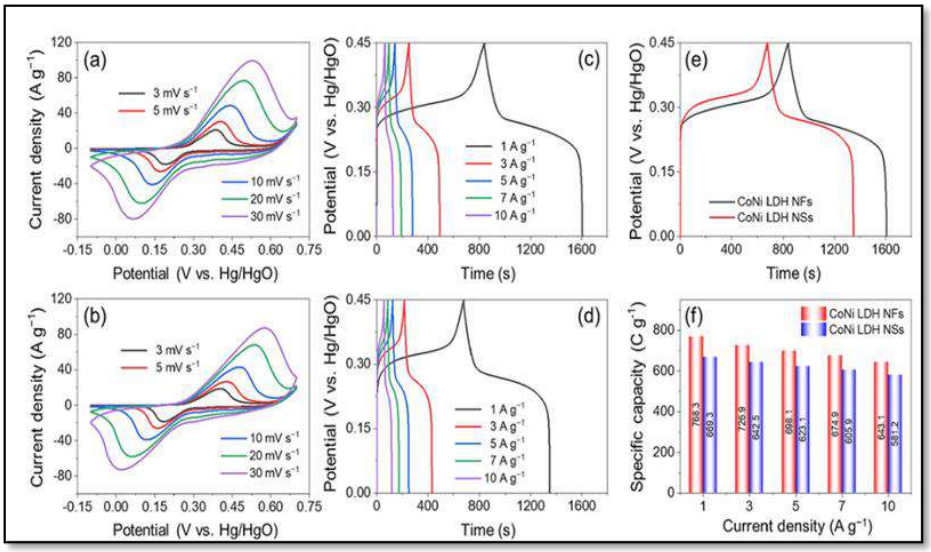

Fig. 3: Electrochemical Performance of NiCo LDH via three electrode system [19].

The specific capacitance of CoNi LDHs calculated from the discharge curve. For the CoNi LDH NFs electrode, it exhibits a specific capacitance 643.1C g-1 at the current density of 10 A g-1, while the CoNi LDH NSs exhibits 581.2C g-1, accordingly. The GCD curves of CoNi LDH NFs and NSs at the current load of 1 Ag-1 were presented in Fig. 3e, and it shows the discharge time of NFs was longer than that of NSs, indicating the higher specific capacity that the NFs could deliver. The CoNi LDH NFs possessed larger surface area and could provide more active sites for Faradic reactions. Fig. 3f showed the rate performance of these CoNi LDHs, and CoNi LDH NFs retained 83.7 % of initial capacity as the current density from 1 to 10 A g-1 and the CoNi LDH NSs gives a similar rate of capability with 86.8 % retention [19].

Comparative study of electrochemical studies of NiCo LDH based nanocomposite.

Composite	***Specific capacitance (F/g)***	***Energy Density (Wh/kg)***	***Power Density (W/kg)***	***Ref.***
ZIF-9 derived rGO/$NiCo_2S_4$	1242.2	79.87	750	03
NiCo LDH on CC	1540	37	27.3	04
NiCo LDH@rGO	2640	58.4	3732	05
NiCo LDH /Ag	2920.6	42.9	800	06
NiCo LDH/Gr	2690	50.2	8002	07
PPy/g-C_3N_4/MnO_2 on NiCo LDH	2389	82	750	10
NiCoP @ NiCo – LDH	1951	57	850	13

NiCo-LDH@rGO	1703	47.1	399.9	14
2D ZIF NiCo LDH on rGO/Ni Foam	2408.8	32.2	235.5	15
NiCo LDH/Graphene	175.1 mAh/g	40.6	400	16
Ce doped NiCo LDH@ CNT	187.2	-	-	17
MOF NiCo LDH	1652	32.9	74.6	18
CoNi LDH	768.3 C/g	31	748	19

Conclusion

Hydrothermally synthesized NiCo-LDH nanocomposites demonstrate significant potential for energy storage applications due to controllable nanostructure and enhanced electrochemical properties. The synergistic interaction between nickel and cobalt promotes efficient redox activity, leading to improved pseudocapacitive behavior. Incorporation of conductive carbon materials and hybrid architectures further enhances electrical conductivity and structural stability. Additionally, optimized porous and three-dimensional morphologies facilitate effective electrolyte diffusion and increase the availability of active sites. As a result, NiCo-LDH-based composites exhibit high reversibility, good rate capability, and excellent cycling durability, making them promising composite for advanced hybrid supercapacitor systems.

References

1. Gonçalves et al., RSC Adv., 2016.
2. Wang et al., Appl. Clay Sci., 2020, 198, 105820.
3. Cui et al., Microchem. J., 2023, 190, 108718.
4. Li et al., J. Mater. Sci.: Mater. Electron., 2019.
5. Kiran et al., Carbon, 2019.
6. Guan et al., J. Alloys Compd., 2019, 799, 521–528.
7. Liu et al., J. Alloys Compd., 2018.
8. Qu et al., J. Energy Storage, 2025, 107, 114986.
9. Shen et al., Inorg. Chem. Commun., 2019.
10. Rangaraju et al., FlatChem, 2025, 52, 100897.
11. Chu et al., J. Colloid Interface Sci., 2020.
12. Guo et al., Energy Fuels, 2025, 39, 20950–20956.
13. Gao et al., Chem. Eng. J., 2019.
14. Long et al., J. Alloys Compd., 2019.
15. Liu et al., Electrochim. Acta, 2024, 475, 143507.
16. Zou et al., Appl. Surf. Sci., 2022, 571, 151322.
17. Dinari et al., Energy Fuels, 2021, 35, 1831–1841.
18. Xiao et al., ACS Nano, 2019.
19. Bao et al., J. Energy Storage, 2024, 82, 110535.

Supercapacitor: Principles and Types

Rushikesh S. Shete, Amol R. Pardeshi

Dada Patil Mahavidyalaya, Karjat, Dist: Ahilyanagar 414 402

Email: amolrp111@gmail.com

Article DOI Link: https://zenodo.org/uploads/19792507

DOI: 10.5281/zenodo.19792507

Abstract

The accelerating uses of fossil fuel and the environmental consequences of greenhouse gas emissions have intensified the transition toward sustainable energy technologies. Because renewable energy sources are often intermittent, reliable and efficient energy storage systems are essential. Supercapacitors, also known as electrochemical capacitors or ultracapacitors, are considered promising devices that fill the gap between traditional capacitors and rechargeable batteries. They provide high power output, fast charge-discharge behavior, long cycling stability, and good operational reliability with moderate energy storage capability.

This chapter provides a detailed examination of the fundamental principles governing supercapacitor operation, including charge-storage mechanisms at the electrode electrolyte interface. The distinctions between electric double-layer capacitors (EDLCs), pseudocapacitors, and hybrid supercapacitors are systematically discussed, with emphasis on their electrochemical behavior, material selection, structural configuration, and performance metrics. Important factor such as capacitance, energy density, and power density are analyzed to elucidate the factors influencing device efficiency. Furthermore, the classification of hybrid supercapacitors including asymmetric, symmetric, and battery-type configurations is presented to highlight recent advancements aimed at enhancing energy storage performance. Through comprehensive analysis, this chapter outlines the scientific foundation and technological strategies required for the development of next-generation supercapacitor systems for advanced energy applications.

Keyword: Supercapacitor, Charge Storage Mechanism, Energy Density, Power Density.

Introduction

The rapid use of fossil fuel reserves & the escalating environmental concerns associated with greenhouse gas emissions have intensified global efforts toward the deployment of sustainable energy systems. Renewable energy sources such as

solar, wind, and hydroelectric power are increasingly being integrated into modern power grids; however, their intermittent and fluctuating nature necessitates efficient and reliable energy storage solutions. In this context, electrochemical energy storage play a pivotal role in stabilizing power output, enhancing grid resilience, and enabling efficient energy utilization.

Conventional storage technologies - including batteries, capacitors, and fuel cells have been extensively developed and commercialized. Each system, exhibits intrinsic performance constraints. Electrochemical batteries are well recognized for their high energy density, enabling prolonged energy supply, but they often suffer from limited power density and slower charge-discharge kinetics. Conversely, dielectric and electrolytic capacitors demonstrate exceptional power density and rapid energy delivery, yet their energy storage capacity remains comparatively low. Consequently, neither system independently satisfies the simultaneous demand for high energy density and high-power density for advanced renewable energy applications. To bridge this performance gap, supercapacitors also referred to as electrochemical capacitors or ultracapacitors have emerged as a promising energy storage technology [1-2]. Supercapacitors combine the advantageous characteristics of batteries and conventional capacitors by delivering substantially higher power density than batteries while offering greater energy density than traditional capacitors. Although their energy density remains lower than that of batteries, their rapid charge - discharge capability, long cycle life, high coulombic efficiency, and superior operational stability make them particularly suitable for applications involving peak power support, regenerative braking systems, and hybrid energy storage configurations [3].

This chapter presents a comprehensive discussion of the fundamental working principles of supercapacitors, including charge storage mechanisms at the electrode - electrolyte interface. Various classifications highlighting their structural configurations, material compositions, and electrochemical performance characteristics. Such an in-depth exploration provides essential insight into the design strategies and functional attributes that govern the performance of supercapacitor systems.

Fundamental of Supercapacitors

Supercapacitors, often referred to as ultracapacitors or electrochemical capacitors, are modern energy storage devices that combine characteristics of traditional capacitors and rechargeable batteries. They store and release energy very quickly because charge builds up at the boundary between the electrode and the electrolyte. As a result, supercapacitors provide high power density and can operate for a large number of charge-discharge cycles. Energy storage in supercapacitors mainly occurs through two mechanisms. In Electric Double-Layer Capacitors (EDLCs), energy is stored through electrostatic charge

accumulation on the surface of electrodes with large surface areas. This process does not involve chemical reactions, which allows rapid charging and long operational life. On the other hand, pseudocapacitors store energy through quick and reversible redox reactions at the electrode surface, leading to higher capacitance compared to purely electrostatic storage. Fig. 1 represent the energy and power densities of various energy storage devices [4].

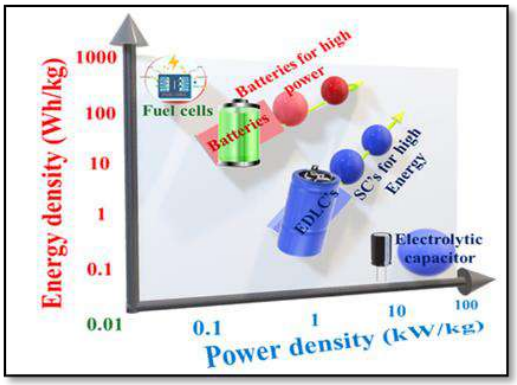

Fig 1: Energy and power densities of various energy storage devices [4]

The performance of supercapacitors depends on key components such as high-surface-area conductive electrodes, ionically conductive electrolytes, separators to prevent short circuits, and efficient current collectors. Due to their rapid electrochemical kinetics, high power capability, and superior cycling stability, supercapacitors are widely utilized in applications requiring quick energy delivery and long operational life. [4]

Working Mechanism of Supercapacitor

The working mechanism of supercapacitor based on the capacitive performance a) Electrochemical Double - Layer Capacitor (EDLC) which store the electric charge via interface between the electrode and electrolyte, b) Pseudocapacitance grown form rapid and reversible surface of redox reaction, it's a combination of non – faradaic and faradaic process, 3) hybrid capacitor take the advantages of EDLC and PC mechanism [5-8].

Eletric Double-Layer Capacitor (EDLC)

Fig. 2a: EDLC are most of common type of supercapacitor which work on principle of store charge via electrostatic phenomena due to offer unique properties like high surface area, high power density and fast charging discharging process with high capacitance [2].

EDLC consist of two conducting plates separated by a dielectric material.

Its capacitance is $\boldsymbol{C = \frac{Q}{V} = \frac{\varepsilon A}{d}}$

where Q = Stored charge and V = Applied Potential, A = Area and

d = distance between two plates [4].

Pseudocapacitor

Fig. 3b: Pseudocapacitor work on principle of store charge via reversible redox reaction of charge storage mechanism of the pseudocapacitor include the transfer of charge between the electrode and electrolyte, when voltage applied between electrode material undergoes an oxidation and reduction process [2]. Specific capacitance of pseudocapactive materials is $C = \frac{nF}{MV}$

Where n = number of electron transfer, F = Faraday's Constant, M = Molar Mass and V = Voltage window.

Energy density and power density are calculated as

$$\boldsymbol{Energy\ density = \frac{1}{2}CV^2,\ Power\ Density = \frac{1}{4R}CV^2}$$

Where, C = Capacitance, V = Voltage and R = Equivalent Series Resistance.

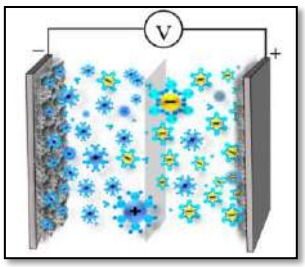

Fig. 2a: EDLC

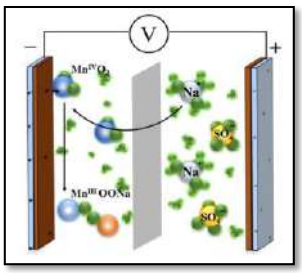

Fig.2b: Pseudocapacitor

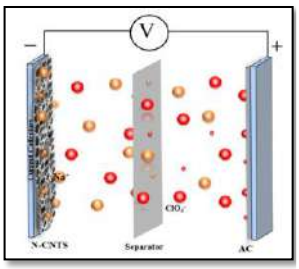

Fig. 2c: Hybrid capacitor

Hybrid Supercapacitor

Fig. 3c: Hybrid supercapacitor gives high performance of energy storage application. It's overcome the limitation of EDLC and Pseudocapacitors and combine the advantages of both. Hybrid supercapacitor provides the high energy density and power density along with retaining fast charging having long cycle life properties [2].

Hybrid supercapacitor divided into three groups.

- Asymmetric Hybrid Supercapacitor
- Symmetric Hybrid Supercapcitor
- Battery type hybrid supercapacitor

In hybrid supercapacitor mostly activated carbon employed as negative electrode material due to large surface area and metal oxide electrode as negative electrode.

- **Asymmetric Hybrid Supercapacitor:** it is fabricated to exhibits excellent energy and power density of device, asymmetric hybrid supercapacitor fabricated by two different electrode material with different operating potetial such as high capacitive negative electrode and highly redox active pseudocapacitve positive electrode.
- **Symmetric Hybrid Supercapacitor:** it's fabricated via both same electrode material. Mostly composite material is used to electrode material for supercapacitor, its advance over simple supercapacitor and providing high potential window and high energy density.
- **Battery Type Hybrid Supercapacitor:** it is fabricated by two different type of electrode materials one of high capacitive type another one is battery type electrodes. [7]

Conclusion

Supercapacitors are an important class of electrochemical energy storage devices designed to deliver high power and long operational stability. They combine the rapid charge-discharge capability of conventional capacitors with the improved energy storage capacity typically associated with batteries, making them suitable for applications requiring quick energy delivery and reliable cycling performance.

This chapter described the main energy storage mechanisms involved in different supercapacitor systems, including electric double-layer capacitors, pseudocapacitors, and hybrid devices. Electric double-layer capacitors store energy through electrostatic charge separation at the electrode-electrolyte interface, whereas pseudocapacitors rely on fast and reversible redox reactions to increase capacitance. Hybrid systems integrate these mechanisms to enhance energy density while maintaining high power capability. Additionally, factors such as electrode materials, electrolyte composition, device configuration, and internal resistance significantly influence overall device performance.

References

1. Kavishka Dissanayake et. al, Journal of Energy Storage 96 (2024) 112563.
2. Iqbal Singh et. al, Next Research 2 (2025) 100228.
3. Jie Zhang et. al. MNE 21 (2023) 100229.
4. Sonali A. Beknalkar et. al. Journal of Alloys and Compounds 1024 (2025) 180169.
5. Saswata Bose et. al. J. Mater. Chem., 2012, 22, 767
6. Yonggang Wang et. al. Chem. Soc. Rev., 2016, 45, 5925
7. Elumalai Dhandapani et. al. Journal of Energy Storage 52 (2022) 104937
8. Sajjad Gharanli et. al. Journal of Energy Storage 122 (2025) 116509

Recent Advances in Samarium-Doped Ferrites for Supercapacitor Applications: A Concise Review

Kangude Sahadev Hanumant, Mhaske Mangal Kailas

Rayat Shikshan Sanstha's Dada Patil Mahavidyalaya Karjat, Dist- Ahilyanagar-414402

Email: sahadevkangude72832@gmail.com

Article DOI Link: https://zenodo.org/uploads/19792654

DOI: 10.5281/zenodo.19792654

Abstract

The increasing demand for efficient energy storage systems has stimulated extensive research on advanced electrode materials for supercapacitors. Among these materials, samarium (Sm^{3+})-doped ferrites have gained significant attention due to their improved structural, magnetic, and electrochemical properties. The incorporation of Sm^{3+} ions into the ferrite lattice enhances electrical conductivity, increases active redox sites, and improves charge storage capability. This chapter discusses the structure, properties, and synthesis methods of samarium-doped ferrites and highlights their potential applications as electrode materials in supercapacitors. Their enhanced electrochemical performance makes them promising candidates for next-generation energy storage technologies.

Keywords: Samarium-doped ferrites; Supercapacitors; Spinel structure; Energy storage; Electrode materials.

Introduction

The increasing global energy demand and the rapid integration of renewable energy sources such as solar and wind power have created a strong need for efficient energy storage technologies. Energy storage systems play a crucial role in balancing the gap between energy generation and consumption, ensuring stable and reliable power supply. Among various energy storage devices, supercapacitors have attracted considerable attention because of their high-power density, fast charge–discharge capability, and long cycling life compared with conventional batteries and capacitors (1,2). Supercapacitors store energy mainly through charge accumulation at the electrode–electrolyte interface or through fast surface redox reactions. Because of these mechanisms, they are widely used in applications such as portable electronic devices, electric vehicles, and renewable energy systems. The electrochemical performance of supercapacitors strongly depends on the nature and properties of the electrode materials. In recent years, transition-metal ferrites and rare-earth-doped ferrites have been extensively

investigated as potential electrode materials due to their good electrochemical activity, chemical stability, and relatively low cost (3). Ferrite materials possess a spinel crystal structure and high surface area, which facilitate efficient ion diffusion and charge transport during electrochemical reactions. These characteristics make ferrites promising candidates for high-performance energy storage applications. Furthermore, doping with rare-earth elements such as samarium (Sm^{3+}) can significantly modify the structural and electrochemical properties of ferrite materials. The incorporation of Sm^{3+} ions can alter the crystal lattice, enhance electrical conductivity, and increase the number of electrochemically active sites. As a result, samarium-doped ferrites show improved charge storage capability and enhanced electrochemical performance, making them attractive materials for supercapacitor electrodes (4,5).

Structure and Properties of Samarium-Doped Ferrites

- **Spinel Structure of Ferrite**

The spinel ferrite structure ($MeFe_2O_4$) consists of a cubic close-packed arrangement of oxygen atoms with metal cations occupying two types of interstitial sites: tetrahedral (A) and octahedral (B). In this structure, eight A-sites and sixteen B-sites are present per unit cell. Depending on the distribution of Me^{2+} and Fe^{3+} ions, spinels can be classified as normal, inverse, or mixed spinels. The antiparallel alignment of magnetic moments between A and B sites results in ferrimagnetic behaviour [6], shown in Fig. 1.

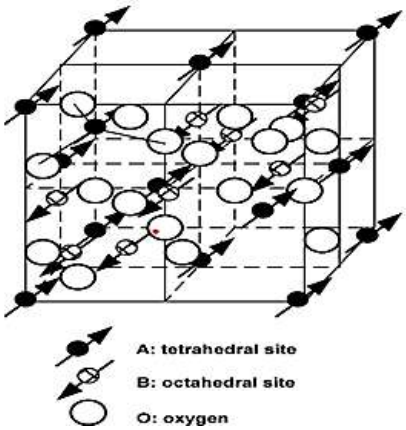

Figure 1. Spinel ferrite ($MeFe_2O_4$) crystal structure showing tetrahedral (A) and octahedral (B) cation sites in a cubic close-packed oxygen lattice, with metal ions occupying interstitial positions (adapted from Ref. [6]).

- **Samarium Substitution**

Samarium (Sm^{3+}) ion substitution in ferrite materials significantly influences their structural, magnetic, and electrochemical properties. Due to its larger ionic radius compared to Fe^{3+} ions, Sm^{3+} ions tend to occupy the octahedral (B) sites of the spinel lattice, leading to lattice distortion and

modification of cation distribution. This substitution can alter magnetic interactions and improve electrical conductivity and redox activity. As a result, Sm^{3+}-doped ferrites exhibit enhanced electrochemical performance, making them promising materials for supercapacitor electrode applications (7).

- **Structural Properties**

Sm^{3+} ion substitution in ferrites leads to lattice distortion due to its larger ionic radius compared to Fe^{3+} ions. This modification can influence the crystal structure, lattice parameters, and cation distribution within the spinel lattice (8).

- **Magnetic Properties**

The incorporation of Sm^{3+} ions affect the magnetic interactions between A and B sites, resulting in changes in saturation magnetization and magnetic anisotropy of the ferrite material (9).

- **Electrochemical Properties**

Sm^{3+} doping enhances electrical conductivity and redox activity, which improves the charge storage capability and electrochemical performance of ferrite electrodes in supercapacitor applications (10).

In samarium (Sm^{3+})-doped ferrites, particle size, electrical conductivity, and surface area significantly influence electrochemical performance. Sm^{3+} substitution can reduce particle size and create lattice distortions, which increase the surface area and the number of active sites. This enhanced surface area improves electrolyte accessibility and ion diffusion. Additionally, Sm^{3+} doping can improve electrical conductivity, facilitate efficient charge transport, and enhance the overall performance of ferrite-based supercapacitor electrodes (11).

Synthesis Methods of Sm-Doped Ferrites

- **Sol–Gel Method**

The sol–gel method is widely used for the synthesis of samarium-doped ferrites due to its simplicity and ability to produce highly homogeneous materials. In this method, metal precursors undergo hydrolysis and condensation reactions to form a gel, which upon calcination yields ferrite nanoparticles with controlled particle size and uniform composition. This technique also allows precise control over stoichiometry and structural properties (12).

- **Co-precipitation Method**

The co-precipitation method is one of the most common techniques for preparing ferrite nanoparticles because of its low cost and simple processing. In this method, metal salts are precipitated simultaneously in an alkaline medium to form hydroxide precursors, which are then converted into ferrite nanoparticles

after drying and calcination. The method provides good control over particle size and composition (13).

- **Hydrothermal Method**

The hydrothermal method involves chemical reactions of metal precursors in a sealed autoclave at high temperature and pressure. This technique promotes the formation of highly crystalline ferrite nanoparticles with controlled morphology and improved structural properties. It is widely used for synthesizing doped ferrites with enhanced electrochemical and magnetic performance (14).

- **Combustion Method**

The combustion synthesis method is a rapid and energy-efficient technique for producing ferrite nanoparticles. In this process, metal nitrates react with a suitable fuel such as urea or glycine, resulting in a self-sustaining exothermic reaction that produces ferrite powders. This method is advantageous for obtaining fine particles with high purity and good crystallinity (15).

4. Supercapacitor Applications of Sm-Doped Ferrites (Rewritten)

Samarium-doped ferrites have emerged as promising electrode materials for supercapacitor applications because of their improved electrochemical characteristics. The incorporation of Sm^{3+} ions into the ferrite lattice can enhance electrical conductivity and increase the availability of active redox sites, which contribute to improved charge storage performance. These materials often exhibit good cyclic stability, high specific capacitance, and efficient charge–discharge behavior during electrochemical cycling (16). In supercapacitor systems, Sm-doped ferrites mainly store energy through pseudocapacitive mechanisms involving fast and reversible redox reactions at the electrode surface. The nanoscale structure and relatively large surface area of these materials facilitate rapid ion transport and effective electrolyte interaction. Consequently, samarium-doped ferrite nanomaterials are considered promising candidates for advanced energy storage devices and next-generation high-performance supercapacitor technologies (17).

Conclusion

Samarium-doped ferrites exhibit improved structural stability, enhanced electrical conductivity, and increased electrochemical activity, making them attractive materials for energy storage applications. These properties make them promising electrode materials for high-performance supercapacitors with good capacitance and cycling stability. Future research should focus on the development of nanocomposites, optimization of synthesis parameters, and scalable fabrication methods to enhance their practical applicability in advanced energy storage devices.

References

1. Czagany, M., et al. (2024). Supercapacitors for energy storage. Materials, 17, 702.
2. Wang, Y., Song, Y., & Xia, Y. (2016). Electrochemical capacitors. Chem. Soc. Rev., 45, 5925–5950.
3. Simon, P., & Gogotsi, Y. (2020). Electrochemical capacitor perspectives. Nat. Mater., 19, 1151–1163.
4. Conway, B. E. (1999). Electrochemical Supercapacitors: Scientific Fundamentals and Technological Applications. New York: Kluwer Academic/Plenum Publishers.
5. Goldman, A. (2006). Modern Ferrite Technology (2nd ed.). New York, NY: Springer.
6. Mathew, D. S., & Juang, R. S. (2007). Spinel ferrite nanoparticles. Chem. Eng. J., 129, 51–65.
7. Siddiqui, M. A., et al. (2024). Sm-doped spinel ferrites. Ceram. Int.
8. Cullity, B. D., & Graham, C. D. (2011). Introduction to Magnetic Materials. Wiley.
9. Smit, J., & Wijn, H. (1959). Ferrites. Philips Technical Library.
10. Wang, Y., Song, Y., & Xia, Y. (2016). Electrochemical capacitors. Chem. Soc. Rev., 45, 5925–5950.
11. Sahu, A., et al. (2024). Sm^{3+} doped ferrite for supercapacitors. Mater. Chem. Phys.
12. Liu, C., et al. (2000). Spinel ferrite nanoparticles. J. Am. Chem. Soc., 122, 6263–6267.
13. Massart, R. (1981). Magnetic liquids preparation. IEEE Trans. Magn., 17, 1247–1248. Byrappa, K., & Adschiri, T. (2007). Hydrothermal nanotechnology. Prog. Cryst. Growth Charact. Mater., 53, 117–166.
14. Patil, K. C., et al. (2002). Combustion synthesis. Curr. Opin. Solid State Mater. Sci., 6, 507–512. https://doi.org/10.1016/S1359-0286(02)00123-7
15. Simon, P., & Gogotsi, Y. (2008). Electrochemical capacitor materials. Nat. Mater., 7, 845–854.
16. Wang, Y., Song, Y., & Xia, Y. (2016). Electrochemical capacitors. Chem. Soc. Rev., 45, 5925–5950.

NiMn Layered Double Hydroxide Based Nanocomposites for Supercapacitor: Hydrothermal Approach and Electrochemical Performance

[1]Amol R. Pardeshi, [2]Vishnu S. Shinde

[1]Department of Physics, Dada Patil Mahavidyalaya, Karjat, Dist: Ahilyanagar, 414402

[2]Department of Physics, YC college Karmala, Dist: Solapur 413 203

Email: amolrp111@gmail.com

Article DOI Link: https://zenodo.org/uploads/19792910

DOI: 10.5281/zenodo.19792910

Abstract

The depletion of fossil fuels and growing environmental concerns have driven interest in sustainable energy storage, with supercapacitors gaining attention for their high power, fast charging, long life, and safety. This chapter presents a NiMn layered double hydroxide (LDH) nanocomposite electrode synthesized via a hydrothermal method. A core–shell structure was formed by growing Co_3O_4 on nickel foam followed by NiMn-LDH nanosheets, enhancing redox activity, ion transport, and charge transfer. Electrochemical studies in an alkaline electrolyte show excellent capacitive performance, rate capability, and cycling stability. Overall, the results demonstrate that hydrothermally synthesized NiMn LDH nanocomposites are promising for high-performance supercapacitor electrodes.

Introduction

The depletion of fossil fuels and environmental issues such as global warming have increased the need for renewable and sustainable energy storage systems, including fuel cells, batteries, and supercapacitors. Among these technologies, supercapacitors are widely studied because of their high-power density, good energy density, rapid charge–discharge capability, long cycle life, and operational safety. Electrochemical supercapacitors are generally categorized into three types based on their charge storage mechanism: (i) electric double-layer capacitors (EDLCs), (ii) pseudocapacitors, and (iii) hybrid supercapacitors. EDLCs store charge at the electrode–electrolyte interface, pseudocapacitors involve reversible Faradaic redox reactions, while hybrid supercapacitors combine both storage mechanisms. [1-3].

Material is designed for electrode require electrochemical properties, among which the metal Layered double hydroxide exhibits the superior owing the high capacitance, high conductivity due to composite and large surface [4]. The LDH

contain Ni, Mn are most of promising material for supercapacitor due to their excellent specific capacitance, long cyclic life, inexpensive and easy to synthesis. Electrochemical studies of LDHs improved if they combined with carbon/conducting polymers & other materials to form composite [5-6]. This chapter studies the hydrothermal synthesis of NiMn LDH based nanocomposite and electrochemical studies for supercapacitor.

Hydrothermal Approach to Synthesis NiMn LDH based Nanocomposites electrode

- **Material Required for Composite**

Manganese Nitrate Hexahydrate $Mn(NO_3)_2.6H_2O$ Cobalt Nitrate Hexahydrate $Co(NO_3)_2.6H_2O$ Urea / Hexamethylenetetramine (HMT), Nickel Nitrate Hexahydrate $Ni(NO_3)_2.6H_2O$ and NH_4F, Nickel foam, distilled water, all regents were analytical grade and used without purification. All aqueous solutions were prepared with distilled water [7-8]

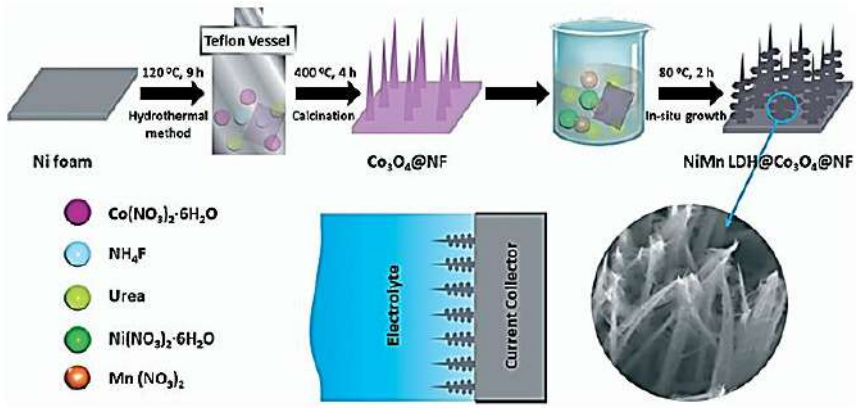

Fig. 1: Hydrothermally synthesis of NiMn LDH@Co3O4@NF (Nickel Foam) [7].

Pretreatment Nickel Foam: the nickel foam (used as electrode) of 2 cm ×4cm ×0.1 cm. It was cleaned with distilled water, acetone, absolute ethanol in ultrasonicate bath for 15 min to remove the surface oxide layer, after washing Nickel foam dried at 60^o for 12 hrs [7- 9]

- **Composite Preparation**

i. **Synthesis Co_3O_4 Nanoneedle @ NF:** The Co_3O_4@Ni foam Cleaned nickel foam was immersed in an aqueous solution containing Co $(NO_3)_2 \cdot 6H_2O$ (2 mmol), NH_4F (8.1 mmol), urea (20 mmol), and 50 mL deionized water under stirring. The mixture with the foam was sealed in a Teflon-lined autoclave and heated at 120 °C for 9 h. After natural cooling, the sample was washed with water and ethanol and dried at 60 °C

overnight. The dried material was then calcined in air at 400 °C for 4 h, producing crystalline Co_3O_4 nanoneedles on the nickel foam surface.

ii. **Synthesis of Core-shell NiMn LDH/Co_3O_4@NF:** n a typical procedure, nickel nitrate hexahydrate, manganese nitrate solution, and 6.6 mmol of urea were added one by one into 60 mL of distilled water. The mixture stirred strongly until a clear and uniform solution obtained. After that, the previously prepared Co_3O_4-coated nickel foam (Co_3O_4@NF) was placed into this solution. The beaker containing the mixture was kept in a water bath at 80 °C for 2.5 hours with continuous stirring. When the reaction was completed, the beaker was removed from the water bath and allowed to cool naturally to room temperature. The final core–shell product was washed several times with deionized water to remove any remaining impurities and then dried at 60 °C overnight. During the preparation, the total amount of Ni^{2+} and Mn^{2+} ions was fixed at 2 mmol. To study the effect of composition, three different molar ratios of Ni^{2+} to Mn^{2+} were used: 3:1 (Ni_3Mn_1), 1:1 (Ni_1Mn_1), and 1:3 (Ni_1Mn_3), also represented in fig, 1 [7].

There is one of the examples of preparing NiMn LDH based nanocomposite for supercapacitor via. Hydrothermal method.

Electrochemical Studies

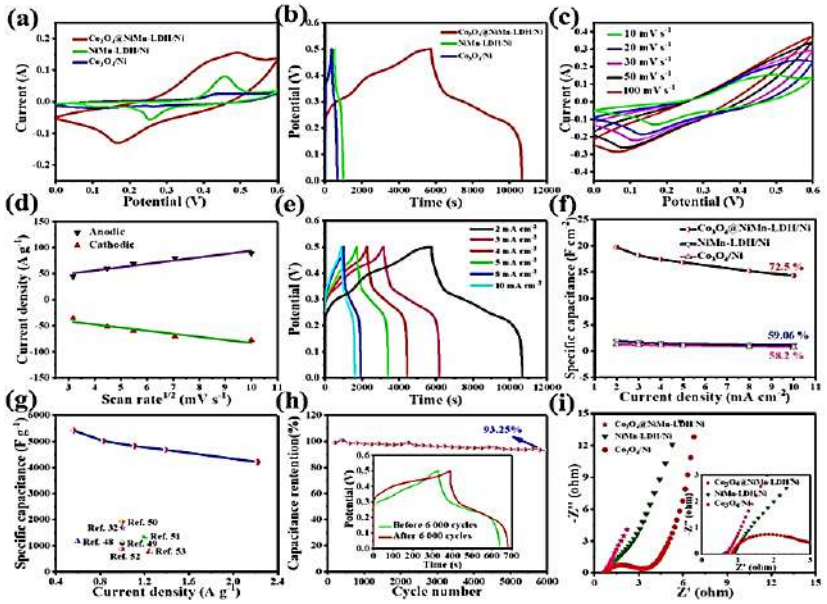

Fig. 2: Electrochemical performance of the Co_3O_4–NiMn LDH/Ni electrode in a three-electrode system, including CV, GCD, scan-rate and current-density dependent studies, specific capacitance comparison, and cyclic stability with EIS analysis (Ref. [4]).

Specific capacitance of the electrode calculated by $\boldsymbol{C_s = \frac{I \int V dt}{sV^2}}$, where I represent the discharge current, dt represented discharge time, V represent the potential window and s represent effective area of electrode, charge stored of electrode represented by $\mathbf{q = C \times m \times v}$, m represent mass of active material also energy & power density calculated by $\boldsymbol{E = \frac{1}{2} CV^2}$ and $\boldsymbol{P = \frac{E}{dt}}$.

Electrochemical performance for this composite material is excellent which exhibit specific capacitance upto 5419.7 F/g at 0.56 A/g current density with outstanding cyclic stability upto 93.25 % capacitance maintained after 6000 cycles, also energy density and power density exhibits a upto 47.15 Wh/kg and 376 W/kg [4].

Comparative Studies of NiMn LDH based Nanocomposites.

Composite	**Specific capacitance**	**Energy density**	**Power density**	**Retention per cycle**	**Electrolyte solution in KOH**	**Ref.**
Cu_2S@NiMn-LDH@Co_4S^3	14.78 F/cm^2	2.32 mWh/cm^2	9 mW/cm^2	76.22% after 10000	2 M	02
NiMn-LDH@$MnCo_2S_4$@NF	1228 C/g	-	-	95% after 10000	3 M	03
Co_3O_4@NiMn-LDH/Ni	5419 F/g	47.15 Wh/kg	376 W/kg	93.25% after 6000	6 M	04
$MgCo_2O_4$@NiMn LDH	3757.2 F/g	62.33 Wh/kg	750 W/kg	93.7 % after 6000	6 M	05
NiMn LDH@Co_3O_4	607.9 F/g	26.49 Wh/kg	350 W/kg	97 % after 1000	6 M	07
NiMn LDH/rGO	1635 F/g	33.8 Wh/kg	0.85 kW/kg	74.1 % after 2000 cycle	2 M	08
NiMn LDH@NF	1916 F/g	33.7 Wh/kg	378.13 W/kg	91 % after 5000	1 M	09
NiMn-LDH/MXene	1575 F/g	126 Wh/kg	0.74 kW/kg	90.3 % after 10000	6 M	10
NiMn LDH	2128.3 F/g	-	-	94.3 %	1 M	11

				after 5000		
NiMn LDH	682 mAh/g	49 Wh/kg	815 W/kg	102 % after 10000	1 M	12
CeO_2/NiMn LDH	1956 F/g	51.8 Wh/kg	809 W/kg	91.9% after 5000	1 M	13

Conclusion

In this chapter, a NiMn layered double hydroxide–based nanocomposite electrode was successfully synthesized through a hydrothermal strategy and engineered into a hierarchical core–shell architecture on nickel foam. The integration of NiMn LDH with a conductive oxide backbone provides enhanced redox activity, improved charge transport, and efficient electrolyte accessibility. As a result, the composite exhibits excellent capacitive performance, good rate capability, and stable long cycling behavior. The study demonstrates that rational structural design and compositional tuning of LDH-based material offer an effective pathway for developing advanced and durable supercapacitor electrodes.

References

1. Yanqun Tang et. al. Adv. Funct. Mater. 2020, 1908223
2. Xiaocheng Liu et. al. ACSAppl.EnergyMater.2025,8,10071−10081
3. Muhammad Arslan Raza et. al. EnergyFuels2023,37,1310−1317
4. Weiguo Huang et. al. JournalofPowerSources440(2019)227123
5. ZhiqiangLiu et. al. Journal of Colloid and Interface Science 592 (2021) 455–467
6. Ai-Lan Yan et. al. Nanomaterials 2018, 8, 747; doi:10.3390/nano8100747
7. Huihua Peng et al. CrystEngComm,2019,21, 470
8. M. Li et. al. Electrochimica Acta 206 (2016) 108–115
9. Hongyan Chen et. al. j. electacta 2016 06 038
10. Dongdong Zhang et. al. ACS Appl. Energy Mater 202
11. Daming Chen et. al. Electrochimica Acta 292 (2018) 374e382
12. Yan Cheng et. al. ElectrochimicaActa429(2022)141039
13. Xiaoliang Wang et. al. Journal of Alloys and Compounds 810 (2019) 151911.

Synthesis and Electrochemical Characterization of $ZnFe_2O_4$ Nanostructures for Supercapacitor Applications

Pooja U. Kashid, Sampada D. Karpe

Department of Physics, Dada Patil Mahavidyalaya, Karjat, Dist: Ahilyanagar 414 402.

Email: kashidpooja78@gmail.com

Article DOI Link: https://zenodo.org/uploads/19793106

DOI: 10.5281/zenodo.19793106

Abstract

Transition metal oxides have attracted considerable attention for electrochemical energy storage devices because of their high theoretical capacitance and excellent redox activity. Among various metal oxides, zinc ferrite ($ZnFe_2O_4$) has emerged as a promising electrode material for supercapacitor applications due to its unique spinel crystal structure, good chemical stability, and environmental friendliness [1,2]. Nanostructured $ZnFe_2O_4$ materials provide a large surface area and shorter ion diffusion pathways, which significantly enhance electrochemical performance [3]. In this study, $ZnFe_2O_4$ nanostructures are synthesized using a hydrothermal method followed by thermal annealing. The synthesized material is characterized using structural and electrochemical techniques. Electrochemical properties are investigated using cyclic voltammetry, galvanostatic charge–discharge, and electrochemical impedance spectroscopy. The results indicate that $ZnFe_2O_4$ nanostructures exhibit promising capacitive behavior and good cycling stability, making them potential candidates for next-generation supercapacitors.

Keywords: $ZnFe_2O_4$, nanostructures, supercapacitor, electrochemical characterization, energy storage

Introduction

The increasing demand for efficient energy storage systems has stimulated extensive research on advanced electrode materials for electrochemical devices. Supercapacitors have attracted significant attention because they offer high power density, rapid charge–discharge capability, and long cycle life compared to conventional batteries [4].

Supercapacitors are generally classified into two categories: electrical double layer capacitors (EDLCs) and pseudocapacitors. EDLCs store energy through electrostatic charge accumulation at the electrode–electrolyte interface, while pseudocapacitors store energy through fast and reversible Faradaic redox reactions occurring on the surface of electrode materials [5].

Transition metal oxides such as MnO_2, NiO, Co_3O_4, and $ZnFe_2O_4$ have been widely investigated as electrode materials for pseudocapacitors due to their high theoretical capacitance and excellent electrochemical activity [6]. Among these materials, $ZnFe_2O_4$ has gained significant attention because of its spinel crystal structure, good electrical conductivity, and chemical stability [7].

The spinel structure of $ZnFe_2O_4$ allows the presence of multiple oxidation states of iron ions, which facilitates reversible redox reactions during electrochemical processes [8]. Moreover, the nanoscale morphology of $ZnFe_2O_4$ provides a large active surface area and shorter ion diffusion pathways, resulting in improved electrochemical performance [9]. Therefore, the synthesis of $ZnFe_2O_4$ nanostructures and investigation of their electrochemical behavior are important for developing high-performance supercapacitor materials.

Synthesis of $ZnFe_2O_4$ Nanostructures

Several synthesis techniques have been reported for the preparation of $ZnFe_2O_4$ nanostructures, including sol–gel synthesis, hydrothermal synthesis, co-precipitation, and microwave-assisted methods [10].

Among these methods, the hydrothermal synthesis technique is widely used because it enables controlled growth of nanostructured materials with uniform particle size and morphology [11]. In a typical hydrothermal synthesis process, zinc nitrate ($Zn(NO_3)_2$) and ferric nitrate ($Fe(NO_3)_3$) are used as precursor materials. These metal salts are dissolved in distilled water under continuous stirring to obtain a homogeneous solution. A precipitating agent such as sodium hydroxide or ammonia solution is gradually added to the solution to adjust the pH value [12]. The prepared solution is transferred into a Teflon-lined stainless-steel autoclave and heated at temperatures between 160–200 °C for several hours. During the hydrothermal reaction, nucleation and crystal growth of $ZnFe_2O_4$ nanoparticles occur under controlled temperature and pressure conditions [13]. After completion of the reaction, the obtained precipitate is washed several times with distilled water and ethanol to remove residual impurities. The product is then dried and calcined at elevated temperature to improve crystallinity and phase purity [14].

Electrochemical Characterization

Electrochemical characterization techniques are used to evaluate the performance of $ZnFe_2O_4$ electrode materials for supercapacitor applications.

- **Cyclic Voltammetry (CV)**

Cyclic voltammetry is one of the most widely used electrochemical techniques to study the redox behavior of electrode materials. In this technique, the potential of the working electrode is scanned at a constant rate and the resulting current response is recorded [15]. The CV curves of $ZnFe_2O_4$ electrodes generally exhibit

distinct redox peaks corresponding to reversible Faradaic reactions involving iron ions. These redox reactions contribute to the pseudocapacitive behavior of the material [16].

- **Galvanostatic Charge–Discharge (GCD)**

Galvanostatic charge–discharge measurements are performed to evaluate the specific capacitance and energy storage capability of electrode materials. In this method, the electrode is charged and discharged at a constant current and the voltage variation with time is recorded [17]. The triangular shape of the charge–discharge curves indicate good capacitive behavior and high reversibility of electrochemical reactions.

- **Electrochemical Impedance Spectroscopy (EIS)**

Electrochemical impedance spectroscopy provides information about the charge transfer resistance and ion diffusion processes in electrode materials. The Nyquist plot obtained from EIS measurements consists of a semicircle at high frequency and a straight line at low frequency [18]. A small semicircle diameter indicates low internal resistance and good electrical conductivity of the electrode material.

Results and Discussion

The structural properties of $ZnFe_2O_4$ nanostructures are typically analyzed using X-ray diffraction (XRD). The XRD pattern confirms the formation of a cubic spinel structure corresponding to $ZnFe_2O_4$, which is consistent with previously reported studies [19].

Morphological analysis using scanning electron microscopy (SEM) and transmission electron microscopy (TEM) reveals that the synthesized $ZnFe_2O_4$ nanoparticles possess uniform distribution and nanoscale dimensions. The nanosized particles provide large surface area for electrochemical reactions and facilitate efficient ion transport during charge–discharge processes [20].

Electrochemical measurements demonstrate that $ZnFe_2O_4$ nanostructures exhibit good capacitive behavior with stable cycling performance.

Table 1: Reported electrochemical performance of $ZnFe_2O_4$ nanostructures

Material	Synthesis Method	Specific Capacitance	Ref.
$ZnFe_2O_4$ nanoparticles	Hydrothermal	310 F/g	[9]
$ZnFe_2O_4$ nanospheres	Sol–gel	280 F/g	[10]
$ZnFe_2O_4$/graphene composite	Hydrothermal	420 F/g	[11]

Conclusion

$ZnFe_2O_4$ nanostructures have attracted significant attention as promising electrode materials for supercapacitor applications due to their unique spinel structure, high redox activity, and good chemical stability. The hydrothermal

synthesis method provides an effective approach for preparing $ZnFe_2O_4$ nanostructures with controlled morphology and high surface area. Electrochemical characterization techniques such as cyclic voltammetry, galvanostatic charge–discharge, and impedance spectroscopy demonstrate that $ZnFe_2O_4$ nanostructures exhibit good capacitive performance and excellent cycling stability. Therefore, $ZnFe_2O_4$ nanostructures are considered potential candidates for future high-performance energy storage devices.

References

1. P. Simon, Y. Gogotsi, Nature Materials, 7 (2008) 845–854. https://doi.org/10.1038/nmat2297
2. B. E. Conway, Journal of The Electrochemical Society, 138 (1991) 1539–1548. https://doi.org/10.1149/1.2085829
3. J. R. Miller, P. Simon, Science, 321 (2008) 651–652. https://doi.org/10.1126/science.1158736
4. H. Wang, H. S. Casalongue, Y. Liang, H. Dai, Journal of the American Chemical Society, 132 (2010) 7472–7477. https://doi.org/10.1021/ja102267j
5. Y. Wang, Y. Song, Y. Xia, Chemical Society Reviews, 45 (2016) 5925–5950. https://doi.org/10.1039/C5CS00580A
6. X. Liu, J. Wang, G. Zhang, Journal of Power Sources, 273 (2015) 105–111. https://doi.org/10.1016/j.jpowsour.2014.09.099
7. L. Yu, B. Guan, X. Lou, Nano Energy, 11 (2015) 138–145. https://doi.org/10.1016/j.nanoen.2014.10.012
8. Y. Zhang, X. Li, H. Wang, Materials Letters, 65 (2011) 2523–2526. https://doi.org/10.1016/j.matlet.2011.05.053
9. H. Chen, Y. Liu, J. Zhang, Electrochimica Acta, 190 (2016) 105–112. https://doi.org/10.1016/j.electacta.2015.12.123
10. B. Zhao, P. Liu, J. Jiang, Journal of Electroanalytical Chemistry, 688 (2013) 1–10. https://doi.org/10.1016/j.jelechem.2012.10.010
11. S. Kumar, R. Kumar, Materials Research Bulletin, 48 (2013) 251–257. https://doi.org/10.1016/j.materresbull.2012.10.024
12. X. Li, Y. Wang, Journal of Materials Chemistry A, 2 (2014) 1174–1182.https://doi.org/10.1039/C3TA13961C
13. Mo, X., Wang, Y., Liu, Z. et al., Nanomaterials, 13 (2023) 1034. https://doi.org/10.3390/nano13061034
14. Askari, M.B., Salarizadeh, P., Seifi, M. et al., Journal of Alloys and Compounds, 860 (2021) 158497. https://doi.org/10.1016/j.jallcom.2020.158497
15. Reddy, A.E. et al., New Journal of Chemistry, 42 (2018) 3910–3918. https://doi.org/10.1039/C7NJ04269H.

NiFe LDH Based Nanocomposite for Supercapacitor: Material, Methods & Electrochemical Performance

Amol R. Pardeshi, Renuka Sonmali

Department of Physics, Dada Patil Mahavidyalaya, Karjat, Dist: Ahilyanagar 414 402

Email: amolrp111@gmail.com

Article DOI Link: https://zenodo.org/uploads/19793239

DOI: 10.5281/zenodo.19793239

Abstract

Layered double hydroxide-based nanomaterials is promising electrode material for advanced supercapacitor systems due to their modifiable structure, rich redox activity, and high surface reactivity. This chapter discusses the synthesis of NiFe-LDH based nanocomposites via a hydrothermal approach and their structural, morphological, and electrochemical characteristics. Advanced characterization techniques confirm the formation of ultrathin nanosheet architectures with porous frameworks that promote efficient ion transport and enhanced electroactive surface sites. Electrochemical investigations reveal pronounced pseudocapacitive behaviour with improved charge storage capability and favourable electron transfer kinetics. The study shows the potential of NiFe-LDH based nanostructures as efficient materials for high-performance energy storage applications.

Keywords: NiFe LDH, Supercapacitor, Nanocomposites, Hydrothermal Method.

Introduction

The growing use of fossil fuels has intensified environmental problems such as global warming, increasing the need for advanced energy storage technologies. Several energy conversion and storage systems, including lithium-ion batteries, fuel cells, solar cells, and supercapacitors, are widely investigated. Among them, supercapacitors are attractive because they provide higher power density than batteries and greater energy density than conventional dielectric capacitors. Based on their charge storage mechanism, supercapacitors are classified into three types: (i) electric double-layer capacitors (EDLCs), (ii) pseudocapacitors that operate through redox reactions, and (iii) hybrid supercapacitors combining both mechanisms. EDLCs store charge at the electrode–electrolyte interface using porous carbon electrodes, while pseudocapacitors store energy through reversible redox reactions at the electrode surface, resulting in higher capacitance and energy density. Various techniques such as hydrothermal synthesis, chemical

vapor deposition, and physical vapor deposition are commonly used to prepare nanostructured electrode materials. [1-4].

NiFe LDH based nanocomposite material are promising electrode material of performing electrochemical studies for energy storage devices due to higher conductivity which allows the fast and reversible faradaic reaction also having high attention due to ion-exchange ability, higher surface area [5-10]. This chapter reveals the NiAl LDH based nanocomposite preparation technique and material required to prepare NiAl LDH also reveals the electrochemical behavior of NiAl LDH based nanocomposite materials.

Material & Method

Synthesis material required for prepare NiAl LDH is given: Ferric Nitrate Nonahydrate, Nickel Nitrate Hexahydrate, Urea/Hexamine, Ammonium Fluoride, distilled water.

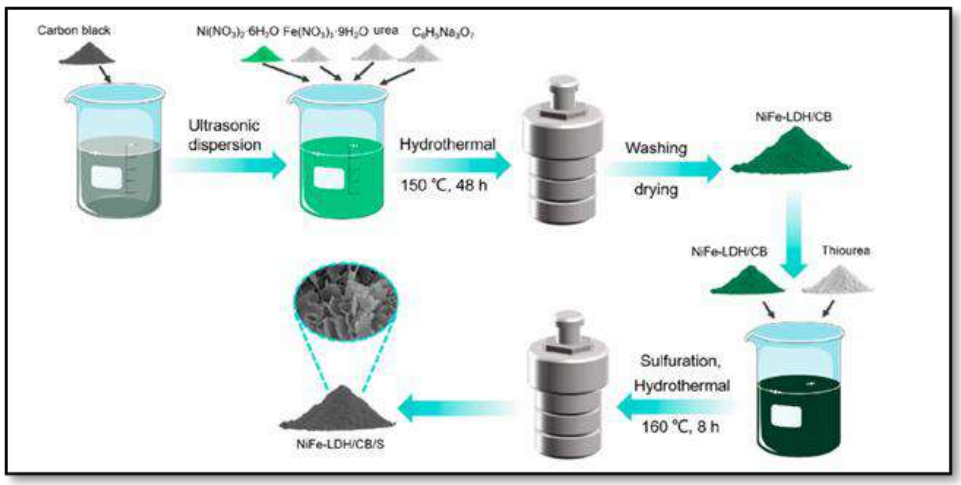

Fig. 1: Hydrothermal method to prepare NiAl LDH based Nanocomposite [1]

For the synthesis of the NiAl-LDH/CB composite fig, 1., 4 mg of carbon black was first dispersed in 80 mL of deionized water by sonication for 30 min. Afterward, $Ni(NO_3)_2 \cdot 6H_2O$ (1.6 mmol), $Fe(NO_3)_3 \cdot 9H_2O$ (0.67 mmol), $C_6H_5Na_3O_7$ (0.023 mmol), and urea (3.6 mmol) were added with continuous stirring. The mixture was then sealed in a Teflon-lined autoclave and heated at 150 °C for 48 h. The product was washed with ethanol and deionized water and dried under vacuum at 60 °C. For comparison, NiFe-LDH was prepared using the same procedure but without carbon black [1]. In such manner, prepare different nanocomposite for supercapacitor application [2-10].

Structural, Morphological and Function Group Studies of Nanocomposite

In Fig. 2. Show the surface study of NiFe-LDH, NiFe-LDHS-1, NiFe-LDHS-2, and NiFe-LDHS-3 was examined using SEM, revealing the significant influence

of sulfidation reagents on structural evolution. Pristine NiFe-LDH exhibits vertically aligned nanosheets uniformly grown on the Ni foam substrate, forming a nanowall architecture with an average wall thickness of approximately 10 nm.

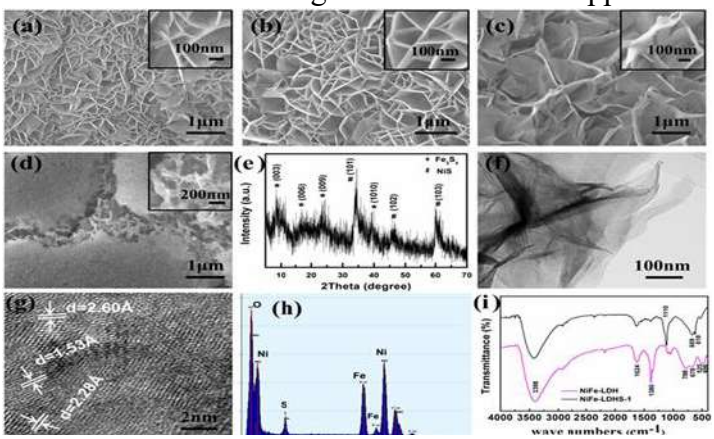

Fig. 2: (a) pristine NiFe-LDH, (b) NiFe-LDHS-1, (c) NiFe-LDHS-2, and (d) NiFe-LDHS-3. (e) XRD pattern of NiFe-LDHS-1. (f–g) TEM and HRTEM images of NiFe-LDHS-1. (h) EDS analysis of NiFe-LDHS-1. (i) FTIR spectra of NiFe-LDH and NiFe-LDHS-1 [4].

After sulfidation, NiFe-LDHS-1 largely retains this nanosheet arrangement without noticeable structural degradation. In contrast, NiFe-LDHS-2 displays weakened nanosheet rigidity, resulting in partially collapsed walls. For NiFe-LDHS-3, the morphology transforms into a sponge-like framework containing visible cracks, while higher-magnification observations indicate the presence of an interconnected porous network. XRD analysis of NiFe-LDHS-1 confirms the coexistence of crystalline NiS and Fe_3S_4 phases. TEM imaging reveals ultrathin and highly transparent nanosheets, consistent with the nanoscale layered morphology. HRTEM lattice analysis shows interplanar spacings of 2.28 Å, 2.60 Å, and 1.53 Å, which correspond to the (1010) plane of Fe_3S_4 and the (101) and (103) planes of NiS, respectively, supporting the XRD results. Elemental analysis by EDS identifies Ni, Fe, and S as the dominant elements, along with a substantial oxygen signal, likely originating from residual amorphous oxide species that were not completely converted during sulfidation. The approximate elemental molar ratio of Ni:Fe:S:O is estimated to be 2.9:2:1:20.7, indicating partial transformation of the NiFe-LDH precursor. FTIR spectroscopy was further employed to probe the chemical structure before and after sulfidation. For NiFe-LDH, a broad absorption band around 3428 cm^{-1} is attributed to O-H stretching vibration from hydroxyl group & interlayer water molecules [4].

Electrochemical Performance

Electrochemical behavior of electrodes was evaluated via. cyclic voltammetry (CV), galvanostatic charge-discharge (GCD), and electrochemical impedance spectroscopy (EIS), as presented in Fig. 3. The CV profiles (Fig. 3a) compare

NiFe-LDH, Ni $(OH)_2$, and bare Ni foam electrodes, The negligible current response of Ni foam confirms its minimal contribution to the overall capacitance. The Ni $(OH)_2$ electrode exhibits a distinct redox couple around 0.3 V, corresponding to the reversible Ni^{2+}/Ni^{3+} transition associated with the Ni $(OH)_2$/NiOOH conversion.

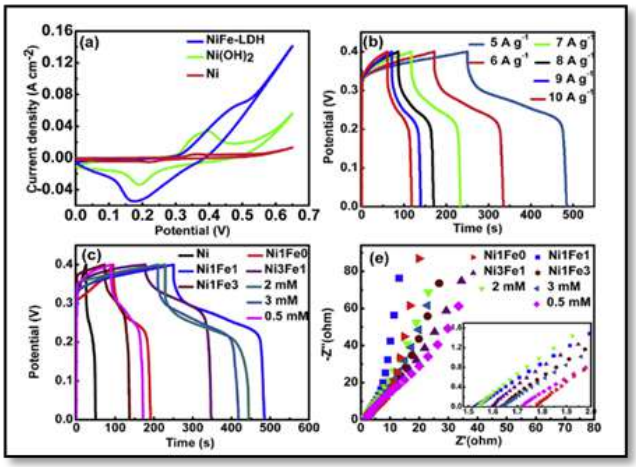

Fig. 3: (a) CV comparison of Ni_1Fe_1-LDH, Ni $(OH)_2$, and Ni foam at 5 mV s^{-1}. (b) GCD profiles of Ni_1Fe_1-LDH at various current densities. (c) Galvanostatic charge–discharge behavior [7].

A similar redox feature is observed for the NiFe-LDH electrode; however, the significantly higher current density and larger enclosed CV area indicate enhanced electrochemical activity and superior charge storage capability. This improvement can be attributed to Fe incorporation within the $Ni(OH)_2$ lattice and the presence of ultrathin LDH nanosheets, which provide electroactive sites and facilitate fast ion diffusion. The GCD profiles recorded at current densities ranging from 5 to 10 A g^{-1} (Fig. 3b) exhibit pronounced charge–discharge plateaus, characteristic of Faradaic pseudocapacitive behavior. The Ni_1Fe_1-LDH electrode delivers high specific capacitances of 2708, 2149, 1874, 1694, 1566, and 1456 F g^{-1} at 5, 6, 7, 8, 9, and 10 A g^{-1}, respectively, while maintaining a high coulombic efficiency of ~95.8% at 5 A g^{-1}, confirming efficient and reversible charge storage. The influence of metal ion concentration and Ni/Fe molar ratio on electrochemical performance is shown in Fig. 3c. Increasing Fe incorporation initially enhances the capacitance due to synergistic redox activity; however, excessive Fe content (Ni:Fe = 1:3) leads to performance deterioration. Similarly, increasing the precursor concentration from 0.5 to 1 mmol significantly improves the capacitance, reaching a maximum of ~2708 F g^{-1}, whereas further increases to 2 and 3 mmol slightly reduce the capacitance, likely due to structural thickening that limits electrolyte accessibility. EIS analysis (Fig. 3e) provides further insight into the charge transfer & ion diffusion

characteristics. Absence of a pronounced semicircle in the high-frequency region suggests minimum charge-transfer resistance & efficient interfacial electron transport [7].

Table 1: Comparative study of NiAl LDH based nanocomposite

Electrode Material	***Specific Capacitance (F/g)***	***Energy Density (Wh/kg)***	***Power Density(W/kg)***	***Ref.***
NiFe – LDH/CB/S	1397.9	38.22	799.95	**01**
NiFe LDH/rGO	1224	-	-	**03**
NiFe -LDH	992 mF/cm^2	39.9 mWh/cm^2	211.4 350 mW/cm^2	**04**
NiFe LDH/rGO/CNFs	1330.2	33.7	785.8	**05**
NiFe LDH on NF	2708	52	800	**07**
MnO_2@NF/NiFe LDH	4274.4 mF/cm^2	24.6 mWh/cm^2	350 mW/cm^2	**08**
NiFe LDHs/rGO/NF	1462.5	17.71	348.49	**09**

Conclusion

NiFe-LDH based nanocomposites were successfully synthesized and systematically examined for supercapacitor applications. Structural and morphological analyses confirm the formation of layered nanosheet architectures with porous features that facilitate rapid ion diffusion and effective electrochemical reactions. Electrochemical studies demonstrate enhanced pseudocapacitive behaviour arising from synergistic redox interactions within the layered framework. Overall, the results emphasize the significant potential of NiFe-LDH nanostructured materials as promising electrode systems for energy storage technologies.

References

1. Cheng Chen et. al. Energy Fuels 2023, 37, 12416 – 12426
2. Fang Zheng et. al. Energy Fuels 2024, 38, 6290-6299
3. Sadegh Azizi et. al. Physica B 600 (2021) 412606
4. Ting Xiao et. al. Journal of Alloys and Compounds 2018 32780-4
5. Feifei Wang et. al. https://doi.org/10.1038/s41598-018-27171-0.
6. Linli Chen et. al. ACS Appl. Mater. Interfaces 2024, 16, 8751 -8762
7. Yi Lu et. al. Journal of Alloys and Compounds 714 (2017) 63e70
8. Min Li et. al. Journal of Energy Storage 11 (2017) 242–248
9. Min Li et. al. Electrochimica Acta 2019 30221 – x
10. Jun Chi et. al. ACS Appl. Mater. Interfaces.

Synthesis Strategies of Ternary Layered Double Hydroxides (LDHs) Nanocomposites for High-Performance Supercapacitors

[1]Amol R. Pardeshi, [2]Rutuja Bhosale

[1]Department of Physics, Dada Patil Mahavidyalaya, Karjat, Dist: Ahilyanagar 414 402.

[2]Department of Physics, SM Joshi College, Hadapsar 411 028.

Email: amolrp111@gmail.com

Article DOI Link: https://zenodo.org/uploads/19793419

DOI: 10.5281/zenodo.19793419

Abstract

Rising global energy demands and the search for sustainable storage solutions have encouraged the exploration of high - performance electrode materials for supercapacitor applications. Ternary layered double hydroxides (LDHs) have gained considerable interest owing to their adaptable chemical composition, rich redox-active centers, and superior electrochemical properties. This chapter presents an overview of different synthesis strategies for ternary LDH-based nanocomposites, including hydrothermal, solvothermal, co-precipitation, ion-exchange, and electrodeposition approaches. Various ternary systems such as NiCoCu-LDH, ZnNiCo-LDH, NiCoFe-LDH, NiCoZn-LDH, and NiCoCr-LDH integrated with conductive supports or functional nanostructures are discussed. The incorporation of multiple transition metal ions and conductive matrices improves electrical conductivity, structural stability, and charge transfer kinetics, thereby enhancing the electrochemical performance. A comparative study of energy density, power density, and specific capacitance demonstrates the superior charge storage capability of ternary LDH nanocomposites for supercapacitor applications. This chapter examines how the synthesis approach for Ternay LDHs and structural design influence electrochemical performance, offering guidance for the development of advanced electrode materials for future energy storage systems.

Keywords: Ternary LDH, Nanocomposite, Supercapacitor.

Introduction

The extensive use of fossil fuel-derived energy has significantly increased greenhouse gas emissions, which contribute to global warming and various environmental problems. In this regard, the development of advanced energy storage devices with both high-power density and high energy density is critically important. Electrochemical capacitors are considered promising energy storage

systems because they offer rapid charge–discharge capability, high power density, long cycle life, and excellent operational stability [1-3]. Based on their energy storage mechanisms, supercapacitors are generally classified into three categories: (i) Electric Double Layer Capacitors (EDLCs), which store energy through electrostatic charge accumulation at the electrode-electrolyte interface, (ii) pseudocapacitors, where energy storage occurs through Faradaic redox reactions, and (iii) hybrid supercapacitors, which combine the characteristics of both EDLCs and pseudocapacitors [4 - 5].

Layered Double Hydroxides (LDHs) are classified into two categories: (i) binary LDHs and (ii) ternary LDHs. These materials possess a tunable layered structure, high specific capacitance, and strong redox activity. Their electrochemical performance originates from redox reactions involving the transfer of electrons between transition metal ions along with the participation of interlayer anions. The incorporation of multiple metal ions enhances cycling stability, rate capability, overall capacitance, and energy density. Compared with conventional binary transition metal LDHs, ternary transition metal layered hydroxides usually demonstrate higher specific capacitance and more pronounced redox activity [1-7]. This chapter reveals the synthesis strategies and electrochemical performance for Ternary LDH Based nanocomposite for supercapacitor application.

Synthesis Strategies

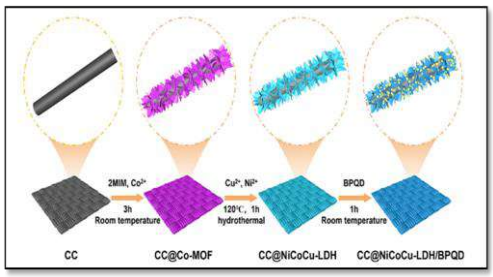

Fig. 1: Carbon Cloth @ NiCoCu - LDH/ Black Phosphorus Quantum Dots (BPQD) [1]

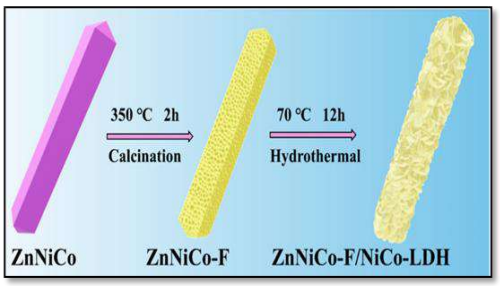

Fig. 2: Preparation of ZnNiCo - F/NiCo LDH [2].

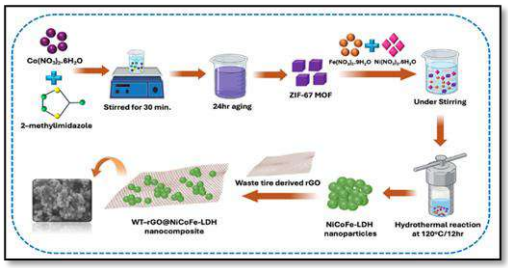

Fig. 3: Synthesis of Whatman-rGO @ NiCoFe-LDH composite [3].

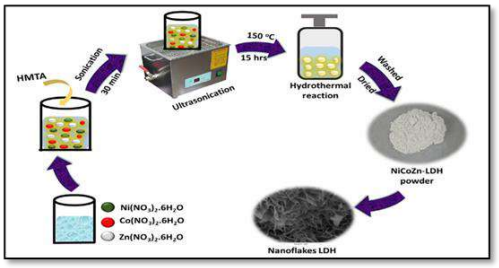

Fig. 4: Schematic Representation of Hydrothermal preparation of NiCoZn -LDH [4].

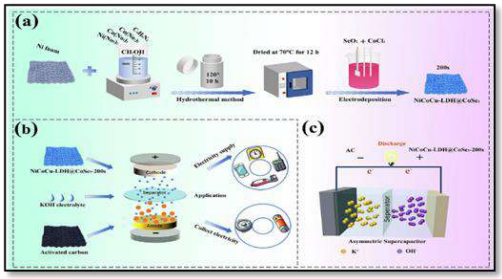

Fig 5: a) Sythesis of NiCoCu LDH @ CoSe2, b) Asemble Nickel Cobalt Aluminium (NCA) asymmetric Supercapacitor, c) Ion Transport in NCA device [5].

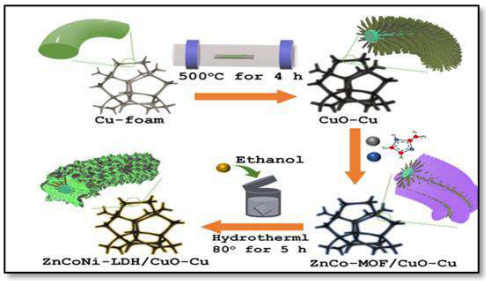

Fig. 6: Preparation ZnNiCo LDH / CuO-Cu [6]

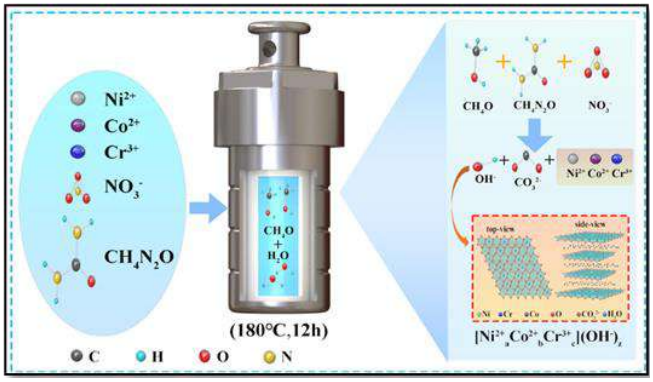

Fig. 7: Schematic Diagram of NiCoCr – X sample prepared by one step hydrothermal method [7].

Figure 1. The CC@NiCoCu-LDH/BPQD nanocomposite was synthesized through a sequential process. Initially, triangular Co-MOF nanosheets were grown on carbon cloth (CC) using a precipitation method with $Co(NO_3)_2 \cdot 6H_2O$ and 2-methylimidazole. The obtained CC@Co-MOF was then transformed into CC@NiCoCu-LDH via an ion-exchange reaction in a mixed Ni^{2+} and Cu^{2+} solution under hydrothermal conditions. Finally, BPQD were attached to the NiCoCu-LDH surface through a simple immersion step, producing the CC@NiCoCu-LDH/BPQD composite electrode.[1]. In Figure 2. ZnNiCo precursor nanorods were first synthesized via a co-precipitation method by dissolving Ni $(CH_3COO)_2$-$4H_2O$, Co $(CH_3COO)_2$-$4H_2O$, Zn $(CH_3COO)_2$-$2H_2O$, and polyvinylpyrrolidone (PVP) in ethanol and stirring at 85 °C for 4 h. The obtained precipitate was washed with ethanol and dried at 70 °C under vacuum to obtain ZnNiCo powder. Subsequently, the precursor was fluorinated by mixing with NH_4F and calcining at 350 °C for 2 h under a nitrogen atmosphere, producing porous ZnNiCo-F. For the fabrication of ZnNiCo-F/NiCo-LDH, ZnNiCo-F precursor was dispersed in a mixed solution containing urea, Ni $(NO_3)_2$-$6H_2O$, and Co $(NO_3)_2$-$6H_2O$ in deionized water and methanol. The mixture was sonicated and maintained at 70 °C for 12 h to allow the hydrothermal growth of

NiCo-LDH nanosheets on the ZnNiCo-F surface. The final ZnNiCo-F/NiCo-LDH composite was collected via. centrifugation, washed with distilled water & ethanol, and dried [2]. Figure 3. WT-rGO was first ultrasonically dispersed in ethanol to form a stable suspension. Separately, nickel nitrate, iron nitrate, and the ZIF-67 precursor were dissolved in deionized water and then mixed with the WT-rGO solution under stirring. The mixture was transferred to a Teflon-lined autoclave and treated solvothermally at 120 °C for 12 h, enabling in-situ growth of NiCoFe-LDH on the WT-rGO surface. After cooling, the product was filtered, washed with water and ethanol, and dried at 60 °C to obtain the WT-rGO@NiCoFe-LDH composite. A control NiCoFe-LDH sample was also prepared under the same conditions without WT-rGO [3]. The schematic illustration of NiCoZn-LDH formation via hydrothermal treatment at 150 °C for 15 h is also presented. in Figure 4 [4]. Figure 5. Fabrication of the NiCoCu-LDH@$CoSe_2$ electrode and the assembly of the asymmetric device. Initially, nickel foam was employed as the conductive substrate and immersed in an aqueous precursor solution containing nickel, cobalt, and copper nitrates along with hexamethylenetetramine. The mixture was subjected to a hydrothermal treatment, enabling the in-situ growth of NiCoCu layered double hydroxide (NiCoCu-LDH) nanosheets on the nickel foam surface. After washing and drying, the obtained NiCoCu-LDH electrode was further modified through an electrodeposition process in a cobalt–selenium electrolyte to deposit a $CoSe_2$ layer, thereby forming the hierarchical NiCoCu-LDH@$CoSe_2$ composite electrode. Subsequently, an asymmetric supercapacitor device was assembled using NiCoCu-LDH@$CoSe_2$ as the positive electrode and activated carbon as the negative electrode, with KOH serving as the electrolyte. The resulting device, denoted as NCA (NiCoCu-LDH@$CoSe_2$//activated carbon), facilitates efficient charge storage through rapid ion diffusion and electron transport during the charge-discharge process [5]. Figure 6. Synthesis of ZnNiCo-LDH/CuO-Cu hierarchical electrode. Initially, ZnCo-MOF nanosheets were grown on a CuO–Cu substrate by immersing it in a mixed aqueous solution of Zn^{2+}, Co^{2+}, and 2-methylimidazole, followed by aging at room temperature to obtain ZnCo-MOF/CuO–Cu. The obtained precursor was then treated with an ethanolic $Ni(NO_3)_2 \cdot 6H_2O$ solution under hydrothermal conditions, where ion-exchange and etching processes converted the ZnCo-MOF into ternary ZnNiCo-LDH. The final ZnNiCo-LDH/CuO–Cu composite was washed, vacuum-dried, and used for electrochemical evaluation. During subsequent thermal treatment at 500 °C, partial phase transformation of the copper oxide layer resulted in the formation of Cu_2O [6]. Figure 7. Hydrothermal synthesis of NiCoCr-X LDHs. Ni^{2+}, Co^{2+}, and varying concentrations of Cr^{3+} precursors dissolve in a mixed solvent of distilled water and methanol, followed by ultrasonic dispersion. Urea was then introduced as a hydrolysis agent, and the homogeneous solution was transferred into a

Teflon-lined autoclave for hydrothermal treatment at 180 °C for 12 h. During the reaction, the gradual decomposition of urea generated an alkaline environment that promoted the co-precipitation of Ni, Co, and Cr hydroxide species, resulting in the formation of NiCoCr-X layered double hydroxides. The obtained products were washed, dried, and labeled as NiCoCr-X according to the Cr precursor concentration, while the undoped sample was denoted as NiCo-LDH [7].

Comparative Study of Electrochemical performance for Ternary LDH Nanocomposites

Electrode Material	***Specific Capacitance (F/g)***	***Energy Density (Wh/kg)***	***Power Density (W/kg)***	***Ref.***
NiCoCu-LDH	1810.6	202.2	800	***01***
ZnNiCo-F/NiCl – LDH	819.4 C/g	61.9	735.3	***02***
WT-rGO@NiCoFe-LDH	1232.6	39.36	1098.41	***03***
NiCoZn – LDH	176.5	24.51	121.53	***04***
NiCoCu LDH@$CoSe_2$	1570.75	58.7	650	***05***
ZnNiCl-LDH/CuO-Cu	378.10 mAh/g	117.5	576.9	***06***
NiCoCr -LDH	2712	27.38	267.34	***07***

Conclusion

Ternary layered double hydroxide (LDH) nanocomposites demonstrate significant potential as advanced electrode materials for supercapacitors due to their enhanced redox activity, tunable composition, and improved electrochemical properties. Various synthesis approaches such as hydrothermal, co-precipitation, ion-exchange, and electrodeposition of hierarchical structure with higher surface area and efficient ion transport pathways. The incorporation of multiple transition metals and conductive supports improves electrical conductivity, cycling stability, and overall charge storage performance. Therefore, ternary LDH-based nanocomposites are promising candidates for the development of high-performance energy storage devices.

References

1. Xuan Wei et. al. Applied Surface Science 686 (2025) 162203
2. Weina Bi et. al. Journal of Energy Storage 143 (2026) 119591
3. Diksha Bhatt et. al. Journal of Power Sources 673 (2026) 239656
4. Madappa C. Maridevaru et. al. Journal of Energy Storage 102 (2024) 114125
5. Yuxin Sun et. al. Chemical Engineering Journal 508 (2025) 161062
6. Milan Babu Poudel et. al. Journal of Energy Storage 72(2023)108220
7. Yongtao Tan et. al. Materials Chemistry and Physics 320(2024)129456

Binary Layered Double Hydroxide – Based Electrode Material for Electrochemical Studies: Electrode Fabrication, Charge-Storage Mechanisms and Electrochemical Analysis

Amol R. Pardeshi, Jaya Rokade

Department of Physics, Dada Patil Mahavidyalaya, Karjat, Dist: Ahilyanagar 414 402.

Email: amolrp111@gmail.com

Article DOI Link: https://zenodo.org/uploads/19793589

DOI: 10.5281/zenodo.19793589

Abstract

Binary layered double hydroxides (LDHs) have promising electrode materials for Excellent performance supercapacitors due to their controllable composition, layered structure, and redox-active sites. This chapter discusses the fabrication of binary LDH-based electrodes and their charge storage behavior. Carbon-supported NiCo LDH composites demonstrate improved electrochemical properties due to the synergistic interaction between the conductive carbon framework and redox-active LDH nanosheets. Electrochemical studies using cyclic voltammetry (CV) and galvanostatic charge – discharge (GCD) measurements show enhanced capacitance, rapid ion transport, and improved rate capability. The hybrid architecture combines electric double-layer capacitance and pseudocapacitive reactions, leading to superior energy storage performance.

Keywords: Binary LDH, supercapacitor, charge storage mechanism, Electrochemical Characterization.

Introduction

Issues of energy storage devices, climate change due to heavily use of fossil fuels and environmental challenges, demanded high performance energy storage devices such as batteries, fuel cell, electrolyte capacitor, supercapacitor. Supercapacitor is promising energy storage device due it its unique properties such as high surface area, fast charge discharge, cyclic stability, high power density. Supercapacitor is divided into three parts based on charge storage mechanism a) Electric Double Layer Capacitor (EDLC) which work on the principal energy storage via electrostatic force (two electrode separated by separator), b) Pseudocapacitor which work on the principle of faradaic reaction, and c) Hybrid capacitor work on both principle (combination of EDLC and Pseudocapacitor) [1-5].

Layered Double Hydroxide have significant attention for the high theoretical specific capacitance, commonly such material known as hydrotalcite. It has unique layered structure, rich redox active site which help for charge storage mechanism, specific surface area [6-12]. This chapter reveals the study of electrode fabrication, charge storage mechanism and electrochemical studies of binary LDH based composite for supercapacitor applications.

Electrode Fabrication & Charge Storage Mechanism

- **Electrode Fabrication:** Initially prepare the Binary LDH composite via. Any synthesis method. Fig. 1 represent the preparation of NiMn LDH material via. Hydrothermal method. There are many electrode fabrication methods, most common method are discussing in this section:

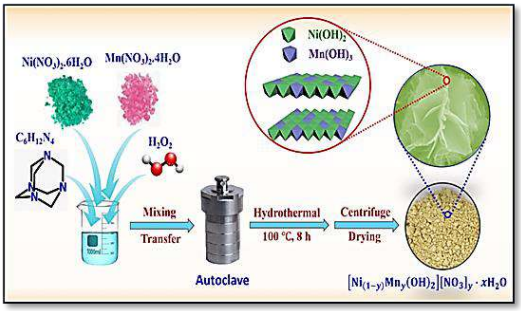

Fig. 1: Schematic diagram for synthesis NiMn LDH

- **Fabrication of Working Electrode and Electrochemical Measurements:** The working electrode was prepared using a stainless-steel plate shaped in a T-configuration. A slurry was prepared by dissolving 10 wt% polyvinylidene fluoride (PVDF) in a solvent mixture of 1 mL N, N-dimethylformamide (DMF) and 1 mL acetone at 80 °C. The synthesized nanoparticles (90 wt%) were added to the binder solution and mixed thoroughly to obtain a uniform slurry. The slurry was then coated onto a 1 × 1 cm^2 surface area of the stainless-steel electrode and dried at 60 °C in a hot air oven. Electrochemical measurements were performed using a three-electrode system with Ag/AgCl as the reference electrode, platinum wire as the counter electrode, and the coated stainless-steel plate as the working electrode. All experiments were conducted in 1 M KOH electrolyte to evaluate the electrochemical performance of the electrode material for supercapacitor applications [6].
- **Charge Storage Mechanism:** The charge storage behavior of Ni/Co layered double hydroxide (LDH) based composites is strongly influenced by their structural and compositional characteristics. In this system, the Ni/Co LDH nanosheets are integrated with a conductive carbon framework, which plays a crucial role in improving the electrochemical studies shown in fig. 2. During

synthesis, Ni and Co hydroxide species are deposited onto the surface of the carbon architecture, forming ultrathin nanosheets. These nanosheets expose a large number of electrochemically active sites, which participate in reversible redox reactions during the charge-discharge process. In alkaline electrolyte, the Ni^{2+}/Ni^{3+} and Co^{2+}/Co^{3+} redox couples contribute significantly to the pseudocapacitive behavior of the material. These faradaic reactions allow the electrode to store charge through fast surface or near-surface electrochemical processes.

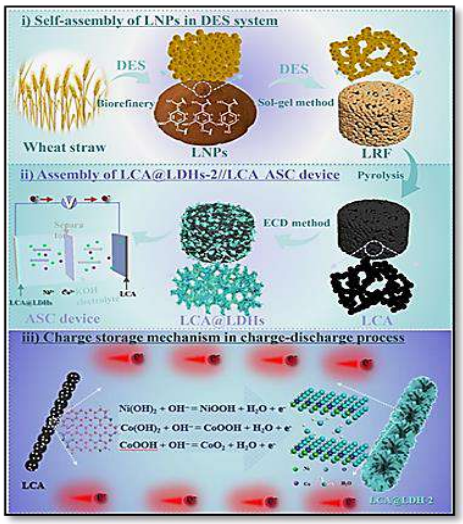

Fig. 2: LCA (carbon aerogels) @LDHs Fabrication and Charge Storage Mechanism [12].

At the same time, the porous carbon matrix offers additional electric double-layer capacitance by allowing electrolyte ions to accumulate at the electrode–electrolyte interface. The presence of micro- and mesoporous channels also shortens the ion diffusion pathways, which improves charge transfer kinetics. As a result, the synergistic interaction between the conductive carbon network and the Ni/Co LDH nanosheets enhances the overall capacitance, promotes rapid electron and ion transport, and improves the energy storage capability of the composite electrode. Therefore, the charge storage in this hybrid system arises from a combined mechanism involving electric double-layer capacitance from the carbon framework and pseudocapacitive redox reactions from the Ni/Co LDH active sites, leading to improved supercapacitor performance [8-12].

Electrochemical Studies

Electrochemical characteristics of synthesized electrode were examined through CV and GCD measurements in an alkaline electrolyte using a three-electrode configuration. The CV curves records at 50 mV s^{-1} reveal distinct differences among the electrodes. The carbon sphere (CS) electrode exhibits a quasi-

rectangular profile with relatively low current response, indicating that its charge storage mainly arises from electric double-layer capacitance.

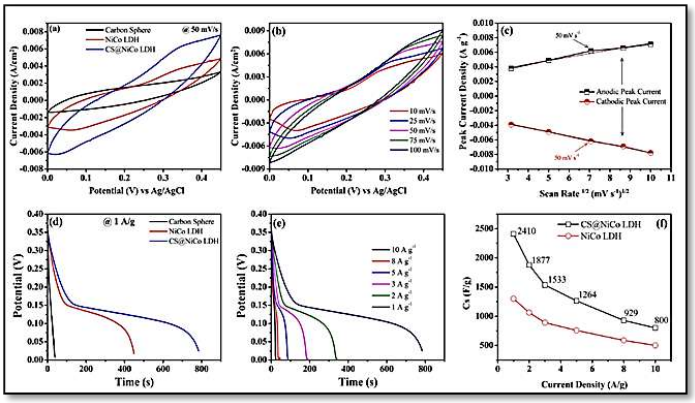

Fig. 3: CV and GCD analyses of CS, NiCo LDH, and CS@NiCo LDH electrodes, including scan rate and current density effects, peak current relationships, and specific capacitance comparison (Ref. [8]).

In distinction, both NiCo LDH and the CS@NiCo LDH composite display prominent redox peaks, confirming a pseudocapacitive behavior governed by reversible faradaic reactions associated with Ni^{2+}/Ni^{3+} and Co^{2+}/Co^{3+} redox couples. Notably, the CS@NiCo LDH electrode shows a larger enclosed CV area and higher current density than pristine NiCo LDH, reflecting enhanced electrochemical activity and improved charge storage capability. When the scan rate is increased, the overall shape of the CV curve remains largely preserved, suggesting favorable electrochemical reversibility and rapid ion transport within the electrode structure

The CS @ NiCo LDH hybrid, however, presents the longest discharge duration, signifying a significantly higher charge storage capacity. Current density of 1 A g^{-1}, the specific capacitance values are approximately 124 F g^{-1} for CS, 1264 F g^{-1} for NiCo LDH, and 2410 F g^{-1} for the CS @ NiCo LDH electrode. Even at elevated current densities, the composite maintains considerable capacitance, demonstrating excellent rate capability. This cooperative architecture shortens ion diffusion pathways, enhances electrolyte accessibility, and effectively mitigates particle aggregation, ultimately leading to improved capacitance and energy storage efficiency, it represents in fig. 3[8].

Table 1: Comparative Electrochemical Study of Binary LDH based Electrode Material

Electrode Material	Specific Capacitance (F/g)	Energy Density (Wh/kg)	Power Density (W/kg)	Ref.
NiCl LDH/Carbon Dots	5157 mF/cm^2	0.45 mWh/cm^2	20 mW/cm^2	03

CoMn-S LDH	792.4 C/g	82.63	985	04
Fe doped CoNi LDH	2115	41.3	750	05
NiSn LDH	821	-	-	06
NiCo LDH	1264	40.2	1368	08
Ni-CoV LDH/NF	508	21.2	801.2	09
MoS2/g-C3N4/NiCo LDH	968 C/g	74.13	400	10
NiMn LDH	612 C/g	60	1770	11

Conclusion

Binary LDH nanostructures integrated with conductive carbon materials exhibit remarkable electrochemical performance for supercapacitor applications. The hybrid electrode architecture provides abundant electroactive sites, improved electrical conductivity, and efficient ion diffusion pathways. As a result, the electrode display significantly excellent capacitance and high rate of capability compared to each component. The synergistic coupling between carbon frameworks and LDH layers plays a crucial role in enhancing charge storage efficiency, making binary LDH-based composites promising candidates for energy storage system.

References

1. Wenxuan Hu et. al. Journal of Energy Storage 134 (2025) 118278
2. Chuan Jing et. al. Progress in Materials Science 150 (2025) 101410
3. Xin Zhu et. al. Diamond & Related Materials 148 (2024) 111514
4. Mahdi Moradi et. al. Journal of Power Sources 629 (2025) 235993
5. Siwen Yang et. al. Journal of Energy Storage 136 (2025) 118461
6. M. Mohanasundari et. al. Results in Engineering 27 (2025) 105772
7. Syed Shaheen Shah et. al. Materials Science & Engineering R 166 (2025) 101041
8. John Peter I et. al. Journal of Power Sources 655 (2025) 237897
9. Abhijith R. Nair et. al. Journal of Power Sources 659 (2025) 238352
10. Qicheng Chen Journal of Power Sources 666 (2026) 239197
11. Abebaw Eshetie Kidie et. al. Journal of Industrial and Engineering Chemistry133(2024)550–56.

Electrochemical Principles and Energy Storage Mechanisms of Supercapacitors

Gita B. Jadhav, Rutuja S. Malave

Department of Physics, Dada Patil Mahavidyalaya, Karjat, Dist: Ahilyanagar 414 402.

Email: jadhavgita590@gmail.com

Article DOI Link: https://zenodo.org/uploads/19793729

DOI: 10.5281/zenodo.19793729

Abstract

Supercapacitors or Electrochemical capacitors have emerged as high performance devices that store energy and work between capacitors and batteries. They exhibit high power density, rapid charge-discharge capability, and long operational life. Unlike batteries that rely on slow bulk chemical reactions, supercapacitors energy store through rapid surface charge storing and fast reversible electrochemical reactions. This chapter presents a comprehensive review of the underlying electrochemical principles and highlights the two main energy collection mechanisms: electric double-layer capacitance (EDLC) and pseudocapacitance. The effects of electrode materials, electrolyte types, and device configuration on performance are examined. Additionally, common electrochemical characterization techniques and recent material innovations are discussed. Understanding these mechanisms is critical for improving energy and power density while ensuring long-term stability in practical applications.

Keywords: Supercapacitor, Electric Double Layer, Pseudocapacitance, Electrochemical Energy Storage, Nanostructured Electrodes.

Introduction

The need for efficiency, reliable, and enduring energy storage solutions has increased rapidly due to the growth of transportable electronics, electric vehicles, and renewable energy systems [2]. Traditional batteries offer high energy density but are limited by slow charge/discharge rates and shorter lifespans. Conventional capacitors provide high power density but store relatively little energy. Supercapacitors combine the advantages of both, offering density of high power, rapid charging capability, and extremely long-life cycle, making them perfect for applications requiring quick energy delivery. Supercapacitors differ fundamentally from batteries in their storage of energy mechanism. While batteries rely on diffusion-controlled bulk redox reactions, supercapacitors store energy primarily at the electrode-electrolyte interface. This results in fast

charge/discharge rates and exceptional stability [2]. To optimize performance, researchers focus on designing high-surface-area electrode materials and selecting electrolytes that expand the operational voltage window.

Electrochemical Principles of Supercapacitor: A supercapacitor consists of two electrodes, a separator, and an electrolyte [3]. The electrodes are conductive plates separated by a dielectric material, and their performance depends on design and structure. The separator prevents electrical contact while allowing ion flow. The electrolyte provides mobile ions that maintain charge balance during operation. When voltage is applied, electrons flow through the external circuit and ions accumulate at the electrode surfaces, storing energy either electrostatically or through reversible redox reactions [1].

Energy Storage Mechanisms

Energy store of supercapacitors through two primary mechanisms: electric double-layer capacitance and pseudocapacitance. Both can operate simultaneously in hybrid devices.

- **Electric Double-Layer Capacitance (EDLC):**

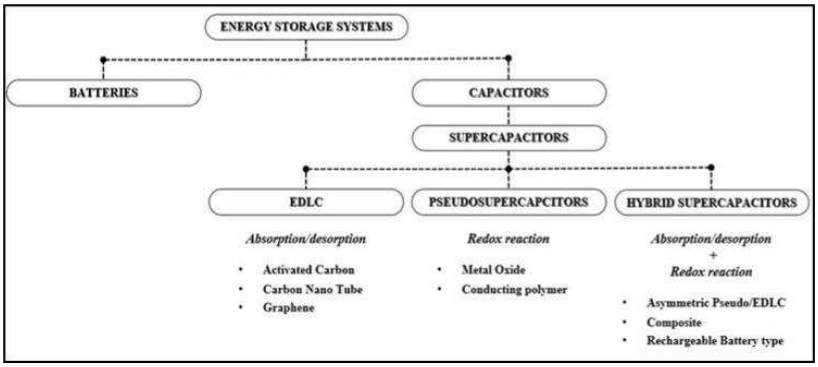

Fig. 1 Summary of supercapacitor types and electrode material systems[4].

EDLC is a non-faradaic mechanism relying on electrostatic charge separation. If voltage is applied then ions in the electrolyte accumulate near electrode surfaces, forming a double layer. No chemical reaction occurs, which ensures excellent reversibility and extremely long cycle life [1]. factors affecting EDLC performance: Electrode surface area, Pore size and distribution, Electrolyte ion size and mobility, Dielectric properties of the medium [1].

Carbon-based materials such as activated carbon, graphene, and carbon nanotubes are commonly used in EDLC because of their large surface area and high conductivity [4].

- **Pseudocapacitance:** Pseudocapacitance include quick, reversible charge-transfer reactions occurring at or near the electrode surface. Unlike EDLC,

this mechanism relies on electron transfer between the electrode and electrolyte species [5]. Materials demonstrating pseudocapacitance include:

- Transition metal oxides (e.g., RuO_2, MnO_2, NiO) [1].
- Conducting polymers (e.g., polyaniline, polypyrrole) [2].

Pseudocapacitive reactions store additional charge, increasing the effective capacitance. However, repeated cycling may lead to slight structural degradation, impacting long-term stability [5].

- **Hybrid Supercapacitors:** Hybrid supercapacitors integrate EDLC and pseudocapacitive materials in asymmetric configurations to optimize both energy density and power capability. This approach balances rapid charge/discharge performance with enhanced total charge storage [6].

Electrode Materials and Electrolytes

- **Electrode Materials**

Electrode material selection is critical

Carbon Materials: Carbon have superior performance in heat, catalysis, adsorption, etc., Most materials have porous structure, also have excellent conductivity [10].

Metal Oxides: High specific capacitance via redox reactions [1].

Conducting Polymers: High pseudocapacitance but moderate stability [1]. Nano structuring and composite designs improve ion transport and enhance active surface area.

- **Electrolytes**

Electrolytes influence operating voltage and ion mobility:

Aqueous Electrolytes: High ionic conductivity, limited voltage (1 V) [3].

Organic Electrolytes: Wider voltage window (~2.5–3 V) [3].

Ionic Liquids: Extended voltage stability, lower conductivity [3]. Increasing the voltage window enhances energy density quadratically, as per the energy equation (1).

Electrochemical Characterization Techniques

Common methods for evaluating supercapacitor performance:

- **Cyclic Voltammetry (CV):** Current response under voltage sweep; rectangular curves indicate EDLC, peaks indicate pseudocapacitance [7].
- **Galvanostatic Charge–Discharge (GCD):** Measures capacitance, internal resistance, energy/power density [7].
- **Electrochemical Impedance Spectroscopy (EIS):** Analyzes frequency-dependent response, providing insights into ion transport and interfacial resistance [8]. These techniques enable accurate assessment of charge storage

mechanisms and device efficiency.

Discussion

Supercapacitors offer higher power density than batteries due to fast surface-based energy storage. However, energy density is lower because storage is limited to surface interactions [1]. The main challenge is enhancing energy density without surrendering power performance and cycle life [9]. Hybrid supercapacitors and nanostructured electrodes have shown promising improvements. Optimizing pore size, electrode composition, and electrolyte selection further improves performance [9]. Future research aims at integrating supercapacitors with renewable energy systems, flexible electronics, and electric vehicles.

Conclusion and Future Scope

Supercapacitors are effective-performance electrochemical energy storage devices offering fast charge/discharge and long cycle life. Energy storage occurs through EDLC and pseudocapacitance mechanisms. Material selection, electrolyte optimization, and hybrid designs are critical for performance enhancement [2].

Future Directions Include

- Development of nanostructured electrodes for higher energy density [9].
- Flexible and solid-state supercapacitors for wearable electronics [2].
- Improved electrolyte systems for wider voltage windows [3].
- Cost-effective scalable manufacturing [2].

With these advancements, supercapacitors will continue to play a vital role in sustainable energy and high-power applications.

References

1. Niraj Kumar et.al., Nanomaterials 2022,12,3708.
2. Niraj Singh et.al., Volume 121, 15 June 2025, 116498.
3. Swati Sharma et.al., Result in Chemistry 5(2023)100885
4. Jae Muk Lim et.al.,Nanoscale Adv,2023,5,615-626.
5. Arpit Mendhe et.al., Discover Material (2023)3:29.
6. Sahila Cansu Gorgula et.al., Journal of Mechatronics and Artificial Intelligence in Engineering. December 2024, Volume 5, Issue 2 143.
7. Nargish Parvin et.al., J. Mater. Chem. A, 2025, 13, 24320-24386.
8. Mate Czagany et.al., Materials 2024,17,702.
9. Niraj Kumar et.al.,Volume 41, March 2026,101251
10. Jiang Li et.al., Manufacturing Riv. 10 (2023) 13.

CoMn Layered Double Hydroxide Based Nanocomposite for Supercapacitor Application: Synthesis Strategies and Electrochemical Behaviour

Amol R. Pardeshi, Pranali S. Kothare

Department of Physics, Dada Patil Mahavidyalaya, Karjat, Dist: Ahilyanagar 414 402.

Email: amolrp111@gmail.com

Article DOI Link: https://zenodo.org/uploads/19793837

DOI: 10.5281/zenodo.19793837

Abstract

Increasing demand for efficient energy storage systems has accelerated the development of advanced electrode materials for supercapacitors. Among them, cobalt - Manganese layered double hydroxides (CoMn-LDHs) have attracted considerable attention due to their multiple redox states, high electrochemical activity, and structural versatility. In this study, CoMn-LDH based electrodes were synthesized through hydrothermal and in-situ growth strategies on conductive substrates such as nickel foam and stainless steel. The layered architecture and synergistic interaction between cobalt and manganese provide abundant electroactive sites, improved charge transport, and enhanced ion diffusion. Electrochemical investigations reveal excellent capacitive behaviour, good rate capability, and stable cycling performance.

Keywords: CoMn LDH, Supercapacitor, NDH based nanocomposites.

Introduction

In current scenario researchers are endeavoring to develop excellent efficient energy storage and conversion technologies due to globally increasing environmental problems. Various reason for researcher shifts towards the energy storage devices such as pollution, global warming due to high use of fossil fuels. Supercapacitor have promising energy storage device due to fast charge – discharge rate, higher power density and excellent cycling stability. Supercapacitor basically divided into three types on the basis of charge storage mechanism i. Electric Double Layer Capacitor (EDLCs) which made up by carbon material such as carbon nanotubes, activated carbon, graphene and high rate of capabilities but having low specific capacitance and low energy density, ii. Pseudocapactor which made up by Ru, Mn oxides which delivers higher specific capacitance as compare to EDLCs materials, iii. Hybrid supercapacitor which

made up by combination of EDLCs and Pseudocapactor, it's divided into three type 1. Ion adsorption at surface, 2. Faradaic electron transfer, and 3. Reversibility intercalation of ions [1-4].

LDHs materials exhibit a layer -by-layer structure involving tow metal ion in the oxidation state of 2+ and 3+. Metal cations occupy the octahedral centres coordinated by hydroxyl groups positioned along the edges. Edge-sharing octahedra assemble into two - dimensional layered frameworks. The resulting positive layer charge electrostatically accommodates anionic species within the interlayer galleries, where the interlayer distance is governed by the steric dimensions of the inserted anions. Cobalt - Manganese LDH exhibits favourable electrochemical characteristics as a cathodic material in KOH electrolyte. Cobalt and manganese are attractive electrode constituents for supercapacitors owing to their variable oxidation states, favourable electrochemical activity, and economic viability. The Co^{2+}/Co^{3+} redox pair contributes high electrical conductivity and efficient charge-transfer kinetics, whereas the Mn^{2+}/Mn^{3+} couple offers high theoretical capacitance, chemical robustness, and cost effectiveness. Integrating these transition metals in cobalt–manganese layered double hydroxides (CoMn - LDHs) generates a synergistic framework that enhances redox accessibility, ion diffusion, and electronic transport. The intrinsic layered architecture, high surface area, and abundant electroactive sites facilitate rapid faradaic reactions and efficient electrolyte penetration. Consequently, CoMn - LDHs represent a promising class of electrode materials for high - performance supercapacitors with improved capacitance, rate capability, and cycling durability [5-13]. This chapter shows the synthesis strategies for CoMn based nanocomposite and Electrochemical studies.

Synthesis Strategies

- **Materials required to prepare CoMn LDH**

Manganese Chloride Tetrahydrate (MnCL2.4H2O), Cobalt (II) Nitrate Hexahydrate Co (NO3)2.6H2O, Methylimidazole, Distilled water, Aceton, Ethanol, Hydrochloric Acid, Polyvinylidene Fluoride (PVDF), Acetylene Black, and N – Methyl pyrrolidone (NMP).

- **Methods**

In Fig. 1: in stage – I: The CoMn–LDH/NF electrode was prepared via a sequential in-situ growth approach. promoting the in-situ formation of a cobalt based metal – organic framework (Co-MOF) layer on the conductive scaffold. The obtained Co-MOF/Nickel foam (NF) F was washed with deionized water & dried at 60 °C for 8 h. In Stage -II:, the Co-MOF/NF precursor was subjected to hydrothermal treatment in a Teflon-lined autoclave containing an ethanol solution with controlled concentrations of $MnCl_2 \cdot 4H_2O$ (0.50, 0.75, and 1 mM).

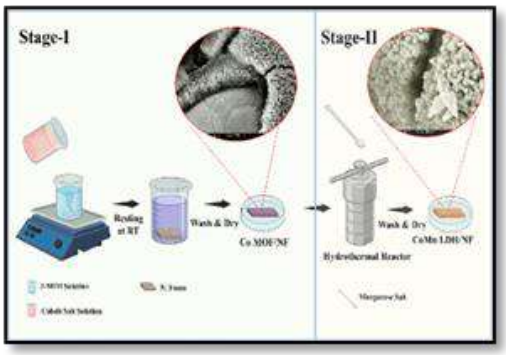

Fig. 1: Sythesis of CoMn LDH/NF, Stage 1: Co-MOF, Stage 2: CoMn LDH [2].

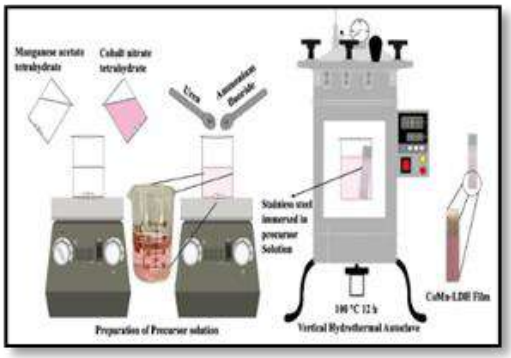

Fig. 2: Synthesis Process of CoMn LDH film on stainless steel substrate [6].

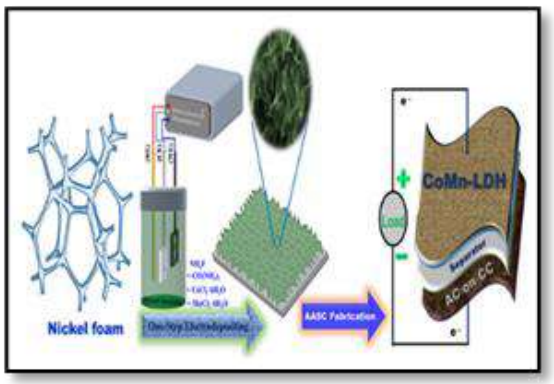

Fig. 3: CoMn-LDH@NF nanostructure on NF and Asymmetric Supercapacitor [11].

The reactor was heat at 70 °C for 1 h, enabling the conversion of the Co-MOF precursor into CoMn-LDH through a metal-ion mediated transformation process. The resulting CoMn-LDH/NF electrodes exhibited a uniform hazelnut-brown coating with an average active mass loading of 1.2 ± 0.2 mg cm^{-2}, determined by the mass difference between bare and coated Ni foam [2]. The pretreated stainless - steel (SS) substrate immersed in the reaction mixture which prepared using given materials and subjected to hydrothermal treatment at 100 °C for 12 h, facilitating the in-situ nucleation & growth of CoMn layered double hydroxide on the substrate surface. After natural cooling, the coated substrate was thoroughly rinsed with deionized water and ethanol, followed by drying at 60 °C to obtain a uniform CoMn-LDH film [6]. The typical fabrication process for the CM-LDH cathodes and AASCs is illustrated in Fig. 3. [11].

Electrochemical Studies

After individual electrode assessment, an asymmetric aqueous supercapacitor (AASC) was assembled using CoMn-LDH as the cathode, activated carbon (AC) as the anode, and 2.0 M KOH as the electrolyte. The cyclic voltammetry profiles

of the cathode and anode at 30 mV s^{-1} within the potential ranges of 0.0–0.5 V and −1.1–0 V are presented in Fig. 4a, confirming balanced charge storage. CV curves recorded at various scan rates within 0.0–1.6 V (Fig. 4b) maintain similar shapes, indicating favourable electrochemical reversibility. Galvanostatic charge–discharge curves (Fig. 4c) exhibit nearly symmetric profiles, demonstrating high Coulombic efficiency. The device delivers specific capacitances of 274.26, 263.37, 253.12, 223.87, 213.50, and 208.75 F g^{-1} at current densities of 1, 2, 3, 6, 8, and 10 A g^{-1}, respectively, and retains ~137.10 F g^{-1} at 30 A g^{-1}, reflecting good rate capability. Long-term cycling performance (Fig. 4d) shows 89.2% retention after 5000 cycles at current density 5 A g^{-1} with nearly 100% Coulombic efficiency. The Ragone plot (Fig. 4e) demonstrates a maximum energy density of 97.5 Wh kg^{-1} at a power density of 800 W kg^{-1}, while 74.3 Wh kg^{-1} is maintained at 8000 W kg^{-1}. For practical demonstration, two series-connected 2016-coin cells successfully powered a 3.2 V red LED for over 16 minutes (Fig. 4f), confirming the practical applicability of the fabricated AASC device [1].

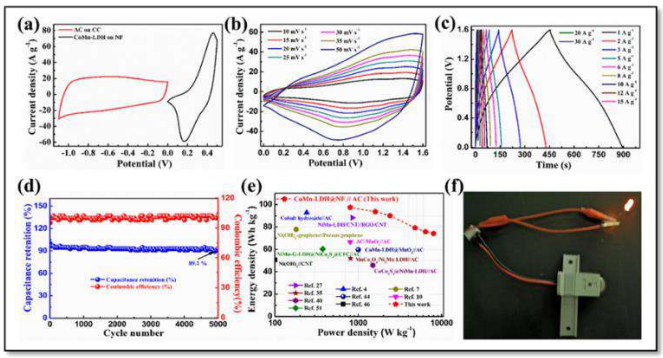

Fig. 4: AASC performance: (a) CV of cathode and anode, (b) CV at varying scan rates, (c) GCD at different current densities, (d) cycling stability and Coulombic efficiency over 5000 cycles, (e) Ragone plot comparison, and (f) practical demonstration lighting a 3.2 V red LED.

Table: Comparative Study of CoMn Based LDH Nanocomposite for Supercapacitor Application Tabulate in Table 1.

Electrode Material	*Specific Capacitance (F/g)*	*Energy Density (Wh/kg)*	*Power Density (W/kg)*	*Ref.*
CoMn LDH	*2673.6 F/g*	*97.5 Wh/kg*	*800 W/g*	***01***
CoMn LDH	*1305 F/g*	*23.8 Wh/kg*	*300 W/g*	***02***
CoMn LDH	*1062.6 F/g*	*4.4 Wh/kg*	*2500 W/g*	***03***
CoMn LDH/PPy	*220 mAh/g*	*29.6 Wh/kg*	*500 W/g*	***04***
Co-HKUST@CoMn -LDH	*313.8 F/g*	*90.2 Wh/kg*	*719.0 W/kg*	***07***
CoMn LDH	*65 F/g*	*20.3 Wh/kg*	*435 W/kg*	***08***

CoMn LDH	*36.38 mF/cm²*	*6.82 μ Wh/cm²*	*-*	***09***
CoMn LDH	*1091 C/g*	*84 Wh/kg*	*1191.4 W/kg*	***10***
CoMn LDH	*1231.2 mF/cm²*	*0.409 mWh/cm²*	*-*	***12***
CoMn LDH	*1409 F/g*	*58.9 Wh/kg*	*163.2 W/kg*	***14***

Conclusion

In summary, CoMn-LDH nanostructured electrodes were successfully synthesized using facile in-situ and hydrothermal approaches on conductive substrates. The unique layered morphology and synergistic redox activity of cobalt and manganese significantly enhance electrochemical performance by providing efficient charges transfer pathways & accessible active sites. The fabricated asymmetric supercapacitor device delivers high capacitance, favorable and other chemical parameters.

References

1. Adil Emin el. al. Journal of Energy Storage 50 (2022) 104667
2. Megha Prajapati et. al. Journal of Electroanalytical Chemistry 961 (2024) 118242
3. Ajay D. Jagadale et. al. Journal of Power Sources 306 (2016) 526e534
4. Yujin Guo et. al. Journal of Alloys and Compounds 832 (2020) 154899
5. Ximeng Liu et. al. ACS Appl. Mater. Interfaces, 2019.
6. K.R. Kumbhar et. al. Journal of Energy Storage 146 (2026) 119854
7. X. Liu et. al. Materials Today Sustainability 17 (2022) 100092
8. F.O. Ochai-Ejeh et. al. Electrochimical Acta http://dx.doi.org/10.1016/j.electacta.2017.08.163
9. Ankit Tyagi et. al. Electrochimica Acta 2019
10. Mahdi Moradi et. al. Journal of Energy Storage 71 (2023) 108177
11. Adil Emin et. al. Fuel 381 (2025) 133335
12. Songbiao Tian et. al. Electrochimica Acta 539 (2025) 146660
13. Daming Chen et. al. Journal of Alloys and Compounds 729 (2017) 866e873 .

Metal Oxide Framework Nanocomposite for Supercapacitor Application: Review

Rutuja S. Malave, Amol R. Pardeshi

Department of Physics, Dada Patil Mahavidyalaya, Karjat, Dist: Ahilyanagar 414 402.

Email: malaverutuja2001@gmail.com

Article DOI Link: https://zenodo.org/uploads/19793969

DOI: 10.5281/zenodo.19793969

Abstract

The increasing need for sustainable storage energy systems has accelerated research on progressive electrochemical devices such as supercapacitors. Supercapacitors show high power density, rapid charge-discharge capability, and long cycle life contrast to conventional capacitors and batteries. Metal-Organic frameworks (MOFs), owing to their highly porous structure, large surface area, and tuneable chemical composition, have emerged as promising electrode materials. Their unique framework structure provides abundant active sites and facilitates efficient ion transport. Furthermore, MOF-based nanocomposites such as MOF/carbon, MOF/metal oxide, and MOF/conducting polymer materials significantly enhance electrical conductivity and electrochemical performance. This chapter briefly discusses the fundamentals of supercapacitors, structural characteristics of MOFs, as well as the role of MOF-based nanocomposites in improving energy storage performance.

Keywords: Supercapacitors, Metal-organic frameworks (MOFs), Electrochemical performance.

Introduction

The world rapidly expands economically, technologically and in industrial things. It demands large energy sources. Because of more need of energy, we use conventional energy till know. Excess use of conventional energy it creates bad impact on the environment so for protect the Environment we studied the development of renewable energy [1]. Supercapacitors are energy collection devices that can collect and deliver energy at a rapid rate. Compared to regular capacitors, they provide higher energy and power density, can work over a vast temperature range, and have a much longer cycle life [2]. Normal capacitors stored small amount of energy and released it very quickly. They pass energy very fast. Batteries are used in large amount of energy for long term use and they delivered energy slowly. Metal–organic frameworks (MOFs) are extremely

crystalline porous materials that are widely used as starting materials to produce metal oxides and metal oxide–carbon hybrid materials [3]. Metal–organic frameworks (MOFs) have possible applications in gas partition, catalysis, fluorescence sensing, magnetism, and drug delivery. The organic conjugated units in MOFs help improve electrical conductivity, while the metal ions provide active sites. Because of these properties, MOFs are considered hopeful electrode materials for supercapacitors [2]. In this chapter we study about supercapacitors and MOF materials its chemical behaviour.

Fundamentals of Supercapacitor

Supercapacitor categorized in three sections on the root of ion storage mechanism

- **Electric Double Layer Capacitor:** An electrical double layer capacitor (EDLC) is a classification of supercapacitor that stores energy by collecting charges at the boundary between an electrode and an electrolyte, using electrostatic forces and not chemical reactions.
- **Pseudocapacitor:** In pseudocapacitors, energy is stored through various electrochemical processes, such as electro sorption, redox (oxidation-reduction) reactions, and ion intercalation. These processes involve the transfer of charge between electrode as well as electrolyte, which depends on the applied voltage. For this reason, is called a pseudo-capacitor [4].
- **Hybrid Capacitor:** Hybrid supercapacitors (HSCs) offer a promising way to fill the space between batteries and supercapacitors. By uniting battery-like and capacitor-like materials, HSCs can provide both high energy storage and high-power output [5]. Fig, 1: classified the different type of flexibility mode of MOFs.

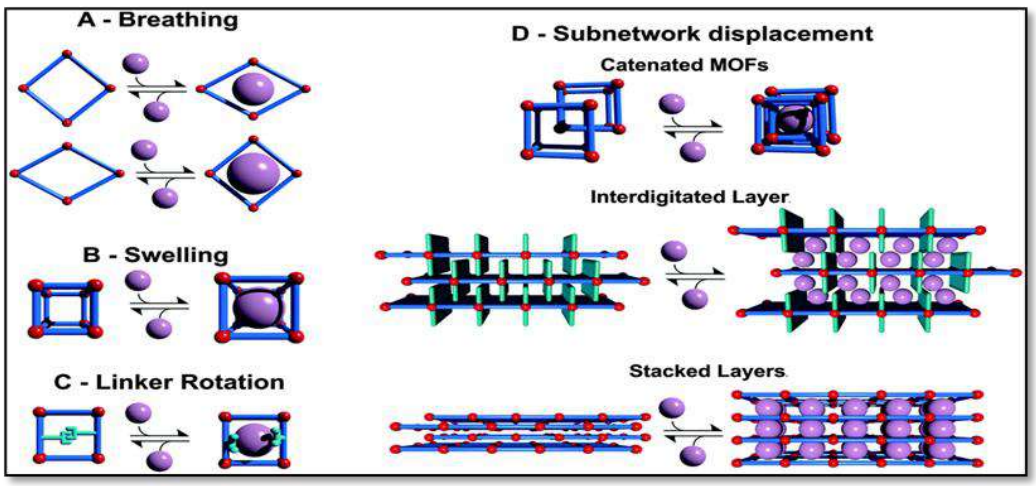

Fig 1: Different flexibility modes of MOFs. [8]

Metal Organic Framework

- **Meaning and Structure**

Metal-organic frameworks (MOFs) are highly crystalline porous materials that are widely used as precursor materials for synthesizing metal oxides and metal oxide carbon hybrid structures [3]. Metal-Organic Frameworks (MOFs) are hopeful materials for devices of energy storage, especially supercapacitors, because of their unique structures and adjustable functional properties [6]. Metal-organic frameworks (MOFs) are formed by connecting inorganic and organic part through strong bonds. The organic part are diatonic or polytopic carboxylate molecules (or similar negatively charged molecules) that connect with metal units to form strong crystalline MOF structures, typically having porosity greater than 50% of the crystal volume. The ability to change the size and properties of MOF structures without altering their basic topology led to the is reticular principle, allowing the creation of MOFs with very large pores (98 Å) and very low density (0.13 g/cm^3) [7].

- **Properties of Metal–Organic Frameworks (MOFs)**

1. High Surface Area

A high surface area allows ions to be quickly adsorbed and desorbed in Supercapacitors and increases the material's gas storage capacity [9].

2. Tuneable Pore Size

Pore size influences how easily ions and molecules can access the material, which is important for supercapacitor performance and selective gas storage [10].

3. Structural Diversity

Pore size influences how easily ions and molecules can access the material, which is important for supercapacitor performance and selective gas storage [11].

4. Redox Activity

Redox activity enhances energy storage by combining electric double-layer capacitance (EDLC) with Faradaic charge storage mechanisms [12].

MOF-Based Nanocomposites

- **Concept of Nanocomposites**

A nanocomposite material creates several stages, with at least one, two, or three dimensions at the nanometre range. Decreasing material size to the nanoscale make phase interfaces, which are crucial for improving material properties. The surface-to-volume ratio of reinforced material in a nanocomposite plays a significance role in understanding the relationship between structure and properties [13].

- **Types of MOF-Based Nanocomposites**

1. MOF/Carbon Composites

Pure MOFs often suffer from low electrical conductivity and limited stability, which limit their practical applications. To overcome these limitations, MOFs are frequently combined with carbon materials such as, carbon nanotubes (CNTs), graphene and activated carbon, forming MOF/carbon composites with improved conductivity, stability, and catalytic performance [14].

2. MOF/Metal Oxide Composites

When MOFs are thermally treated or chemically converted, they can produce metal oxide composites such as NiO, Co_3O_4, and MnO_2 while maintaining the original porous structure of the MOF. These materials exhibit improved electrical conductivity, high surface area, and large-scale active sites, making them promising for energy storage, catalysis, and sensing applications [15].

3. MOF/Conducting Polymer Composites

Most MOFs experience poor electrical conductivity, which restricts their application in electrochemical devices storage energy like supercapacitors and batteries [16].

To overcome this limitation, MOFs are often combined with conducting polymers like a polyaniline (PANI) as well as polypyrrole (PPy) to form MOF/conducting polymer composites with improved electrical conductivity and electrochemical performance These composites integrate the high conductivity and redox activity of conducting polymers with the porous structure of MOFs, leading to enhanced charge transfer, increased active sites, and improved electrochemical stability [17].

Conclusion

Metal-organic frameworks possess remarkable structural and physicochemical characteristics that make them attractive materials for supercapacitor applications. Their large surface area, tuneable pore architecture, as well as redox-active metal centres support efficient charge storage. However, the limited electrical conductivity of pristine MOFs can restrict their electrochemical performance. The formation of MOF-based nanocomposites with metal oxides, carbon materials or conducting polymers effectively improves conductivity, stability, and capacitance behaviour. Therefore, rational design and modification of MOF-derived materials can play a significant role in developing very good-performance supercapacitors for future storage energy technologies.

References

1. Y. Liu, X. Xu, Z. Shao, S. P. Jiang, Energy Storage Mater., 2020, 25, 170–193.

2. L. Yue, X. Wang, T. Sun, H. Liu, Q. Li, N. Wu, H. Guo, W. Yang, Chem. Eng. J., 2020, 381, 121959.
3. S. Shin, M. W. Shin, Appl. Surf. Sci., 2020, 529, 148295.
4. S. C. Gorgulu, I. Yazar, T. H. Karakoc, J. Mech. Autom. Instrum. Eng., 2024, 8, 24103.
5. N. Parvin, D. Merum, M. Kang, S. W. Joo, J. H. Jung, T. K. Mandal, J. Mater. Chem. A, 2015, 3, 14964–14973.
6. S. R. Dash, M. S. Yadav, R. K. Sahoo, A. L. Sharma, Appl. Energy, 2026, 351, 127349.
7. H. Furukawa, K. C. Cordova, M. O'Keeffe, O. M. Yaghi, Science, 2013, 341, 1230444.
8. Schneemann, V. Bon, I. Schwedler, I. Senkovska, S. Kaskel, R. A. Fischer, Chem. Soc. Rev., 2014, 43, 6062–6096.
9. H. Furukawa, K. E. Cordova, M. O'Keeffe, O. M. Yaghi, Science, 2013, 341, 1230444.
10. O. M. Yaghi, M. O'Keeffe, N. W. Ockwig, et al., Nature, 2003, 423, 705–714.
11. S. Kitagawa, R. Kitaura, S. Noro, Angew. Chem. Int. Ed., 2004, 43, 2334–2375.
12. L. Zhang, et al., Chem. Soc. Rev., 2020, 49, 8361–8394.
13. Nanocomposites: A Brief Review, 2020, 10, 51–59.
14. S. Lu, F. Xie, H. Liu, Y. Liu, Z. Zhang, W. Shang, J. Jiang, Y. Wen, Electrochim. Acta, 2023, 452, 143063.
15. D. Yue, P. Rosaiah, K. Mallikarjuna, M. R. Karim, J. S. Alnawmasi, T. J. Ko, G. P. Nunna, Polyhedron, 2024, 260, 117062.
16. M. Z. Iqbal, M. M. Faisal, S. R. Ali, S. Farid, A. M. Afzal, Electrochim. Acta, 2020, 346, 136039.
17. V. N. Kendre, V. N. Narwade, S. S. Patil, K. A. Bogle, M. Shariq, M. L. Tsai, M. D. Shirsat, Emergent Mater., 2025, 8, 5577–5589.

Ternary LDH Based Nano Composite for Super Capacitors Application: Electrochemical Performance

Sushama M. Saykar, Rutuja S. Malave

Department of Physics, Dada Patil Mahavidyalaya, Karjat, Dist: Ahilyanagar 414 402.

Email: sushamasaykar81@gmail.com

Article DOI Link: https://zenodo.org/uploads/19794543

DOI: 10.5281/zenodo.19794543

Abstract

The development of durable and high-performance thin films with outstanding energy storage and conversion properties has gained significant interest in the areas of super capacitors and elctrocatalysis [2]. Electrochemical energy storage systems including batteries and super capacitor offer significant promise for a wide range of applications [7]. The microstructures and chemical composition of the different composite materials were examined using techniques such as scanning and transmission electron microscopy (SEM and TEM),X-Ray diffraction (XRD) Raman spectroscopy and nitrogen(N2) physisorption analysis, among other methods[7]This research examined how adding graphene foam (GF) to a ternary transition metal hydroxide matrix composed of nickel , cobalt and manganese influences its electrochemical properties with the aim of enhancing its performance as asupercapacitor electrode[6]. In this work, hierarchical Nano sheet structured ternary CONife layered double hydroxide thin films were fabricated using a simple and cost-effective electro deposition techniques, their structural, morphological and electrochemical characteristics where thoroughly examined and compared with these of the corresponding binary material.

Introduction

The continuously rising global energy demand and the rapid depletion of conventional energy resources have driven significant interest in developing advanced electrochemical energy storage systems .these systems include technologies such as fuel cells, metal-ion , batteries and super capacitors which are designed to deliver high performance and improved efficiency.supercapacitors have high power density and fast charges- storage properties which attracts the attention of many researchers[4]layered double hydroxide LDHs are 2d layered anionic clays also known as hydrotalcite which attracted the interest in various potential application in which electrochemical energy storage and conversion included [5].

Super capacitors and batteries are both energy storage devices that play a central role in modern technologies. Batteries offer high specific energy which makes them especially suitable for extended periods. Such as throughout the day .to the best of our knowledge, only a limited number of studies have been published on ternary met hydroxide -carbon composites. Combining ternary metal hydroxides with carbon nanostructured materials offers a promising approach for the development of advanced super capacitors design [6]. The aim of this study was to fabricate a composite material that enhance the synegistic interaction between the ternary hydroxide and the highly conductive graphene foam [6]. In recent years, transition metal - based layered double hydroxide (LDHs) have gained significant interest in applications such as super capacitors (SCs), elctrocatalysis and electrochemical sensing due to their highly reversible redox behaviour, low cost and outstanding flexibility in structure and composition tuning. supercapacitors (SCs) are generally divided into two types : (1) electric double layered capacitors (EDLCs) and (2) psuedocapacitors .In comparison to electric double – layered capacitors, pseudo capacitors exhibits enhanced capacitance performance because they involve rapid redox reactions along with extensive electrostatic charge diffusion and strange processes[2].

Layered doubled hydroxides (LDHs) have the genral chemical composition **[M1-x ^2+ Mx 3+(OH)2]^x+[Ax/n^n-.mH2o]^x-** in this formula m2+ and m3+ represents divalent and trivalent metal cations respectively while An- denotes the integer layer charge compensating anion with a valence of n.the parameter x corresponds to the molar ration of trivalent metal cations defined as

$$X = m^{3+} / m^{2+} + m^{3+}$$

Recently, several LDH systems such as NiCO, COAL, COMn, NiAl, and NiMn have gained significant attentions as high performance electrodes materials for electrochemical energy storage and conversion applications. Among the alpha-phase NiCO LDH has been particularly widely investigated for its effectiveness in super capacitors devices and electrochemical catalytic applications [2].

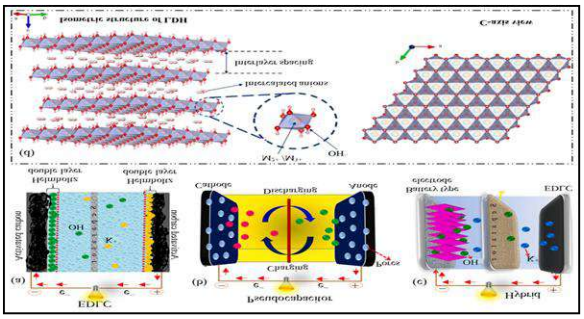

Fig (1):- schematic illustration of charge storage mechanism of EDLCs Pseudo capacitor and hybrid SCs.[8]

Electrode materials play a vital role in super capacitor systems (SCS), as they largely influence electrochemical performance more than electrolytes or separators. A wide range of materials have been explored as effective electrodes for super capacitors, including porous carbons, activated carbons (ACs), conducting polymers (CPs), graphene oxide (GO), reduced graphene oxide (ergo), metal oxides, carbon nanotubes (CNTs), layered double hydroxides (LDHs), MXenes, and metal chalcogenides [8].

Synthesis of LDHs

The preparation of binary/ternary LDHs was achieved by electrodeposition using a three-electrode system. The stainless steel (SS) (exposed area 1 × 1 cm2), Ag/AgCl (3M NaCl) and coiled platinum were used as a working, reference and counter electrodes, respectively. Prior to deposition, SS electrodes (1 × 6 cm2) were cleaned with deionized water and ethanol using an ultrasonic. The electrodeposition bath for ternary CONiFe LDH was prepared by mixing 0.1 M Co (NO3)2.6H2O, 0.1 M Ni (NO3)2.6H2O and 0.1 M FeSO4.7H2O in the ratio of 1:1:1. To this solution, 0.1 M of NaNO3 was added to increase the concentration of OH−ions, accelerating the rate of deposition which resulted into in high-quality uniform thin films. The electrolyte for binary LDHs such as CoNi, CoFe and NiFe was prepared by adding the corresponding nitrate sources to the deionized water in the ratio of 1:1. All the depositions were carried out at the cathodic current density of 1 mA cm-2 for 5 minute Binary and ternary LDHs were synthesized by electrodeposition using a three-electrode system with stainless steel (SS, 1 × 1 cm^2 exposed area) as the working electrode, Ag/AgCl (3 M NaCl) as the reference electrode, and coiled platinum as the counter electrode. Prior to deposition, SS electrodes (1 × 6 cm^2) were ultrasonically cleaned with deionized water and ethanol. For ternary CoNiFe LDH, the bath contained 0.1 M Co $(NO_3)_2 \cdot 6H_2O$, 0.1 M Ni $(NO_3)_2 \cdot 6H_2O$, and 0.1 M $FeSO_4 \cdot 7H_2O$ in a 1:1:1 ratio. Additionally, 0.1 M $NaNO_3$ was added to increase OH^- ion concentration, enhancing the deposition rate and producing uniform thin films. Binary LDHs (CoNi, CoFe, NiFe) were prepared using the respective nitrate salts in a 1:1 ratio. All depositions were performed at a cathodic current density of 1 mA cm^{-2} for 5 minutes [2].

Electrochemical Performance

The electrochemical performance of CONi-LDH,FeCoNi-LDH, FeCoNi-LDH -1, FeCoNi-LDH -2 and FeCoNi-LDH -3 was evaluated using a three-electrode system with 1 M KOH as the electrolyte [9]. The excellent electrochemical performance of the ternary FeCoNi-LDH mainly results from its increased specific surface area and mesoporous structure which are achieved through the formation of a three-dimensional architecture composed of nanosheets [9]. The

electrode fabrication, the active materials were combined with polyvinylidene difluoride (PVDF) as a binder and conductive carbon acetylene black (CAB) to compensate for the reduction in conductivity caused by the addition of the binder [6]. the analysis was performed using EC-lab(R) v11.33 software with a bio-logic VMP300 potential at (knoville,TN 37.930, USA) in a three-electrode measurement configuration.in this,glassy carbon served as the counter electrode Ag/Agcl was used as the referance electrode and synthesized materials acted as the working electrode [6].

Conclusion

The development of advanced electrochemical energy storage systems has become increasingly important due to the rapid growth in global energy demand and the depletion of conventional energy resources. Among the various energy storage technologies, supercapacitors have attracted significant attention because of their high-power density, rapid charge–discharge capability, and long cycle life. Compared with conventional batteries, supercapacitors provide faster energy delivery and improved operational stability, making them suitable for a wide range of modern applications. Layered double hydroxides (LDHs), particularly transition metal–based LDHs such as NiCo, CoAl, CoMn, NiAl, and NiMn systems, have emerged as promising electrode materials for supercapacitor applications. Their unique layered structure, tunable composition, high redox activity, and low cost make them highly suitable for electrochemical energy storage. The incorporation of multiple metal ions in ternary LDH systems further enhances electrochemical performance due to the synergistic interaction between different metal cations, which improves electrical conductivity, redox activity, and structural stability.

In this chapter, binary and ternary LDHs were successfully synthesized through an electrodeposition technique using a three-electrode system. The electrodeposition method offers advantages such as controlled growth, uniform thin film formation, and strong adhesion to the substrate. The electrochemical performance of the synthesized materials was evaluated using a three-electrode configuration in an alkaline electrolyte. The results demonstrated that ternary FeCoNi-LDH exhibits superior electrochemical performance compared to binary LDHs, mainly due to its larger specific surface area, mesoporous structure, and three-dimensional nanosheet architecture that facilitates efficient ion diffusion and rapid redox reactions. Furthermore, the incorporation of conductive carbon materials and suitable binders during electrode fabrication improves the electrical conductivity and structural integrity of the electrode, leading to enhanced charge storage capability. The synergistic combination of ternary metal hydroxides with conductive carbon materials represents a promising strategy for designing next-generation high-performance supercapacitor electrodes.

References

1. Hongbo wang et.al. journal of alloys and compounds 870(2021) 159317
2. R.C.Rohit et.al. journal of alloys and compounds 2020. 158081
3. Chuan Jing et.al. RCS.ADV 2019,9. 9604
4. Caihong Yang et.al. journal of alloys and compounds 2020.157933
5. Duang Wang et al. Journal of alloys and compounds 726 (2017),306-314
6. V.N.Kintage et.al. materials for renewable and sustainable energy (2021).10:7
7. Ayaman E.Elkholy et .al.journal of the international society of electrochemistry (electrochemical Acta-2018
8. Ganesan sriram et.al.Energies 2025 18(18) 4846.
9. Fuzhi Li, et .al.batteries and energy storage 2026

Layered Double Hydroxide based Nanocomposite Electrode Materials for Supercapacitor: Mini Review

Priti S. Kharade, Amol R. Pardeshi

Department of Physics, Dada Patil Mahavidyalaya, Karjat, Dist: Ahilyanagar 414 402.

Email: amolrp111@gmail.com

Article DOI Link: https://zenodo.org/uploads/19794643

DOI: 10.5281/zenodo.19794643

Abstract

Layered double hydroxide (LDH) - based nanocomposites have emerged as promising electrode materials for advanced supercapacitor systems due to their tunable metal composition, layered structure, and abundant redox-active sites. Integration with conductive carbon frameworks significantly improves electrical conductivity, structural integrity, and ion transport dynamics. This chapter outlines the synthesis strategies, electrode fabrication, and electrochemical characteristics of several LDH-derived nanocomposites. Comparative analysis highlights the influence of compositional engineering and nanostructural design on capacitive behavior, demonstrating the potential of LDH hybrids for high-performance electrochemical energy storage applications.

Keywords: LDHs, Supercapacitor, Electrochemical

Introduction

Fossil fuel-based energy has intensified greenhouse gas emission that accelerate the global warming and environmental challenges. To change the dependency on fossil fuel demanding renewable and clean energy sources & storage devices. Batteries, fuel cell and supercapacitor are energy storage devices, electrochemical supercapacitors are gaining attention due to fast charge-discharge kinetics, high-power density, excellent cyclic life and long-term durability. They can be divided into two categorized on the base of charge storage mechanism: Electric double-layer capacitor (EDLCs) that store the energy through electrostatic force, and pseudocapacitors that store energy on the basic of faradaic reaction to achieve higher energy density but shorten lifespan. Overcome the limitation of EDLCs and Pseudocapacitor that develop the hybrid condition of supercapacitor which work on EDLCs and Pseudocapacitor [1-5].

Layered double hydroxides (LDHs) having potential application such as electrode material, catalysts, adsorbents, additive in polymers, photochemistry and precursors to mixed metal oxide catalysts due to tunable properties. LDHs,

also known as hydrotalcite like compounds or anionic clays, are a group of compounds which consist layer's metal cations and intercalated anions [6-9]. LDHs exhibits high specific surface area, which supported for fast ion transfer. This chapter reveals that the LDHs based nanocomposites material for electrode materials for supercapacitors.

Synthesis Approach

Synthesis of LDH Nanocomposite

Fig. 1 represent the WT-rGO@NiCoFe-LDH nanocomposite was synthesized via a solvothermal method. Briefly, 0.1 g of WT-rGO was ultrasonically dispersed in ethanol for 1 h to obtain a homogeneous suspension (Solution A). Separately, equimolar amounts of $Ni(NO_3)_2 \cdot 6H_2O$, $Fe(NO_3)_3 \cdot 9H_2O$, and ZIF-67 MOF were dissolved in deionized water under magnetic stirring to form Suspension B. Solution A was then added to Suspension B under vigorous stirring and mixed for 30 min to ensure uniform dispersion. The resulting mixture was transferred into a Teflon-lined stainless-steel autoclave and subjected to solvothermal treatment at 120 °C for 12 h. After naturally cooling to room temperature, the obtained precipitate was collected by filtration, thoroughly washed with deionized water and ethanol, and dried at 60 °C for 12 h to obtain the WT - rGO@NiCoFe - LDH nanocomposite. For comparison, NiCoFe - LDH was synthesized under identical conditions without the addition of WT - rGO [1]. In such manner different LDH based nanocomposite synthesized via. Different methods [2-5].

Electrode Fabrication of LDH Nanocomposite

The $rGO/Ni_xCo_\gamma S$ positive electrode was fabricated through a sequential hydrothermal growth and anion-exchange sulfurization strategy using nickel foam (NF) as a conductive scaffold. Initially, graphene oxide (GO) was coated onto the three-dimensional porous NF to introduce abundant oxygen-containing functional groups, facilitating heterogeneous nucleation and strong interfacial adhesion. Subsequently, mixed Ni^{2+} and Co^{2+} precursors with urea were subjected to hydrothermal treatment, resulting in the in-situ formation of NiCo oxide/hydroxide nanosheets ($rGO/Ni_xCo_\gamma O$) uniformly anchored on the GO-modified NF surface. The obtained intermediate was then converted into $rGO/Ni_xCo_\gamma S$ via a hydrothermal anion-exchange sulfurization process using Na_2S as the sulfur source for 8 h, where O^{2-} ions were partially replaced by S^{2-} ions. This topochemical sulfurization produced a hierarchically structured $rGO/Ni_xCo_\gamma S$ nanostructure with enhanced electroactive surface area, electrical conductivity, and redox-active sites. The Ni:Co molar ratio in the NiCo sulfide framework was systematically tuned to optimize the electrochemical performance

of the rGO/$Ni_xCo_\gamma S$/NF positive electrode [9].

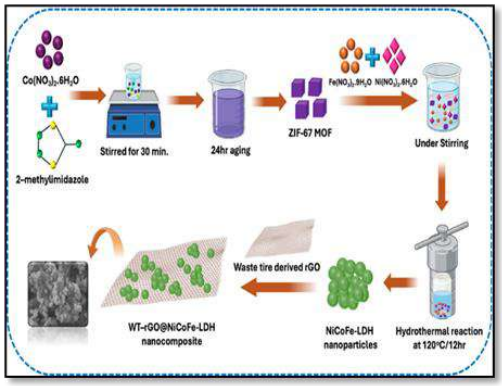

Fig. 1: Synthesis of WT-rGO@NiCoFe-LDH nanocomposite [1].

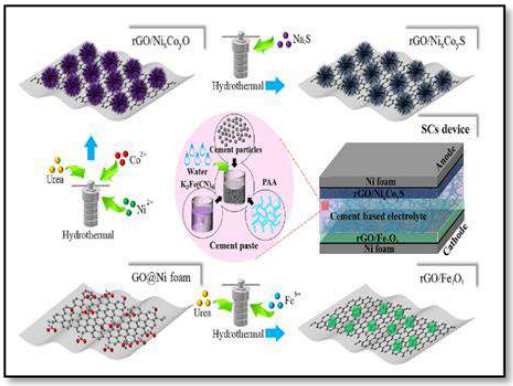

Fig. 2: Fabrication of Electrode and quasi-solid cement-based device [9].

Electrochemical Behavior

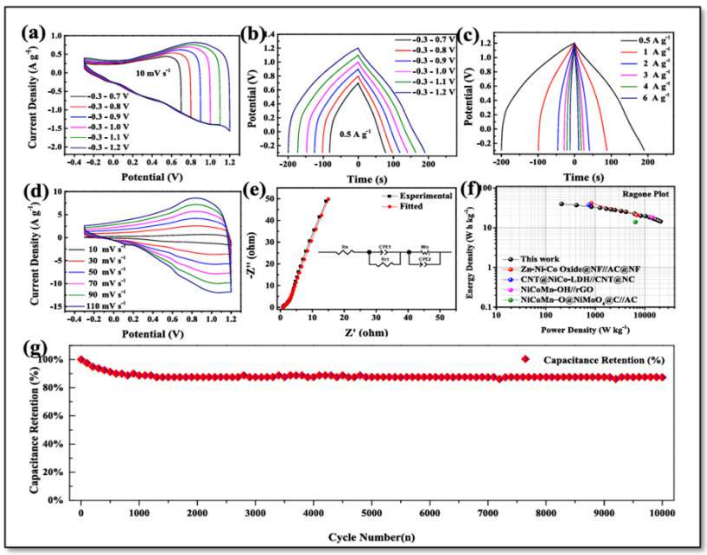

Fig. 3: Electrochemical performance of the CoNi/rGO // 3D rGO aerogel asymmetric supercapacitor: CV and GCD at varying voltage windows, scan rates, and current densities, along with EIS, Ragone plot comparison, and cycling stability over 10,000 cycles (Ref. [2]).

The electrochemical behavior of the assembled NiCo/rGO // 3D rGO aerogel asymmetric supercapacitor is illustrated in Fig. 3. The cyclic voltammetry curves recorded at 10 mV s^{-1} within different potential windows (1.0-1.5 V) are shown in Fig. 3(a). At 1.0 V, the negative electrode mainly exhibits electric double-layer characteristics, whereas the positive electrode displays a distinct faradaic redox peak. As the operating voltage window increases, the redox peak becomes more pronounced, indicating enhanced charge storage capability. The absence of

significant distortion even at 1.5 V confirms that this extended voltage window is electrochemically stable for the device. Galvanostatic charge–discharge (GCD) profiles obtained at 0.5 A g^{-1} under different voltage windows are presented in Fig. 3(b). The appearance of shoulder-like features during charging and discharging reflects the contribution of redox reactions. The nearly symmetric and parallel charge–discharge curves further verify the suitability of the 1.5 V operating window.The GCD curves measured within the 1.5 V window at current densities ranging from 0.5 to 6 A g^{-1} are shown in Fig. 3(c). With increasing current density, the redox-related shoulders gradually diminish due to limited reaction kinetics at higher rates. The nearly identical durations of the charge and discharge processes suggest a high coulombic efficiency of the asymmetric device. Electrochemical impedance spectroscopy results are presented in Fig. 3(e). The Nyquist plot shows a small semicircle in the high-frequency region and a nearly vertical line in the low-frequency region, which are typical features of capacitive systems. The intercept on the real axis corresponds to an internal resistance of approximately 0.8 Ω, while the semicircle diameter indicates an interfacial charge transfer resistance of about 0.5 Ω. The steep slope at low frequency suggests efficient ion diffusion within the electrode–electrolyte interface. The Ragone plot in Fig. 3(f) demonstrates the relationship between energy density and power density. The device delivers a high energy density of 39.58 Wh kg^{-1} at a power density of 200 W kg^{-1}. Even at a high-power density of 20,833.33 W kg^{-1}, an energy density of 14.375 Wh kg^{-1} is maintained, indicating good rate capability compared with previously reported Ni-Co based asymmetric supercapacitors. Long-term cycling stability was evaluated for 10,000 charge-discharge cycles at 10 A g^{-1}, as shown in Fig. 3(g). The device retains about 87.4 % of its initial capacitance, corresponding to a loss of only 12.6 %, which demonstrates excellent electrochemical durability. In addition, the assembled coin-type asymmetric supercapacitor is capable of powering a light-emitting diode, confirming its practical energy storage capability [2].

Comparative study of LDH based Nanocomposites for Supercapacitor

LDH Nanocomposite	Specific Capacitance (F/g)	Energy Density (Wh/kg)	Power Density (W/kg)	Ref.
WT-rGO@NiCoFe – LDH	110.7 F/g	39.36 Wh/kg	1098.41 W/kg	***01***
CoNi/rGO	5229.5 F/g	39.58 Wh/kg	14.38 W/kg	***02***
rGO@NiCoAl – LDHs	2291.6 F/g	91.4 Wh/kg	875 W/kg	***03***
NiFe2O4-NiCo-LDH@rGO	750 C/g	50 Wh/kg	-	***04***
2D NiMn LDH	612 C/g	60 Wh/kg	17.7 kW/kg	***05***

NiCoAl – LDH	592 C/g	22.18 $\mu Wh/cm^2$	3.0 mW/cm^2	***06***
CuCo LDH	1009 F/g	58.6 Wh/kg	850 W/kg	***07***
NiCo LDH	1454.2 F/g	56.4 Wh/kg	882.5 W/kg	***08***
rGO/NiCoS	4.55 F/cm^2	3.6 μWh/cm2	163.2 $\mu W/cm^2$	***09***

Conclusion

Layered double hydroxide–based nanocomposites have demonstrated strong potential as electrode materials for supercapacitor applications due to their layered structure, tunable composition, and abundant electroactive sites. The integration of LDHs with conductive carbon materials, particularly graphene derivatives, enhances electrical conductivity, ion transport, and structural stability during repeated electrochemical processes. Various LDH nanocomposites reported in this chapter exhibit improved capacitive behaviour and reliable cycling stability when utilized in asymmetric supercapacitor systems. Comparative analysis indicates that compositional tuning and nano structural design play a critical role in optimizing electrochemical performance. Therefore, LDH -derived hybrid materials provide an effective platform for the development of advanced and efficient energy storage devices.

References

1. Diksha Bhatt et. al. Journal of Power Sources 673 (2026) 239656
2. Honglu Wu et. al. Journal of Energy Storage 84 (2024) 110864
3. Dongxuan Guo et. al. chemical engineering journal 356 (2019) 955-963
4. Dawei Chu et. al. Journal of Colloid and Interface Science 568 (2020) 130–138
5. Abebaw Eshetie Kidie et. al. Journal of Industrial and Engineering Chemistry 133 (2024) 550–560
6. Chi Zhang et. al. Applied Surface Science 598 (2022) 153796
7. Xiaojie Xu et. al. Journal of Colloid and Interface Science 649 (2023) 355–363
8. Liyang Jiang et. al. Applied Surface Science 426 (2017) 148–159
9. Juan Wang et. al. Journal of Energy Storage 70 (2023) 107938

Supercapacitors for Sustainable Energy Storage: A Mini Review

[1]Amol R. Pardeshi, [2]Avinash R. Gaikwad

[1]Department of Physics, Dada Patil Mahavidyalaya, Karjat, Dist: Ahilyanagar 414 402.

[2]Department of Physics, Vivekanand College, Kolhapur, Dist: Kolhapur 416 003.

Email: amolrp111@gmail.com

Article DOI Link: https://zenodo.org/uploads/19794766

DOI: 10.5281/zenodo.19794766

Abstract

The growing global demand for sustainable energy solutions and the environmental impact associated with fossil fuel consumption have intensified research on advanced energy storage systems. Among the available electrochemical storage technologies, supercapacitors have emerged as attractive devices owing to their superior power capability, rapid charge - discharge response, long operational durability, and enhanced safety compared with conventional batteries. Positioned between dielectric capacitors and rechargeable batteries in terms of energy and power characteristics, supercapacitors provide an effective balance between fast energy delivery and moderate energy storage capacity. This chapter outlines the fundamental principles of supercapacitor technology, including device architecture, classification, and underlying charge storage processes. The operational mechanisms of electrical double-layer capacitors, pseudocapacitors, and hybrid supercapacitors are briefly discussed, along with their technological relevance in modern energy storage applications.

Keywords: Supercapacitor, EDLCs, Pseudocapacitor, Hybrid Supercapacitor, Charge Storage

Introduction

High energy production demand and new energy storage technology and devices. Thus, there is a growing technology needs high-performance, environment friendly and energy storage devices.

Currently, energy storage systems are depended on fossil fuel which main cause to global warming. Among these option, electrochemical energy storage gives possibility of directly storing electrical energy include electrostatic capacitors, rechargeable batteries, supercapacitors, fuel cells, etc. biofuel or batteries face the challenges about their lifespan, and other technical limitations.

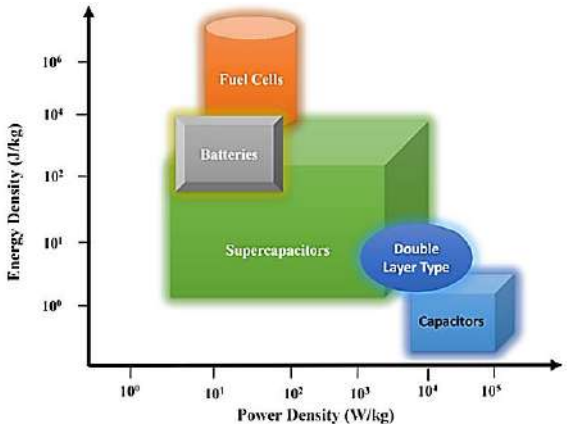

Fig. 1: Ragone Plot of Different Energy Storage Devices [01].

Supercapacitor are different form the conventional capacitor due to its exceptional electrochemical properties, excellent charge-discharge cycle, high specific power density, high energy density. a plot of energy density and power density called Ragone plot for various Electrochemical Energy storage device including supercapacitor in fig. 1. [1-6]. Supercapacitor fall between rechargeable batteries and capacitors and provide the high-power density and fast charging and discharging. Moreover, supercapacitor tend to be safer than lithium-ion batteries, supercapacitor exhibit high power density as compare to batteries and high energy density as compare to normal capacitor [7-14]. This chapter reveals that the fundamental knowledge about supercapacitor, energy storage mechanism and application regarding supercapacitor.

Fundamentals of Supercapacitor

Supercapacitor mainly classified into three types i. Electric Double Layer Capacitor (EDLCs), ii. Pseudocapacitor, and iii. Hybrid Supercapacitor which represented in fig. 2, also fig. 3 represent the structure of supercapacitor.

- **Electric Double Layer Capacitor (EDLCs):** EDLCs operate on the principle of electrostatic force and electrode material of EDLCs fabricated via active porous materials such as graphene, activated carbon etc. contact between electrode and electrolyte where electric charge stored. The capacitor of EDLCs electrode is estimated by given equation

$$\boldsymbol{C = \frac{\varepsilon_r \varepsilon_o A}{d}}$$

Where, ε_r= relative permittivity of electrolyte,ε_o=is the permittivity

in space,d=separation distance between charge in EDL,and A-area of porous electrode material [7].

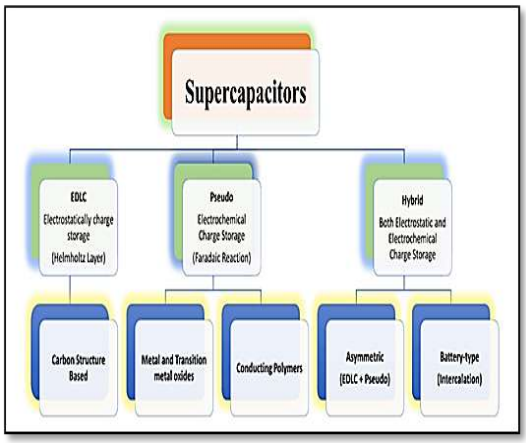

Fig. 2: Classification of Supercapacitor [01].

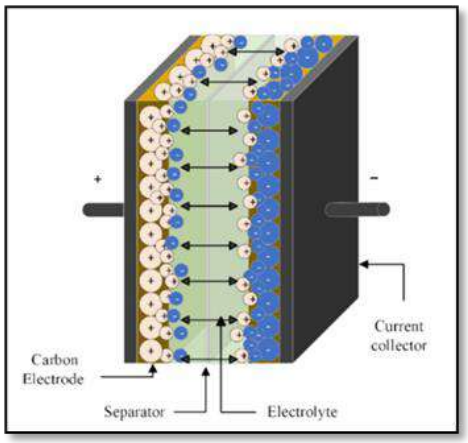

Fig. 3: Structure of Supercapacitor [04].

- **Pseudocapacitor:** Pseudocapacitor electrode material work on the principle of reversible redox reaction which take place to electrode surface. Specific capacitance of Pseudocapacitor is higher compare to EDLCs. Pseudcapacitor are divided into three parts due to charge storage mechanism a) Adsorption Pseudocapacitance, b) Redox Pseudocapacitor and c) Intercalation supercapacitor [7-9].

- **Hybrid Supercapacitor:** Hybrid supercapacitors have attracted considerable attention as promising candidates for next-generation high-performance energy storage technologies. The development of these devices is primarily intended to address the inherent limitations associated with both electrical double-layer capacitors (EDLCs) and pseudocapacitors while simultaneously integrating the beneficial characteristics of each system. By combining different charge-storage mechanisms within a single device architecture, hybrid supercapacitors are capable of delivering enhanced electrochemical performance. These systems are typically designed to achieve improved energy density while maintaining high power output, rapid charge-discharge capability, and extended cycling durability. The synergistic interaction between capacitive and faradaic processes allows hybrid configurations to balance energy storage capacity and power delivery more effectively than conventional supercapacitor types. Furthermore, overcoming the performance constraints of individual capacitor systems opens the possibility of developing economically viable hybrid supercapacitors suitable for practical large-scale energy storage applications [1-8].

Energy Storage Mechanism of Supercapacitor

Fig. 4 represent the energy storage mechanism for supercapacitor.

Supercapacitors are electrochemical energy storage devices consisting of two oppositely charged electrodes, an electrolyte, a separator, and protective encapsulation. The separator prevents electrical contact between the electrodes while allowing ion movement through the electrolyte. Based on their charge storage mechanisms, supercapacitors are generally classified into three types: electrical double-layer capacitors (EDLCs), pseudocapacitors, and hybrid supercapacitors. In EDLCs, energy storage occurs through electrostatic accumulation of ions at the electrode-electrolyte interface, forming an electrical double layer. This process is non-faradaic, meaning that no redox reactions or electron transfer take place. As a result, EDLCs exhibit highly reversible charge storage, fast charge-discharge capability, and excellent cycling stability without significant structural changes in the electrode material. Pseudocapacitors store energy through rapid and reversible faradaic reactions occurring at or near the electrode surface. These reactions involve charge transfer processes such as surface redox reactions, ion adsorption, or intercalation within the electrode material. In practical systems, both double-layer capacitance and pseudocapacitance may coexist and contribute to the overall capacitance. Hybrid supercapacitors combine the characteristics of EDLCs and pseudocapacitors by employing different types of electrodes, typically a battery-type electrode and a capacitive electrode. This configuration enables higher energy storage capacity while maintaining high power density and rapid charge-discharge performance [9-14]. Fig. 5 represent the application of supercapacitor in several industry, electric vehicle, renewable energy and consumer electronics [9].

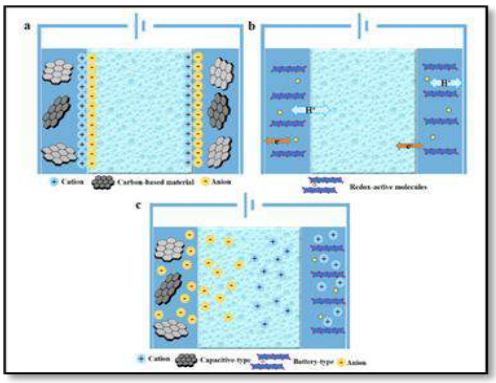

Fig 4: Energy storage Mechanism in Supercapacitor [14].

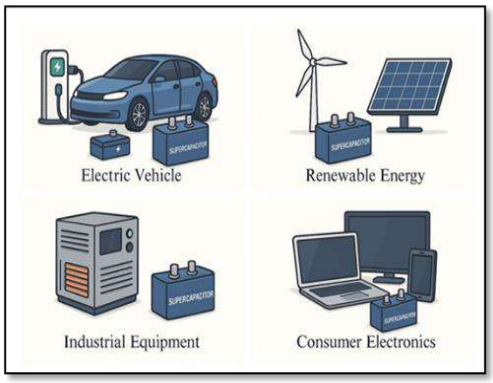

Fig. 5: Application of Supercapacitor [09]

Conclusion

Supercapacitors constitute an important category of electrochemical energy storage devices capable of delivering high power output, rapid electrochemical response, and extended cycling stability. The energy storage behaviour of these systems is governed by two principal mechanisms: electrostatic ion accumulation

at the electrode-electrolyte interface and reversible faradaic reactions occurring within the electrode material. Electrical double-layer capacitors rely predominantly on interfacial charge separation, whereas pseudocapacitors store energy through fast surface redox processes. Hybrid supercapacitors integrate both mechanisms to achieve improved electrochemical performance. Owing to their distinctive characteristics, supercapacitors have become increasingly important in applications such as renewable energy systems, electric mobility, and portable electronic technologies. Continued progress in material engineering and device optimization is expected to further enhance their efficiency and expand their role in future energy storage systems.

References

1. Neeraj Singh et. al. Journal of Energy Storage 121 (2025) 116498
2. S.M. Sultan Mahmud Rahat et. al. Journal of Energy Storage 73 (2023) 108847
3. Saeid Zahedi Asl et. al. Journal of Molecular Structure 1342 (2025) 142703
4. Kavishka Dissanayake et. al. Journal of Energy Storage 96 (2024) 112563
5. Wenxuan Hu et. al. Journal of Energy Storage 134 (2025) 118278
6. Vinodhini S.P et. al. Journal of Power Sources 669 (2026) 239429
7. Ranjan Kumar Maurya et. al. Journal of Power Sources 640 (2025) 236818
8. Iqbal Singh et. al. Next Research 2 (2025) 100228
9. Sudhana J et. al. Results in Engineering 29 (2026) 108720
10. Nidhi Puri et. al. Bioresource Technology Reports 33 (2026) 102506
11. Sajjad Gharanli et. al. Journal of Energy Storage 122 (2025) 116509
12. Gülcan Aydın Journal of Energy Storage 150 (2026) 120234
13. V.J. Vipu Vinayak et. al. Journal of Energy Storage 100 (2024) 113551
14. Chenyu Du et. al. Journal of Alloys and Compounds 1054 (2026) 186363

$MnFe_2O_4$ Based Nanocomposites for High-Performance Supercapacitor Applications: A Concise Review

S. A. Sagade, S. A. Bagwan, B. S. Maharnavar

Rayat Shikshan Sanstha's Dada Patil Mahavidyalaya Karjat Dist- Ahilyanagar-414402

Email: balbhimph022@gmail.com

Article DOI Link: https://zenodo.org/uploads/19794870

DOI: 10.5281/zenodo.19794870

Abstract

The growing global energy demand requires efficient energy storage systems to support renewable sources, and manganese ferrite ($MnFe_2O_4$), a spinel-structured transition metal oxide with rich redox activity and good conductivity, has developed as a promising pseudocapacitive material designed for high-performance supercapacitors. $MnFe_2O_4$ can be synthesized using hydrothermal, sol–gel Method which allow precise control over particle size, morphology, and crystallinity. Electrochemical studies using cyclic voltammetry (CV) and galvanostatic charge–discharge (GCD) indicate combined electric double-layer and pseudocapacitive behavior, with reversible Mn^{2+}/Mn^{3+} and Fe^{2+}/Fe^{3+} redox reactions enhancing charge storage. $MnFe_2O_4$-based composites, such as polyaniline (PANI)/$MnFe_2O_4$ and reduced graphene oxide (rGO)/$MnFe_2O_4$, exhibit better specific capacitance, rate capability, and cycling stability due to synergistic effects. These findings demonstrate that $MnFe_2O_4$ and its composites are promising candidates for high-performance, cost-effective supercapacitor electrodes, contributing to advanced energy storage solutions.

Keywords: Supercapacitor, cyclic voltammetry, Spinel ferrite, Power Density

Introduction

Today's global energy demand is increasing rapidly due to population growth, Industrial development, urbanization [1]. The rising use of electricity in homes, industries, Electric vehicles has significantly contributed to this growth [2]. To support the long-term developmental needs of modern society, there has been a significant shift toward integrating renewable energy sources such as solar, wind, and tidal power into the energy sector [3–4]. However, the intermittent and variable nature of these energy sources prevents their direct and stable integration into the power grid. Therefore, the development of efficient and reliable electrical energy storage systems has become urgently necessary to ensure continuous and stable energy supply [5]. Supercapacitors are high-power energy storage devices

with fast charging, long cycle life, and expanding applications, though improving their energy density remains a key research focus [6]. Some ferrite materials such as NiFe2O4, ZnFe2O4, CoFe2O4, CuFe2O4 and MnFe2O4, emphasizing their potential to enhance energy density and overall performance in advanced energy storage systems [7].

Supercapacitors play a vital role, because of their superior power output and quick charging ability and long cycle life. Advance materials like MnFe2O4 are being developed to enhance performance for renewable energy. Energy density can be improved using several strategies, such as widening the operating potential window of supercapacitors, enhancing the ratio of active to inactive components within the cell, employing porous electrode materials, and tailoring the surface characteristics of both anode and cathode materials. Furthermore, combining a pseudocapacitive electrode with an electric double-layer mechanism, as implemented in hybrid supercapacitor devices, can effectively increase both capacitance and operating voltage [8–9]. Manganese ferrite ($MnFe_2O_4$) is a spinel-structured transition metal oxide that has attracted interest as a pseudocapacitive electrode material due to its high redox activity and relatively high electrical conductivity, which enhance charge storage in supercapacitors. Recent studies show that designing $MnFe_2O_4$ in nanostructured or composite forms significantly improves its electrochemical performance, including higher specific capacitance and cycling stability, making it a hopeful candidate for advanced renewable storage devices [10-11]

Energy density may be enhanced by various approaches, with growing the supercapacitor working potential window, increasing the amount of active to inactive material in the cell, using porous materials in supercapacitors, and improve the surface characteristics of the anode and cathode materials. moreover, the capacitance and voltage can be intensified by combination a pseudocapacitive electrode with an electric double layer as in of hybrid supercapacitor device [12].

Synthesis Methods of MnFe2O4

$MnFe_2O_4$ nanoparticles can be synthesized using various methods, including sol–gel, auto-combustion, hydrothermal, co-precipitation and chemical bath deposition (13). The hydrothermal method (fig.1 a) involves reacting metal precursors and graphene oxide in a sealed autoclave at elevated temperature and pressure, promoting controlled nucleation and growth of $MnFe_2O_4$ on rGO sheets. By adjusting precursor concentration, particle size, morphology, and dispersion on rGO can be tuned, directly influencing supercapacitor performance (14). The sol–gel method (fig.1 b) converts a solution into a solid gel via hydrolysis and condensation, offering high purity, homogeneity, and controlled particle size. Using natural polymers, $MnFe_2O_4$ nanoparticles were synthesized with tunable size, morphology, and surface properties, resulting in well-dispersed particles

with adjustable structural, optical, magnetic, catalytic, and biological characteristics. This technique is simple, versatile, and operates at low temperatures (15).

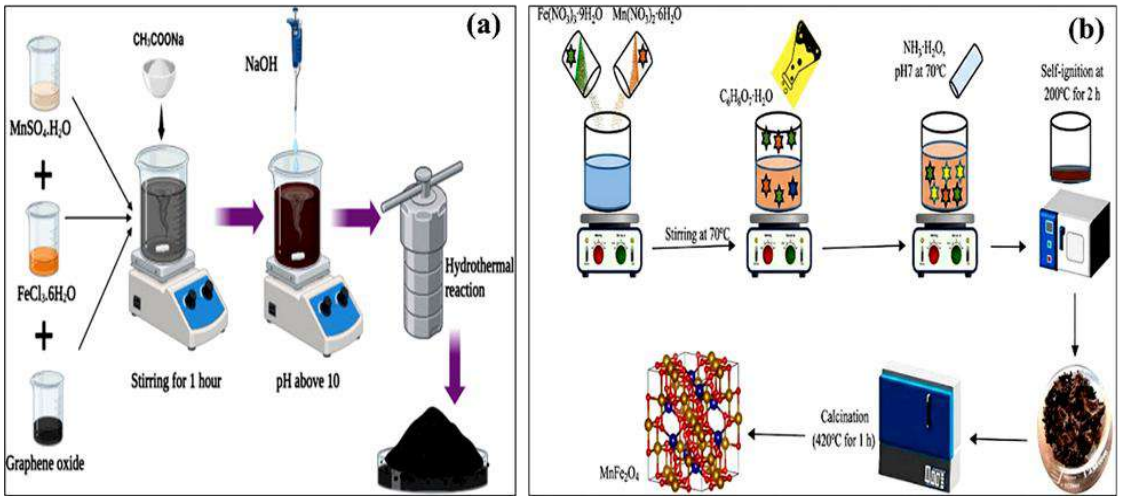

Fig.1. Synthesis of MnFe2O4 and Its Composites from (a) Hydrothermal method and (b) Sol Gel Auto combustion Method [14-15]

Structural, Morphological and Elemental Study

The structural, morphologic, and elemental characteristics of $MnFe_2O_4$ and its composites are commonly analyzed using techniques such as XRD for phase identification and crystallinity, SEM for particle size and shape, and EDS for elemental composition. When combined with other phases, such as ZnO or $BaTiO_3$, the composites display heterogeneous but well-distributed morphologies with distinct structural domains confirmed by XRD and microscopic analyses [16,17]. Pure $MnFe_2O_4$ nanoparticles typically exhibit a cubic spinel structure with spherical or near-spherical morphology and nanoscale particle sizes (~20–40 nm), often showing some agglomeration due to high surface energy, these combined characterization methods provide comprehensive insights into the crystallographic, morphological, and compositional evolution of $MnFe_2O_4$ systems, which is essential for tailoring their functional properties [18].

Electrochemical Study

The electrochemical behavior of the prepared electrodes was analyzed using EIS, CV, and GCD techniques. The CV curves of the $MnFe_2O_4$/rGO composite electrode (Fig.2 a) at scan rates of 10–70 mV s^{-1} show distinct redox peaks, confirming its pseudocapacitive behavior due to Faradaic reactions of $MnFe_2O_4$. The CV curves retain similar shapes at different scan rates, indicating good reversibility and rate capability. The larger CV area of $MnFe_2O_4$/rGO compared to pure $MnFe_2O_4$ suggests a higher specific capacitance (Fig.2 b). GCD

measurements within the 0–0.5 V potential window further confirm the pseudocapacitive nature of the electrode. The $MnFe_2O_4$/rGO composite shows a specific capacitance of 195 F g^{-1} at 1 A g^{-1} (fig.2 c), which is higher than pure $MnFe_2O_4$ (77 F g^{-1}) and rGO (67 F g^{-1}) (fig. 2 d). This improved performance results from the synergistic effect of $MnFe_2O_4$ providing active sites and rGO enhancing electrical conductivity and charge transport (19).

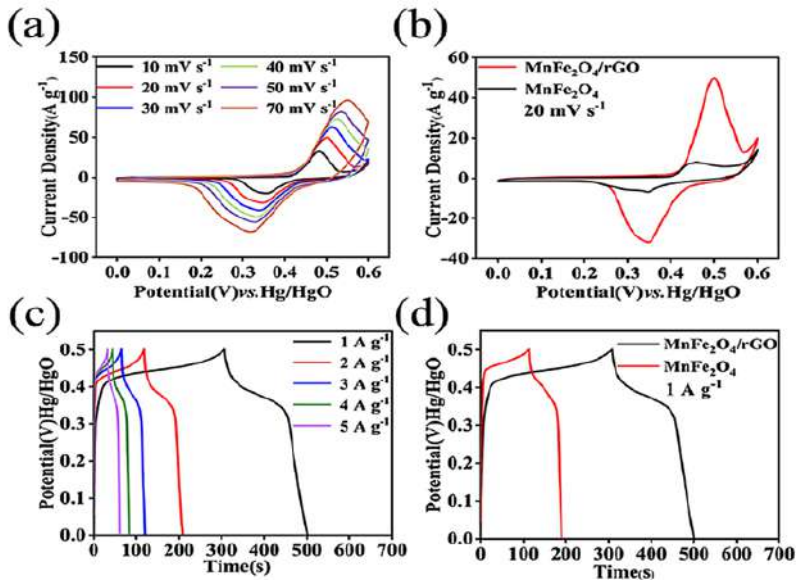

Fig. 2. Comparison of electrochemical performance through cyclic CV and GCD curves of $MnFe_2O_4$ and $MnFe_2O_4$/rGO electrodes at different scan rates.

Conclusion

$MnFe_2O_4$ is a hopeful pseudocapacitive material for supercapacitor electrodes due to its multiple oxidation states, good stability, and suitable electrical conductivity. Various synthesis methods like sol–gel, hydrothermal, co-precipitation, and chemical bath deposition allow the controlled preparation of $MnFe_2O_4$ nanostructures. XRD, SEM, and EDX provide information about crystallinity and particle distribution. The incorporation of reduced graphene oxide (rGO) improves electrical conductivity, prevents particle aggregation, and enhances electrochemical performance. Electrochemical studies using CV, GCD, and EIS show that $MnFe_2O_4$/rGO composites exhibit higher specific capacitance and better rate capability than pure $MnFe_2O_4$. Therefore, $MnFe_2O_4$-based nanocomposites are promising materials for advanced supercapacitors and future energy storage applications.

References

1. Zhou, J., Zhang, S., Zhou, Y. N., Tang, W., Yang, J., Peng, C., & Guo, Z. (2021). Electrochemical Energy Reviews, 4(2), 219–248.

2. Jiang, Y., & Liu, J. (2019). Energy & Environmental Materials, 2(1), 30–37.
3. Hao, J., Liu, H., Han, S., & Lian, J. (2021). ACS Applied Nano Materials, 4(2), 1330–1339.
4. Meftahi, A., Reisi-Vanani, A., & Shabani-Nooshabadi, M. (2023). Fuel, 331, 125683.
5. Zahedi, F., & Shabani-Nooshabadi, M. (2023). Fuel, 335, 127083.
6. Gopi, M., V. V., C., Alzahmi, S., Narayanaswamy, V., Vinodh, R., Issa, B., & Obaidat, I. M. (2023). 61, 106773
7. Kumbhar, A. A., Bachankar, S. S., Lokhande, V. C., Kim, C., & Ji, T. (2025). Journal of Solid-State Electrochemistry, 30, 519–566.
8. Bhosale, S. V., & Bhosale, S. V. (2025). Chemical Science, 16(23), 10159–10227.
9. Kumbhar, A. A., Bachankar, S. S., Lokhande, V. C., Kim, C., & Ji, T. (2025). Journal of Solid-State Electrochemistry, 30, 519–566.
10. Zahedi, F., & Shabani-Nooshabadi, M. (2023). Fuel, 335, 127083.
11. Devi, R., Patra, J., Tapadia, K., Sutar, A. K., Chang, J.-K., & Maharana, T. (2023). 67, 107548.
12. Bhosale, R., Bhosale, S., Sankannavar, R., Chavan, V., Jambhale, C., Kim, H., & Kolekar, S. (2024). ACS Applied Nano Materials, 7(4), 4078–4091.
13. Sun, Y., Feng, J., Zhu, W., Hou, R., Zhang, B., & Ishag, A. (2024). Science of The Total Environment, 954, Article 176378.
14. Chavan, P. P., Babar, U. D., Redekar, R. S., Chougale, A. D., Tarwal, N. L., & Kamble, P. D. (2024). Journal of Alloys and Compounds, 999, 171-185
15. Nadafan, M., Puladrak, M., Majidi, R., Karimi, Z., & Mousavi, M. (2023). Journal of the Australian Ceramic Society, 59(2), 491–500.
16. Li, S., Liu, R., & Xiong, X. (2025). Metals, 15(8), 903.
17. Medina, J. A. L. López. (2025). ACS Omega, 10(17), 17595–17610.
18. Zhu, Q., et al. (2025). Journal of Magnetism and Magnetic Materials, 628, 173178.
19. Chai, S., Zheng, R., Guo, R., Luo, H., Cai, H., Liang, L., Huang, H., & Cheng, Z. (2023). Journal of Materials Science: Materials in Electronics, 34, 1–12.

Carbon-Based Materials for Energy Storage Devices: A Review

Suhani M. Karande, Tejswini Y. Farande, Balbhim S. Maharnavar

Rayat Shikshan Sanstha's Dada Patil Mahavidyalaya Karjat Dist- Ahilyanagar-414402

Email: balbhimph022@gmail.com

Article DOI Link: https://zenodo.org/uploads/19794984

DOI: 10.5281/zenodo.19794984

Abstract

Carbon-based nanomaterials have attracted significant attention as advanced electrode materials for energy storage devices due to their high electrical conductivity, large specific surface area (1000–3000 $m^2\ g^{-1}$), chemical stability, and tunable porous architecture. Nanostructured carbons such as activated carbon, graphene, reduced graphene oxide, and carbon nanotubes exhibit superior electrochemical performance with rapid charge transfer and high capacitance. Several synthesis methods including chemical vapor deposition (700–1000 °C), hydrothermal synthesis (120–200 °C), template-assisted techniques, and biomass-derived carbonization (600–900 °C) enable controlled morphology and porosity. Furthermore, carbon-based composites such as graphene/MnO_2, CNT/$NiCo_2O_4$, rGO/$MnFe_2O_4$, and graphene/PANI demonstrate enhanced specific capacitance (≈350–400 F g^{-1}) and improved electrochemical stability due to synergistic redox and conductive interactions

Keywords: Carbon, hybrid composites, electrochemical, power density.

Introduction

The rising global need for efficient and sustainable energy storage systems has driven significant research toward the development of advanced electrode materials for batteries and supercapacitors. Among various candidates, carbon-based materials have gained considerable attention owing to their outstanding electrical conductivity, large surface area, excellent chemical stability, and adaptable porous architectures. These materials are extensively employed in electrochemical energy storage devices due to their superior conductivity, remarkable stability, and high specific surface area. These properties enable efficient charge storage and rapid electron transport, which are essential for high-performance supercapacitors and batteries [1]. Several types of carbon nanomaterials have been investigated for energy storage applications. The most commonly used carbon materials include are Activated Carbon (AC), Graphen (GR), Reduced Graphene Oxide(rGO), Carbon Nanotube (CNT), Multiwalled carbon nanotube (MWCNT), single walled carbon nanotube (SWCNT), carbon

nanofiber (CNF), mesoporous carbon, Hierarchical porous carbon (HCP), Graphite carbon. ACs is one of the most widely used electrode materials in commercial supercapacitors due to its extremely high surface area (typically 1000–3000 $m^2\ g^{-1}$) and well-developed porous structure. These features enable efficient adsorption of electrolyte ions, which enhances the electric double-layer capacitance [2]. Graphene's two-dimensional layered framework enables fast electron movement and effective electrolyte ion transport, thereby overall enhancing the electrochemical behaviour of energy storage systems [3]. CNTs show excellent electrical conductivity and mechanical strength. Their tubular structure provides efficient pathways for electron transport, which enhances the power density of supercapacitors and batteries [4].

In addition to pure carbon materials, researchers have developed carbon-based composites that combine carbon nanostructures with metal oxides, sulfides, or conductive polymers. These composites exhibit synergistic effects that improve electrochemical activity and stability. Some Common carbon-based composites used in energy storage include are Graphene /MnO2, rGO/Fe2O4, CNT/NiCo2O4, Graphene/Co3O4, rGO/MnFe2O4, CNT/MnO2, Graphene/PANI, rGO/PPY, Carbon nanofibre/NiO and Activated Carbon/MnO2. For example, graphene/MnO_2 composites have shown specific capacitance values as high as 350–400 F g^{-1}, which is significantly higher than pure carbon electrodes [5]. Similarly, CNT/$NiCo_2O_4$ nanocomposites exhibit excellent electrochemical performance due to improved electrical conductivity and enhanced redox activity [6].

Synthesis Methods of Carbon-Based Materials

The preparation method significantly influences the structural characteristics and electrochemical performance of carbon-based materials

- **Chemical Vapor Deposition (CVD)**

Chemical vapor deposition is widely used for synthesizing high-quality graphene and carbon nanotubes. During this process, hydrocarbon gases like methane (CH_4) or acetylene (C_2H_2) undergo thermal decomposition at elevated temperatures (700–1000°C) in the presence of metal catalysts such as Fe, Co, or Ni. The carbon atoms then deposit on the catalyst surface to form graphene sheets or CNT structures. CVD-produced graphene exhibits excellent electrical conductivity and crystallinity, which is beneficial for energy storage applications [7].

- **Hydrothermal Method**

The hydrothermal method is commonly used to synthesize graphene oxide, reduced graphene oxide, and carbon-based nanocomposites. The reaction occurs in a sealed autoclave at temperatures between 120–200°C and high pressure. This

method allows the formation of porous carbon structures and hybrid nanocomposites with controlled morphology [8].

- **Template-Assisted Method**

Template-assisted synthesis is used to produce porous carbon materials with controlled pore size and structure. Templates such as silica nanoparticles or polymer spheres are used to create pores in carbon frameworks. After carbonization, the template is removed by chemical etching, resulting in highly porous carbon materials suitable for energy storage applications [9].

- **Biomass-Derived Carbon**

Biomass-derived carbon materials are produced from natural resources such as coconut shells, rice husks, banana peels, and sugarcane bagasse. These materials are carbonized at high temperatures (600–900°C) and activated using chemical agents such as KOH or $ZnCl_2$. Biomass-derived carbons often exhibit hierarchical pore structures and high surface area, making them attractive for supercapacitor electrodes [10].

Structural and Study of Carbon-Based Materials

- **X-ray Diffraction (XRD)**

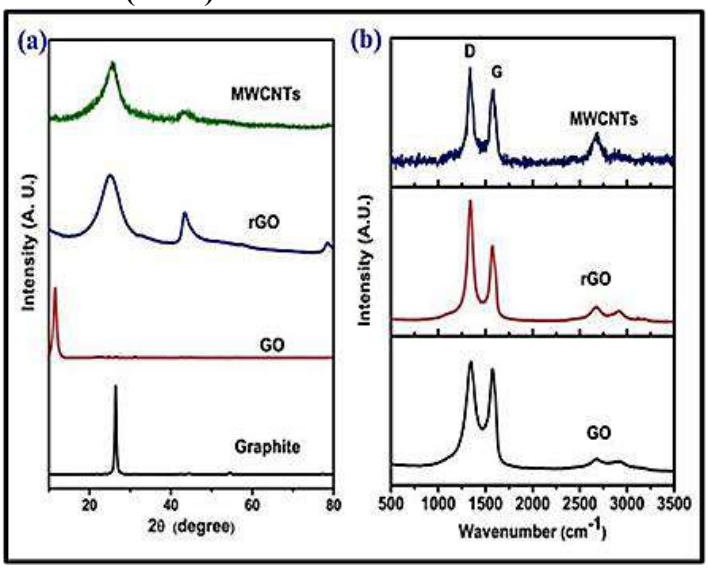

Fig. 1 (a) XRD pattern of graphite, GO, rGO and MWCNTs, (b) Raman spectra of GO, rGO and MWCNTs. [11]

The XRD pattern shows a sharp diffraction peak of graphite at $2\theta \approx 26.5°$ (002 plane), which shifts to ~10–11° in GO due to oxidation and increased interlayer spacing (~0.8 nm). After reduction, rGO exhibits a broad peak around 24–25°, indicating partial restoration of the graphitic structure and reduced layer spacing. The Raman spectra show two characteristic bands: the D band (~1340–1350

cm^{-1}) related to structural defects and the G band (~1580–1600 cm^{-1}) corresponding to the sp^2 carbon network. The ID/IG intensity ratio increases from GO to rGO, confirming the formation of defects and successful reduction of graphene oxide [11].

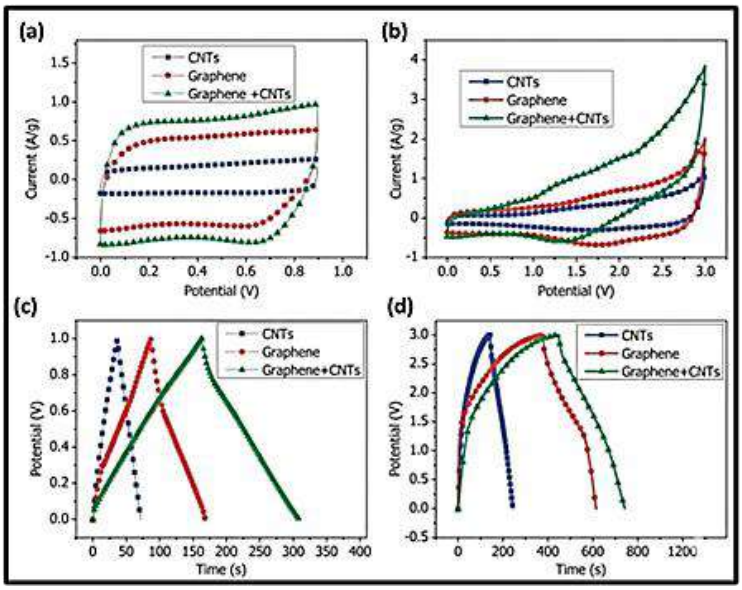

Fig. 2 Electrochemical properties of various electrodes made of CNTs and Graphene, graphene, and graphene/CNT composite [12]

Electrochemical Study

The electrochemical performance of CNTs, graphene, and graphene@CNTs composite electrodes is shown in Fig.3 (a–d). In the Cyclic Voltammetry curves (a) within the potential window of 0–1 V, the graphene@CNTs electrode exhibits the largest current response about 1.0 A g^{-1} compared to graphene 0.6 A g^{-1} and CNTs 0.2 A g^{-1}, indicating higher capacitance. Similarly, in the wider potential range of 0–3 V (b), the graphene@CNTs composite shows the highest current density reaching about 3.5–4.0 A g^{-1}, while graphene and CNTs reach around 2.0 A g^{-1} and 1.2 A g^{-1}, respectively. The Galvanostatic Charge–Discharge curves (c) at 0–1 V show that CNTs discharge within about 70 s, graphene within 150 s, and graphene@CNTs extend up to 350 s, indicating improved charge storage. A similar trend is observed at 0–3 V (d), where CNTs discharge around 200 s, graphene around 600 s, and graphene@CNTs reach approximately 1200 s, confirming the superior capacitance and electrochemical performance of the graphene@CNTs composite electrode due to its enhanced conductivity and larger effective surface area [12].

Applications of Carbon-Based Materials in Energy Storage Devices

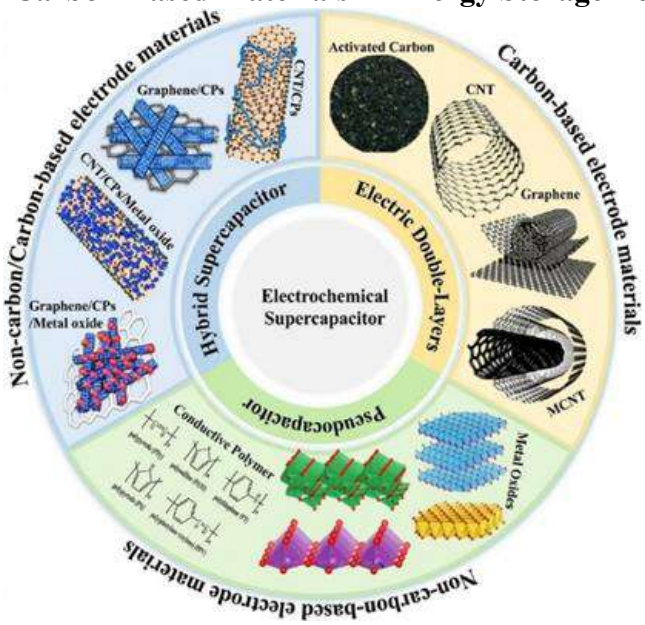

Fig.3 Common electrode materials used in different types of SCs. Adapted with permission from Hu et al. [13].

The diagram (Fig.3) presents the categorization of electrochemical supercapacitors into electric double-layer capacitors (EDLCs), pseudocapacitors, and hybrid supercapacitors, emphasizing their distinct charge storage mechanisms. It further shows common electrode materials, including carbon-based materials (activated carbon, graphene, CNTs), metal oxides, conducting polymers, and their composites used to enhance electrochemical performance [13]. Carbon-based materials play a crucial role in various electrochemical energy storage systems. In supercapacitors, electrodes made of activated carbon and graphene deliver high power density and outstanding cycling stability owing to their large surface area and superior electrical conductivity [14]. In lithium-ion batteries, graphene and carbon nanotubes are commonly used as conductive additives and anode materials to improve electron transport and structural stability [15]. Porous carbon materials are also hopeful anode materials for sodium-ion batteries, where their large interlayer spacing allows efficient sodium ion insertion and extraction [16].

Carbon nanomaterials are also used in hybrid energy storage devices, such as lithium-ion capacitors, where carbon electrodes provide high power density while battery-type materials contribute to high energy density [17]. Flexible carbon nanomaterials such as carbon nanofibers, graphene films, and CNT networks have enabled the development of flexible and wearable supercapacitors for portable electronics [18]. Carbon-based electrodes play a crucial role in large-scale energy storage systems, enabling the storage of

electricity produced from renewable sources such as solar and wind energy [19].

Conclusion

Carbon-based nanomaterials and their composites exhibit excellent electrochemical characteristics due to high electrical conductivity, hierarchical porosity, and large active surface area. Hybrid structures such as graphene/MnO_2, CNT/$NiCo_2O_4$, and rGO/PPY significantly enhance capacitance and cycling stability, making them promising electrode materials for high-performance supercapacitors and next-generation energy storage systems.

References

1. Simon, P., & Gogotsi, Y. (2020). Nature Materials, 19(11), 1151–1163.
2. Sevilla, M., & Mokaya, R. (2014). Energy & Environmental Science, 7(4), 1250–1280.
3. Novoselov, et al. (2012. Nature, 490(7419), 192–200.
4. Iijima, S. (1991). Nature, 354(6348), 56–58
5. Yu, G., Hu, et al. (2011). Nano Letters, 11(10), 4438–4442.
6. Wang, H et al. (2012). Nature Communications, 3, 917.
7. Li, X., et al. (2009. Science, 324(5932), 1312–1314.
8. Marcano, D. C et al. (2010). ACS Nano, 4(8), 4806–4814.
9. Lee, J., et al. (2006). Advanced Materials, 18(16), 2073–2094.
10. Titirici, M. M, et al. (2015). Chemical Society Reviews, 44(1), 250–290.
11. Sa, K., Mahakul, et al. (2018.IOP Conference Series: Materials Science and Engineering, 338(1), 012055.
12. Zhang, Y., et al. (2025). Journal of Energy Storage, 137, 118566
13. Hu, W., et al. (2021). Materials 14 (16), 4571.
14. Liu, Y., et al. (2024). Journal of Power Sources, 617, 235140.
15. Zhang, Q., et al. (2023. Journal of Energy Storage, 63, 106995.
16. Liang, Y., et al. (2020). RSC Advances, 10, 22663–22667.
17. Wang, F., et al. (2017. Chemical Society Reviews, 46(22), 6816–6854.
18. Han, Y., et al. (2023). Applied Sciences, 13(5), 3290.
19. Mishra, S., et al. (2025). Energy & Fuels, 39(28), 13151–13182.

Carbon-Based $ZnFe_2O_4$ Advanced Electrodes for Supercapacitor Application: A Review

Dhawale Sagar, Kangude Sahadev H., Torkad Aaditya S.

Department of Physics, Rayat Shikshan Sanstha's Dada Patil Mahavidyalaya Karjat,

Dist- Ahilyanagar-414402

Email: sagardhawale842@gmail.com

Article DOI Link: https://zenodo.org/uploads/19795075

DOI: 10.5281/zenodo.19795075

Abstract

Ferrite ($ZnFe_2O_4$) composites have emerged as favourable material because of their excellent electrical conductivity, high surface area, and strong redox activity. Charge transfer and electrochemical stability are enhanced when ZnFe2O4 nanoparticles are combined with carbon materials such graphene, reduced graphene oxide (rGO), carbon nanotubes (CNTs), activated carbon, and carbon nanofibers. Composites such as $ZnFe_2O_4$/rGO, $ZnFe_2O_4$/CNT, and $ZnFe_2O_4$/activated carbon provide enhanced ion diffusion and abundant electroactive sites. This chapter reviews synthesis methods, structural characterization, and electrochemical performance of carbon-based $ZnFe_2O_4$ composites for high-performance supercapacitor applications.

Keywords: ZnFe2O4, Composites, Electrochemical stability, Supercapacitor.

Introduction

The need for effective and dependable energy storage devices has grown dramatically due to the quick development of contemporary technology, including as portable electronics, hybrid electric cars, and renewable energy systems. Supercapacitors have drawn a lot of interest among different energy storage systems because of its high-power density, quick charge-discharge capability, extended cycle life, and superior stability when compared to traditional batteries [1,2]. These advantages make supercapacitors highly suitable for applications requiring fast energy delivery and long operational lifetimes. The materials utilized for the electrodes have a major impact on supercapacitor performance. Because of their high electrical conductivity, huge specific surface area, and good chemical stability, carbon-based materials like activated carbon, graphene, carbon nanotubes, and carbon nanofibers are employed extensively. [3]. However, carbon materials primarily store charge through electrostatic adsorption, which often results in relatively low capacitance and limited energy

density.To enhance the energy storage capability of supercapacitors, transition metal oxides and ferrite materials have been incorporated into carbon matrices. Zinc ferrite ($ZnFe_2O_4$) has attracted noteworthy attention as an electrode material because of its environmental friendliness, cheap in cost, high theoretical capacitance, and multiple oxidation states that facilitate reversible redox reactions [4]. The spinel structure of $ZnFe_2O_4$ provides a stable framework for electrochemical reactions and efficient ion diffusion during charge–discharge processes.

However, pure $ZnFe_2O_4$ electrodes often suffer from poor electrical conductivity and limited electrochemical performance. To overcome these limitations, researchers have developed carbon-based $ZnFe_2O_4$ composites, where $ZnFe_2O_4$ nanoparticles are integrated with conductive carbon frameworks such as $ZnFe_2O_4$/graphene, $ZnFe_2O_4$/reduced graphene oxide (rGO), $ZnFe_2O_4$/carbon nanotubes (CNTs), $ZnFe_2O_4$/activated carbon, and $ZnFe_2O_4$/carbon nanofibers [5]. These hybrid structures significantly improve electrical conductivity, increase accessible surface area, and enhance electrolyte penetration within the electrode material. Recent research has shown that $ZnFe_2O_4$ nanoparticles and conductive carbon matrices work in concert to enhance electron transport and electrochemical activity, leading to increased capacitance, better rate capability, and superior cycling stability [6]. For example, $ZnFe_2O_4$/graphene and $ZnFe_2O_4$/CNT composites have shown significantly higher electrochemical performance compared with pure $ZnFe_2O_4$ due to their hierarchical porous structures and enhanced charge transport pathways. $ZnFeO_4$ nanocomposites based on carbon are therefore thought to be viable electrode materials for high-performance supercapacitors of the future.

Synthesis Methods of Carbon-Based $ZnFe_2O_4$ Materials

Various synthesis strategies have been developed to prepare carbon-based $ZnFe_2O_4$ nanocomposites with controlled morphology and improved electrochemical performance.

- **Hydrothermal Method**

One of the most popular methods for creating $ZnFe_2O_4$ nanostructures is the hydrothermal process. In this method, zinc and iron precursors are dissolved in an aqueous solution containing carbon materials such as graphene oxide or activated carbon. After that, the mixture is put in a sealed autoclave and cooked to high temperatures. During the hydrothermal process, $ZnFe_2O_4$ nanoparticles nucleate and grow on the carbon surface, forming composites such as $ZnFe_2O_4$/graphene and $ZnFe_2O_4$/activated carbon with improved conductivity and electrochemical activity [7].

- **Sol–Gel Method**

The sol-gel method entails creating a homogenous solution using carbon sources and metal precursors. A gel-like network is created by hydrolysis and condensation processes. $ZnFe_2O_4$ nanoparticles are evenly dispersed throughout the carbon matrix following drying and calcination to create composites like $ZnFe_2O_4$/carbon and $ZnFe_2O_4$/CNT hybrids. This technique enables exact control over the size and shape of the particles. [8].

- **Electrospinning Method**

Electrospinning is widely used to fabricate $ZnFe_2O_4$/carbon nanofiber composites with more surface area and porous structures. In this technique, polymer solutions containing zinc and iron salts are electrospun into nanofibers, followed by carbonization at high temperatures. The resulting materials consist of $ZnFe_2O_4$ nanoparticles embedded within conductive carbon nanofibers, forming $ZnFe_2O_4$/CNF composites with enhanced electron transport and structural stability [9].

- **Chemical Bath Deposition**

Chemical bath deposition is a simple and cost-effective technique for synthesizing $ZnFe_2O_4$ nanostructures on conductive carbon substrates such as carbon cloth or carbon fiber papers. The controlled precipitation process results in uniform coating of $ZnFe_2O_4$ nanoparticles on carbon frameworks, improving the electrochemical performance of the composite electrodes [10].

Structural Characterization and Electrochemical Performance

Several characterisation techniques are used to study the structural and electrochemical properties of $ZnFe_2O_4$ composites based on carbon. Structural analysis is commonly performed using XRD to confirm the confirmation of the spinel $ZnFe_2O_4$ crystal structure and phase purity of the composite materials [11]. The distribution of $ZnFe_2O_4$ nanoparticles within carbon matrices, such as graphene, carbon nanotubes, or carbon fibers, is revealed by morphological analysis using scanning electron microscopy (SEM) and transmission electron microscopy (TEM), which also provides information about particle size, morphology, and porosity [12]. Furthermore, the specific surface area and pore structure of the composites are determined using Brunauer–Emmett–Teller (BET) surface area analysis, which has a significant impact on ion diffusion and electrochemical performance [13].

Both electrical double-layer capacitance (EDLC) and pseudocapacitive processes are used in supercapacitors based on carbon–$ZnFe_2O_4$ electrodes. EDLC behavior originates from electrostatic adsorption of electrolyte ions on the carbon surface, while pseudocapacitance arises from fast and reversible redox reactions of Zn^{2+}/Fe^{3+} ions in $ZnFe_2O_4$ [14]. Hybrid supercapacitors combine both

mechanisms, providing improved energy and power density.

Cyclic voltammetry (CV), galvanostatic charge-discharge (GCD), and electrochemical impedance spectroscopy (EIS) are commonly used to assess electrochemical performance. CV curves usually display quasi-rectangular shapes with redox peaks, indicating combined EDLC and pseudocapacitive behavior. Pure $ZnFe_2O_4$ electrodes generally exhibit relatively lower capacitance values around 200–300 F g^{-1}, whereas carbon-based composites show significantly improved performance. For example, $ZnFe_2O_4$/graphene composites have demonstrated capacitance values around 450–500 F g^{-1}, while $ZnFe_2O_4$/CNT composites exhibit capacitance values of approximately 420–480 F g^{-1} due to enhanced conductivity and electron transport. Similarly, $ZnFe_2O_4$/carbon nanofiber electrodes have reported capacitance values approaching 500–600 F g^{-1} with excellent rate capability [15].

EIS analysis reveals reduced charge transfer resistance in carbon-based composites because conductive carbon networks facilitate rapid electron transport. In addition, these electrodes exhibit excellent cycling stability, often retaining more than 90–95% capacitance after 5000–10000 cycles, demonstrating their potential for high-performance supercapacitor applications.

Conclusion

Carbon-based $ZnFe_2O_4$ nanocomposites, including $ZnFe_2O_4$/graphene, $ZnFe_2O_4$/CNT, and $ZnFe_2O_4$/carbon nanofiber systems, show excellent potential as advanced supercapacitor electrodes because of their better electrical conductivity, large surface area, and strong redox activity. Continued optimization of composite structures and synthesis strategies will further enhance their electrochemical performance for next-generation energy storage technologies

References

1. Devi, R., et al. (2024). ACS Applied Polymer Materials, 6(21), 12973–12982.
2. Yang, C., et al. (2019). ACS Applied Materials & Interfaces, 11(16), 14713–14721.
3. Abdulhamid, Z. M., et al. (2025). Journal of Energy Storage, 131, 117544.
4. Vadiyar, M. M., et al. (2019)., 2(10), 7133–7142.
5. Li, J., et al. (2019). ACS Applied Materials & Interfaces, 11(35), 32520–32528.
6. Fu, Y., & Wang, X. (2011). Industrial & Engineering Chemistry Research, 50(12), 7210–7218.
7. Mandal, M., et al. (2023). Diamond & Related Materials, 139, 110300.
8. Mandal, M., et al. (2021). Inorganic Chemistry Communications, 123, 108332.

9. Deshagani, S., et al. (2022 ACS Applied Energy Materials, 5(11), 13520–13534
10. Gazi, S., et al. (2026). Journal of Alloys and Compounds, 1050, 185718.
11. Seong, J.-G., et al. (2021). Green Energy & Environment, 6(4), 549–558.
12. Appiah-Ntiamoah, R., et al. (2022). ACS Applied Nano Materials, 5(3), 3657–3666.
13. Yang, S., at al. (2018). Carbon, 136, 1–10.
14. Hu, X.-W., et al. (2015) ACS Applied Materials & Interfaces, 7(19), 10322–10329.
15. Yang, S., et al (2020). Journal of Power Sources, 451, 228416.

Role of NiCo LDH for Supercapacitor: Synthesis Approach, Electrochemical Study

Yogita Shinde, Rutuja S. Malave, A. R. Pardeshi

Department of Physics, Dada Patil Mahavidyalaya, Karjat, Dist: Ahilyanagar 414 402

Email: amolrp111@gmail.com

Article DOI Link: https://zenodo.org/uploads/19795210

DOI: 10.5281/zenodo.19795210

Abstract

The increasing demand for effective and sustainable energy storage systems have speed up research on innovative electrode materials for supercapacitors. Among various candidates, transition-metal-based layered double hydroxides (LDHs) have drawn to considerable interest due to their multiple redox states and high theoretical capacitance. In this chapter, the synthesis and electrochemical evaluation of NiCo LDH-based nanocomposites are discussed for high-performance supercapacitor applications. The irregular supercapacitor device constructed with NiCo-LDH-based electrodes shows improve energy density and power density equated with many before reported NiCo-based systems. The results confirm that rational design of NiCo LDH nanocomposites with conductive and catalytic components is an effective strategy for developing next-generation storage energy materials.

Keywords: NiCo LDH, Supercapacitor, Energy Density, Power Density.

Introduction

Currently, growth of society rests on efficient and environmentally friendliness storage energy devices as well as conversion devices. Supercapacitor, hopeful energy storage device because high power density, fast recharge capability as well as stable cycle stability. Supercapacitor categorized in three parts on the basis of storage charge mechanism, Electric Double Layer Capacitor (EDLCs) which has improv cyclic stability however decrease storage capacity, Pseudocapacitor structure based on Faradaic redox reaction, and Hybrid Supercapcitor which work on combination of EDLCs and Pseudocapacitor. Electrochemical performance of electrode material depends upon material used in electrode fabrication [1-7].

Transition Metal compounds undergo rich redox reaction because of multiple valence state of Transition metals. Transition Metal Hydroxide (TMHs) attracted attention due to high theoretical specific capacitance. TMHs are utilize as

electrode material, the microstructure will little change or collapse because of insertion and deintercalation of ion between electron layer in the action of electrochemical procedure. Layered Double Hydroxide (LDH) has advantages of high electrochemical properties, non-toxic and highly stable. NiCo LDH is on the large hopeful electrode material because of unique interlayer spacing and shape. The double electron layer structure can supply the electrochemical active site which upgrade the electrochemical execution of composite [8-15]. This chapter reveals the information about the fabrication process of NiCo LDH based composite, study the electrochemical performance.

NiCo LDH Based Nanocomposite Fabrication Method

In this section, study the preparation of NiCo baed LDH nanocomposite for supercapacitor. Fig. 1 represent the fabrication of CC@MOF – 74 (NiO)@NiCo Based Nanocomposite for supercapacitor. The CC@MOF-74(NiO)@NiCo LDH electrode was synthesized through a sequential three-step procedure. First, flower-like MOF-74(Ni) structures were directly developed on conductive carbon cloth via hydrothermal method. Second, the obtained material was thermally treated at 450 °C for 2 h under a nitrogen atmosphere, converting MOF-74(Ni) into NiO while preserving the porous architecture. Finally, NiCo layered double hydroxide (NiCo LDH) nanosheets were uniformly deposited onto the CC@MOF-74(NiO) surface using an electrodeposition technique. This process produced a three-dimensional hierarchical CC@MOF-74(NiO)@NiCo LDH composite with a multilevel nanostructure [2].

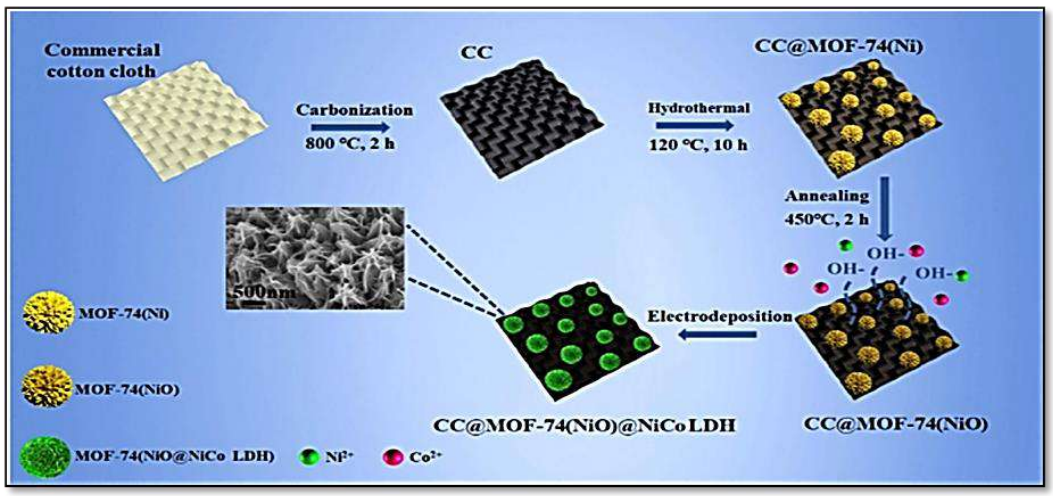

Fig. 1: Schematic diagram for the fabrication of 3D multiphase structure

Electrochemical Studies

Fig. 2: reveals the electrochemical execution of NiCo LDH@rGO//AC is to assess its practical performance, an unsymmetric supercapacitor (ASC) device

was organized using NiCo-LDH@rGO as the positive electrode as well as activated carbon (AC) as the negative electrode in 1 M KOH electrolyte, as illustrated in Fig. 2a. The AC electrode exhibited quasi-rectangular cyclic voltammetry (CV) profiles as well as nearly symmetric triangular galvanostatic charge-discharge (GCD) curves, indicating typical electric double-layer capacitive behavior. The stable potential windows of AC and NiCo-LDH@rGO electrodes were -1.0-0 V as well as 0-0.6 V, respectively, allowing the organized device to operate within an extended voltage window of 1.6 V. To maintain charge balance, mass ratio between NiCo-LDH@rGO as well as AC electrodes was optimized to 0.5. The CV curves of the NiCo-LDH@rGO//AC device at scan rates ranging from 5 to 100 mV s^{-1} are shown in Fig. 2b. The curves maintain quasi-rectangular shapes with slight redox features, indicating the combined contribution of faradaic reactions from NiCo-LDH@rGO and capacitive behavior from AC. The negligible distortion of the CV curves at higher scan rank suggests rapid charge transfer and favorable electrochemical kinetics. The GCD profiles recorded at current densities from 1 to 10 A g^{-1} (Fig. 2c) display slightly distorted triangular shapes, confirming the hybrid storage charge mechanism involving both diffusion-controlled as well as capacitive processes. The specific capacitance values calculated from the discharge curves (Fig. 2d) were 110.4, 92.3, 77.2, 59.7, and 35.9 F g^{-1} at current densities of 1, 2, 3, 5, as well as 10 A g^{-1}, respectively.

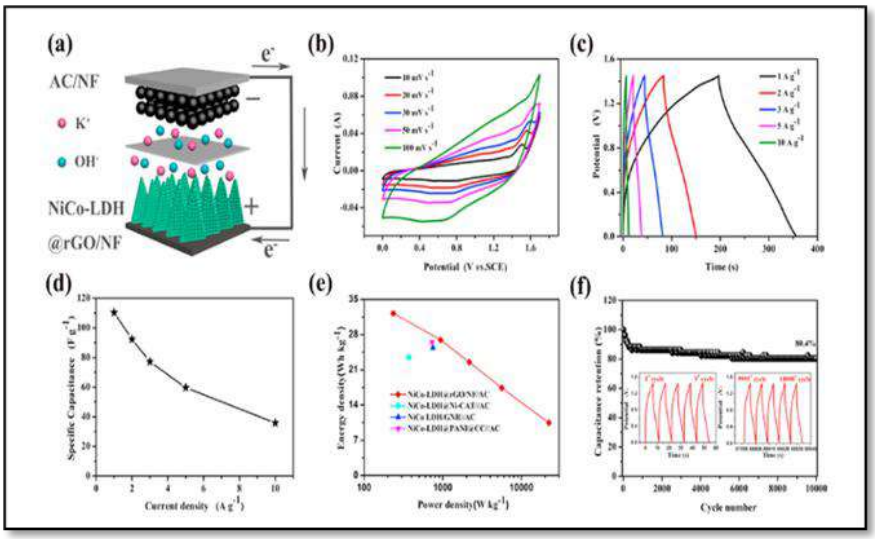

Fig. 2: Schematic illustration of the NiCo-LDH@rGO//AC (a). CV curves of NiCo-LDH@rGO//AC (b). GCD curves of NiCo-LDH@rGO//AC (c). Specific capacitance values of NiCo-LDH@rGO//AC obtained from GCD curves (d). Ragone plots of NiCo-LDH@rGO//AC along with representative data reported in literature (e). rGO//AC was evaluated (Fig. 6f). The ASC is insured during the first 500 cycles [4].

The Ragone plot presented in Fig. 2e. demonstrates that the device delivers a highest energy density of 32.2 Wh kg^{-1} at a power density of 235.5 W kg^{-1}, which is greater than several lastly reported NiCo-based supercapacitor systems. These results indicate that the NiCo-LDH@rGO nanocomposite exhibits excellent electrochemical performance as well as promising potential for maximun-performance energy storage applications.

Comparative Study of NiCo LDH Based Nanocomposite

Composite Material	**Specific Capacitance (F/g)**	**Energy Density (Wh/kg)**	**Power Density (W/kg)**	**Ref.**
Mn_3O_4/NiCo-LDH@Carbon Nanotube	-	16.01Wh/m^2	69.77 W/m^2	**01**
CC@MOF-74(NiO)@NiCo LDH	9.73 F/cm^2	22.85 Wh/kg	1750 W/kg	**02**
CNTs@NiCo LDH/	176.33 mAh/g	37.38 Wh/kg	800 W/kg	**03**
NiCo LDH@rGO/NF	2408.8 F/g	32.2 Wh/kg	235.5 W/g	**04**
Ce Doped NiCo LDH@CNT	187.2 F/g	-	-	**05**
CuO/CoNi LDH	7791 C/g	39.2 Wh/kg	368.3 W/kg	**06**
NiCo MOF@La_2O_3@rGO	3595 C/g	45 Wh/kg	1600 W/kg	**07**
Fe_2O_3-rGO & NiCo LDH rGO	1850 F/g	108 Wh/kg	884 W/kg	**08**
Ni@NC@NiCo - LDH	1761.8 F/g	39.27 Wh/kg	757.21 W/kg	**09**
$NiCo_2O_4$/NiCo LDH	3.85 F/cm^2	0.48 mWh/cm^2	40 mW/cm^2	**10**
NiCo LDH/$Ti_3C_2T_x$	635.7 C/g	44.6 Wh/kg	852.5 W/kg	**11**
Ni-P@NiCo LDH	3470.5 F/g	35.1 Wh/kg	770.8 W/kg	**12**
PPy/g-C_3N_4/MnO_2	2389 F/g	82 Wh/kg	750 W/kg	**13**
V doped NiCo LDH	1835 F/g	60.9 Wh/kg	800 W/kg	**14**
MXene@NiCo LDH/Co_9S_8	586.2 F/g	96.4 Wh/kg	800 W/kg	**15**

Conclusion

NiCo LDH-based nanocomposites represent a promising category of electrode materials for advanced supercapacitor systems due to their rich redox activity, layered structure, and high theoretical capacitance. In this chapter, different fabrication strategies were discussed for constructing hierarchical NiCo LDH composites, including MOF-derived structures and hybrid materials integrated

with La_2O_3 nanoparticles and reduced graphene oxide. The combination of porous frameworks and conductive carbon networks significantly improves ion diffusion, electrical conductivity, and electrochemical stability. Electrochemical characterization of the fabricated materials demonstrates notable specific capacitance and favourable energy-power density characteristics in asymmetric supercapacitor configurations.

References

1. Yu Jun Yang et. al. Journal of Alloys and Compounds 930 (2023) 167466.
2. Lili Wang et. al. Journal of Alloys and Compounds 885 (2021) 160899.
3. Fangfang Zhu et. al. Chemical Engineering Journal 383 (2020) 123150.
4. Zheng Yang et. al. Journal of Alloys and Compounds 850 (2021) 156864.
5. Mohammad Dinari et. al. Energy Fuels 2021, 35, 1831-1841
6. Gaini Zhang et. al. Journal of Energy Storage 83 (2024) 110426.
7. Sohail Mumtaz et. al. Journal of Industrial and Engineering Chemistry xxx (2026)
8. FanTang et. al. Journal of Colloid and Interface Science 634 (2023) 357–368.
9. Yuan Chen et. al. international journal of hydrogen energy 47 (2022) 29636-29647
10. Yi Gao et. al ACS App. Nano Mater 8 (2025) 9448-9459
11. Yanzhong Wang et. al. Electrochimica Acta 376 (2021) 138040
12. Jiale Xing et. al. J. Name., 2013, 00, 1-3
13. Hariprasath Rangaraju et. al. FlatChem 52 (2025) 100897
14. Shidong Li et. al. Materials Chemistry and Physics 318 (2024) 129226
15. Ye Qu et. al. Journal of Energy Storage 107 (2025) 114986

$ZnMn_2O_4$-Based Composite Electrodes: Synthesis, Electrochemical Behaviour, and Supercapattery Applications

Kangude Sahadev H, Chavan Diksha A.

Department of Physics Rayat Shikshan Sanstha's Dada Patil Mahavidyalaya Karjat,

Dist- Ahilyanagar-414402

Email: sahadevkangude7283@gmail.com

Article DOI Link: https://zenodo.org/uploads/19795291

DOI: 10.5281/zenodo.19795291

Abstract

The increasing demand for efficient energy storage has encouraged the development of advanced electrochemical systems with both high energy and power densities. Traditional batteries store large amounts of energy but deliver power slowly, while supercapacitors provide rapid charge–discharge and long cycle life but store less energy. To combine these advantages, hybrid devices called supercapatteries have been introduced. Among potential electrode materials, spinel-type ternary metal oxides such as $ZnMn_2O_4$ are promising due to their multiple redox states, stability, and low cost. However, poor electrical conductivity limits performance. Forming composites with conductive materials like graphene or carbon improves electron transport, ion diffusion, and structural stability, enhancing their suitability for advanced hybrid energy storage systems.

Keywords: $ZnMn_2O_4$, Supercapatteries, Composite electrodes, Graphene, Electrochemical energy storage.

Introduction

The growing use of portable electronics, electric vehicles, and renewable energy has increased the need for efficient energy storage. Rechargeable batteries and supercapacitors are commonly studied to meet this demand. While batteries store large amounts of energy but deliver limited power, supercapacitors offer fast charge–discharge and long cycle life, though with lower energy density [1,2]. To combine the advantages of both technologies, hybrid energy storage systems known as supercapatteries have been developed. These devices integrate battery-type electrodes with capacitive materials, allowing them to achieve both high energy density and high-power density in a single system [3]. The overall performance of supercapatteries strongly depends on the properties of the electrode materials, prompting extensive research into advanced materials that offer high electrical conductivity, strong redox activity, and good structural

stability. Among the various candidates, transition metal oxides have attracted significant attention due to their multiple oxidation states and high theoretical capacities [4]. Zinc manganite ($ZnMn_2O_4$) is promising due to its spinel structure, enabling efficient redox reactions and ion transport. Its low electrical conductivity and structural changes during cycling can limit performance. To address this, nanostructuring and composite formation with conductive materials have been used to improve conductivity, surface area, and overall electrochemical behavior [5,6].

Structural Characteristics of $ZnMn_2O_4$

$ZnMn_2O_4$ is a spinel-type metal oxide with the general formula AB_2O_4, in which metal cations occupy both tetrahedral and octahedral lattice sites. In this structure, Zn^{2+} ions preferentially occupy tetrahedral sites, while Mn^{3+} ions reside in octahedral positions coordinated by oxygen atoms. This cation arrangement within the spinel framework enhances ion diffusion and facilitates redox reactions essential for electrochemical applications [7]. A key advantage of $ZnMn_2O_4$ as an electrode material is the presence of multiple oxidation states of manganese, enabling reversible Faradaic reactions during electrochemical cycling. These redox processes allow efficient storage and release of electrical energy [8]. Moreover, zinc and manganese are abundant, low-cost, and environmentally friendly, making $ZnMn_2O_4$ a sustainable electrode material. However, its performance is hindered by low electrical conductivity and nanoparticle aggregation. These limitations can be effectively addressed by forming composites with conductive materials, which enhance charge transport and structural stability [9].

Synthesis Strategies for $ZnMn_2O_4$ Nanostructures

Various synthesis techniques have been developed to prepare $ZnMn_2O_4$ nanostructures with controlled morphology and improved electrochemical performance.

- **Hydrothermal Method**

The hydrothermal technique enables the controlled synthesis of well-defined nanostructures (e.g., nanorods, nanosheets) with high surface area, enhancing electrochemical performance [10].

- **Sol–Gel Method**

The sol–gel process involves the formation of a homogeneous solution containing metal precursors that gradually transform into a gel through hydrolysis and condensation reactions. Subsequent thermal treatment results in crystalline $ZnMn_2O_4$ nanoparticles with controlled composition and particle size [11].

- **Microwave and Combustion Techniques**

Microwave-assisted synthesis and combustion methods have also been highlighted for producing $ZnMn_2O_4$ nanomaterials rapidly. These approaches allow uniform heating and fast nucleation, which can improve crystallinity and electrochemical performance [12].

$ZnMn_2O_4$-Based Composite Materials

$ZnMn_2O_4$ electrochemical performance is improved by forming composites with conductive materials. Carbon-based materials and graphene enhance electron transport and surface area, while hybrid metal oxides boost capacitance and stability. Flexible electrodes on conductive substrates further enable applications in wearable energy devices [13–16].

Electrochemical Mechanism in Supercapatteries

In supercapattery systems, $ZnMn_2O_4$ stores energy through Faradaic redox reactions involving reversible manganese oxidation states. Combining it with conductive materials improves electron transport, enhancing energy density, power capability, and cycling stability [17].

Recent Progress and Performance of $ZnMn_2O_4$ Supercapattery Electrodes

Recent studies have reported significant improvements in the electrochemical performance of $ZnMn_2O_4$-based composites. The incorporation of conductive carbon materials enhances charge transport and cycling stability. Table 1 summarizes the electrochemical performance of various $ZnMn_2O_4$ composite electrodes reported in recent studies [18-20].

Table 1. Electrochemical performance of $ZnMn_2O_4$-based composite electrodes for supercapattery applications [Ref. 18-20].

Material System	Specific Capacitance	Energy Density (Wh kg^{-1})	Cycle Stability
$ZnMn_2O_4$ nanoparticles	~350 F g^{-1}	18	85% after 2000 cycles
$ZnMn_2O_4$/Graphene	~720 F g^{-1}	32	92% after 5000 cycles
$ZnMn_2O_4$/CNT composite	~650 F g^{-1}	30	90% after 4000 cycles
$ZnMn_2O_4$/Porous carbon	580 F g^{-1}	27	91% after 3000 cycles

Conclusion

$ZnMn_2O_4$ is a promising electrode material for hybrid energy storage due to its spinel structure, redox activity, and eco-friendliness, but its low conductivity and structural limitations hinder practical use. Forming composites with conductive

carbon or other metal oxides significantly enhances its performance. Ongoing advances in nanostructure design and device engineering are expected to further improve $ZnMn_2O_4$ composites, making them strong candidates for next-generation supercapattery applications.

References

1. Simon, P., & Gogotsi, Y. (2008). Nature Materials, 7(11), 845–854.
2. Conway, B. E. (1999). Springer.
3. Wang, H., Yi, Z., Zhang, X., & Lu, L. (2020). Energy Storage Materials, 27, 40–55.
4. Liu, Z., Zhang, H., & Wang, Y. (2020). Nano Energy, 71, 104603.
5. Zhang, Y., Liu, J., & Wang, H. (2021). Journal of Alloys and Compounds, 853, 157231.
6. Li, Y., Zhang, Q., & Chen, X. (2020). Electrochimica Acta, 338, 135823.
7. M. H. L., Kumar, P., & Singh, R. (2023). Solid State Sciences, 136, 107110.
8. Wang, H., Liu, D., & Chen, X. (2021). Journal of Power Sources, 490, 229536.
9. Zhang, Y., Liu, J., Wang, H., & Chen, X. (2021). Journal of Alloys and Compounds, 853, 157231.
10. Kumar, R., Singh, A., & Patel, S. (2020). Materials Letters, 272, 127833.
11. Singh, R., Sharma, P., & Kumar, A. (2019). Journal of Materials Science, 54, 11234–11247.
12. Yang, S., Liu, Q., & Chen, H. (2020). Chemical Engineering Journal, 396, 125236.
13. Chen, R., Zhao, T., Wu, F., & Li, L. (2020). Progress in Materials Science, 113, 100637.
14. Zhang, Y., Liu, X., Chen, H., & Wang, J. (2024). Journal of Energy Storage, 76, 109636.
15. Kumar, N., Dubal, D. P., & Gomez-Romero, P. (2020). Materials Today Energy, 17, 100431.
16. Wang, T., Zhang, Y., & Li, J. (2021). Energy Storage Materials, 38, 220–231.
17. Ramesh, J. K., Rostami, S., Rajesh, J., Bhackiyavathi Princess, R. M., Govindaraju, R., Kim, J., … Abdollahifar, M. (2025). Journal of Materials Chemistry A, 13,
18. Liu, D., Kim, S., & Choi, W. M. (2024). Materials, 17, 884.
19. Zhang, Y., Liu, X., Chen, H., & Wang, J. (2024). Journal of Energy Storage, 76, 109636.
20. Li, X., Zhang, Y., & Wang, J. (2026). Energy & Fuels.

Fundamental Concepts and Types of Supercapacitors: A Mini Review

Kanchan R. Chavan, Aarti S. Modhale, Balbhim. S. Maharnavar

Rayat Shikshan Sanstha's Dada Patil Mahavidyalaya Karjat Dist- Ahilyanagar-414402

Email: balbhim02@gmail.com

Article DOI Link: https://zenodo.org/uploads/19795549

DOI: 10.5281/zenodo.19795549

Abstract

Supercapacitor have promising electrochemical properties due to their high-power density, rapid charge-discharge capability, and long cycling stability. This chapter summarizes the fundamental concepts, working principles, and major basic types of supercapacitors, including electrical double-layer capacitors, pseudocapacitors, and hybrid supercapacitors. In addition, electrochemical performance parameters such as specific capacitance, energy, and power density are discussed to highlight their importance in evaluating and optimizing supercapacitor performance for modern energy storage applications.

Keywords: Electrochemical, Energy Storage Devices, Hybrid, Specific Capacitance.

Introduction

The accelerating demand of energy and the rapid development of modern electronic devices have created a strong need for efficient energy storage technologies. Conventional energy storage devices such as batteries and dielectric capacitor have several limitations, including minimum power density, low charge-discharge rates, and limited cyclic life. As a result, advanced electrochemical energy storage devices known as supercapacitors have attracted significant attention due to excellent electrochemical performance and long operational stability [1]. Supercapacitors, also referred to as electrochemical capacitors, bridge the gap between capacitor and batteries by providing both high-power density & moderate energy density [2]. Supercapacitors store energy via. fast redox reactions at the electrode-electrolyte interface. Compared with conventional batteries, supercapacitors exhibit rapid charge-discharge, high-power density, long cycling stability (often exceeding 100,000 cycles), and excellent efficiency [3]. These characteristics make them suitable applications in hybrid vehicles, renewable energy storage systems, portable electronics, and smart grid technologies [4]. In recent years, significant attention has been

directed toward enhancing the electrochemical properties of supercapacitors through the design of advanced electrode materials, including carbon-based nanostructures, transition metal oxides, conducting polymers, and ferrite nanomaterials. The use of nanostructured materials offers distinct advantages such as large surface area, improved electrical conductivity, and increased electrochemical reactivity, which collectively contribute to higher capacitance and improved energy storage capability [5]. As a result, supercapacitors are increasingly recognized as potential candidates for next-generation energy storage applications in sustainable energy technologies [6].

Basic Concept of Supercapacitors

Supercapacitor is electrochemical energy storage device which stores electrical energy through charge accumulation at the electrode-electrolyte interface. Unlike conventional capacitors that store energy through dielectric polarization, supercapacitors utilize either electrostatic charge separation or reversible electrochemical on the electrode surface [7]. This unique mechanism enables them to deliver high-power density and rapid charge-discharge ratio. Properties of electrode are affecting electrodes electrochemical behaviour electrolyte. High surface area components such as activated carbon, graphene, and carbon nanotubes are commonly used as electrodes because they provide numerous active sites for ion-adsorption and charge-storage [8]. The electrolyte facilitates ion transport between the electrodes during the charging and discharging processes. In general, the energy storage capability of supercapacitors lies between that of conventional capacitors and rechargeable batteries. While batteries store energy through slow chemical reactions in the bulk material, supercapacitors rely on rapid surface processes, allowing them to charge and discharge within seconds while maintaining excellent cycle life [9].

Working Principle of Supercapacitors

The operation of a supercapacitor relies on charge accumulation at the interface between the electrode and electrolyte. Upon applying a potential, electrolyte ions migrate toward oppositely charged electrodes, forming an electrical double layer that serves as the primary charge storage region [10]. During charging, ions are adsorbed onto the electrode surface, while during discharging they return to the electrolyte, releasing stored energy. In addition, some systems exhibit fast and reversible faradaic reactions at the electrode surface, further enhancing capacitance [11]. The performance of supercapacitors is influenced by factors such as electrode surface area, electrical conductivity, pore structure, and ion mobility, with high surface area nanomaterials improving charge storage efficiency [12].

Classification of Supercapacitors

Supercapacitors are classified into three types based on their charge storage mechanism: electrical double-layer capacitors, pseudocapacitors, and hybrid supercapacitors [13]. These categories differ mainly in their storage processes and electrode materials.

- **Electrical Double-Layer Capacitors (EDLCs):** EDLCs store energy through electrostatic charge separation at the electrode–electrolyte interface without any chemical reactions. Carbon-based materials such as activated carbon, graphene, and carbon nanotubes are widely used due to their high surface area and good electrical conductivity [14].
- **Pseudocapacitors:** Pseudocapacitors store the energy through reversible Faradaic redox reactions occurring at the electrode surface. Transition metal oxides as RuO_2, MnO_2, NiO and conducting polymers are typically used as electrode materials. These materials provide higher capacitance compared to EDLCs [15].
- **Hybrid Supercapacitors:** Hybrid supercapacitors combined with EDLCs and pseudocapacitors to achieve improved energy and power density. They use asymmetric electrode configurations, where one electrode behaves like a battery-type material and the other acts as a capacitive electrode [16]. Hybrid systems provide enhanced electrochemical performance compared with single-mechanism supercapacitors [17].

Electrochemical Performance Parameters of Supercapacitors

Electrochemical parameters are used to evaluate the performance of supercapacitors, such as specific capacitance, energy density, and power density. These parameters are commonly determined using cyclic voltammetry (CV) and galvanostatic charge–discharge (GCD) techniques.

Specific Capacitance from Cyclic Voltammetry (CV)

The capacitance of an electrode calculated from the CV curve is given

$$C_p = \frac{\int i(V)\, dV}{m \times s \times \Delta V}$$

Where,

C_p= Specific capacitance (F g^{-1}), i(V) = Current response in the CV curve (A),

m = Mass of active electrode material (g), s = Scan rate (V s^{-1}), ΔV = Potential window (V)

Surface Area Occupied by Hydrated Ions

The effective surface area occupied via hydrated ions on the electrode surface can

be estimated as:

$$S = \frac{C_p \times \Delta V \times \sigma \times N}{F}$$

Where, S = Surface area occupied by hydrated ions (m^2), C_p = Specific capacitance (F g^{-1}), ΔV = Potential window (V), σ = Cross-sectional area of hydrated ions (m^2), N = Avogadro's number (6.022×10^{23} mol^{-1}), F = Faraday constant (96485 C mol^{-1}) [18]

Specific Capacitance from Galvanostatic Charge–Discharge (GCD)

The capacitance obtained from GCD measurements is calculated using:

$$C_s = \frac{i \times \Delta t}{m \times \Delta V}$$

Where,

C_s = Specific capacitance, i = Discharge current,

Δt = Discharge time, m = Mass of active material (g), ΔV = voltage window (V)

Number of Electrochemically Active Sites

The number of active sites participating in the electrochemical reaction can be estimated using:

$$z = \frac{C_s \times n \times F \times \Delta V}{M}$$

Where, z = Number of active sites, C_s= Specific capacitance (F g^{-1}),

n= Number of electrons transferred, F= Faraday constant,

M= Molecular weight of the active material (g mol^{-1}), ΔV= Potential window (V)

Energy Density and Power Density

The energy density and power density of a supercapacitor device are calculated using the following relations Energy Densit given as $E_{cell} = \frac{1}{2} C(\Delta V)^2$ Power Density given as $P_{Celll} = \frac{E_{cell}}{\Delta t}$

Where, E_{cell}= Energy density (Wh kg^{-1}), C_{cell}= Specific capacitance of the device (F g^{-1}), P_{cell}= Power density (W kg^{-1}), ΔV = Potential window (V), Δt = Discharge time (s)[19].

Conclusion

Supercapacitors are electrochemical energy storage devices known for their high-power density, rapid charge-discharge behavior, and long cycling stability. Energy storage occurs through either electrostatic ion accumulation at the electrode-electrolyte interface or fast surface redox reactions. Based on these mechanisms, they are classified as electrical double-layer capacitors (EDLCs), pseudocapacitors, and hybrid systems. Among these, hybrid supercapacitors offer improved performance by combining both charge storage processes. KeY factor such as specific capacitance, energy density, and power density is commonly used to evaluate their electrochemical performance and practical applicability.

References

1. Borenstein, A., et al. (2017). Journal of Materials Chemistry A, 5(25), 12653–12672.
2. Simon, P., & Gogotsi, Y. (2020). Nature Materials, 19, 1151–1163.
3. Wang, Y., Song, Y., & Xia, Y. (2019). Chemical Society Reviews, 48, 162–199.
4. Zhang, L. L., & Zhao, X. (2019. Chemical Society Reviews, 48, 2520–2531.
5. Shao, Y., et al. (2020). Chemical Reviews, 118, 9233–9280.
6. Liu, C., Li, F., Ma, L., & Cheng, H. M. (2021). Advanced Materials, 33, 2000732.
7. Conway, B. E. (2018). Electrochemical supercapacitors: Scientific fundamentals and technological applications. Springer.
8. Miller, J. R., & Simon, P. (2018). Science, 321, 651–652.
9. Yu, G., Hu, L., & Cui, Y. (2020). Energy & Environmental Science, 13, 2114–2140.
10. Dubal, D. P., et al. (2019). Chemical Society Reviews, 44, 1777–1790.
11. Pandolfo, A. G., & Hollenkamp, A. F. (2018). Journal of Power Sources, 157, 11–27.
12. Frackowiak, E., & Béguin, F. (2019). Carbon, 39, 937–950.
13. Gogotsi, Y., & Simon, P. (2022). Science, 334, 917–918.
14. Zhai, Y., et al. (2019). Advanced Materials, 23, 4828–4850.
15. Liu, T., et al. (2020). Nano Letters, 14, 2522–2527.
16. Wang, G., et al. (2019). Chemical Society Reviews, 41, 797–828.
17. Choi, C., et al. (2020). Nature Reviews Materials, 5, 5–19.
18. Miller, J. R., et al. (2008). Science, 321(5889), 651–652.
19. Dubal, D. P., et al. (2015). Chemical Society Reviews, 44(7), 1777–1790.

A Review on Sodium-Ion Batteries: Materials, Mechanisms, and Energy Storage Applications

[1]Sampada D. Karpe, [2]Vishal M. Khetmalis, [1]Balbhim S. Maharnavar

[1]Rayat Shikshan Sansthas Dada Patil Mahavidyalaya Karjat dist- Ahilyanagar(MS), India – 414402

[2]Vidya Pratishthan's Arts, Science and Commerce College Baramati, India.

Email: balbhim02@gmail.com

Article DOI Link: https://zenodo.org/uploads/19795651

DOI: 10.5281/zenodo.19795651

Abstract

This chapter reviews the principles of battery technology, try to develop methods of cathode substances utilized in sodium-ion battery systems (SIBs). While primary batteries are limited to single-use applications, secondary batteries like SIBs offer an affordable and sustainable solution for storing energy on large-scale. The performance of SIBs is primarily governed by four cathode these are classified into Layered Transition Metal Oxides, Polyanionic system, Prussian Blue Analogues, and Organic Materials. By analyzing their structural frameworks, electrochemical capacities, and inherent challenges such as air sensitivity and lattice water. This chapter highlights the material innovations essential for upcoming generation of efficient and safe energy storage systems.

Keywords: battery, energy storage, Na-ion, Anode, Cathode

Introduction

Global energy consumption is increasing day by day. We need to upgrade our energy storage system so as to meet daily requirements. The battery technology is the important to store electrical power. Batteries convert chemical energy into electrical energy. All batteries are made up of three basic components: an anode (the '-ve' side), a cathode (the '+ve' side), and some kind of electrolyte (conductive medium that enables the transport of ions between the cathode and anode).

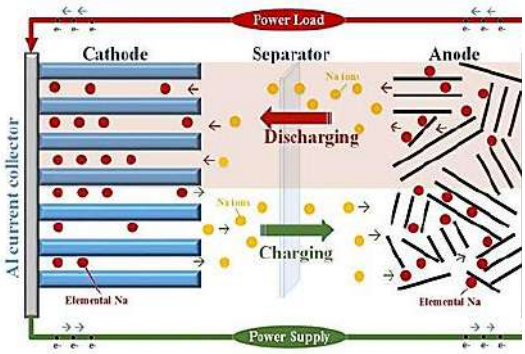

Fig. 1. Working of a battery cell

Fig. 2 Different battery cells

Types of Batteries

Depending on the principle of operation, cells are classified as

- **Primary or Non-Rechargeable**

Batteries these cells undergo irreversible electrochemical reactions. They contain a fixed quantity of reactive compounds and can be discharged only once. As the reactants are consumed during discharge, the cell cannot be reused. For example: Zinc Carbon batteries, Alkaline batteries

- **Secondary or Rechargeable**

batteries which can be recharged several times. This is possible since the electrochemical reaction happening inside these batteries is reversible. For example, Lead acid, Li ion, Na ion, Zn ion, Nickel Cadmium batteries. [1]

Working Principle of Battery Cell

A cell is composed of an anode (negative electrode), a cathode (positive electrode), an electrolyte (which conducts ions), and a separator. When charging, ions travel from the cathode to the anode, storing energy. During discharging, ions return to the cathode, releasing electrons through an external circuit to power devices

Calculation of Theoretical Specific Capacity (Cp) of a battery

$$C_p = \frac{n.F}{3.6\ X\ MW} \qquad [2]$$

Were, n: no. of electrons utilized per formula unit, F: Faraday Constant and MW: Molecular weight of a material

Na-ion Batteries

Materials used for the cathode in sodium-ion batteries (SIBs) are generally classified into four primary categories based on their crystal structure and chemical composition. Each type presents distinct compromises between energy

density, lifespan, and cost.

- **Layered Transition Metal Oxides (Na_xMO_2)**

Layered oxide cathodes are promising for sodium-ion batteries due to their high capacity and structural similarity to lithium-ion cathodes. Based on Meijer/Delmas notation, O3-type structures offer higher capacity but undergo phase transitions, while P2-type structures provide faster ion transport and better rate capability. These materials deliver ~120–180 mAh/g and are cost-effective due to compatibility with existing battery manufacturing technologies [3,4].

- **Polyanionic Compounds**

Polyanionic compounds are important cathode materials for sodium-ion batteries, known for their strong 3D frameworks and high thermal and chemical stability. Their open structures enable efficient sodium-ion diffusion, ensuring good ionic conductivity and cycling stability, while strong X–O bonds enhance safety by suppressing oxygen release [6]. Key subclasses include NASICON-type orthophosphates with high power and durability, pyrophosphates with excellent stability but lower capacity, and fluorophosphates offering higher operating voltages (~3.9–4.0 V) for improved energy density. Emerging sulfates and silicates also show promise as cost-effective alternatives [7–9].

- **Prussian Blue Analogues (PBAs)**

Prussian Blue Analogues (PBAs) are a distinctive types of coordination framework cathode components for sodium-ion batteries, typically represented by the formula $A_xM_1[M_2(CN)_6] \cdot nH_2O$. Their face-centered cubic (FCC) structure forms a highly open three-dimensional network with large channels, enabling rapid sodium-ion diffusion with minimal resistance. Due to the spacious framework, sodium insertion and extraction occur with nearly zero structural strain, resulting in excellent cycling stability and long operational life. Another key advantage of PBAs is the presence of dual redox-active metal centers (M_1 and M_2), which enhance charge storage capacity; for instance, Prussian White ($Na_2Fe[Fe\ (CN)_6]$) delivers a theoretical capacity of around 170 mAh/g. Additionally, PBAs are composed of abundant and environmentally benign elements such as Fe and Mn, making them cost-effective [10]. However, a major challenge is the presence of interstitial water within the lattice, which can degrade performance; thus, current research focuses on developing water-free PBAs through advanced synthesis techniques [11]

- **Organic Cathode Materials**

Organic materials used as cathodes in sodium-ion batteries (SIBs) have gained attention as sustainable, metal-free alternatives to conventional inorganic cathodes due to their environmental compatibility and structural versatility.

Organic materials used as cathodes in sodium-ion batteries Consisting of widely available elements such as C, H, N, O, and S, and often derived from renewable biomass, they reduce reliance on critical metals like cobalt and nickel. Their flexible frameworks can accommodate the large size of sodium ions and tolerate volume changes during cycling, enhancing structural stability. Moreover, their electrochemical properties can be tailored at the molecular level by modifying functional groups, such as introducing electron-withdrawing groups to increase operating voltage and energy density [12]. These materials are broadly classified into carbonyl compounds (e.g., quinones, PTCDA, imides), conjugated polymers (e.g., polypyrrole, polyaniline), and organosulfur or radical-based systems. Despite their advantages, they face challenges including dissolution in liquid electrolytes, low intrinsic electronic conductivity requiring conductive additives, and relatively low operating voltages (<2.2 V), which limit their competitiveness with inorganic cathodes [13].

Anode Materials for Sodium Ion Batteries

Carbon containing materials are among the most commercially viable anodes for sodium-ion batteries (SIBs) because of their abundance and affordable; however, unlike in lithium-ion systems, graphite performs poorly for sodium storage because the larger Na^+ ions cannot effectively intercalate into its small spacing between layers (~0.335 nm), resulting in a very low capacity (~35 mAh/g). As a result, hard carbon has emerged as the leading anode candidate, featuring a disordered, non-graphitizable structure with expanded interlayer spacing and nanopores that enable reversible sodium storage via intercalation and pore-filling mechanisms. Soft carbon, which can be graphitized at high temperatures (>2500 °C), typically offers better rate capability but lower specific capacity compared to hard carbon [14].

In addition to carbon materials, titanium-based oxides such as $Na_2Ti_3O_7$ are promising intercalation-type anodes due to their “zero-strain” behavior, undergoing minimal volume change during cycling, which ensures excellent safety and long cycle life; for example, $Na_2Ti_3O_7$ shows a low working voltage (~0.3 V) and a theoretical having a capacity near 177 mAh/g [15]. Alloy-based materials, including phosphorus (P), tin (Sn), and antimony (Sb), provide extremely high theoretical capacities through the formation of sodium-rich alloys, with phosphorus reaching ~2596 mAh/g, although it suffers from severe volume expansion (~300%), while tin and antimony offer capacities of approximately 847 and 660 mAh/g, respectively [16]. Furthermore, conversion-type materials such as transition metal oxides, sulfides, and phosphides (e.g., Fe_3O_4, MoS_2, and Sb_2S_3) store charge through reversible redox reactions forming metallic nanoparticles, but they face challenges such as large voltage hysteresis and

significant volume expansion during repeated cycling [17].

Conclusion

Sodium-ion batteries provide a viable, economical, and environmentally friendly option for large-scale energy storage. Advances in cathode and anode materials have significantly improved performance, though challenges such as stability, conductivity, and capacity fading remain. Continued material innovation and optimization are essential to achieve high efficiency, safety, and long-term durability.

References

1. R.K. Azegaet. al. (2024). Sustainable Materials and Technologies,41 (2024), e01111
2. Young Lu et. al. (2019),58, 21, (2019) 7020-7024
3. C. Delmaset. al. (2018). Advanced Energy Materials,8(17), 1703137.
4. Hwanget. al. (2017), Chemical Society Reviews, 46(12), 3529-3614.
5. Y Chen et.al. (2023), Batteries, 9(3), (2023).183.
6. C. Masquelier et. al. (2013), Chemical Reviews, 113(8), 6552–6591
7. JianZelanget. al. (2012), Electrochemistry Communications, 14(1), 86-89.
8. P. Barpandaet. al. (2012), Electrochemistry Communications, 24,116-119.
9. R Shakoor et. al., (2012), Journal of Materials Chemistry, 22(38), 20535-20541
10. L. Wang et. al., (2014), Journal of the American Chemical Society, 136(32),11412-11421.
11. Y. Youet. al. (2014), Energy & Environmental Science, 7(5),1643-1647.
12. B. Häupler et. al. (2015), Advanced Energy Materials, 5(11), 1402034.
13. Hao Li et. al., (2014), ECS Meeting Abstract, MA2014-03,189.
14. D. Stevens et. al., (2000), Journal of the Electrochemical Society, 147(4), (2000), 1271.
15. P. Senguttuvan, P., et. al., (2011), Chemistry of Materials, 23(18), (2011), 4109-4111.
16. Kim, Y., et al. (2013), Advanced Materials, 25(21), (2013), 3045-3049.
17. David, L., et al. (2014) " ACS Nano, 8(2), (2014), 1759-1770.

Metal - Organic Framework Assisted Nanocomposites: Synthesis, Morphological Features and Supercapacitive Behaviour

Tejswini S. Ghalme, Amol R. Pardeshi

Department of Physics, Dada Patil Mahavidyalaya, Karjat, Dist: Ahilyanagar 414 402

Email: amolrp111@gmail.com

Article DOI Link: https://zenodo.org/uploads/19795765

DOI: 10.5281/zenodo.19795765

Abstract

Metal-Organic frameworks (MOFs) based nanocomposites have promising consideration attention as advanced electrode materials for supercapacitor applications due to tuneable porous structure, high specific surface area, abundant electroactive sites. In this chapter, MOF-derived nanostructured materials are synthesized and systematically investigated for their structural, morphological, and electrochemical properties. The formation of ultrathin $NiCo_2S_4$ nanoarrays on activated carbon cloth enhances electrolyte accessibility and facilitates efficient charge transfer. Electrochemical studies reveal strong pseudocapacitive behaviour, good reversibility, and excellent rate capability. These results demonstrate that MOF-derived nanocomposites provide an effective strategy for designing excellent performance electrode materials for electrochemical performance.

Keywords: MOF, LDH, Supercapacitor, Morphology and Electrochemical

Introduction

The rapid growth in global energy demand and the environmental impact associated with excessive fossil fuel consumption have intensified the search for sustainable energy technologies. Recently present energy resources such as solar, wind, and tidal power are considered promising alternatives for reducing greenhouse gas emissions and ensuring long-term energy sustainability. However, the intermittent nature of these resources necessitates the development of efficient energy storage systems capable of delivering stable and reliable power. Among the various electrochemical energy storage, supercapacitors have attracted considerable attention because of their high-power density, rapid charge - discharge capability, and long cycling stability. Based on the charge storage mechanism, supercapacitors are generally divided into electric double - layer

capacitors (EDLCs) and pseudocapacitors. EDLCs energy store via electrostatic ion adsorption at the electrode & electrolyte interface and typically employ carbon - based materials such as activated carbon, graphene, and carbon nanotubes. Although these materials provide excellent rate capability and cycling durability, their relatively low capacitance limits the achievable energy density. In contrast, pseudocapacitors utilize fast and reversible Faradaic redox reactions occurring on electroactive surfaces, enabling significantly higher capacitance. However, many conventional pseudocapacitive materials suffer from poor electrical conductivity and limited structural stability during long-term cycling [1-6].

Nowadays, metal–organic frameworks (MOFs) are promising materials for advanced electrodes due to their high porosity, large surface area, and tunable composition. These features enable efficient ion diffusion and abundant electroactive sites. MOFs also serve as precursors for metal oxide/carbon nanocomposites with enhanced conductivity and electrochemical performance, making them attractive for high-performance supercapacitors [7–10].

Synthesis

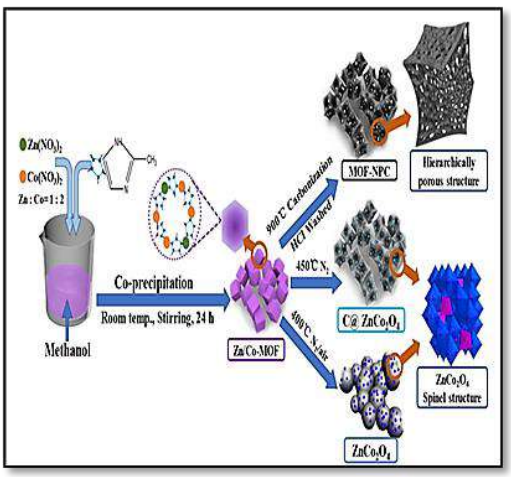

Fig. 1: Synthesis of Zn/Co- MOF [4].

In fig. 1, The bimetallic MOF - derived electrode materials to prepared using a "one-for-all" synthetic approach, as schematically illustrated in Figure 1. The preparation procedure involved two sequential stages. In the first stage, bimetallic Zn/Co metal–organic frameworks with a polyhedral morphology were synthesized through a co-precipitation process. Zinc and cobalt ions were reacted with 2-methylimidazole (MIM) in methanol at ambient conditions, leading to the formation of a uniform Zn/Co-MOF precursor. The obtained precipitate was collected and designated as Zn/Co-MOF.

To achieve the desired stoichiometry for $ZnCo_2O_4$ formation, the molar ratio of Zn to Co was carefully maintained at 1:2 during the synthesis. In the second stage, the as-prepared Zn/Co-MOF served as a sacrificial precursor for generating both nitrogen-doped porous carbon (NPC) and $ZnCo_2O_4$ through controlled thermal treatment. The precursor was subjected to pyrolysis under a nitrogen atmosphere at different temperatures to obtain the corresponding derivatives. Calcination at 900 °C resulted in the formation of nitrogen-doped porous carbon, while heat treatment at 450 °C facilitated the conversion of the MOF framework into $ZnCo_2O_4$. This strategy enables the simultaneous generation of porous carbon and metal oxide structures while preserving the original morphology of the MOF template, which is beneficial for the electrochemical properties of the resulting electrode materials [4].

Morphological Study

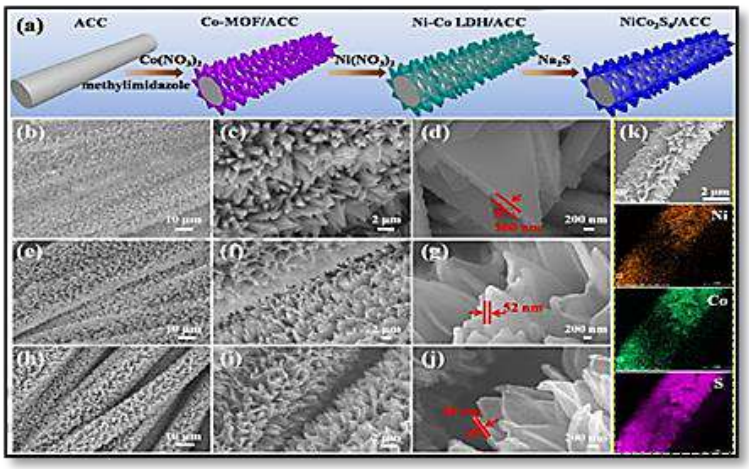

Fig. 2: (a) Schematic illustration of MOF-derived ultrathin $NiCo_2S_4$ nanoarrays on electrochemically activated carbon cloth. (b) Low- and (c, d) high-magnification SEM images; (e) low- and (f, g) high-magnification SEM images; (h) low- and (i, j) high-magnification SEM images; (k) SEM image with corresponding elemental mapping [6]

The morphology of the synthesized materials was investigated via. SEM analysis. The electrochemically activated carbon cloth (ACC) exhibited excellent wettability due to the introduce of oxygen - containing functional groups, which promoted the uniform nucleation and growth of Co-MOF on the carbon fibre surface. As shown in Figure 2a, ACC rapidly absorbs a water droplet, confirming its hydrophilic nature. The SEM images of Co-MOF/ACC (Figure 2b, 2c) reveal a uniform coverage of nanosheet arrays on ACC substrate. The enlarged image (Figure 2d) shows smooth and dense nanosheets with an average thickness of approximately 300 nm. After treatment with Ni $(NO_3)_2$, the nanoarray structure remains intact (Figure 2e, 1f), while the nanosheets become significantly thinner due to a controlled etching process, with the nanowall thickness reduced to about

52 nm (Figure 2g). Following hydrothermal sulfurization, the morphology of Ni-Co-S/ACC-160 is illustrated in Figure 2h-2j, showing dense and uniformly distributed nanosheets anchored on the carbon fibers. The nanosheets become ultrathin (less than 30 nm) with crimped edges and a hollow porous structure, which facilitates rapid electrolyte ion diffusion and efficient charge transfer. Furthermore, the elemental mapping images (Figure 1k) confirm the homogeneous distribution of Ni, Co, and S elements throughout the nanosheet architecture [6].

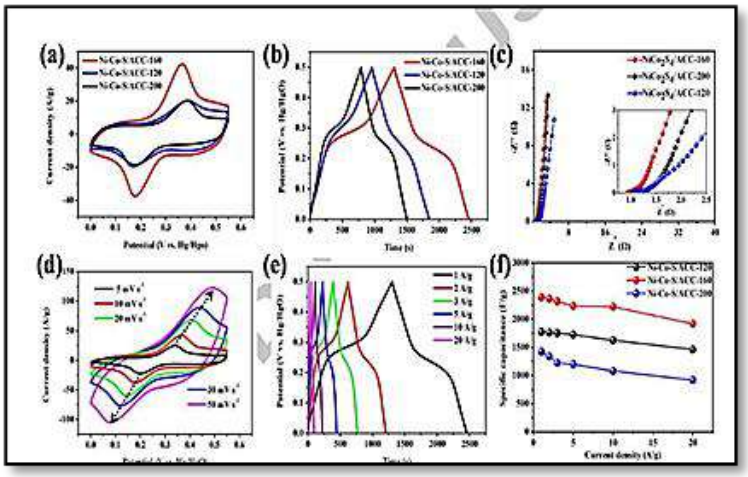

Fig. 3: (a) CV curves of Ni–Co–S/ACC-120, -160, and -200 at 10 mV/s; (b) GCD curves; (c) Nyquist plots; (d) CV curves; (e) GCD curves; (f) specific capacitance plots [6].

Electrochemical Studies

The electrochemical performance of $NiCo_2S_4$/ACC electrodes was evaluated in a three-electrode system using 6 M KOH. The CV curves show clear redox peaks, confirming Faradaic pseudocapacitive behavior, with Ni–Co–S/ACC-160 exhibiting the highest activity. GCD results indicate longer discharge time and higher capacitance for this sample, along with good reversibility and Coulombic efficiency. It delivers a maximum specific capacitance of 2392 F g^{-1} at 1 A g^{-1} and retains ~80.3% at 20 A g^{-1}, demonstrating superior rate capability. Overall, the 160 °C sample shows the best electrochemical performance [6].

Comparative Study Electrochemical Properties of MOF Based Nanocomposite Material

Composite Material	***Specific Capacitance (F/g)***	***Energy Den. (Wh/kg)***	***Power Den. (W/kg)***	***Ref.***
NiCo – MOF	*1202.1 F/g*	*49.4 Wh/kg*	*562.5 W/kg*	***01***
MOF – derived	*328.4 F/cm3*	*10.6*	*0.17 W/cm^3*	***02***

Mn_3O_4@C/rGO		*mWh/cm^3*		
MOF – derived TiO_2/C	*-*	*43.5 Wh/kg*	*865 W/kg*	***03***
MOF – derived NPC (Nanoporous Carbon)	*94.4 F/g*	*28.6 Wh/kg*	*100 W/kg*	***04***
3D porous carbon/Co_3O_4	*423 F/g*	*21.1 Wh/kg*	*790 W/kg*	***05***
NiCo-S/ACC	*2392 F/g*	*30.1Wh/kg*	*800.2W/kg*	***06***
CC/CoNi-MOF	*846 mF/cm^2*	*55.5 Wh/kg*	*175.5 W/kg*	***07***
Ni@Cu – MOF	*48.7 F/g*	*17.3 Wh/kg*	*798.5 W/kg*	***08***
MOF derived CeO^2/rGO	*720 F/g*	*23.5 Wh/kg*	*2917.2 W/kg*	***09***

Conclusion

MOF-derived nanocomposite electrodes demonstrate strong potential for high-performance supercapacitor applications owing to their hierarchical porous architecture and improved electrochemical activity. The adopted synthesis approach enables the formation of ultrathin nanosheet arrays that promote rapid ion diffusion and efficient electron transport. The optimized electrode exhibits superior electrochemical behaviour with enhanced capacitance and good rate capability compared with many previously reported MOF-based materials. Overall, the results highlight the advantages of MOF-derived nanostructures as promising materials for upcoming-generation electrochemical energy storage devices.

References

1. Yanzhong Wang et. al. ACS Appl. Energy Mater
2. By Ruoyu Wang et. al. RSC Adv., 2020, 10,34403
3. Vishal Shrivastav et. al. Int J Energy Res. 2020;1–16.
4. Da He et. al. Frontiers in Chemistry 2020 8 719
5. Sumin Li et. al. Applied Surface Science 2019, https://doi.org/10.1016/j.apsusc.2019.144090
6. Wei Zhao et. al. Chemical Engineering Journal 2019 https://doi.org/10.1016/j.cej.2019.04.070
7. Shusheng Xu et. al. Electrochimica Acta 342 (2020) 136124
8. Yi Wang et. al. Polymers 2019, 11, 821
9. Usman Ali Khan et. al. JournalofEnergyStorage41(2021)102999

Functionalized GO and rGO for Enhanced Electrochemical Properties: A Review

[1]Supriya P. Salunkhe, [2]Balbhim S. Maharnavar

[1]Bharati Vidyapeeth's College of Engineering for Women, Pune -411043

[2]Rayat Shikshan Sanstha's Dada Patil Mahavidyalaya Karjat, Ahilyanagar (MS), India-414402

Email: balbhim02@gmail.com

Article DOI Link: https://zenodo.org/uploads/19795895

DOI: 10.5281/zenodo.19795895

Abstract

The growing global demand for energy and the environmental concerns associated with fossil fuel consumption have accelerated research into sustainable energy storage technologies. Supercapacitors have emerged as promising electrochemical energy storage devices due to their high-power density, long cycle life, and rapid charge–discharge capability. Among various electrode materials, graphene-based nanohybrids have attracted considerable attention because of their excellent electrical conductivity, large specific surface area, and superior electrochemical stability. Graphene oxide (GO), derived from graphite through chemical oxidation methods such as the widely used Hummers' method, serves as an important precursor for the synthesis of reduced graphene oxide (rGO). Various reduction approaches, including thermal, chemical, photocatalytic, and electrochemical methods, have been explored to improve the electrical and structural properties of GO. The incorporation of rGO into electrode materials enhances electron transport and electrochemical activity, thereby improving the overall performance of supercapacitors. Consequently, graphene-based nanostructured materials represent a promising pathway for the development of efficient and sustainable next-generation energy storage systems

Keywords: Graphene Oxide, Reduced graphene oxide, Hummers Method

Introduction

The significant increase in energy use and consumption will result in the depletion of fossil fuels, causing numerous environmental issues, including pollution and global warming. As a result, utilizing renewable energy sources is essential and gaining worldwide attention [1]. Their environmental sensitivity and irregular nature require conversion and storage devices [2]. Modern energy

storage systems include dielectric capacitors, fuel cells, thermal batteries, and supercapacitors (SCs). Batteries provide greater energy density, whereas capacitors offer remarkable power density; however, the power density in batteries and the energy density in capacitors are relatively low SCs have shown significant advantages in this regard, as they provide the benefits of both systems [3]. SCs are extensively utilized as energy storage devices because of their long lifespan, high power density, and rapid charge/discharge capability. Enhancing the energy density of SCs can be achieved by increasing the potential window, specific capacitance (Cs), or both simultaneously (4). Electrochemical energy storage devices exhibit several advantages, including high specific capacitance, wide temperature tolerance, optimal power density, and low self-discharge. Nanohybrid materials demonstrate enhanced electrochemical performance due to their large surface area and tailored morphologies [5]. EDLCs typically exhibit higher power densities and ultra-long cycling stability, whereas PCs provide higher energy density but comparatively lower power density and cycling stability due to reduced conductivity. Transition metal oxides and sulfides have emerged as efficient electrode materials owing to their multiple oxidation states, cost-effectiveness, and enhanced energy storage capacity [6]. Graphene, consisting of one or more layers of two-dimensional carbon sheets, has attracted significant attention as a conductive substrate. Graphene-based nanohybrids have garnered interest due to their unique physicochemical properties when combined with other nanostructured materials [7]. Incorporating graphene into electrode materials enhances electron transport, structural stability, and electrochemically active surface area. Reduced graphene oxide (rGO) is widely used in SC electrodes due to its excellent electrical conductivity, chemical stability, large specific surface area, improved mesopore distribution, and enhanced charge transport. The Fig. 1. illustrates the exfoliation of graphite into graphene sheets, followed by their chemical modification. Different functional groups are introduced onto the graphene surface to tailor its properties for advanced applications such as energy storage and electronics [8].

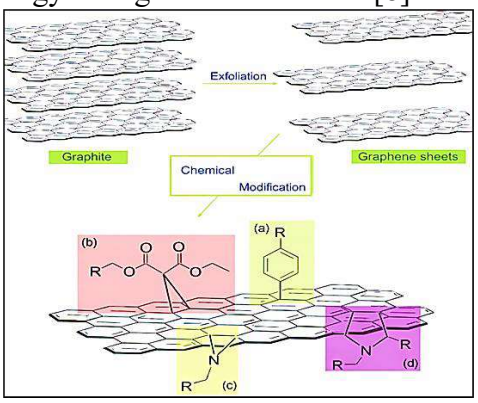

Fig.1 General chemical modification routes for graphene sheets [8]

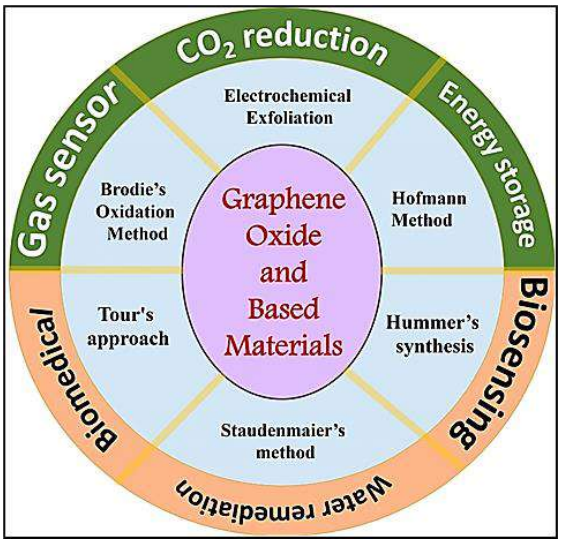

Fig.2 Different methods for the synthesis of GO and Based materials for various application [15]

Slight distortions occur slightly above or below the graphene plane. Due to structural deformation and the presence of covalently bonded functional groups, graphene oxide (GO) sheets are atomically rough. Several researchers have studied the surface of GO and observed highly defective regions, likely due to the presence of oxygen, as well as other nearly intact areas. Reports indicate that the graphene-like honeycomb lattice in GO is preserved, albeit with disorder [10]

Graphene Oxide

Graphite is a layered carbon material composed of stacked honeycomb structures with strong in-plane C–C bonds and weak interlayer van der Waals forces. It follows Bernal stacking and exhibits anisotropic electrical conductivity, with much higher in-plane conduction. Due to its stability, conductivity, and low charge transfer resistance, graphite is widely used in electrodes and energy storage applications. It also shows good oxidation, thermal, and corrosion resistance. Natural graphite exists as vein, flake, and amorphous forms and serves as a precursor for graphene oxide (GO) and reduced graphene oxide (rGO) [11–15].

- **Synthesis of Graphene Oxide (GO)**

Graphene oxide (GO) consists of graphene sheets functionalized with oxygen-containing groups such as hydroxyl and epoxy, which promote layer expansion and exfoliation. It is commonly synthesized using the Hummers method, involving oxidation of graphite with strong acids and oxidizing agents. This method, developed from earlier approaches like Brodie and Staudenmaier methods, remains widely used with various modifications to improve oxidation

efficiency. GO can be further reduced to rGO for enhanced conductivity in advanced applications [16–19].

- **Reduction of GO to rGO**

Efforts to produce materials with properties as close to pristine graphene as possible have led to extensive research focused on removing the oxygen functional groups of graphene oxide (GO) [20]. This reduction can be accomplished through several methods, including thermal, chemical, and electrochemical techniques, each resulting in differences in morphology, electrical properties, and other characteristics. Key factors in GO reduction include optimizing the C/O ratio, selectively removing oxygen functional groups, repairing structural defects, using eco-friendly reducing agents, and maintaining or enhancing properties such as conductivity, mechanical strength, and dispersibility. Thermal reduction of GO relies on the decomposition of oxygen-containing groups into carbon monoxide (CO) and carbon dioxide (CO_2) gases at elevated temperatures [21]. Rapid gas evolution can also exfoliate individual GO nanosheets. Thermal reduction may be achieved through high-temperature annealing in an oxygen-free environment or through alternative methods such as microwave treatment of GO powders or flash reduction of GO films using high-intensity light. Chemical reduction is commonly performed by introducing reducing agents into GO solutions [22]. Widely reported reducing agents include hydrazine, metal hydrides, and hydrohalic acids. Reduced graphene oxide (rGO) can also be synthesized through photocatalytic processes. For example, Williams et al. demonstrated the reduction of GO using ultraviolet (UV) light in the presence of a TiO_2 catalyst [23] Electrochemical reduction represents another viable approach and does not require chemical reducing agents. Instead, it is driven by electron transfer between GO and the electrodes within an electrochemical cell [24].

Conclusion

Among various synthesis techniques, Hummers' method remains the most widely used approach for preparing graphene oxide due to its efficiency and scalability, despite certain environmental and safety limitations. Alternative approaches, such as electrochemical reduction, provide safer and more environmentally friendly routes for producing reduced graphene oxide without hazardous reducing agents. Overall, graphene-based nanohybrids represent a highly promising class of materials for next-generation supercapacitor electrodes. Continued research focused on optimizing synthesis methods, improving material stability, and enhancing electrochemical performance will further advance the development of high-energy, high-power, and environmentally sustainable energy storage systems.

References

1. Huang, X. (2024). npj Climate Action, 3, 107.
2. deyinka, A. M., et al. (2024). Sustainable Energy Research, 11, 26.
3. Patel, A., et al. (2024). Discover Nano, 19, 188.
4. Vessally, E., et al. (2024). RSC Advances, 14, 40141–40160.
5. Khaliq, A. et al. (2024). Journal of Physics and Chemistry of Solids, 192, 112058.
6. Hu, X., et al. (2020). New Journal of Chemistry, 44, 11786–11795.
7. Zaka, A., Hayat, K., & Mittal, V. (2021). ACS Applied Electronic Materials, 3(2), 574–596.
8. Stergiou A, et al. (2014). Beilstein J. Nanotechnology, 5, 1580-1589
9. Boehm, H. P., et al. (1960). Journal de Chimie Physique et de Physico-Chimie Biologique, 58, 141–147.
10. Gómez-Navarro, C., et al. (2007). Nano Letters, 7(11), 3499–3503.
11. Aderibigbe, B., et al. (2016). Journal of Applied Pharmaceutical Science, 6(5), 209–221.
12. Nupearachchi, C., et al. (2017). Groundwater for Sustainable Development, 5, 206–215.
13. Zhang, H., et al. (2020). International Journal of Energy Research, 44(10), 8121–8135
14. Inagaki, M., et al. (2014). Advanced Engineering Materials, 16(5), 494–506.
15. Nosheen Farooq et al. (2024). Ariston Publications, ISSN-2997-8440.
16. Khot, M., & Kiani, A. (2022). International Journal of Energy Research, 46(3), 2700–2733.
17. Kigozi, M., at al. (2020). Results in Materials, 7, 100113.
18. Asthana, N., et al. (2024). Macromolecular Symposia, 406(1), 2300160.
19. Marcano, D. C., et al. (2010). ACS Nano, 4(8), 4806–4814.
20. Stankovich, S., et al. (2007). Carbon, 45(7), 1558–1565.
21. Pei, S., & Cheng, H. M. (2012). Carbon, 50(9), 3210–3228.
22. Thakur, S., & Karak, N. (2015). Carbon, 94, 224–242.
23. Williams, G., Seger, B., & Kamat, P. V. (2008). ACS Nano, 2(7), 1487–1491.
24. Yang, S., et al. (2012). Advanced Materials, 24(26), 3570–3576.

Innovations in Energy Storage Technology for Sustainable Energy Systems

Swapnil N Pawar, B J Lokhande

Lab of electrochemical studies, School of Physical Sciences, P.A.H. Solapur University, Solapur – 413255

Email: bjlokhande@gmail.com

Article DOI Link: https://zenodo.org/uploads/19796301

DOI: 10.5281/zenodo.19796301

Abstract

Energy storage systems are crucial for the transition towards sustainable energy by facilitating the integration of renewables, powering electric vehicles, and supporting smart grids. This chapter discusses last 5 years innovations across four major technologies: lithium-ion batteries, solid-state batteries, advanced supercapacitors, and hydrogen storage. Major findings show that lithium-ion batteries continue to lead with an energy density of up to 220 Wh/kg; solid-state batteries are developing high ionic conductivities; supercapacitors have very high-power densities (18,750 W/kg); and improved hydrogen storage capacity using palladium-graphene composites. Currently, the market is dominated by lithium-ion systems while solid-state and hydrogen technologies have some challenges. Future research areas include silicon anodes, sulphide electrolytes, graphene composites as well as AI-based management and circular economy strategies.

Keywords: Energy storage systems, lithium-ion batteries, solid-state batteries, supercapacitors, hydrogen storage, energy density.

Introduction

The fast global shift to decarbonization has made energy storage systems a key part of modern energy infrastructure. As the share of renewable energy sources like solar and wind grows, their natural intermittency makes it necessary to have efficient ways to store and use energy. At the same time, the electrification of transport with electric vehicles (EVs) and smart power grids demands storage technologies that can meet many performance needs. These include high energy density for longer driving ranges, quick charge-discharge rates for support in grid services, long cycle life for cost-effectiveness, and good safety features for large-scale use. Energy storage technologies include electrochemical, electrostatic, and chemical storage mechanisms that are suited for different operational

requirements. Lithium-ion batteries have become the main technology used in portable electronics and EV applications due to their balanced performance characteristics. [1]

However, there are still safety issues related to limited energy density and critical material availability. Therefore, solid-state batteries have attracted great interest as a next-generation alternative by replacing flammable liquid electrolytes with solid ionic conductors enabling safer operation possibly with high-capacity lithium-metal anodes. Supercapacitors offer extremely high-power density and long cycle life filling the performance gap between conventional capacitors and batteries. Hydrogen-based storage systems coupled with fuel cells present a promising route toward zero-emission transportation plus long-duration energy storage despite material and infrastructure challenges.[2][3]

In the last five years, rapid progress in nanomaterial engineering discovery of materials by computation optimization at interfaces as well as scalable manufacturing has brought these technologies forward into shaping sustainable future energy systems.[1]

Developments in Lithium-Ion Batteries

The technology of lithium-ion batteries is evolving with incremental enhancements in energy density, safety, and performance over the life cycle. Current chemistries such as $LiFePO_4$ and $LiNiMnCoO_2$ achieve energy densities approaching 220 Wh/kg at cycle lives exceeding 2000 cycles. Their dominant position within electric vehicles can be attributed to an optimal balance of energy density, power capability, and process maturity.

Nickel-rich cathodes, advanced electrolytes, and optimized cell architectures have been the main focus in efforts to enhance energy density. Although increasing nickel content improves the capacity of the battery material, it raises thermal stability concerns, necessitating a sophisticated battery management system for safe operation. Modern BMS technologies now feature thermal regulation, state-of-health estimation, and adaptive charging strategies to improve safety and extend operational life. The more batteries are utilized, the more critical recycling has become. Advances in chemical recycling methods enable the retrieval of precious materials and decrease environmental impacts. Yet, economic barriers, infrastructure gaps, and policy inconsistencies persist in hindering large-scale implementation.[2][4]

Solid-State Battery Breakthroughs

Solid-state batteries are a breakthrough technology in energy storage, where the flammable liquid electrolyte is replaced with a solid ionic conductor. This enhances safety and allows for the use of lithium metal anodes with a higher theoretical capacity. Research efforts have focused on sulfide electrolytes that

offer high ionic conductivity, glass-ceramic systems that exhibit better stability in air and compatibility at interfaces, and garnet-type oxide electrolytes known for their excellent chemical and mechanical stability. Polymer hybrid electrolytes come into play as an option with good flexibility but moderate conductivity. A major challenge in this field is the high resistance at solid–solid interfaces which can be improved by means of buffer layers as well as surface modifications. Though advancements have been made, challenges like dendrite growth, degradation of interfaces, low room-temperature conductivity, and high costs still exist before large-scale commercialization can happen.[8]

High-Performance Materials for Supercapacitors

Supercapacitors are used in high-power energy applications because of their high power density and fast charge–discharge process. They do not use electrochemical reactions like batteries to store energy, but rather accumulate electrostatic charge; as a result, they have an extremely long cycle life that exceeds 100,000 cycles. Graphene-based materials are used as electrodes because they have high electrical conductivity and large surface areas with mechanical flexibility. Reduced graphene oxide (rGO) electrodes give high specific capacitance values along with good cycling stability. Three-dimensional graphene structures improve ion transport pathways and structural stability to support flexible and wearable electronics. Metal–organic frameworks and hybrid nanocomposite materials are new material systems that improve capacitance, while hybrid supercapacitors increase energy density at the expense of cycle life. [9]

Hydrogen Energy Systems

Hydrogen storage continues to be a critical issue in hydrogen energy systems due to its low volumetric energy density. Conventional storage techniques, such as compressed gas and liquid hydrogen, necessitate either very high pressures or very low temperatures, which are associated with safety, cost, and efficiency issues. Therefore, solid-state hydrogen storage materials have attracted much attention because of their enhanced safety and possible higher storage density. One mechanism that has been widely studied is the spillover effect in Pd–graphene composite materials. In this mechanism, hydrogen molecules dissociate on palladium catalytic sites, and the resulting hydrogen atoms spill over onto the graphene surface and assist in achieving more adsorption capacity. These materials can improve the kinetics of storage as well as uptake of hydrogen; however, they do not yet meet the performance required for practical vehicular applications. Hydrogen storage systems provide an entire pathway from renewable electricity into hydrogen fuel and back into electrical power when combined with fuel cells although problems like purity of hydrogen, thermal

management, and limited refueling infrastructure still pose significant challenges [5].

Material innovation is essentially what drives advances in energy storage technologies. Lithium-ion batteries keep on improving with silicon-based anodes, advanced electrolytes, and nanostructured electrodes. Solid-state batteries employ defect engineering for ionic conductivity enhancement while supercapacitors use graphene-based hybrid architectures for maximum conductivity and surface area.[6]

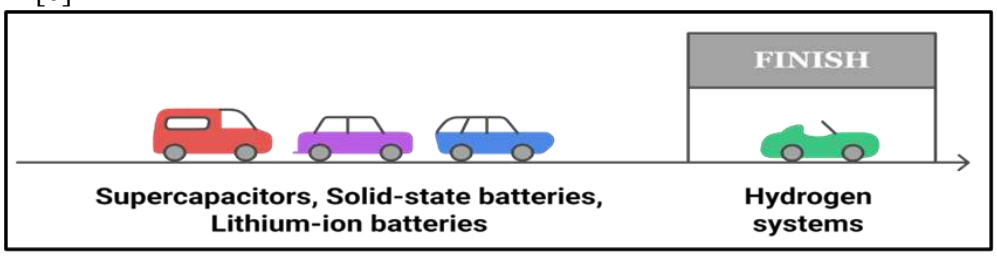

Fig a. Various energy storage technologies withe performance.

Sustainability and Climate Implications

Energy storage systems are used for renewable energy integration and electrification of transport but also create sustainability problems. Lithium-ion batteries usually have lifecycle emission benefits, but their production involves impacts from resource extraction and difficulties in recycling them. Solid-state batteries can provide improvements in safety and lifespan, but they too need to consider sustainable material sourcing and effective recycling strategies. Supercapacitors use carbon-based materials that are widely available with a long operational life, while hydrogen systems will give zero emissions if powered by green hydrogen. The overall sustainability would depend upon responsible manufacturing as well as circular economy practices. AI plays an increasing role in battery management through predictive maintenance, intelligent charging, and digital twin modeling while recycling, second life battery use, and modular design further enhance the long-term environmental performance.[7]

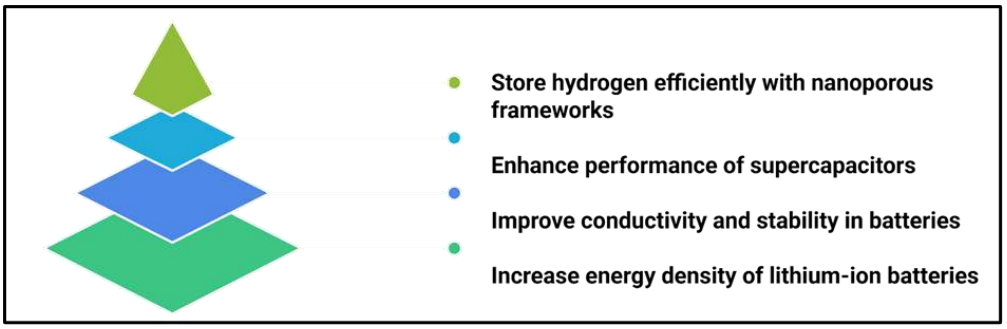

Fig b. Future Research Directions

No one technology is best in every way; it depends on what the application needs.

Conclusion

Recent developments in energy storage technology are vital for the sustainability of energy systems. The most widely used technology is lithium-ion batteries, which have reached maturity in terms of manufacturing and offer reliable performance. Solid-state batteries offer a potential alternative with more safety and higher energy densities. Supercapacitors serve very well in high-power applications, whereas hydrogen storage provides long-duration storage and zero-emission mobility. Since no one technology can fulfill all requirements, future energy systems will use complementary storage solutions backed by advancements in materials science, system integration, and smart energy management.

References

1. Advancements in Electric Vehicle Battery Technology: A Systematic Review – 2024
2. Sutikno et al. – Battery Types and Recent Developments for Energy Storage in Electric Vehicles: Technical Criteria and Battery Management System – 2025
3. Shah et al. – Challenges and Advancements in All-Solid-State Battery Technology for Electric Vehicles – 2024
4. Zhang et al. – Advances and Challenges in Solid-State Battery Technology – 2025
5. Wadodkar et al. – Emerging Materials for Next Generation Supercapacitors: Exploring the Latest Trends and Innovations – 2025
6. Dagdag et al. – Carbon Allotrope-Based Materials as Supercapacitors – 2025
7. Manoharan et al. – High-Power Graphene Supercapacitors for the Effective Storage of Regenerative Energy During the Braking and Deceleration Process in Electric Vehicles – 2021
8. Habibullah et al. – Palladium-Phosphide-Modified Three-Dimensional Phospho-Doped Graphene Materials for Hydrogen Storage – 2023
9. Sun et al. – Solid Hydrogen Storage with Palladium-Graphene Composites: Synthesis, Characterization, and Mechanistic Insights – 2024

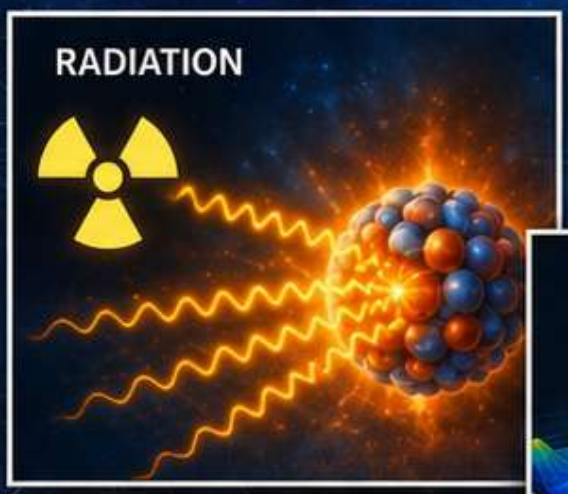

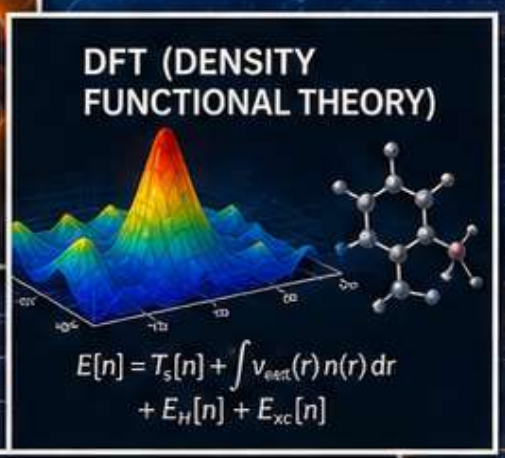

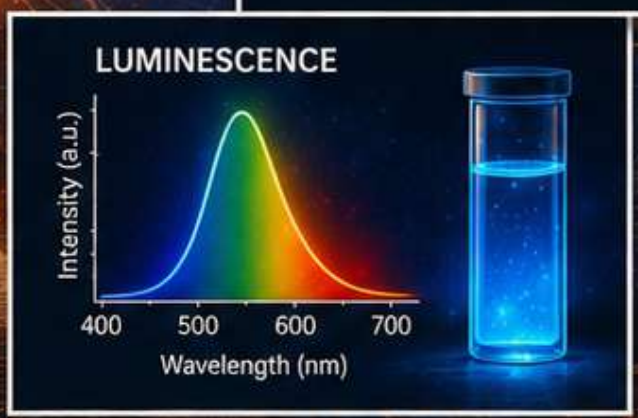

Nature Light Publications

309 West 11, Manjari VSI Road, Manjari Bk.,
Haveli, Pune- 412 307.
Website: www.naturelightpublications.com
Email: naturelightpublications@gmail.com
Contact No: +919822489040 / 9922489040

Nature Light Publications

Nature- 99

ISBN: 978-93-49938-40-3

Price- 999/-